MONASH University

Analysis of Physiologically Relevant Signalling Events via GLP-1R in Insulinoma cells

(Supplementary)

Kavita Pabreja

BPharm, MPharm (Pharmacology)

A thesis submitted for the degree of (*Doctor of Philosophy*) at

Monash University in 2015

Monash Institute of Pharmaceutical Sciences

Table of Contents

APPENDIX-1: SUPPLEMENTARY FIGURES OF CHAPTER 3

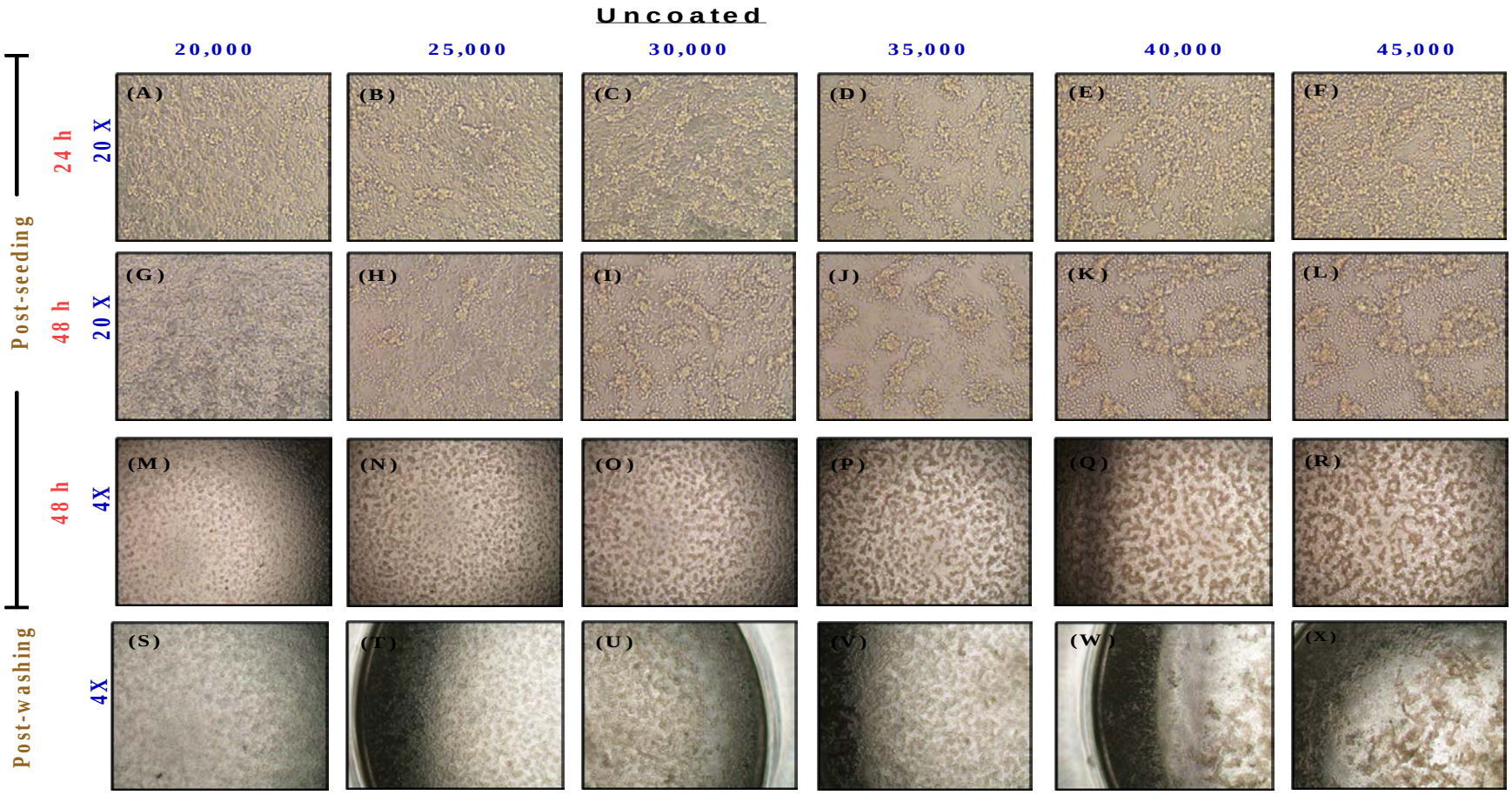

Figure S3.1: Microscopic images of INS-1 832/3 cells on uncoated plates. Images representing the phenotype and distribution of INS-1 832/3 cells after 24 h (panels A-F; 20X) and 48 h (panels G-L; 20 X and panels M-R; 4X) of seeding on uncoated 96 well cell culture plates at different cell densities. Panel S-X (4X) represent the cells after washing the cells.

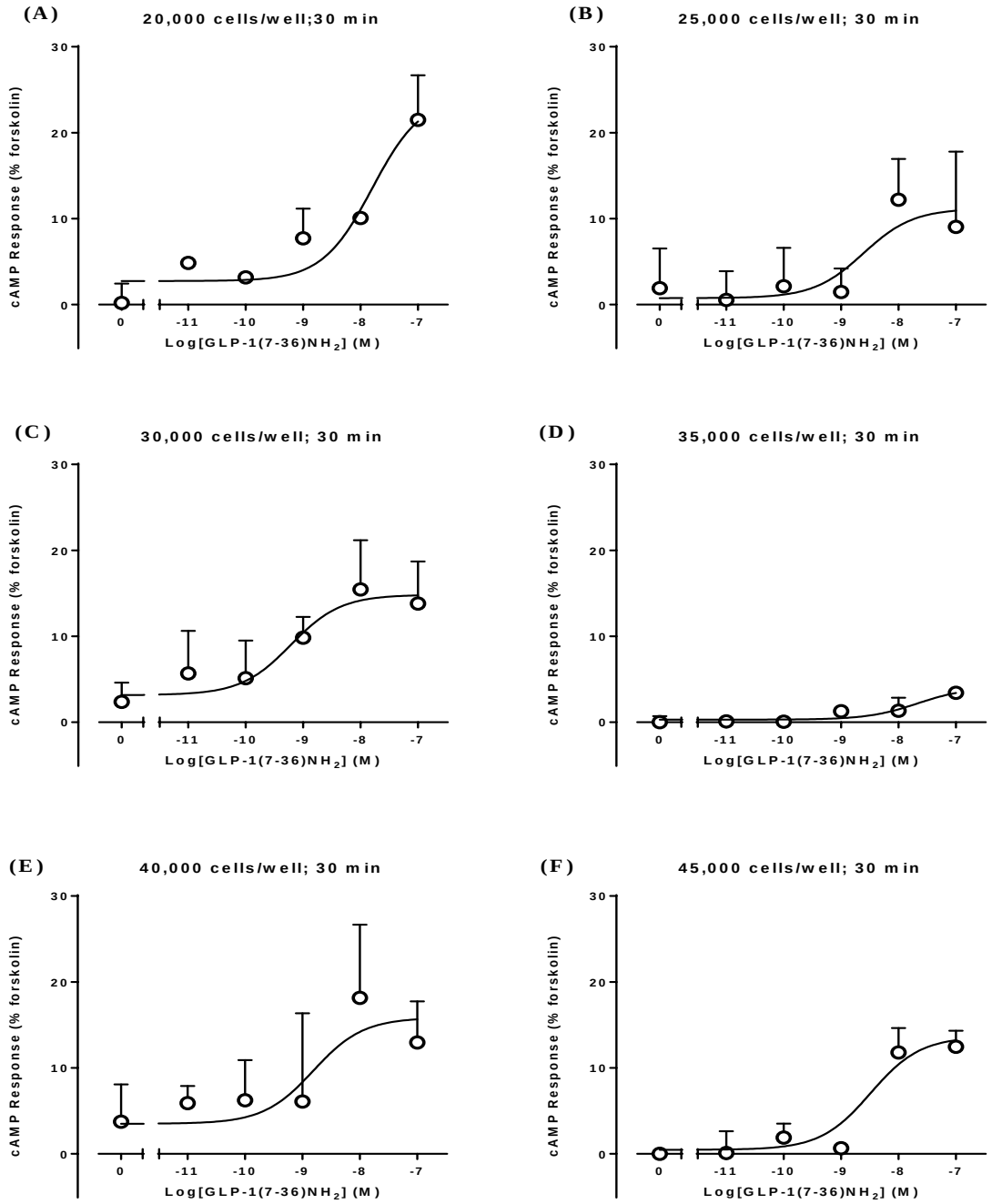

Figure S3.2: cAMP accumulation on cells plated on uncoated plates. Effect of 30 min GLP-1 stimulation in 11 mM glucose on cAMP accumulation in absence of IBMX after 48 h of cell seeding at varying cell densities on uncoated 96-well cell culture plates. (A) 20,000 cells/well; (B) 25,000 cells/well; (C) 30,000 cells/well; (D) 35,000 cells/well; (E) 40,000 cells/well; (F) 45,000 cells/well. Data is normalised to the response elicited by 100 µM forskolin and analysed with a three-parameter logistic equation. All values are mean + SEM of five to ten experiments conducted in triplicate.

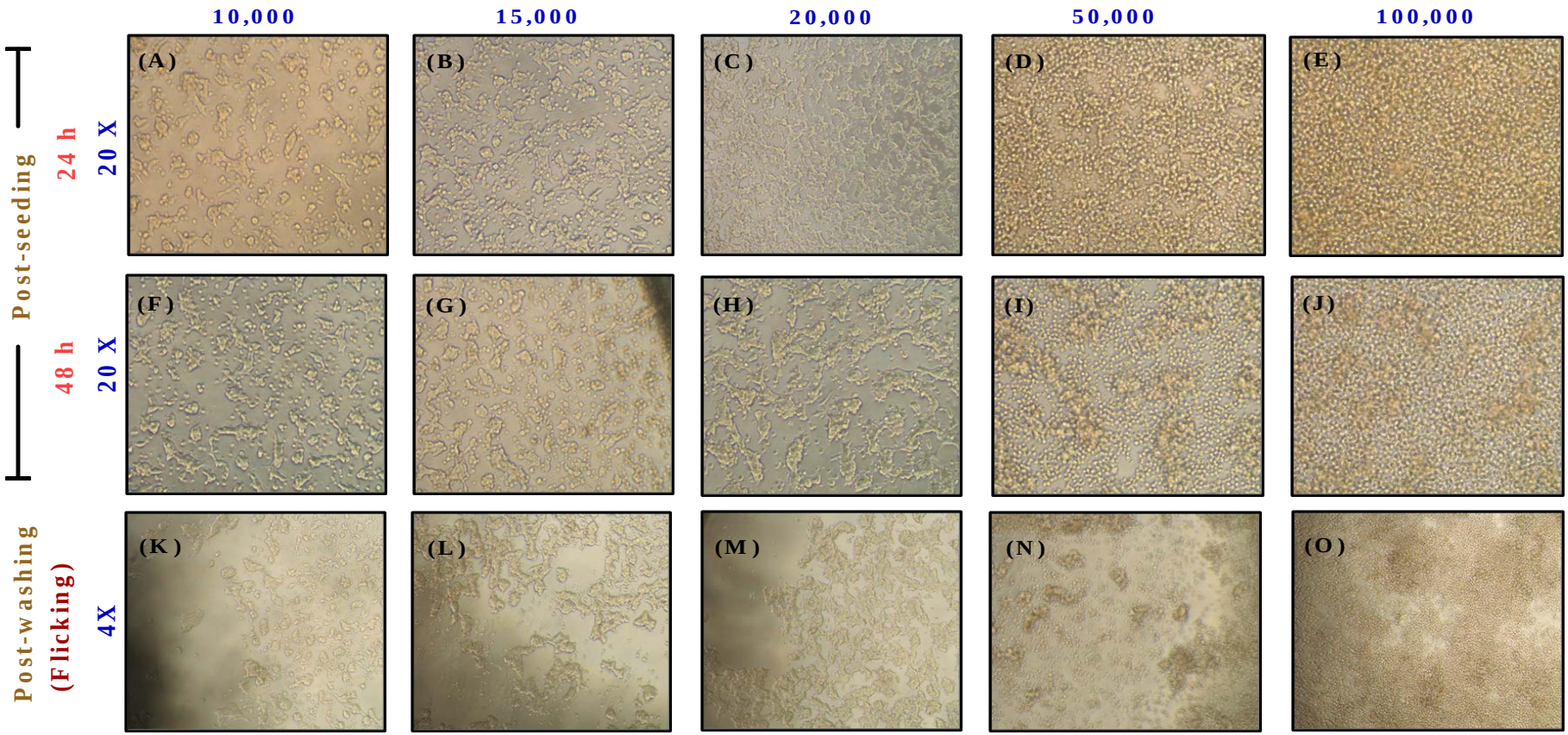

Figure S3.3: Microscopic images of INS-1 832/3 cells on PDL-coated plates. Images representing the phenotype and distribution of INS-1 832/3 cells ar after 24 h (panels A-E; 20X) and 48 h (panels G-J; 20 X) of seeding on poly-D-Lysine coated 96 well cell culture plates at different cell densities. Panels K-O (20X) represent the cells after washing the media on cells prior to assay.

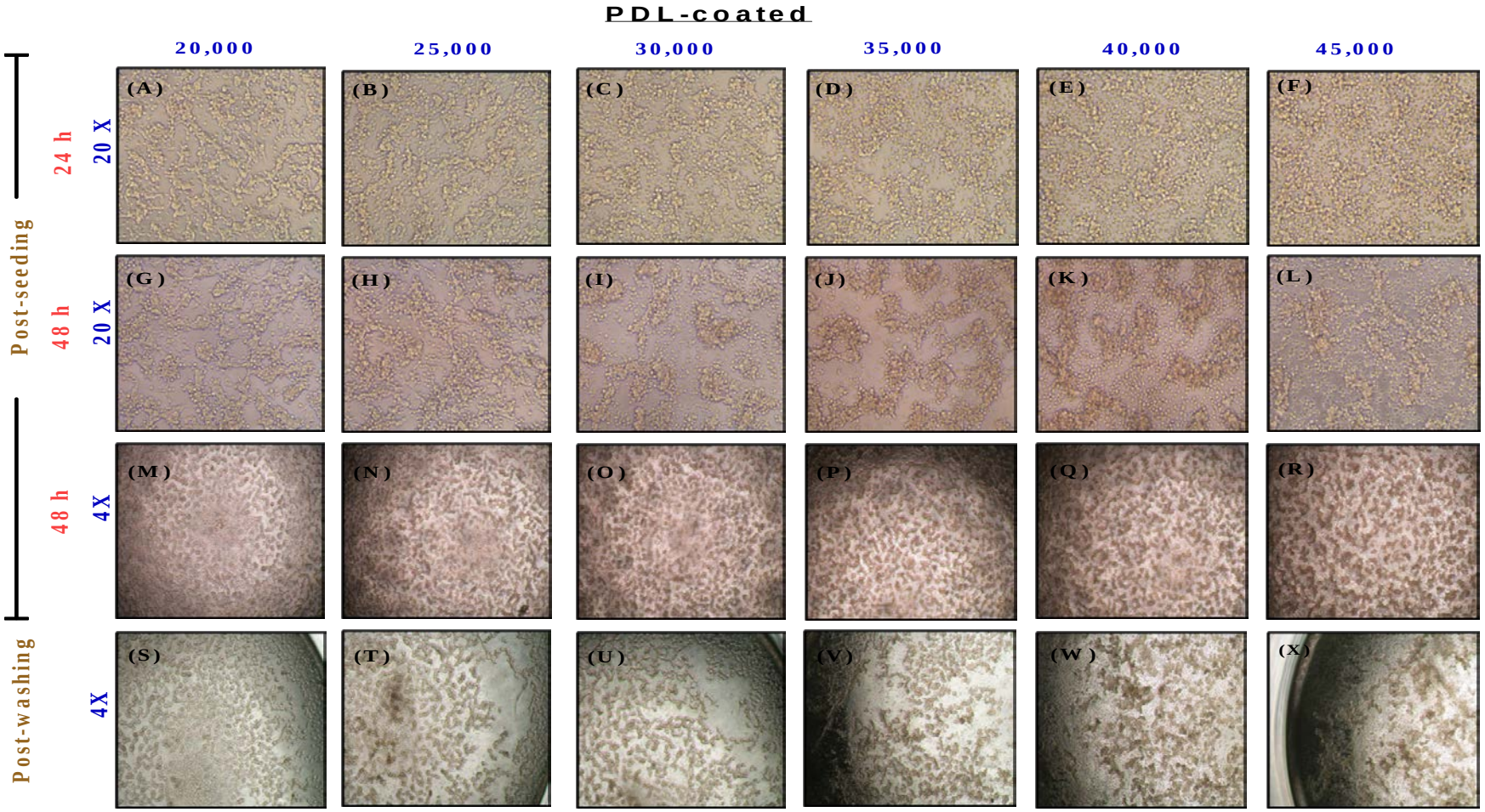

Figure S3.4: Microscopic images of INS-1 832/3 cells on PDL-coated plate at lower cell densities. Images representing the phenotype and distribution of INS-1 832/3 cells after 24 h (panels A-F; 20X) and 48 h (panels G-L; 20 X; panels M-R; 4X) of seeding on poly-D-Lysine coated 96 well cell culture plates at different cell densities. Panels S-X (4X) represent the cells after media aspiration prior to assay.

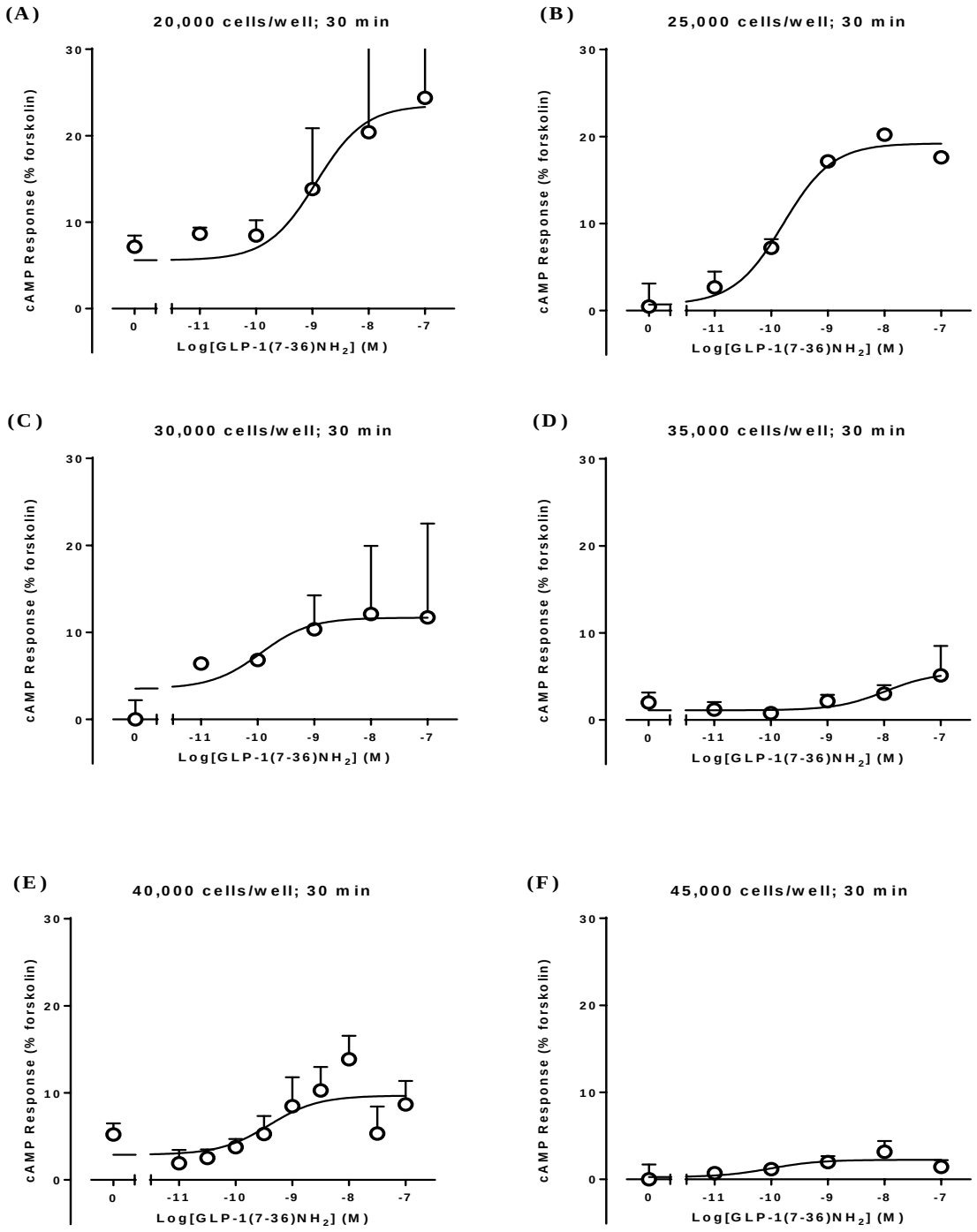

Figure S3.5: cAMP accumulation on cells plated on PDL-coated plates. Effect of 30 min GLP-1 stimulation in 11 mM glucose on cAMP accumulation in presence of IBMX after 48 h of cell seeding at varying cell densities on poly-D-lysine coated 96-well cell culture plates. (A) 20,000 cells/well; (B) 25,000 cells/well; (C) 30,000 cells/well; (D) 35,000 cells/well; (E) 40,000 cells/well; (F) 45,000 cells/well. Data is normalised to the response elicited by 100 µM forskolin and analysed with a three-parameter logistic equation. All values are mean + SEM of five to ten experiments conducted in triplicate.

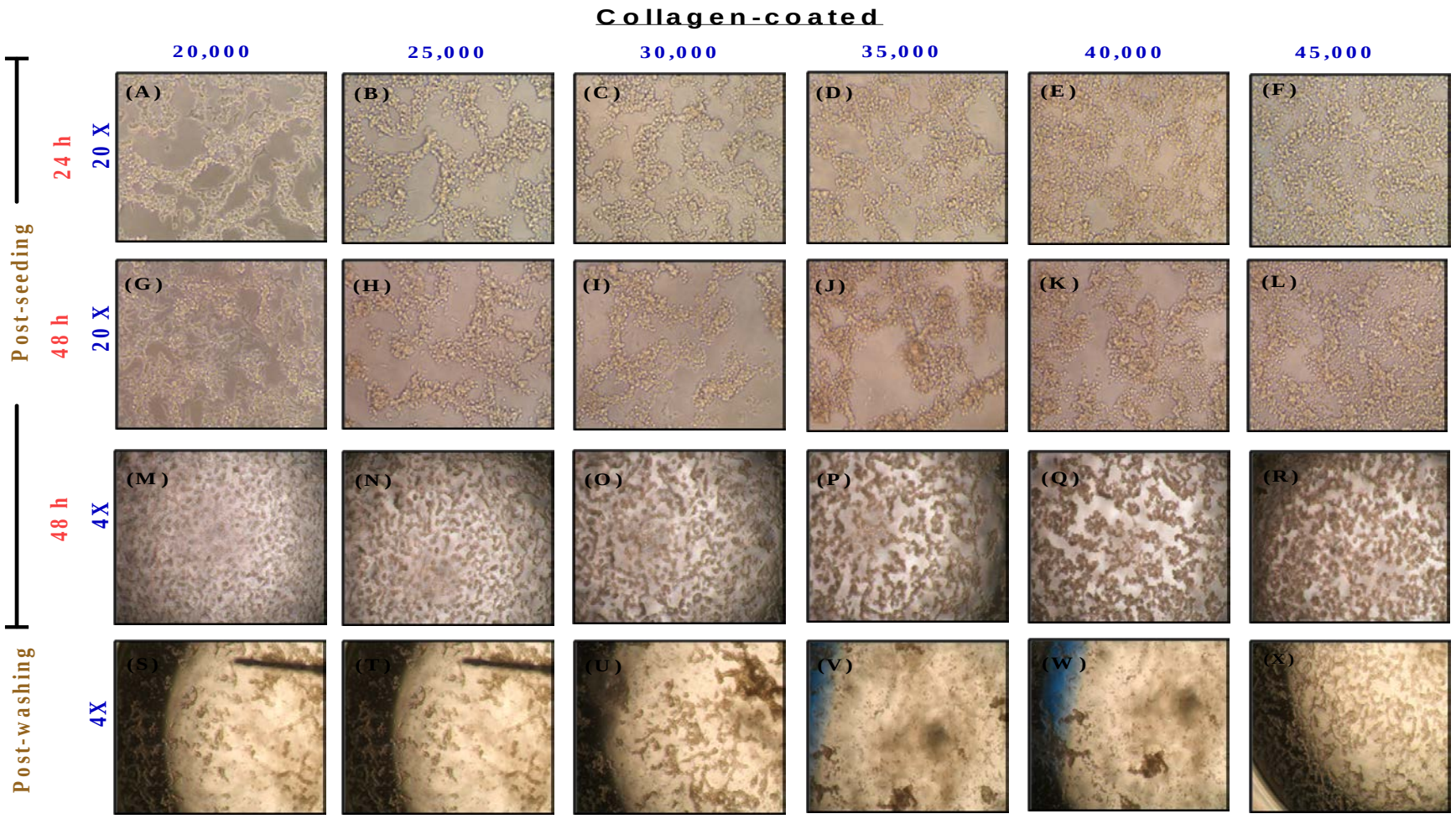

Figure S3.6 Microscopic images of INS-1 832/3 cells on collagen-coated plates. Images representing the phenotype and distribution of INS-1 832/3 cells after after 24 h (panels A-F; 20X) and 48 h (panels G-L; 20 X and panels M-R; 4X) of seeding on collagen coated 96-well cell culture plates at different cell densities. Panels S-X (4X) represent the cells after media aspiration prior to assay.

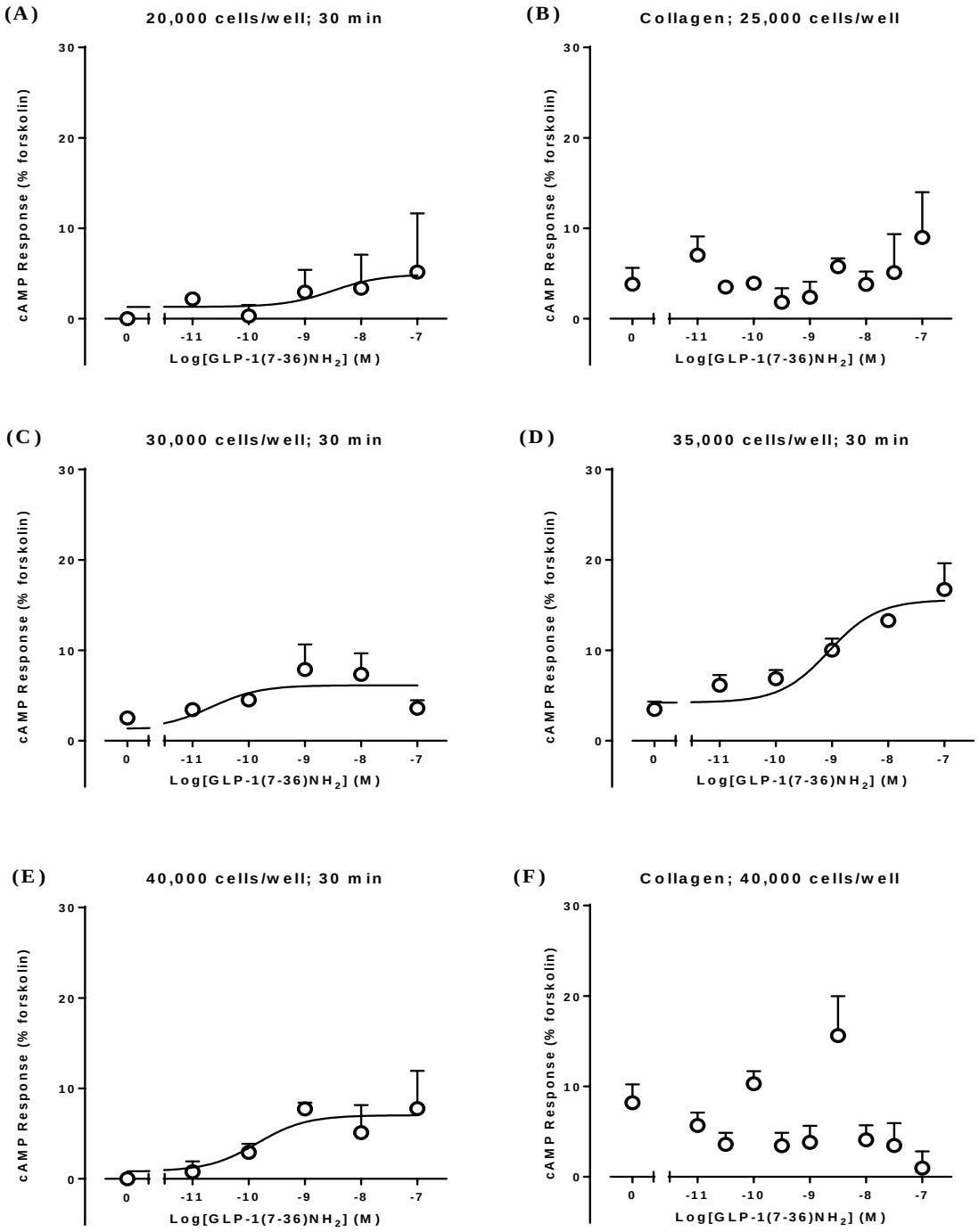

Figure S3.7: cAMP accumulation on cells plated on collagen-coated plates. Effect of 30 min GLP-1 stimulation in 11 mM glucose on cAMP accumulation in presence of IBMX after 48 h of cell seeding at varying cell densities on collagen coated 96-well cell culture plates. (A) 20,000 cells/well; (B) 25,000 cells/well; (C) 30,000 cells/well; (D) 35,000 cells/well; (E) 40,000 cells/well; (F) 45,000 cells/well. Data is normalised to the response elicited by 100 µM forskolin and analysed with a three-parameter logistic equation. All values are mean + SEM of five to ten experiments conducted in triplicate.

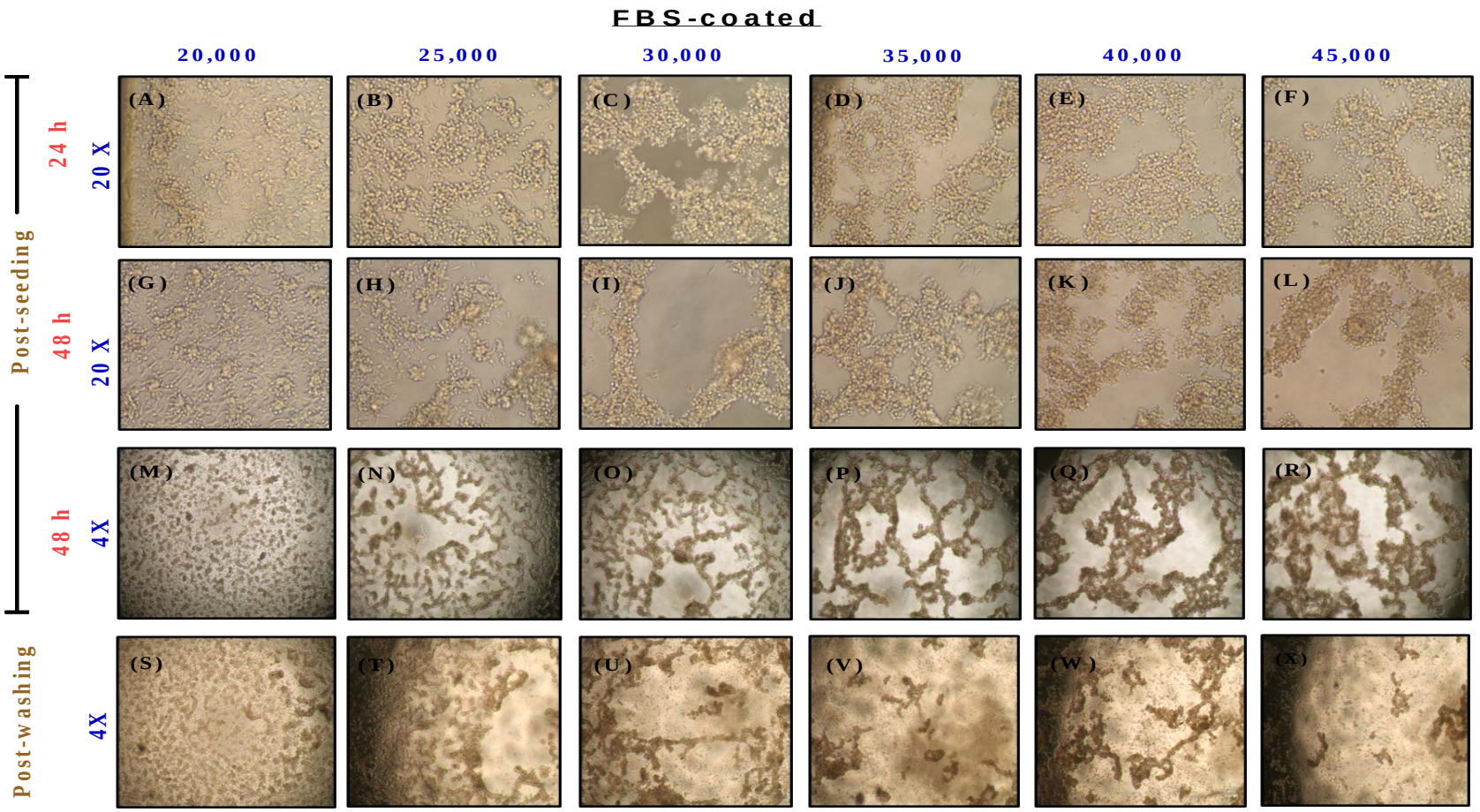

Figure S3.8: Microscopic images of INS-1 832/3 cells on FBS-coated plates. Images representing the phenotype and distribution of INS-1 832/3 cells after after 24 h (panels A-F; 20X) and 48 h (panels G-L; 20 X and panels M-R; 4X) of seeding on foetal bovine serum (FBS) coated 96-well cell culture plates at different cell densities. Panels S-X (4X) represent the cells following media aspiration prior to assay.

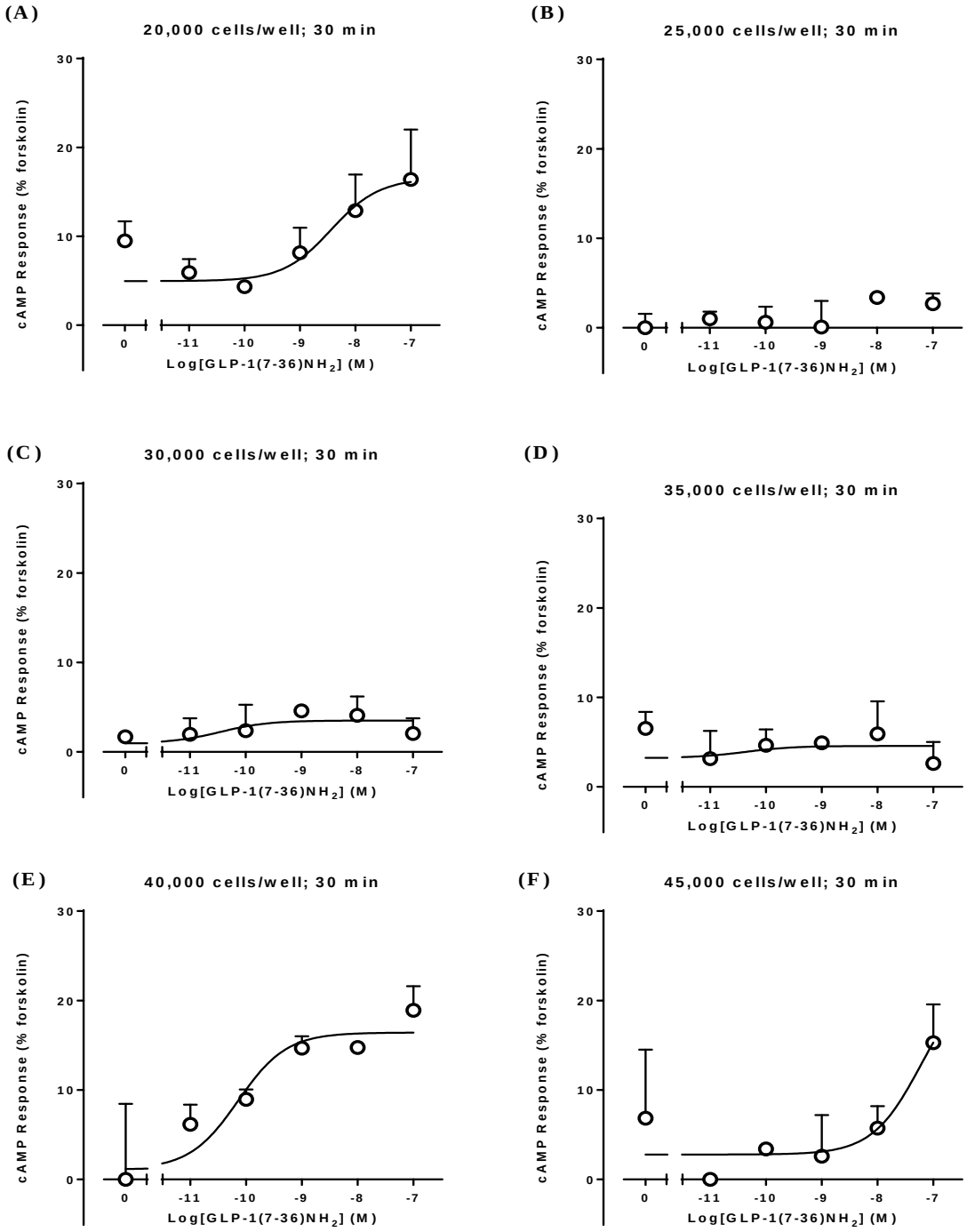

Figure S3.9: cAMP accumulation on cells plated on FBS-coated plates. Effect of 30 min GLP-1 stimulation in 11 mM glucose on cAMP accumulation in presence of IBMX after 48 h of cell seeding at varying cell densities on FBS coated 96-well cell culture plates. (A) 20,000 cells/well; (B) 25,000 cells/well; (C) 30,000 cells/well; (D) 35,000 cells/well; (E) 40,000 cells/well; (F) 45,000 cells/well. Data is normalised to the response elicited by 100 µM forskolin and analysed with a three-parameter logistic equation. All values are mean + SEM of five to ten experiments conducted in triplicate.

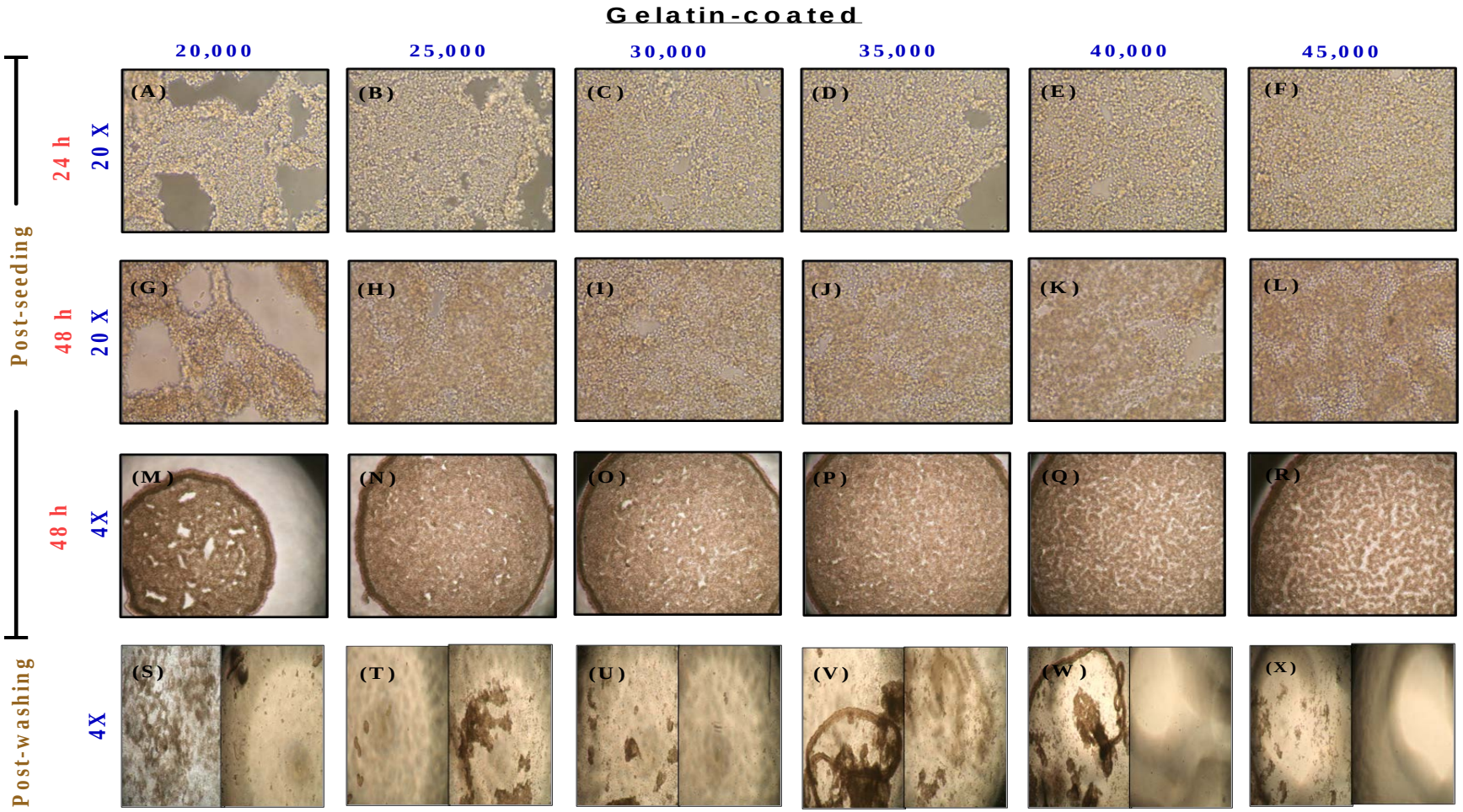

Figure S3.10 Microscopic images of INS-1 832/3 cells on gelatin-coated plates. Images representing the phenotype and distribution of INS-1 832/3 cells after 24 h (panels A-F; 20X) and 48 h (panels G-L; 20 X and panels M-R; 4X) of seeding on gelatin coated 96-well cell culture plates at different cell densities. Panels S-X (4X) represent the cells following media aspiration prior to assay.

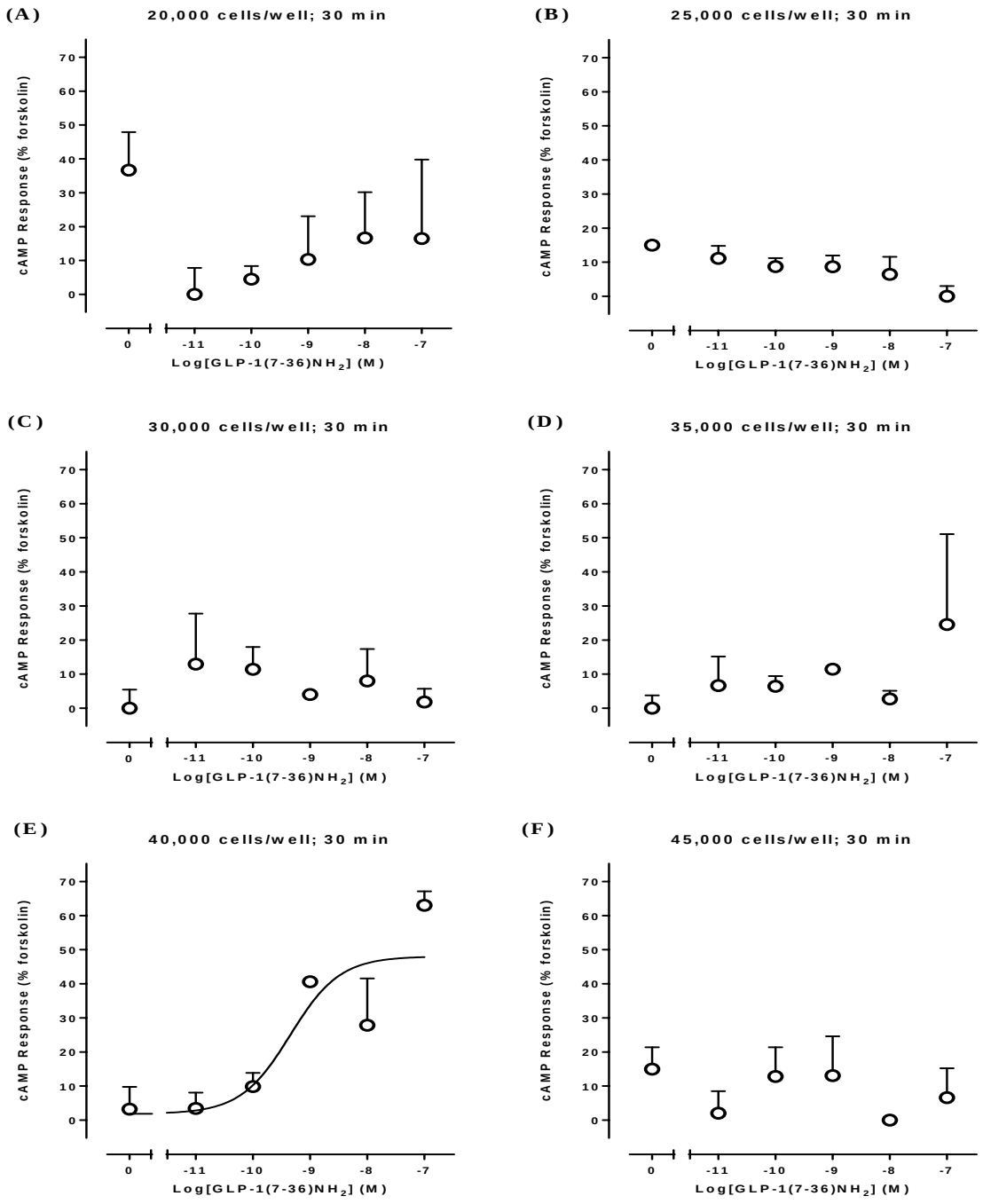

Figure S3.11: cAMP accumulation on cells plated on gelatin-coated plates. Effect of 30 min GLP-1 stimulation in 11 mM glucose on cAMP accumulation in presence of IBMX after 48 h of cell seeding at varying cell densities on gelatin coated 96-well cell culture plates. (A) 20,000 cells/well; (B) 25,000 cells/well; (C) 30,000 cells/well; (D) 35,000 cells/well; (E) 40,000 cells/well; (F) 45,000 cells/well. Data is normalised to the response elicited by 100 µM forskolin and analysed with a three-parameter logistic equation. All values are mean + SEM of five to ten experiments conducted in triplicate.

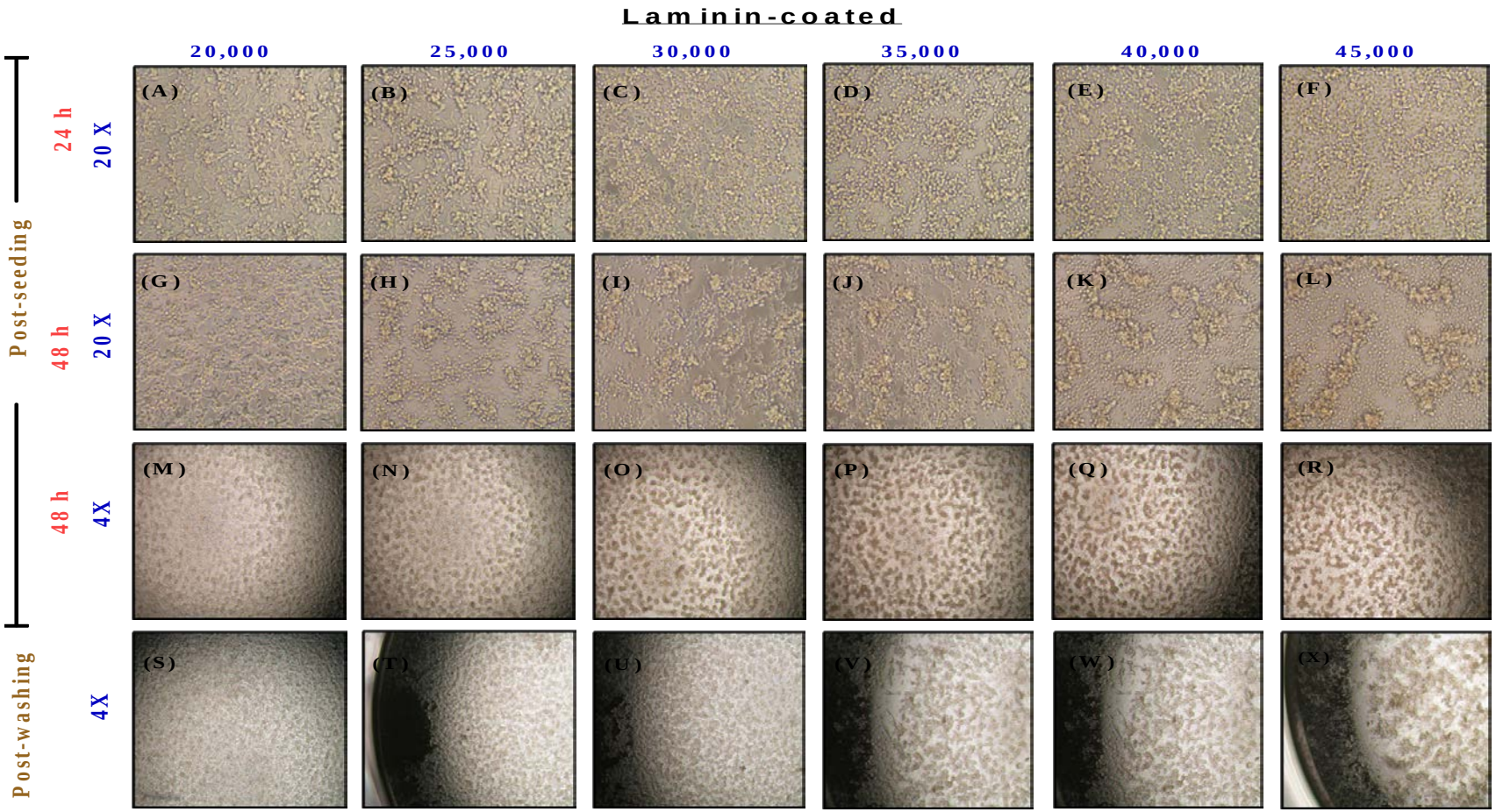

Figure S3.12: Microscopic images of INS-1 832/3 cells on laminin-coated plates. Images representing the phenotype and distribution of INS-1 832/3 cells after 24 h (panels A-F; 20X) and 48 h (panels G-L; 20 X and panels M-R; 4X) of seeding on laminin coated 96-well cell culture plates at different cell densities. Panels S-X (4X) represent the cells following media aspiration prior to assay.

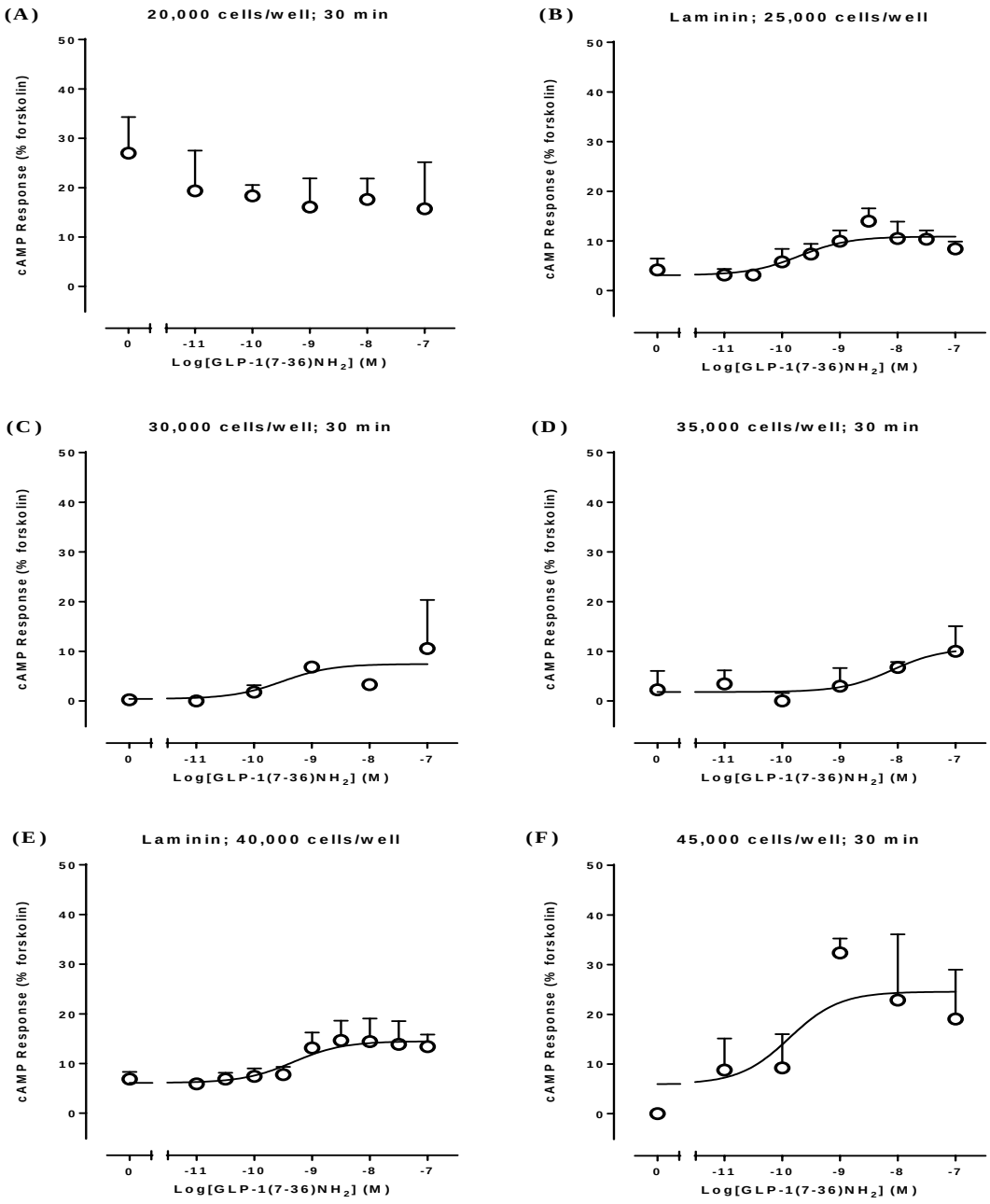

Figure S3.13: cAMP accumulation on cells plated on laminin-coated plates. Effect of 30 min GLP-1 stimulation in 11 mM glucose on cAMP accumulation in presence of IBMX after 48 h of cell seeding at varying cell densities on laminin coated 96-well cell culture plates. (A) 20,000 cells/well; (B) 25,000 cells/well; (C) 30,000 cells/well; (D) 35,000 cells/well; (E) 40,000 cells/well; (F) 45,000 cells/well. Data for cAMP accumulation is normalised to the response elicited by 100 µM forskolin and analysed with a three-parameter logistic equation. All values are mean + SEM of five to ten experiments conducted in triplicate.

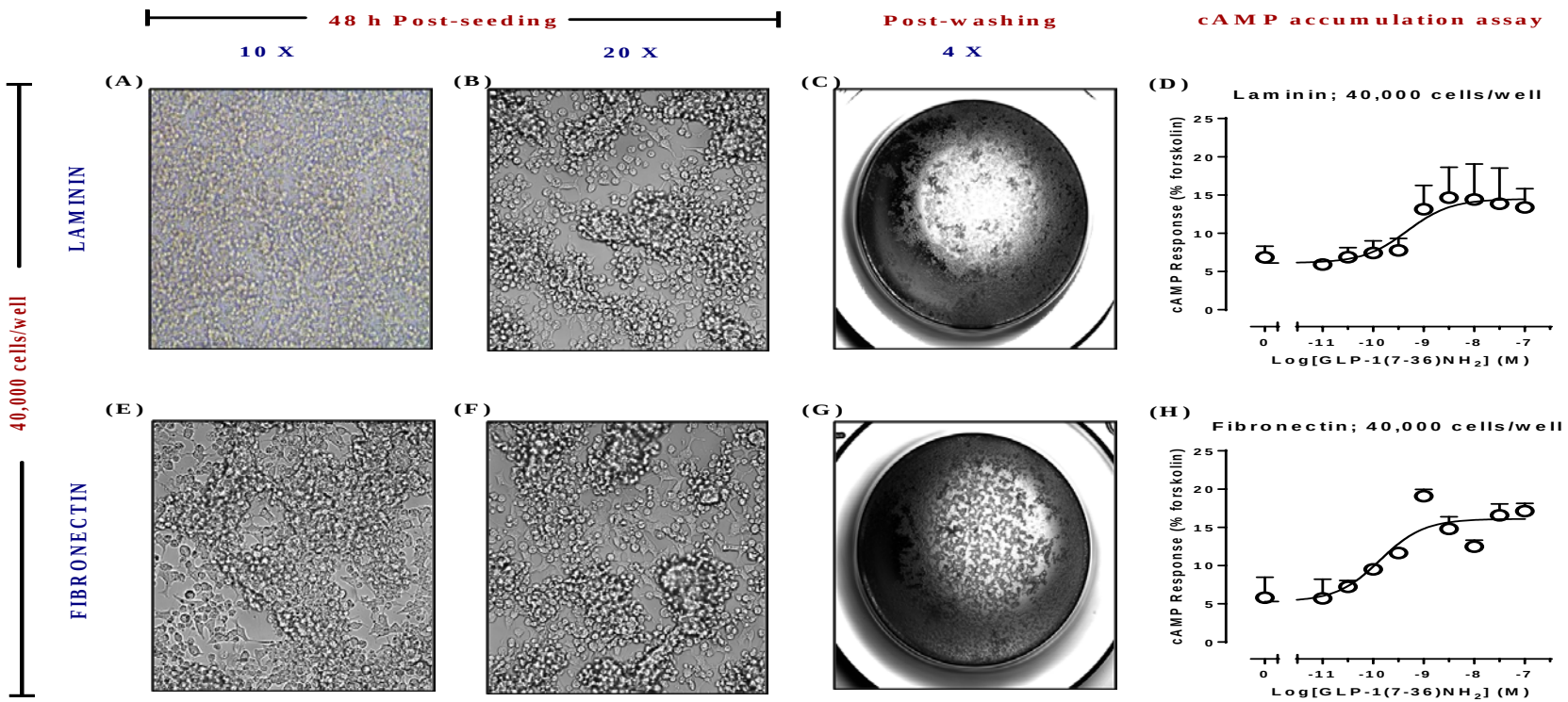

Figure S3.14: cAMP accumulation on cells plated on fibronectin-coated plates. Effect of GLP-1 on cAMP accumulation in INS-1 832/3 cells after 48 h of seeding 40,000 cells/well on laminin (A-D) and fibronectin (E-H) coated 96 well cell culture plates. (A) cell confluence on the day of assay on laminin coated plate, 10X; (B) cell confluence on the day of assay on laminin coated plate, 20X; (C) washing of cells prior to assay on laminin coated plates; (D) concentration dependent cAMP response with cells seeded on laminin coated plate; (E) cell confluence on the day of assay on fibronectin coated plate, 10X; (F) cell confluence on the day of assay on fibronectin coated plate; (G) washing of cells prior to assay on fibronectin coated plates; (H) concentration dependent cAMP response with cells seeded on fibronectin coated plate. Data is normalised to the response elicited by 100 µM forskolin and analysed with a three-parameter logistic equation. All values are mean + SEM of five to ten experiments conducted in triplicate.

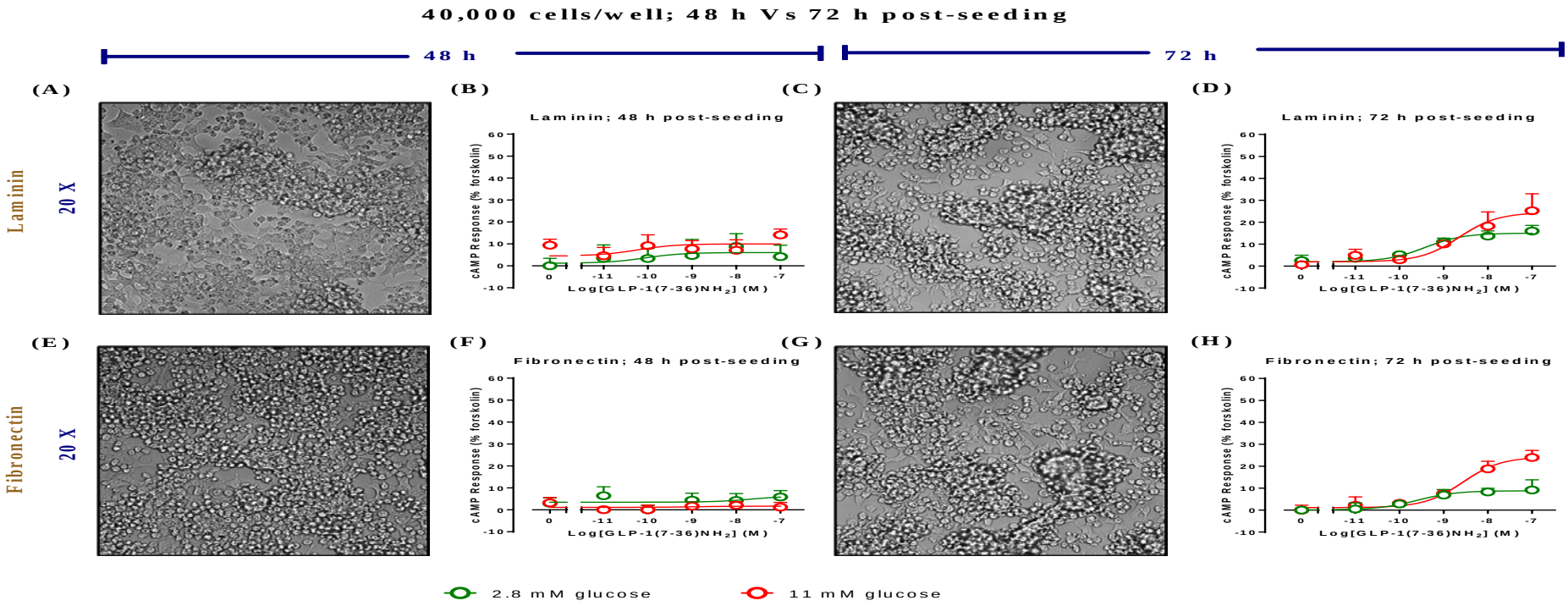

Figure S3.15: Effect of seeding duration on cAMP accumulation on cells plated on laminin-coated plates. Effect of GLP-1 on cAMP accumulation in presence of varying glucose concentration after 48 h (A, B, E and F) and 72 h (C, D, G and H) of seeding 40,000 cells/well on laminin (A-D) and fibronectin (E-H) coated 96 well cell culture plates. (A) 40,000 cells/well on laminin coated plate after 48 h; (B) cAMP assay after 48 h of post-seeding on laminin coated plate; (C) 40,000 cells/well on laminin coated plate after 72 h; (D) cAMP assay after 72 h of post-seeding on laminin coated plate; (E) 40,000 cells/well on fibronectin coated plate after 48 h; (F) cAMP assay after 48 h of post-seeding on fibronectin coated plate; (G) 40,000 cells/well on fibronectin coated plate after 72 h; (H) cAMP assay after 72 h of post-seeding on fibronectin coated plate. Data is normalised to the response elicited by 100 µM forskolin and analysed with a three-parameter logistic equation. All values are mean + SEM of five to ten experiments conducted in triplicate.

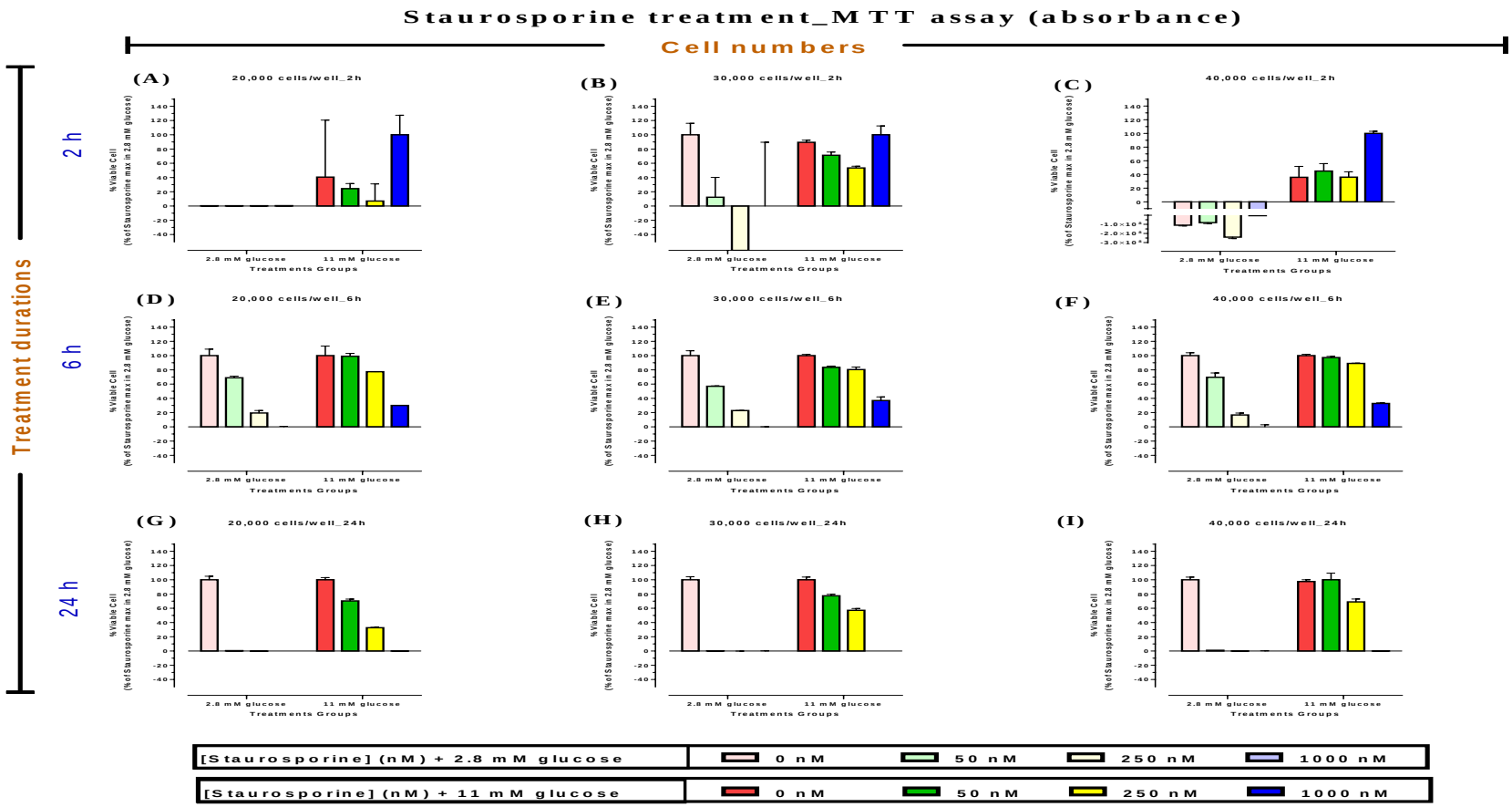

Figure S3.16: Assessment of apoptosis using MTT assay. Staurosporine induced apoptosis assessed using MTT (3-[4,5-dimethylthiazol-2-yl]-2,5 diphenyl tetrazolium bromide) assay at different time points, 2 h (A-C), 6h (D-F) and 24 h (G-I) in INS-1 832/3 cells seeded at varying cell densities, 20,000 cells/well (A, D, G), 30,000 cells/well (B, E, H) and 40,000 cells/well (C, F, I). Percent cell viability was assessed by normalizing to staurosporine maximum (1000 nM) response. Data is presented as mean + SEM of three replicates.

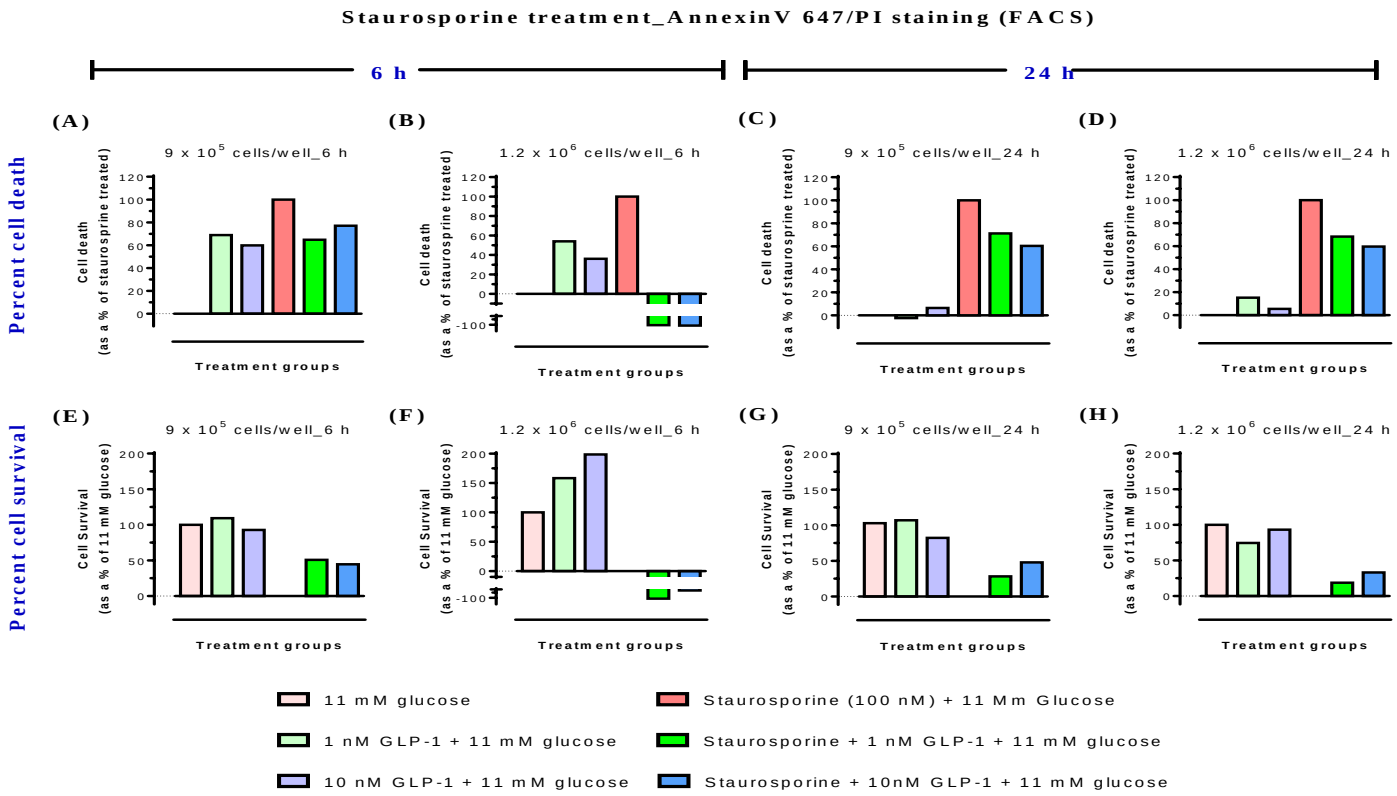

Figure S3.17: Assessment of apoptosis after using FACS. Staurosporine induced apoptosis assessed using annexinV- 647 and propidium iodide staining of INS-1 832/3 cells after 6 h (A, B, E, F) and 24 h (C, D, G, H) incubation in presence and absence of 100 nM staurosporine with and without GLP-1 in RPMI 1640 supplemented with 11 mM glucose. Cell death was assessed as percent of staurosporine treatment with different cell densities. (A) 9 x10^5 cells/well; 6 h incubation (B) 1.2 x 10^6 cells/well; 6 h incubation (C) 9 x10^5 cells/well; 24 h incubation (B) 1.2 x 10^6 cells/well; 24 h incubation. Cell survival (E-H) was assessed as percent of 11 mM glucose media. Data is presented as mean + SEM of three replicates.

APPENDIX 2: SUPPLEMENTARY FIGURES OF CHAPTER 4

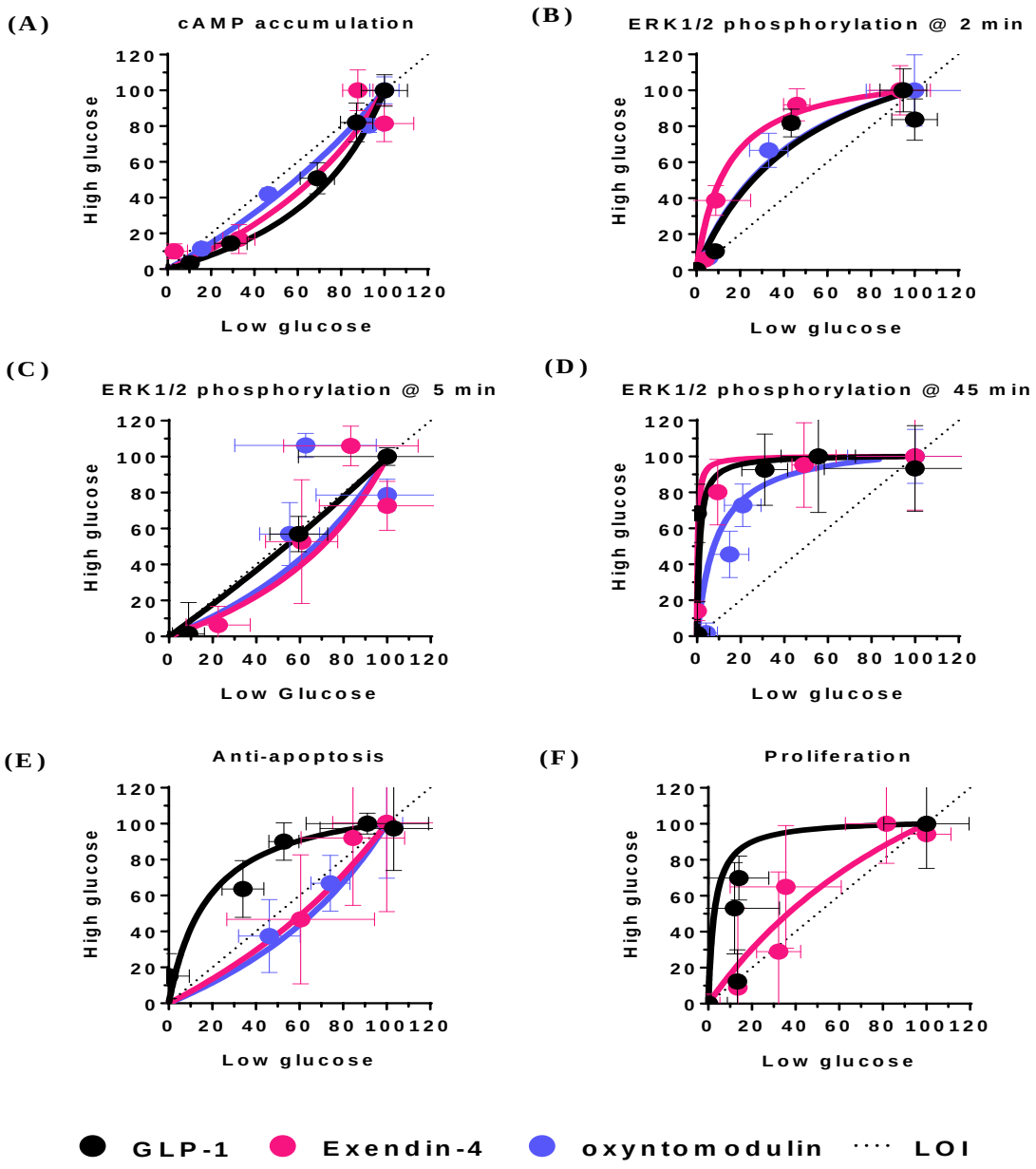

Figure S4.1: Comparison of pathway bias mediated by GLP-1R peptide ligands in low and high glucose. Bias plots of (A) cAMP accumulation, (B) pERK1/2 at 2 min, (C) pERK1/2 at 5 min, (D) pERK1/2 at 45 min, (E) anti-apoptosis and (F) proliferation. Data for each ligand in each pathway was normalised to the maximal peptide response and analysed with three-parameter logistic equation with 150 points defining the curve.

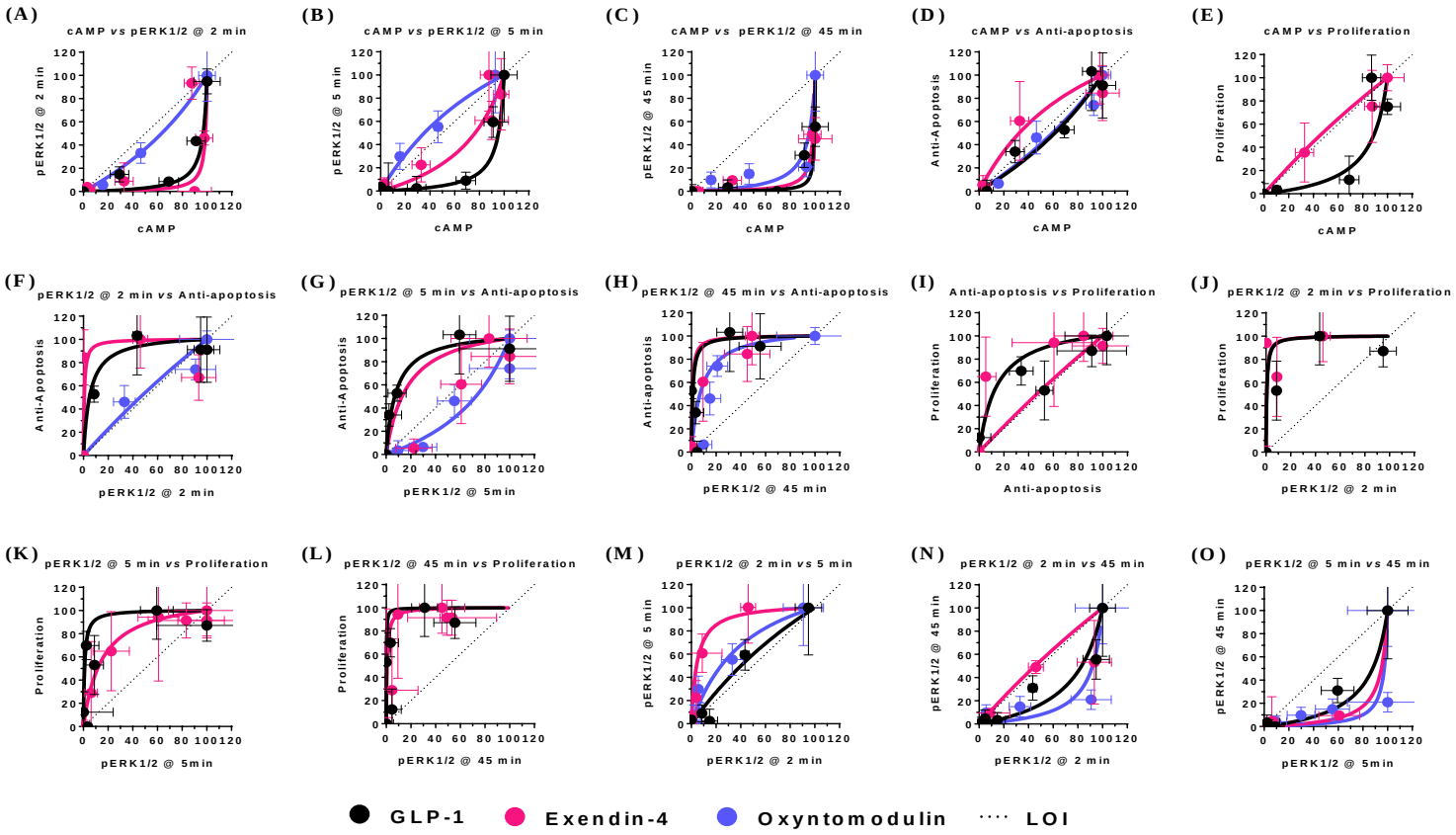

Figure S4.2: Bias plots of GLP-1R peptide ligands in low glucose. Bias plots of (A) cAMP accumulation *vs* pERK1/2 at 2 min, (B) cAMP accumulation *vs* pERK1/2 at 5 min, (C) cAMP accumulation *vs* pERK1/2 at 45 min, (D) cAMP accumulation *vs* anti-apoptosis, (E) cAMP accumulation *vs* proliferation, (F) pERK1/2 at 2 min *vs* anti-apoptosis, (G) pERK1/2 at 5 min *vs* anti-apoptosis, (H) pERK1/2 at 45 min *vs* anti-apoptosis, (I)) anti-apoptosis *vs* proliferation, (J) pERK1/2 at 2 min *vs* proliferation, (K) pERK1/2 at 5 min *vs* proliferation, (L) pERK1/2 at 45 min *vs* proliferation, (M) pERK1/2 at 2 min *vs* pERK1/2 at 5 min, (N) pERK1/2 at 2 min *vs* pERK1/2 at 45 min and (O) pERK1/2 at 5 min *vs* pERK1/2 at 45 min. Data for each ligand in each pathway was normalised to the maximal peptide response and analysed with three-parameter logistic equation with 150 points defining the curve.

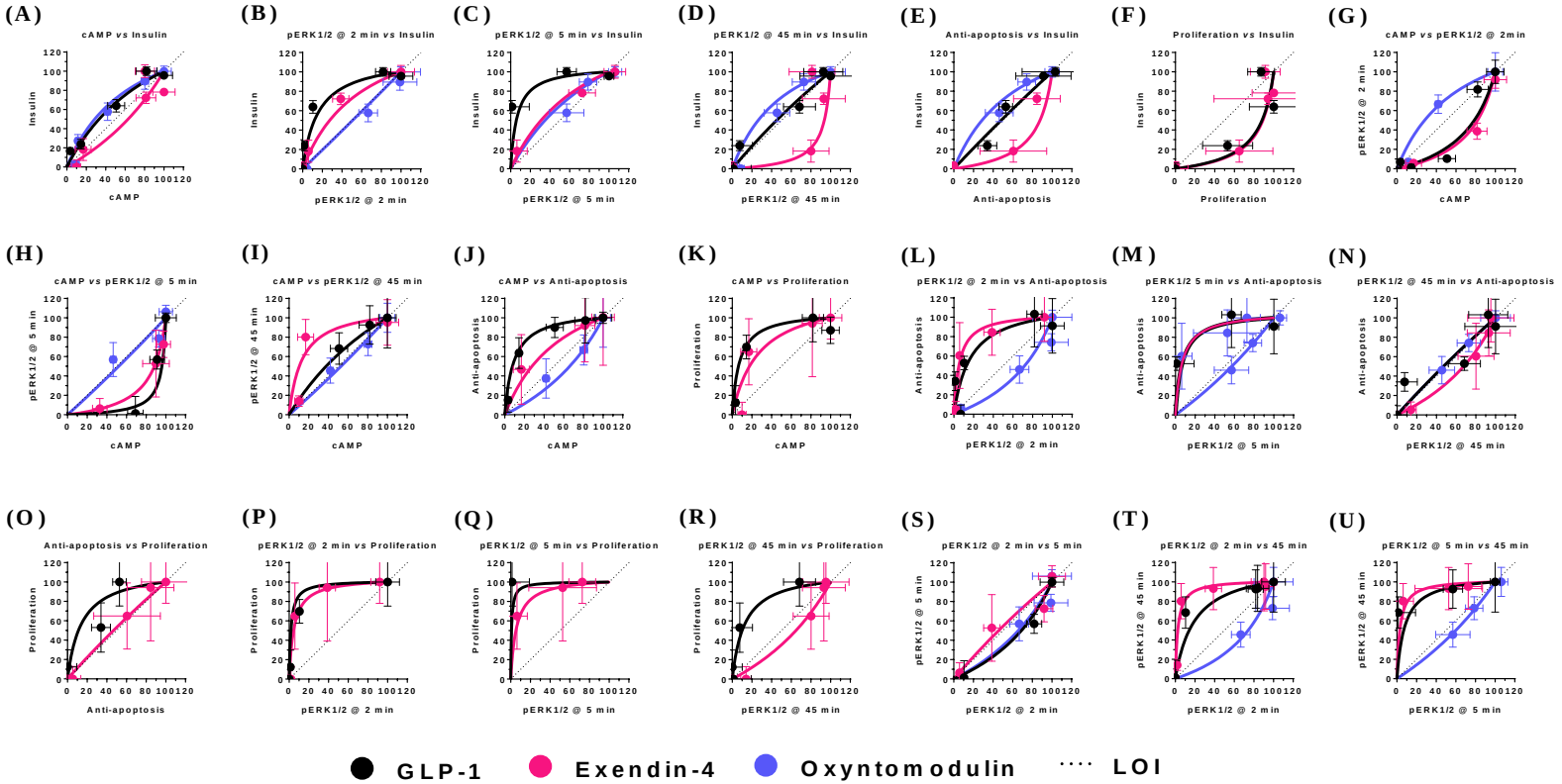

Figure S4.3: Bias plots of GLP-1R peptide ligands in high glucose. Bias plots of (A) cAMP accumulation *vs* insulin, (B) pERK1/2 at 2 min *vs* insulin, (C) pERK1/2 at 5 min *vs* insulin, (D) pERK1/2 at 45 min *vs* insulin, (E) anti-apoptosis *vs* insulin, (F) proliferation *vs* insulin, (G) cAMP accumulation *vs* pERK1/2 at 2 min, (H) cAMP accumulation *vs* pERK1/2 at 5 min, (I) cAMP accumulation *vs* pERK1/2 at 45 min, (J) cAMP accumulation *vs* anti-apoptosis, (K) cAMP accumulation *vs* proliferation, (L) pERK1/2 at 2 min *vs* anti-apoptosis, (M) pERK1/2 at 5 min *vs* anti-apoptosis, (N) pERK1/2 at 45 min *vs* anti-apoptosis, (O)) anti-apoptosis *vs* proliferation, (P) pERK1/2 at 2 min *vs* proliferation, (Q) pERK1/2 at 5 min *vs* proliferation, (R) pERK1/2 at 45 min *vs* proliferation, (S) pERK1/2 at 2 min *vs* pERK1/2 at 5 min, (T) pERK1/2 at 2 min *vs* pERK1/2 at 45 min and (U) pERK1/2 at 5 min *vs* pERK1/2 at 45 min. Data for each ligand in each pathway are normalised to the maximal peptide response and analysed with three-parameter logistic equation with 150 points defining the curve.

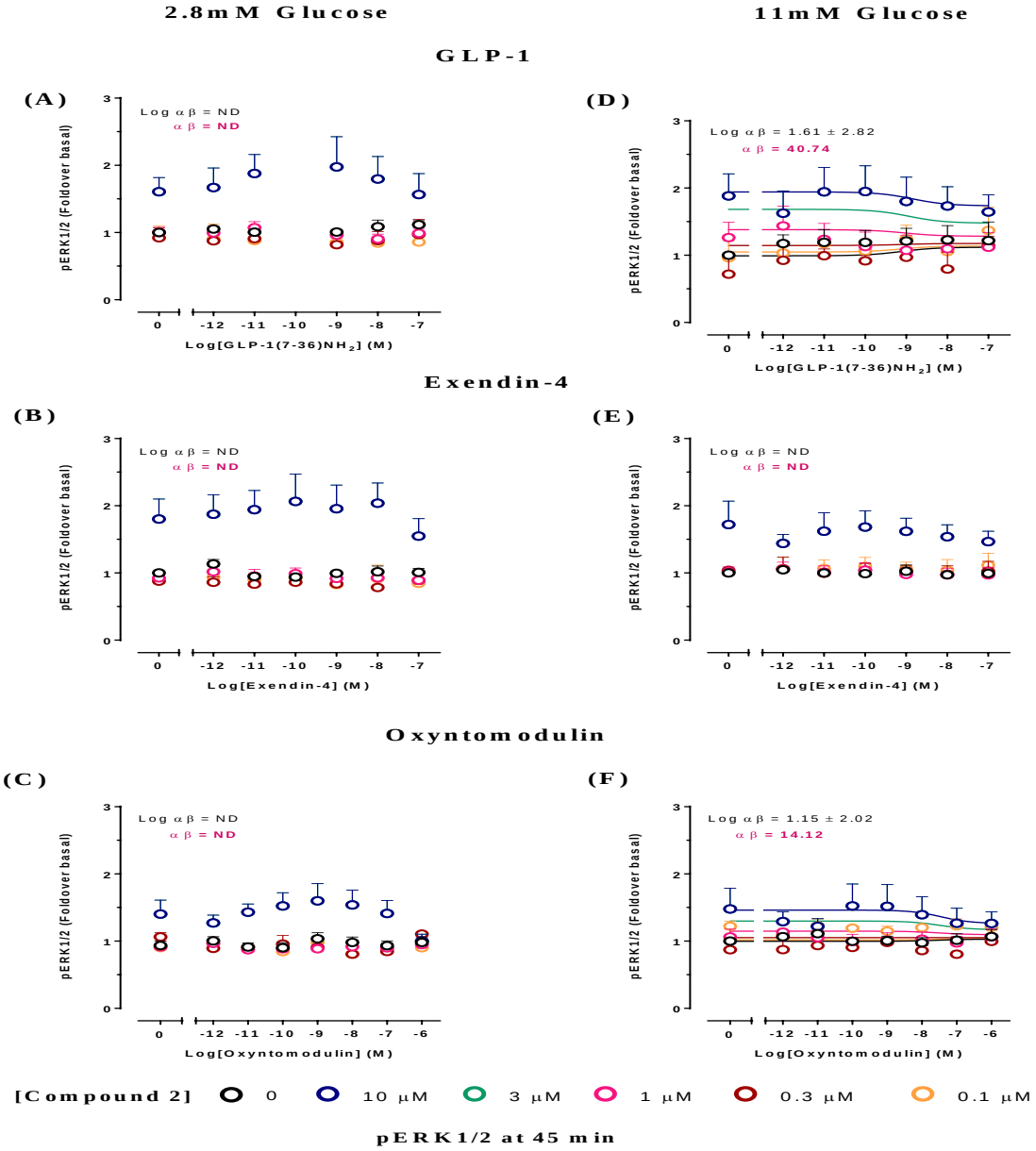

Figure S4.4: Allosteric modulation of GLP-1R peptide responses in pERK1/2 assay performed at the sustained ERK1/2 peak for both peptide and small molecule compound 2. Characterization of the interaction between Compound 2 and GLP-1R peptide ligands under conditions of both low and high glucose in ERK1/2 phosphorylation assay using INS-1 832/3 cells. Concentration response curves were generated for peptide ligand in the absence and presence of increasing concentrations of compound 2 (A) GLP-1, 2.8 mM glucose; (B) Exendin-4, 2.8 mM glucose; (C) Oxyntomodulin, 2.8 mM glucose; (D) GLP-1, 11 mM glucose; (E) Exendin-4, 11 mM glucose; (F) Oxyntomodulin, 11 mM glucose. The compound 2 was co-added with each peptide for 45 min. Data is represented as foldover basal corresponding to respective glucose concentration and analysed using the operational model of allosterism with the curves representing the best global fit. All values are mean + SEM of three to five experiments conducted in triplicate. Calculated log αβ values were analysed with One way ANOVA and Dunnett's post test to determine significant modulation *(*P < 0.05)*.

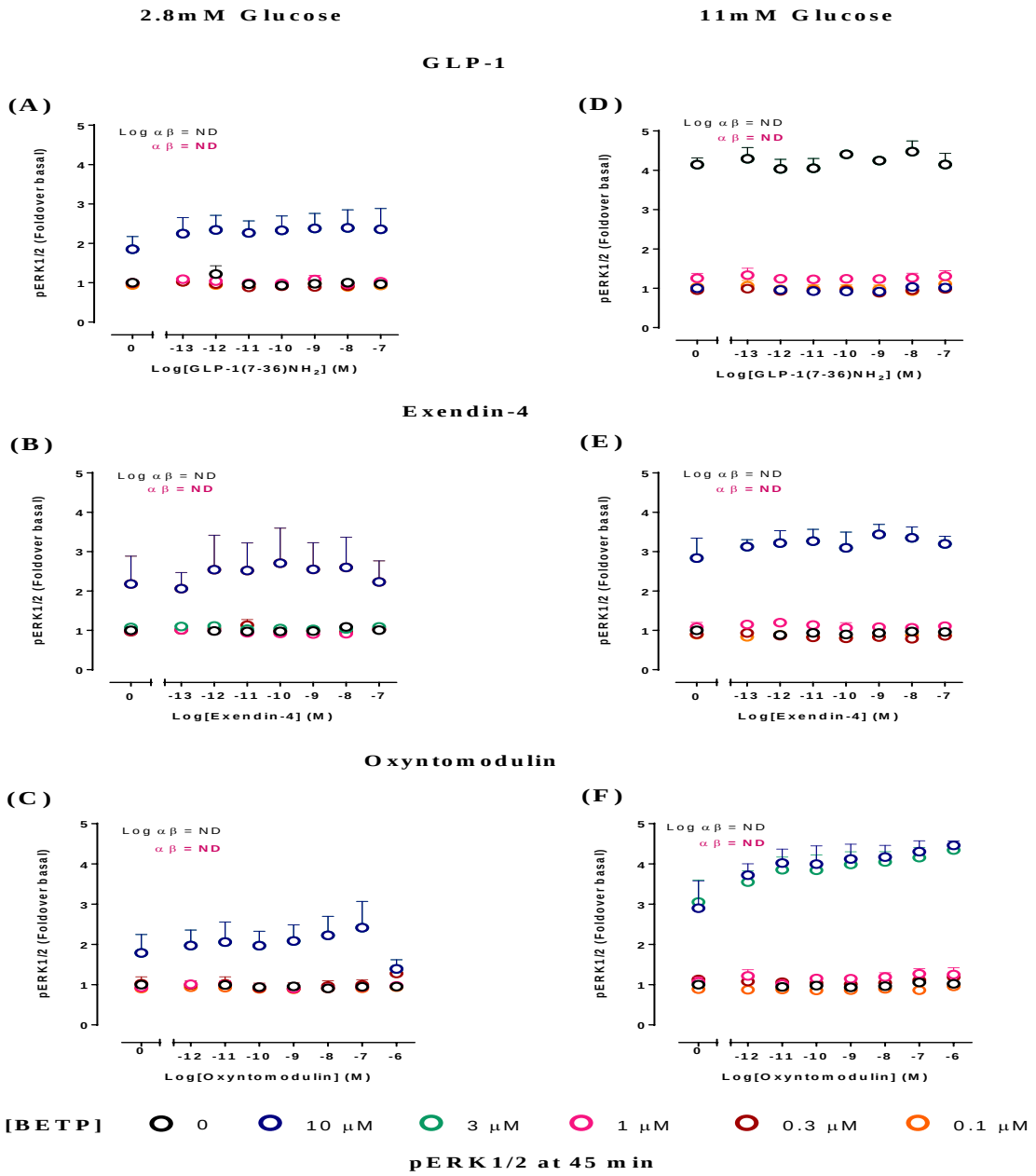

Figure S4.5: Allosteric modulation of GLP-1R peptide responses in pERK1/2 assay performed at the sustained ERK1/2 peak for both peptide and small molecule BETP. Characterization of the interaction between BETP and GLP-1R peptide ligands under conditions of both low and high glucose in ERK1/2 phosphorylation assay using INS-1 832/3 cells. Concentration response curves were generated for peptide ligand in the absence and presence of increasing concentrations of BETP (A) GLP-1, 2.8 mM glucose; (B) Exendin-4, 2.8 mM glucose; (C) Oxyntomodulin, 2.8 mM glucose; (D) GLP-1, 11 mM glucose; (E) Exendin-4, 11 mM glucose; (F) Oxyntomodulin, 11 mM glucose. BETP was co-added with each peptide for 45 min. Data is represented as foldover basal corresponding to respective glucose concentration and analysed using the operational model of allosterism with the curves representing the best global fit. All values are mean + SEM of three to five experiments conducted in triplicate. Calculated log αβ values were analysed with One way ANOVA and Dunnett's post test to determine significant modulation (*$P < 0.05$).

APPENDIX 3: SUPPLEMENTARY FIGURES OF CHAPTER 5

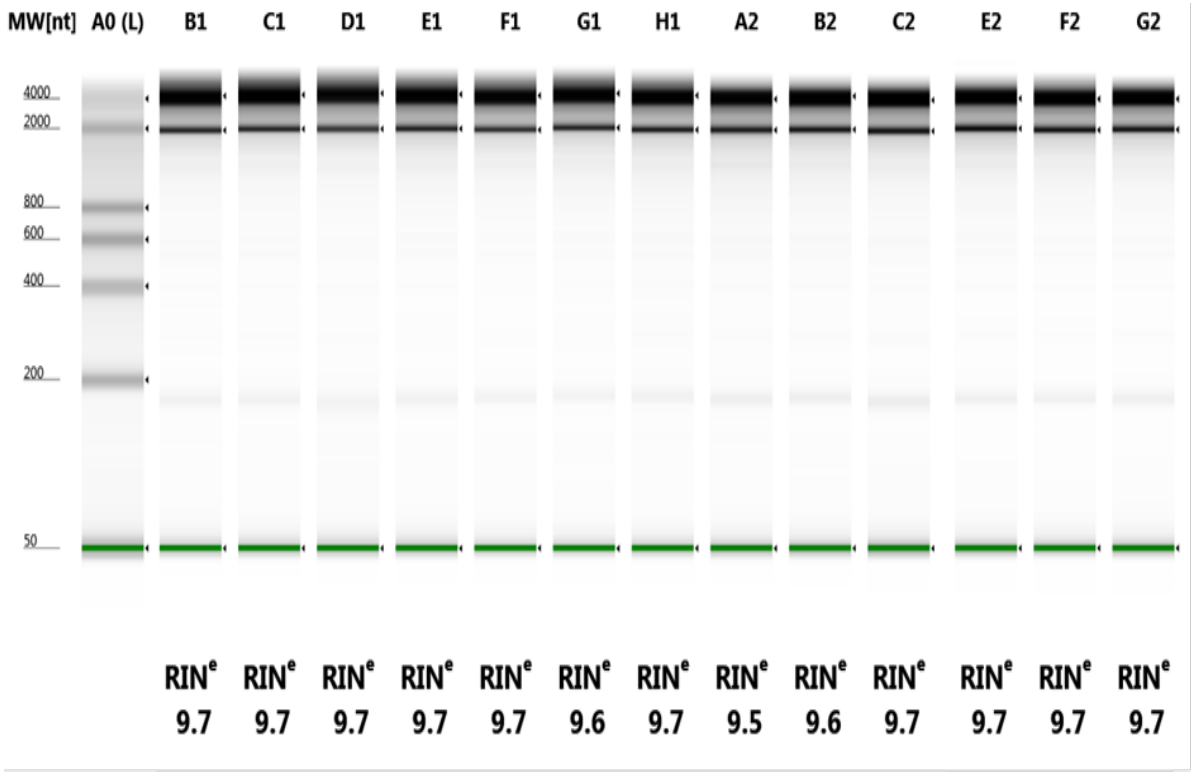

A0 (L)	B1	C1	D1	E1	F1	G1	H1	A2	B2	C2	E2	F2	G2
	U_30	G_30	Ex_30	Ox_30	G_2	G_6	U_24	G_24	Ex_24	Ox_24	U_30	G_30	Ex_30

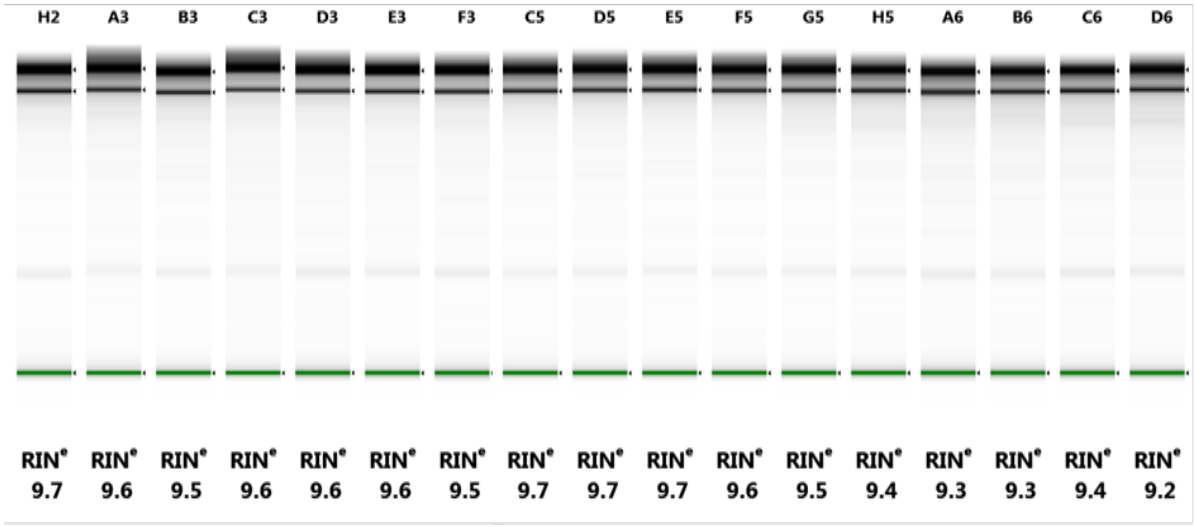

H2	A3	B3	C3	D3	E3	F3	C5	D5	E5	F5	G5	H5	A6	B6	C6	D6
Ox_30	G_2	G_6	U_24	G_24	Ex_24	Ox_24	U_30	G_30	Ex_30	Ox_30	G_2	G_6	U_24	G_24	Ex_24	Ox_24

Figure S5.1: Gel Images and RNA integrity number (RIN) of RNA samples (n=3) prepared for RNA sequencing assessing RNA quality performed using R6K ScreenTape® and 2200 tapeStation Software (A.01.01).

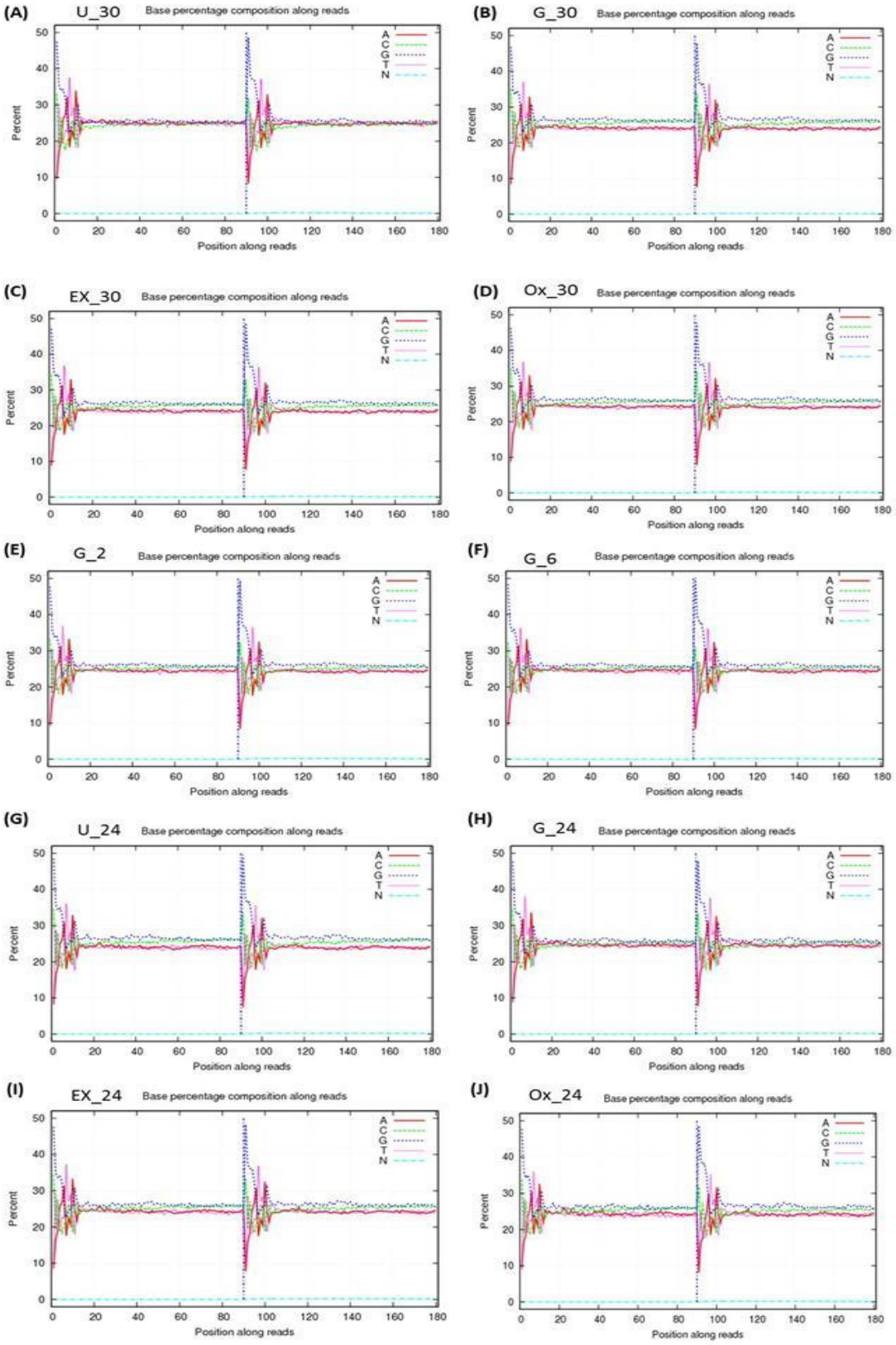

Figure S5.2: Distribution of base sequence content as measure of pre-alignment quality. Even distribution of base sequence content/composition for each sample in the study. On the X axis, position 1 90bp represents read 1, and 91-180bp represents read 2. A curve overlaps with T curve and G curve overlaps with C curve representing balanced composition.

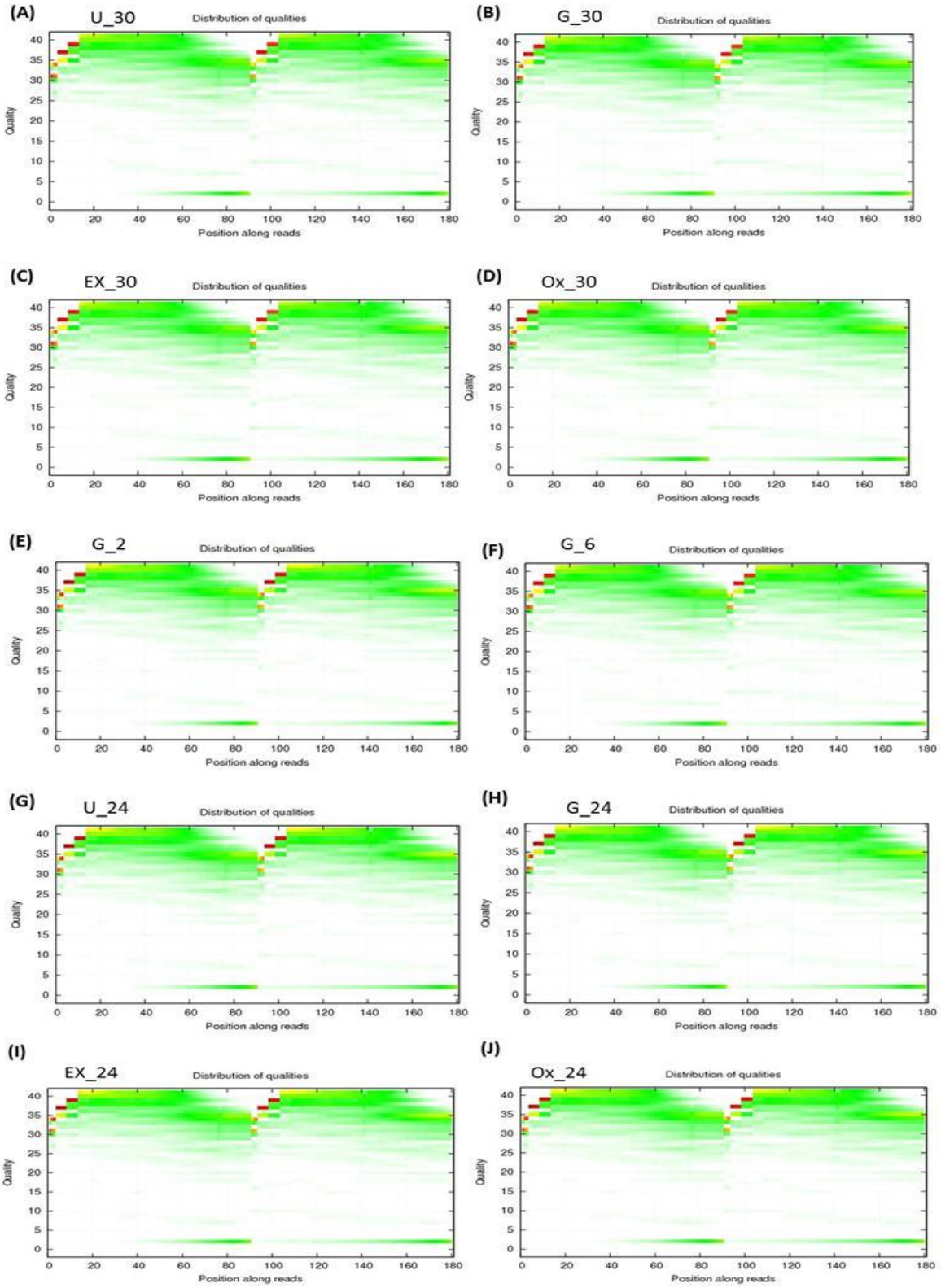

Figure S5.3: Quality distribution of bases as a measure of pre-alignment quality. Quality distribution of bases along reads for each sample in the study. Horizontal axis is the positions along reads. Vertical axis is the quality value. Each dot in the image represents the quality value of the corresponding position along reads. The percentage of the bases with low quality (< 20) is low, thus representing the good quality of sequencing.

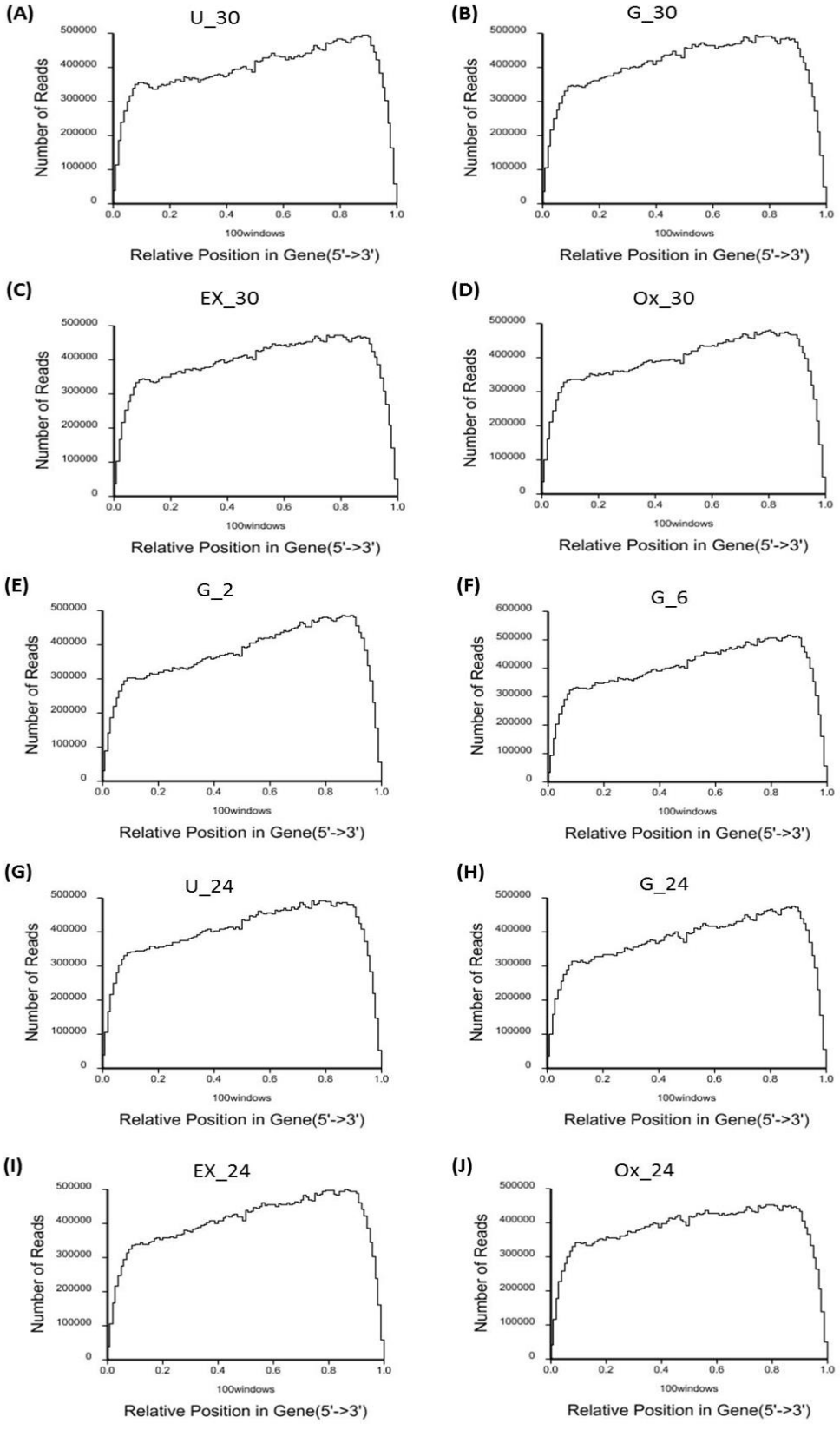

Figure S5.4: Measure of post-alignment quality on reference gene. Distributions of reads on reference genes for each sample in the study. X-axis is relative position in genes, Y-axis is number of reads. Reads are evenly distributed on the reference genes depicting a good randomness.

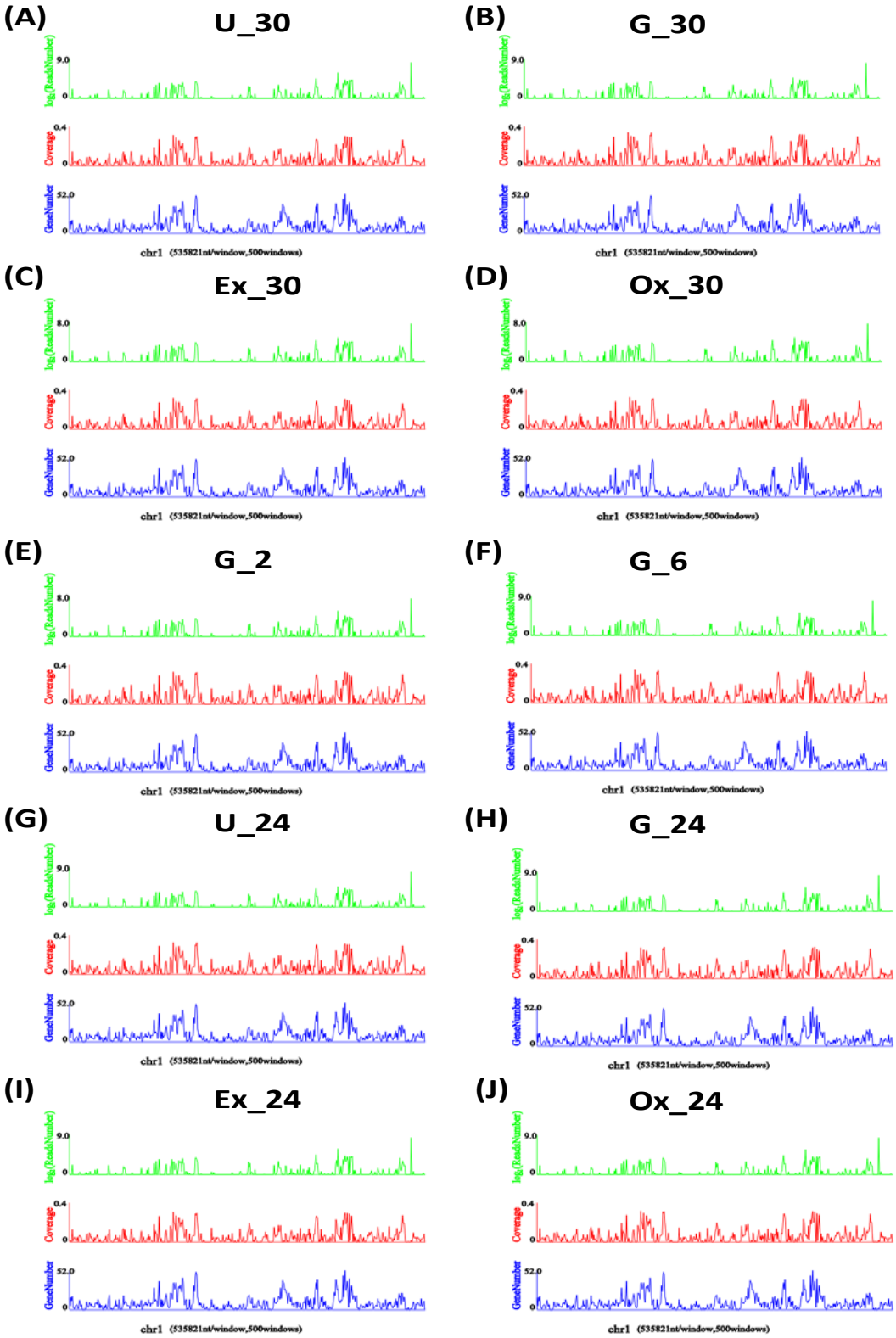

Figure S5.5: Measure of post-alignment quality on reference genome. Distributions of reads on reference genome (chromosome 1). Gene means the number of gene in each window; Coverage means the ratio of the area covered by reads to the length of each windows; Reads mean the average sequence depth in each windows (value = $\log_2$).

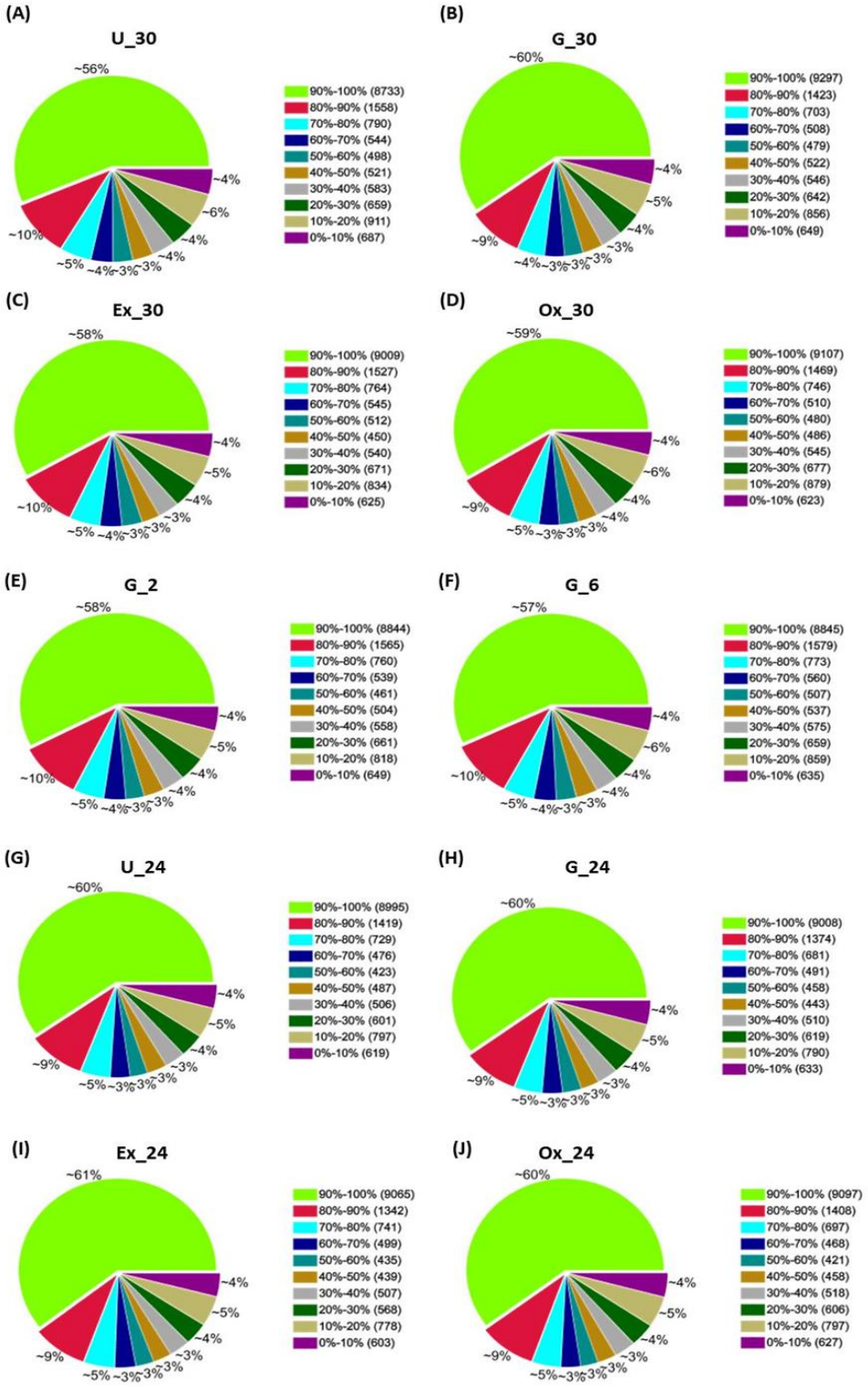

Figure S5.6: Distribution of gene coverage. Pie charts representing gene coverage distribution of each sample used in the study. Pies with different colours represent proportions of genes with certain coverage.

APPENDIX 4: SUPPLEMENTARY TABLES OF CHAPTER 5

Table S5.1: RNA quality analysis. Quality analysis of individual RNA samples assessed using 2200 tapeStation Software (A.01.01) prior to pooling for RNA sequencing.

Sample Name	Replicates	RIN	28S/18S (height)	Concentration (ng/µL)	OD 260/230	OD 260/280
Untreated 30 min (U_30)	A	9.69	1.83	168	2.25	2.07
	B	9.68	1.45	121	2.15	2.10
	C	9.67	1.51	168	2.26	2.08
GLP-1 30 min (G_30)	A	9.70	1.87	190	2.00	2.10
	B	9.69	1.57	139	2.23	2.08
	C	9.66	1.64	185	2.19	2.10
Exendin 30 min (Ex_30)	A	9.72	1.86	126	2.16	2.05
	B	9.69	1.76	118	2.14	2.05
	C	9.68	1.52	189	2.24	2.09
Oxyntomodulin 30 min (Ox_30)	A	9.66	1.76	140	2.16	2.07
	B	9.66	1.75	135	2.19	2.09
	C	9.65	1.67	174	2.26	2.08
GLP-1 2 h (G_2)	A	9.68	1.76	165	2.14	2.06
	B	9.56	1.82	270	2.23	2.07
	C	9.52	1.52	164	2.26	2.08
GLP-1 6 h (G_6)	A	9.62	1.72	205	2.27	2.09
	B	9.54	1.57	143	2.09	2.10
	C	9.43	1.48	130	2.24	2.09
Untreated 24 h (U_24)	A	9.67	1.68	186	2.21	2.09
	B	9.56	2.06	269	2.20	2.08
	C	9.27	1.72	99.7	2.24	2.08
GLP-1 24 h (G_24)	A	9.53	1.54	124	2.18	2.05
	B	9.58	2.24	142	2.24	2.07
	C	9.31	1.49	103	2.11	2.10
Exendin 24 h (Ex_24)	A	9.57	1.52	122	2.19	2.08
	B	9.61	1.91	160	2.21	2.07
	C	9.42	1.39	98.8	2.26	2.09
Oxyntomodulin 24 h (Ox_24)	A	9.69	1.67	94.7	2.17	2.07
	B	9.53	2.01	119	2.16	2.10
	C	9.24	1.48	114	2.25	2.09

Table S5.2: Post-alignment quality assessment (genes within the reference genome) of kinetic treatment with GLP-1. Depiction of alignment statistics (basic read metrics) for 11 mM glucose (30 min and 24 h treatment) and 100 nM GLP-1 treated (30 min, 2 h, 6 h and 24 h) samples in the study depicting alignment statistics. The alignment of reads to the reference gene sequence was performed using alignment tool SOAPaligner/SOAP2.

Column description		U_30		U_24		G_30		G_2		G_6		G_24	
		No.	%age	No.	%age	No.	%age	No.	%age	No.	%age	No.	%age
Total reads		54754112	100	54354240	100	55065942	100	51295996	100	55143072	100	51320690	100
Total base pairs		4927870080	100	4891881600	100	4955934780	100	4616639640	100	4962876480	100	4618862100	100
Total mapped reads		38636769	70.56	39387559	72.46	39979323	72.60	36663719	71.47	39396461	71.44	36768686	71.64
	Perfect match	26330829	48.09	28783718	52.96	28337433	51.46	26249308	51.17	27362658	49.62	25907454	50.48
	≤ 5bp mismatch	12305940	22.47	10603841	19.51	11641890	21.14	10414411	20.30	12033803	21.82	10861232	21.16
	Unique match	36694326	67.02	37607088	69.19	37954035	68.92	34799326	67.84	37408918	67.84	35178334	68.55
	Multiposition match	1942443	3.55	1780471	3.28	2025288	3.68	1864393	3.63	1987543	3.60	1590352	3.10
Total unmapped reads		16117343	29.44	14966681	27.54	15086619	27.40	14632277	28.53	15746611	28.56	14552004	28.36

Table S5.3: Post-alignment quality assessment (genes within the reference genome) of exendin-4 and oxyntomodulin treated samples. Depiction of alignment statistics (basic read metrics) for 100 nM exendin-4 (30 min and 24 h treatment) and 1µM oxyntomodulin treated (30 min and 24 h) samples in the study depicting alignment statistics. The alignment of reads to the reference gene sequence was performed using alignment tool SOAPaligner/SOAP2.

Column description		Ex_30		Ex_24		Ox_30		Ox_24	
		No.	%age	No.	%age	No.	%age	No.	%age
Total reads		52669224	100	54616366	100	52816908	100	52096548	100
Total base pairs		4740230160	100	4915472940	100	4753521720	100	4688689320	100
Total mapped reads		38428194	72.96	39619580	72.54	38040106	72.02	37633501	72.24
	Perfect match	26843277	50.97	29020563	53.14	26948864	51.02	26891542	51.62
	≤ 5bp mismatch	11584917	22.00	10599017	19.41	11091242	21.00	10741959	20.62
	Unique match	36481300	69.26	37834649	69.27	35995519	68.15	36013563	69.13
	Multiposition match	1946894	3.70	1784931	3.27	2044587	3.87	1619938	3.11
Total unmapped reads		14241030	27.04	14996786	27.46	14776802	27.98	14463047	27.76

Table S5.4: Post-alignment quality assessment (reference genome) of kinetic treatment with GLP-1. Depiction of alignment statistics (basic read metrics) for 11 mM glucose (30 min and 24 h treatment) and 100 nM GLP-1 treated (30 min, 2 h, 6 h and 24 h) samples in the study depicting alignment statistics. The alignment of reads to the reference genome sequence was performed using alignment tool SOAPaligner/SOAP2.

Column description		U_30		U_24		G_30		G_2		G_6		G_24	
		No.	%age	No.	%age	No.	%age	No.	%age	No.	%age	No.	%age
Total reads		54754112	100.00	54354240	100.00	55065942	100.00	51295996	100.00	55143072	100.00	51320690	100.00
Total base pairs		4927870080	100.00	4891881600	100.00	4955934780	100.00	4616639640	100.00	4962876480	100.00	4618862100	100.00
Total mapped reads		44060973	80.47	43008103	79.13	43432541	78.87	41224993	80.37	44393738	80.51	41223338	80.32
	Perfect match	27866524	50.89	29135936	53.60	28302947	51.40	27355882	53.33	28582755	51.83	27149581	52.90
	≤ 5bp mismatch	16194449	29.58	13872167	25.52	15129594	27.48	13869111	27.04	15810983	28.67	14073757	27.42
	Unique match	41141628	75.14	40477414	74.47	40510314	73.57	38495044	75.04	41458986	75.18	38834021	75.67
	Multiposition match	2919345	5.33	2530689	4.66	2922227	5.31	2729949	5.32	2934752	5.32	2389317	4.66
Total unmapped reads		10693139	19.53	11346137	20.87	11633401	21.13	10071003	19.63	10749334	19.49	10097352	19.68

Table S5.5: Post-alignment quality assessment (reference genome) of exendin-4 and oxyntomodulin treated samples. Depiction of alignment statistics (basic read metrics) for 100 nM exendin-4 (30 min and 24 h treatment) and 1µM oxyntomodulin treated (30 min and 24 h) samples in the study depicting alignment statistics. The alignment of reads to the reference genome sequence was performed using alignment tool SOAPaligner/SOAP2.

Column description		Ex_30		Ex_24		Ox_30		Ox_24	
		No.	%age	No.	%age	No.	%age	No.	%age
Total reads		52669224	100.00	54616366	100.00	52816908	100.00	52096548	100.00
Total base pairs		4740230160	100.00	4915472940	100.00	4753521720	100.00	4688689320	100.00
Total mapped reads		41710434	79.19	43509904	79.66	42016670	79.55	41148153	78.98
	Perfect match	26808997	50.90	29597371	54.19	27396346	51.87	27398473	52.59
	≤ 5bp mismatch	14901437	28.29	13912533	25.47	14620324	27.68	13749680	26.39
	Unique match	38855944	73.77	40879399	74.85	39070118	73.97	38822654	74.52
	Multiposition match	2854490	5.42	2630505	4.82	2946552	5.58	2325499	4.46
Total unmapped reads		10958790	20.81	11106462	20.34	10800238	20.45	10948395	21.02

Table S5.6: Gene regulation after 30 min exposure to GLP-1 and exendin-4. List of significantly regulated genes, both differentially and commonly, by acute exposure (30 min) of INS-1 832/3 cells to 100 nM GLP-1 and 100 nM exendin-4.

Genes regulated by GLP-1 at 30 min		Genes regulated by exendin-4 at 30 min		Commonly regulated genes by both peptides at 30 min	
Symbol	**Entrez Gene Name**	**Symbol**	**Entrez Gene Name**	**Symbol**	**Entrez Gene Name**
ANKRD35	ankyrin repeat domain 35	ANO9	anoctamin 9	Abcb1b	ATP-binding cassette, sub-family B (MDR/TAP), member 1B
ASTN2	astrotactin 2	CPNE4	copine IV	Akr1c14	aldo-keto reductase family 1, member C14
EGR4	early growth response 4	CYP1A1	cytochrome P450, family 1, subfamily A, polypeptide 1	ADCY1	adenylate cyclase 1 (brain)
EMP3	epithelial membrane protein 3	GATM	glycine amidinotransferase (L-arginine:glycine amidinotransferase)	ADHFE1	alcohol dehydrogenase, iron containing, 1
Hmgn5/Hmgn5b	high mobility group nucleosome binding domain 5B	HTR1D	5-hydroxytryptamine (serotonin) receptor 1D, G protein-coupled	AFAP1	actin filament associated protein 1
LOC100359664	mitochondrial transcription termination factor-like	IL15	interleukin 15	AKR1C1/AKR1C2	aldo-keto reductase family 1, member C2
NXF3	nuclear RNA export factor 3	ITGA10	integrin, alpha 10	ALB	albumin
Trpm8	transient Receptor Potential Cation Channel,	IZUMO1	izumo sperm-egg fusion 1	ANGPTL6	angiopoietin-like 6

	Subfamily M, Member 8				
Ppp1r3e	Protein Phosphatase 1, Regulatory Subunit 3E	LAMA2	laminin, alpha 2	ANKRD63	ankyrin repeat domain 63
Tmem176b	TMEM176B transmembrane protein 176B	LOC100361060	ribosomal protein L36-like	ANTXR1	anthrax toxin receptor 1
Pigx	Phosphatidylinositol Glycan Anchor Biosynthesis, Class X	NXF2/NXF2B	nuclear RNA export factor 2		
		RAMP3	receptor (G protein-coupled) activity modifying protein 3	APOE	apolipoprotein E
		RPL7A	ribosomal protein L7a	ARHGEF26	Rho guanine nucleotide exchange factor (GEF) 26
		RYR3	ryanodine receptor 3		
		SGK2	serum/glucocorticoid regulated kinase 2	ATP6V1G2	ATPase, H+ transporting, lysosomal 13kDa, V1 subunit G2
		SLAMF1	signaling lymphocytic activation molecule family member 1	ATP11C	ATPase, class VI, type 11C
		SLC12A1	solute carrier family 12 (sodium/potassium/chloride	ATXN7L3B	ataxin 7-like 3B

			transporter), member 1		
		STEAP1	six transmembrane epithelial antigen of the prostate 1	BEX4	brain expressed, X-linked 4
		STK32B	serine/threonine kinase 32B	C3orf80	chromosome 3 open reading frame 80
		TIRAP	toll-interleukin 1 receptor (TIR) domain containing adaptor protein	C10orf90	chromosome 10 open reading frame 90
		Hnrnpa1	Heterogeneous Nuclear Ribonucleoprotein A1	C1orf233	chromosome 1 open reading frame 233
		Vom2r52	vomeronasal 2 receptor, 52	C1orf106	chromosome 1 open reading frame 106
		Capn6	Calpain 6	C2CD4A	C2 calcium-dependent domain containing 4A
		Ccr7	C-C chemokine receptor type 7	C8orf59	chromosome 8 open reading frame 59
		Hfm1	ATP-Dependent DNA Helicase Homolog	CALR3	calreticulin 3
		Mep1a	Meprin A, Alpha	CCDC155	coiled-coil domain containing 155
				CD59	CD59 molecule, complement regulatory protein
				CDH3	cadherin 3, type 1, P-cadherin (placental)
				CCKAR	cholecystokinin A receptor

				CD6	CD6 molecule
				CD247	CD247 molecule
				CD164L2	CD164 sialomucin-like 2
				CDO1	cysteine dioxygenase type 1
				Cenpp	centromere protein P
				CHRNA2	cholinergic receptor, nicotinic, alpha 2 (neuronal)
				COL18A1	collagen, type XVIII, alpha 1
				Cox7a2/Cox7a2l2	cytochrome c oxidase subunit VIIa polypeptide 2-like 2
				CPE	carboxypeptidase E
				CRB2	crumbs family member 2
				CREBL2	cAMP responsive element binding protein-like 2
				CREG2	cellular repressor of E1A-stimulated genes 2
				CRIM1	cysteine rich transmembrane BMP regulator 1 (chordin-like)
				D2HGDH	D-2-hydroxyglutarate dehydrogenase
				DCLRE1C	DNA cross-link repair 1C
				DIRAS2	DIRAS family, GTP-binding RAS-like 2
				DNAJB13	DnaJ (Hsp40) homolog, subfamily B, member 13
				DNM3	dynamin 3
				DOC2A	double C2-like domains, alpha
				DTX4	deltex 4, E3 ubiquitin ligase
				EFNA4	ephrin-A4

				EGR1	early growth response 1
				EHHADH	enoyl-CoA, hydratase/3-hydroxyacyl CoA dehydrogenase
				EIF4E1B	eukaryotic translation initiation factor 4E family member 1B
				ERBB3	erb-b2 receptor tyrosine kinase 3
				ERICH2	glutamate-rich 2
				EVA1B	eva-1 homolog B (C. elegans)
				EXTL1	exostosin-like glycosyltransferase 1
				FAM107A	family with sequence similarity 107, member A
				Fam24a	family with sequence similarity 24, member A
				FAM43B	family with sequence similarity 43, member B
				FAM103A1	family with sequence similarity 103, member A1
				FAM109B	family with sequence similarity 109, member B
				FAM65C	family with sequence similarity 65, member C
				FBXO31	F-box protein 31
				FBXL2	F-box and leucine-rich repeat protein 2
				FJX1	four jointed box 1 (Drosophila)
				FLNC	filamin C, gamma
				FOS	FBJ murine osteosarcoma viral oncogene homolog
				GABARAPL2	GABA(A) receptor-associated protein-like 2
				GALM	galactose mutarotase (aldose 1-epimerase)

				GAS8	growth arrest-specific 8
				GBP6	guanylate binding protein family, member 6
				Gimap9	GTPase, IMAP family member 9
				Gm10051	predicted pseudogene 10051
				Gnmt/LOC100911564	glycine N-methyltransferase
				GPR27	G protein-coupled receptor 27
				Gsta4	glutathione S-transferase, alpha 4
				HHAT	hedgehog acyltransferase
				Hist1h1a	histone cluster 1, H1a
				HIST1H2BI	histone cluster 1, H2bi
				HNRNPA0	heterogeneous nuclear ribonucleoprotein A0
				HS1BP3	HCLS1 binding protein 3
				IFNLR1	interferon, lambda receptor 1
				IGDCC3	immunoglobulin superfamily, DCC subclass, member 3
				ITGA2	integrin, alpha 2 (CD49B, alpha 2 subunit of VLA-2 receptor)
				ITGA2B	integrin, alpha 2b (platelet glycoprotein IIb of IIb/IIIa complex, antigen CD41)
				ITGB3BP	integrin beta 3 binding protein (beta3-endonexin)
				KANSL1L	KAT8 regulatory NSL complex subunit 1-like
				KCNJ12	potassium channel, inwardly rectifying subfamily J,

					member 12
				KCNQ1	potassium channel, voltage gated KQT-like subfamily Q, member 1
				KCNG4	potassium channel, voltage gated modifier subfamily G, member 4
				KIAA1161	KIAA1161
				KIAA1671	KIAA1671
				KIAA1045	KIAA1045
				KITLG	KIT ligand
				KLHL18	kelch-like family member 18
				Kng1/Kng1l1	kininogen 1
				KNDC1	kinase non-catalytic C-lobe domain (KIND) containing 1
				LIN9	lin-9 DREAM MuvB core complex component
				LOC685171	similar to protein disulfide isomerase-associated 6
				LOC6887 54	similar to Voltage-dependent anion-selective channel protein 1 (VDAC-1) (mVDAC1) (mVDAC5) (Outer mitochondrial membrane protein porin 1) (Plasmalemmal porin)
				Lag3	Lymphocyte-activation protein 3
				LOC100911966	60S ribosomal protein L7a-like

				LOC102548396 (includes others)	zinc finger protein 951
				LRRC34	leucine rich repeat containing 34
				MAST4	microtubule associated serine/threonine kinase family member 4
				MID1	midline 1
				MSMP	microseminoprotein, prostate associated
				MSS51	MSS51 mitochondrial translational activator
				MT-ND6	NADH dehydrogenase, subunit 6 (complex I)
				MTHFR	methylenetetrahydrofolate reductase (NAD(P)H)
				NFKBID	nuclear factor of kappa light polypeptide gene enhancer in B-cells inhibitor, delta
				NHSL1	NHS-like 1
				Nos1ap	nitric oxide synthase 1 (neuronal) adaptor protein
				NR4A1	nuclear receptor subfamily 4, group A, member 1
				PACSIN1	protein kinase C and casein kinase substrate in neurons 1
				PHACTR3	phosphatase and actin regulator 3
				LHX3	LIM homeobox 3
				LMX1B	LIM homeobox transcription factor 1, beta
				LOC257650	hippyragranin
				LOC498826	LRRGT00165

				LRRC19	leucine rich repeat containing 19
				LRRC14B	leucine rich repeat containing 14B
				MAFA	v-maf avian musculoaponeurotic fibrosarcoma oncogene homolog A
				MITF	microphthalmia-associated transcription factor
				MRGPRX1	MAS-related GPR, member X1
				NDUFC2	NADH dehydrogenase (ubiquinone) 1, subcomplex unknown, 2, 14.5kDa
				NEURL1B	neuralized E3 ubiquitin protein ligase 1B
				NTNG2	netrin G2
				P2RX2	purinergic receptor P2X, ligand gated ion channel, 2
				PAQR5	progestin and adipoQ receptor family member V
				PLXNA2	plexin A2
				PNPLA4	patatin-like phospholipase domain containing 4
				PRRT4	proline-rich transmembrane protein 4
				PSMA8	proteasome (prosome, macropain) subunit, alpha type, 8
				PURG	purine-rich element binding protein G
				RGD1563613	similar to 40S ribosomal protein S25
				RLBP1	retinaldehyde binding protein 1
				Rpl22l1	ribosomal protein L22 like 1
				SEC14L5	SEC14-like 5 (S. cerevisiae)
				SLC16A12	solute carrier family 16, member 12

				SPSB1	splA/ryanodine receptor domain and SOCS box containing 1
				TMEM81	transmembrane protein 81
				TMEM121	transmembrane protein 121
				TMPRSS4	transmembrane protease, serine 4
				TREM3	triggering receptor expressed on myeloid cells 3
				Vom2r52	vomeronasal 2 receptor, 52
				ZNF385B	zinc finger protein 385B

Table S5.7: Gene regulation after 24 h exposure to GLP-1 and exendin-4. List of genes significantly regulated genes both differentially and commonly by long term exposure (24 h) of INS-1 832/3 cells to 100 nM GLP-1 and 100 nM exendin-4.

Genes regulated by GLP-1 at 24 h		Genes regulated by exendin-4 at 24 h		Commonly regulated genes by both peptides at 24 h	
Symbol	**Entrez Gene Name**	**Symbol**	**Entrez Gene Name**	**Symbol**	**Entrez Gene Name**
AR	androgen receptor	ALDH2	aldehyde dehydrogenase 2 family (mitochondrial)	ADM	adrenomedullin
CAPN6	calpain 6	BARHL2	BarH-like homeobox 2	ANXA8/ ANXA8L1	annexin A8-like 1
CCR7	chemokine (C-C motif) receptor 7	CRB1	crumbs family member 1, photoreceptor morphogenesis associated	Cetn4	centrin 4
CYP17A1	cytochrome P450, family 17, subfamily A, polypeptide 1	GRID2	glutamate receptor, ionotropic, delta 2	FOS	FBJ murine osteosarcoma viral oncogene homolog
EPHA5	EPH receptor A5	Hmgb1	high mobility group box 1	MAST4	microtubule associated serine/threonine kinase family member 4
HFM1	HFM1, ATP-dependent DNA helicase homolog (S. cerevisiae)	IGFBP1	insulin-like growth factor binding protein 1	MT-ND3	NADH dehydrogenase, subunit 3 (complex I)
ITGA10	integrin, alpha 10	IL7	interleukin 7	RPL9	ribosomal protein L9
KCNE2	potassium channel, voltage gated subfamily E regulatory beta subunit 2	NOTCH2	notch 2	RPL41	ribosomal protein L41

KIF26A	kinesin family member 26A	OLFML2A	olfactomedin-like 2A	RPS20	ribosomal protein S20
KIFC2	kinesin family member C2	SFRP4	secreted frizzled-related protein 4	Tmem255b	transmembrane protein 255B
Krt10	keratin 10, type I	TLR5	toll-like receptor 5	ADAMTS16	ADAM metallopeptidase with thrombospondin type 1 motif, 16
LSAMP	limbic system-associated membrane protein	CCKAR	Cholecystokinin A Receptor	AOX1	aldehyde oxidase 1
MUC6	mucin 6, oligomeric mucus/gel-forming	CD6	lymphocyte glycoprotein **CD6**	ACTN2	actinin, alpha 2
NEXN	nexilin (F actin binding protein)	CYP1A1	Cytochrome P450, family 1, subfamily A, polypeptide 1	Atp5hl1	ATP synthase, H+ transporting, mitochondrial Fo complex, subunit d-like 1
NPFFR2	neuropeptide FF receptor 2			C15orf27	chromosome 15 open reading frame 27
PLEKHO2	pleckstrin homology domain containing, family O member 2			C5orf28	chromosome 5 open reading frame 28
PROK2	prokineticin 2			CA10	carbonic anhydrase X
S1PR2	sphingosine-1-phosphate receptor 2			BEX4	brain expressed, X-linked 4
SIDT1	SID1 transmembrane family, member 1			C10orf12	chromosome 10 open reading frame 12
SLC26A1	solute carrier family 26 (anion exchanger), member 1			C11orf96	chromosome 11 open reading frame 96

SPAG8	sperm associated antigen 8			CBLN2	cerebellin 2 precursor
SPATC1	spermatogenesis and centriole associated 1			CEP63	centrosomal protein 63kDa
Taar4	trace amine-associated receptor 4			CLCA2	chloride channel accessory 2
TNFRSF25	tumor necrosis factor receptor superfamily, member 25			CNGB3	cyclic nucleotide gated channel beta 3
Tmprssf	Transmembrane protease, serine 2			CASP4	caspase 4, apoptosis-related cysteine peptidase
GPR165	G protein-coupled receptor 165			CCDC94	coiled-coil domain containing 94
Hnrnpa3	Heterogeneous Nuclear Ribonucleoprotein A3			CD59	CD59 molecule, complement regulatory protein
Zfp862	zinc finger protein 862			CHAC1	ChaC glutathione-specific gamma-glutamylcyclotransferase 1
Nxf2	Nuclear RNA Export Factor 2			DEGS2	delta(4)-desaturase, sphingolipid 2
Vom2r52	vomeronasal 2 receptor, 52			DENND2C	DENN/MADD domain containing 2C
				Dmd	dystrophin
				EVA1A	eva-1 homolog A (C. elegans)
				FBXO47	F-box protein 47

				FUT1	fucosyltransferase 1 (galactoside 2-alpha-L-fucosyltransferase, H blood group)
				Gm884	predicted gene 884
				FAM161A	family with sequence similarity 161, member A
				FAM196B	family with sequence similarity 196, member B
				FTL	ferritin, light polypeptide
				GEN1	GEN1 Holliday junction 5' flap endonuclease
				IGSF10	immunoglobulin superfamily, member 10
				HNRNPA1	heterogeneous nuclear ribonucleoprotein A1
				HPX	hemopexin
				HSPA8	heat shock 70kDa protein 8
				IL20RA	interleukin 20 receptor, alpha
				Klhl3	kelch-like family member 3
				Meis1	Meis homeobox 1

				MGC105567	similar to cDNA sequence BC023105
				MORN5	MORN repeat containing 5
				MSC	musculin
				KBTBD6	kelch repeat and BTB (POZ) domain containing 6
				KCNA7	potassium channel, voltage gated shaker related subfamily A, member 7
				LOC498826	LRRGT00165
				LOC688684	similar to 60S ribosomal protein L32
				LOC691427	similar to 6.8 kDa mitochondrial proteolipid
				LOC100360791	tumor protein, translationally-controlled 1
				LOC100361479	hypothetical LOC100361479
				LOC100910017	60S ribosomal protein L31-like
				LOC100911966	60S ribosomal protein L7a-like

				LOC100359522 (includes others)	LRRGT00191-like
				LTB	lymphotoxin beta (TNF superfamily, member 3)
				MGARP	mitochondria-localized glutamic acid-rich protein
				MITF	microphthalmia-associated transcription factor
				MRO	maestro
				Mt1	metallothionein 1
				NID2	nidogen 2 (osteonidogen)
				NRG2	neuregulin 2
				ODF4	outer dense fiber of sperm tails 4
				PCDH17	protocadherin 17
				PLEKHG1	pleckstrin homology domain containing, family G (with RhoGef domain) member 1
				PPARGC1B	peroxisome proliferator-activated receptor gamma, coactivator 1 beta

				RASD2	RASD family, member 2
				RNF225	ring finger protein 225
				RPH3A	rabphilin 3A
				PNMAL1	paraneoplastic Ma antigen family-like 1
				Podxl	podocalyxin-like
				PRRT3	proline-rich transmembrane protein 3
				PRSS12	protease, serine, 12 (neurotrypsin, motopsin)
				PUSL1	pseudouridylate synthase-like 1
				RPL37	ribosomal protein L37
				RSRC1	arginine/serine-rich coiled-coil 1
				SHISA6	shisa family member 6
				SLC10A4	solute carrier family 10, member 4
				SLC30A3	solute carrier family 30 (zinc transporter), member 3

				SPON1	spondin 1, extracellular matrix protein
				SRPK3	SRSF protein kinase 3
				TDRD5	tudor domain containing 5
				THSD7B	thrombospondin, type I, domain containing 7B
				SLC16A12	solute carrier family 16, member 12
				SOX30	SRY (sex determining region Y)-box 30
				STK32B	serine/threonine kinase 32B
				TACO1	translational activator of mitochondrially encoded cytochrome c oxidase I
				TNNI3	troponin I type 3 (cardiac)
				TRMT13	tRNA methyltransferase 13 homolog (S. cerevisiae)
				UBXN10	UBX domain protein 10
				VIM	vimentin
				ZNF862	zinc finger protein 862

Table S5.8: Selection criteria and Primer Sequences. Table presents genes selected for the designing of RT-qPCR array for the validation of RNA-seq data along with the primer sequences and their location on 384 well array plate. The different colors in the table correspond to the selection criteria of the genes which is described as legend at the end of table. Well A01 is set up as no RT (reverse transcriptase enzyme) control having a primer sequence for glutathione-S-transferase alpha-4.

TABLE LEGEND

Colour code	Description	Number of genes
	Control genes	2
	Housekeeping genes	5
	Known as involved in GLP-1 receptor mediated signalling	15
	Differential GLP-1/Exendin-4 treatment @ 30 mins or 24 hours	84
	Common but regulated in different directions by GLP-1/Exendin-4 @ 30mins or 24 hours	9
	Common GLP-1/Exendin-4- genes associated with diabetes or diabetes networks	33
	Common GLP-1/Exendin-4 genes- involved in proliferation/apoptosis/cell signalling - from network clusters with high scores and not already selected as above criteria or clusters containing known genes linked to GLP-1R signalling	44

Well	Gene symbol	Gene ID	Gene Name	The Minimum Information for Publication of Quantitative Real-Time PCR Experiments (MIQE)
A01	No RT control (Gsta4)	(300850)	No RT control (glutathione S-transferase, alpha 4)	No RT control (GCATTTAAGACAAGAATCAGCAACATTCCTACAATTAAGAAGTTCCTGCAACCTGGAAGTCAGAGGAAGCCACCTCCGGATGGCCACTATGTTGACGTGGTCAGGACCGTCCTGAAGTTCTAGTGACAGCGTGCTTTAAAGTGGCTACTGCAAGGGTCCAATCACAGCAGCAGCTACAGAGC)

A02	No primer Control		No primer control	No primer control
A03	Actb	81822	actin, beta	CCTCATGAAGATCCTGACCGAGCGTGGCTACAGCTTCACCACCACAGCTGAGAGGGAAATCGT GCGTGACATTAAAGAGAAGCTGTGCTATGTTGCCCTAGACTTCGAGCAAGAGATGGCCACTGC CGCATCCTCTTCCTCCCTGGAGAAGAGCTATGAGCTGCCTGACGGTCAGGTCATCACTATCGGC AATGAGCGGT
A04	Hprt1	24465	hypoxanthine phosphoribosyltransferase 1	ATGAACCTTCTATGAATTTTATGGTTTTTATTTTTAGAAATGTCTGTTGCTGCGTCCCTTTTGATT TGCACTATGAGCCTGTAGGCAGCCTACCGTCAGGTAGATTGTCACTTCCCTTGTGAGACAGACA GATCTCTTAAATTACCACTGTTAAATAATAATACTGAGATTGTATCTGTAAGAAGGATTTAAAA AGAAGC
A05	Tuba1a	64158	tubulin, alpha 1a	TGGTGCCCTACCCTCGCATCCACTTCCCTCTGGCCACTTATGCCCCTGTCATCTCTGCTGAGAAA GCCTACCATGAACAGCTTTCTGTAGCAGAGATCACCAATGCCTGCTTTGAGCCAGCCAACCAG ATGGTGAAATGTGACCCTCGCCATGGTAAATACATGGCTTGCTGCCTGCTGTACCGTGGTGATG TGGTCCCC
A06	Rpl32	28298	ribosomal protein L32	CGAAACTGGCGGAAACCCAGAGGCATCGACAACAGGGTGCGGAGAAGATTCAAGGGCCAGAT CCTGATGCCCAACATTGGTTACGGGAGTAACAAGAAAACCAAGCACATGCTGCCTAGCGGCTT CCGGAAGTTTCTGGTCCACAATGTCAAGGAGCTGGAAGTGCTGCTGATGTGCAACAA
A07	G6pd	24377	glucose-6-phosphate dehydrogenase	GAGTACCCTTCATCCTGCGCTGTGGCAAAGCTCTGAATGAGCGCAAAGCTGAAGTGAGACTTC AGTTCCGCGATGTGGCAGGTGACATCTTCCACCAGCAGTGCAAGCGTAACGAGCTGGTCATCC GTGTGCAGCCCAATGAGGCGGTATACACCAAGATGATGACCAAGAAGCCTGGCATGTTCTTCA ACCCTGAGGAGTCTGAGCTGGACCTAACCTATGGCAACAGATACAAG
A08	Irs1	25467	insulin receptor substrate 1	TCCAGGGGCTGCTTCCATTTGTAGGCCAACCCGGTCGGTGCCAAATAGCCGTGGTGATTACATG ACCATGCAGATAGGTTGTCCTCGTCAAAGCTATGTGGATACCTCACCAGTGGCCCCAGTCAGCT ATGCTGACATGCGGACAGGCATTGCTGCAGAGAAGGTGAGCCTGCCCAGAACCACAGGAGCT GCCCCCCCTC
A09	Creb1	81646	CAMP responsive element binding protein 1	TTGCCATTACCCAGGGAGGAGCAATACAGCTGGCTAACAATGGTACCGATGGGGTACAGGGCC TGCAGACATTAACCATGACCAATGCAGCTGCCACTCAGCCGGGTACTACCATTCTACAATATGC ACAGACCACTGATGGACAGCAGATTCTAGTGCCCAGCAACCAAGTTGTTGTTCAAG

A10	Ins1	24505	Insulin 1	ATGGCCCTGTGGATGCGCTTCCTGCCCCTGCTGGCCCTGCTCGTCCTCTGGGAGCCCAAGCCTG CCCAGGCTTTTGTCAAACAGCACCTTTGTGGTCCTCACCTGGTGGAGGCTCTGTACCTGGTGTG TGGGGAACGTGGTTTCTTCTACACACCCAAGTCCCGTCGTGAAGTGGAGGACCCGCAAGTGCC ACAACTGGA
A11	Adcy1	305509	adenylate cyclase 1	GTGAGCTGTCTGCCTTGGGCCTGGAGCTCTCACTCCAACAGCTCCCTAGTGGTCCTCGCAGCTG GTGGCCGGCGCACTGTGCTGCCTGCCCTGCCCTGTGAGTCTGCACACCATGGCCTGCTCTGCTG CCTGGTGGGCACCCTCCCACTAGCCATATTCCTGCGGGTGTCCTCCTTGCCAAAGATGATCCTG CTGTCTGGGCTGACGACTTCCTACATCCTTGTCCTGGAGCTCAGTGGATACACCAAGGTTGG
A12	Fos	314322	FBJ murine osteosarcoma viral oncogene homolog	CATCCTTGGAGCCGGTCAAGAACATTAGCAACATGGAGCTGAAGGCTGAACCCTTTGATGACT TCTTGTTTCCGGCATCATCTAGGCCCAGTGGCTCGGAGACTGCCCGCTCTGTGCCAGATGTGGA CCTGTCTGGTTCCTTCTATGCAGCAGACTGGGAGCCTCTGCACAGCAGTTCCCTGGGGATGGGG CCCATGGTC
B01	Nfkbid	308496	nuclear factor of kappa light polypeptide gene enhancer in B-cells inhibitor, delta	GACTCTCTGGATACCCGGCCGTATCCAGAACCTTCCCTGTCACAAGTAGGATCCTGGAGAGTCT CTGGTCTTCCCTCGGGATCCCCACAGTTGCCTCCGTCCACTGGACCCTCCCTGGAGGCAGCCCG AGCTCACATACTGGCTCTGGGCCCCCAACAACTGCTGGCCCAGGATGAGGAAGGAGACAC
B02	Bcl2	24224	B-cell CLL/lymphoma 2	CCTGACGCCCTTCACCGCGAGGGGACGCTTTGCCACGGTGGTGGAGGAACTCTTCAGGGATGG GGTGAACTGGGGGAGGATTGTGGCCTTCTTTGAGTTCGGTGGGGTCATGTGTGTGGAGAGCGT CAACAGGGAGATGTCACCCCTGGTGGACAACATCGCTCTGTGGATGACTGAGTACCTGAACCG GCATCTGCACA
B03	Gck	24385	Glucokinase	GCACTGGCTGCAATGCCTGCTACATGGAGGAAATGCAGAATGTGGAGCTGGTGGAAGGGGAT GAGGGACGCATGTGCGTCAACACGGAGTGGGGCGCCTTCGGGGACTCGGGCGAGCTGGATGA GTTCCTACTGGAGTATGACCGGATGGTGGATGAAAGCTCAGCGAACCCCGGTCAGCAGCT
B04	Foxo1	84482	Forkhead box O1	AGTACATTTCGTCCTCGAACCAGCTCAAACGCTAGCACCATCAGTGGGAGACTTTCTCCCATCA TGACAGAGCAGGATGACCTGGGGGATGGGGATGTGCATTCCCTGGTGTATCCACCCTCTGCTG CCAAGATGGCGTCTACACTGCCCAGTCTGTCTGAAATCAGCAATCCAGAAAACATGGAGAACC TTCTGGATAA
B05	Egr1	24330	Early growth response 1	AGTTATCCCAGCCAAACTACCCGGTTGCCTCCCATCACCTATACTGGCCGCTTCTCCCTGGAGC CTGCACCCAACAGTGGCAACACTTTGTGGCCTGAACCCCTTTTCAGCCTAGTCAGTGGCCTTGT GAGCATGACCAACCCTCCAACCTCTTCATCCTCAGCGCCTTCTCCAGCTGCTTCATCGTCTTCCT CTGCCTC

B06	Igf1r	25718	Insulin-like receptor growth factor 1	CTGGAAAACTGCACGGTGATCGAGGGCTTCCTCCACATCCTGCTCATCTCCAAGGCCGAGGAC TACCGAAGCTACCGCTTCCCCAAGCTCACGGTCATCACCGAGTACTTGCTGCTGTTTCGAGTGG CCGGCCTCGAGAGCCTGGGAGACCTCTTCCCGAACCTCACAGTCATCCGTGGCTGGAAACTCTT CTACAATTA
B07	Mafa	366949	v-maf avian musculoaponeurotic fibrosarcoma oncogene A	GGGTGTTCTGAGATGGGCGCGTCTGCACCGGCTGAGCTCTGGCTTGATCCCGGGTTCTCTGAGG CTCCTTCGTCCTTTGCTGCTCCCAGGTGGCTCCTGCTGAGCCTTCTGAACAGGACGCTAGACAA ATCGTTGGGGAAAATTTTTTGTGTTGTTGGTTTTTGTTGTGTTCTTTTTTTTTCCATTTGTTACAA AACTGA
B08	Pdx1	29535	Pancreatic and duodenal homeobox 1	TACACTCGGGCCCAGCTGCTGGAGCTGGAGAAGGAATTCTTATTTAACAAATACATCTCCCGG CCTCGCCGGGTGGAGCTGGCAGTGATGCTCAACTTGACTGAGAGACACATCAAAATCTGGTTC CAAAACCGTCGCATGAAGTGGAAGAAAGAGGAAGATAAGAAACGTAGTAGCGGGACAACGA GCGGGGGCGGTGG
B09	Crebl2	362453	cAMP responsive element binding protein-like 2	GTGGTCGGAGGCAAAGTGAAGAAGCCTGGTAAGCGAGGGCGGAAGCCAGCCAAAATTGACTT GAAAGCAAAACTTGAGCGAAGCCGGCAGAGTGCAAGAGAGTGCCGGGCCAGGAAAAAGCTGA GATACCAGTACTTGGAGGAGTTGGTGTCCAGTCGGGAAAGAGCTATATGTGCACTCCGAGAGG AACTGGAAATG
B10	Pax6	25509	Paired Box 6	GTGTCCAACGGATGTGTGAGTAAAATTCTGGGCAGGTATTACGAGACTGGCTCCATCAGACCC AGGGCAATCGGAGGCAGTAAGCCAAGAGTGGCGACTCCAGAAGTTGTAAGCAAAATAGCCCA GTATAAACGGGAGTGCCCGTCCATCTTTGCTTGGGAAATCCGAGACAGATTACTCTCCGAGGG GGTCTGTACCAACGACAATATACCCAGT
B11	Tmprss4	367074	transmembrane protease serine 2	GAAATATCTTGACGTGTCCAGCTGGAAGGTGAGGGCCGGCTCAAACAAGCTGGGTAACTCTCC GTCCTTGCCTGTGGCCAAGATCTTCATTGCTGAACCCAATCCCCTGCAACCCAAAGAGAAGGA CATTGCCCTCGTTAAGCTGAAGATGCCGCTCACATTCTCAG
B12	Mep1a	25684	meprin A alpha	ACCTTACCCACTTGAGGCAGACTGAAGTCCCCATTCCCAGCAGAAGCGTGATACCCCGAGGAC TCCTTCTGCAAGGCCAGGAGCCTCTTGCCTTGGGAGACTCCAGAATAGCCATGATGGAGGAAT CCCTGCCAAGAAGGCTGGACCAGAGACAGCCCAGCAGACCAAAGCGCTCAGTGGAAAATACT GGTCCCATGGAG
C01	Trpm8	171384	transient receptor potential cation channel, subfamily M, member 8	TCTGCCGACCTTCAGGAAGTCATGTTCACGGCCCTCATAAAGGACAGGCCCAAGTTTGTCCGCC TCTTCCTGGAGAATGGCCTCAACCTGCAGAAGTTCCTCACCAATGAAGTCCTCACGGAGCTCTT CTCCACCCACTTCAGCACCCTAGTGTACCGGAACCTGCAGATCGCCAAGAACTCCTACAACGA TGCACTCCT

C02	Nxf3	302591	nuclear RNA EXPORT FACTOR 1/2	TCCAGGTCTGAAACTAACCCCTTCCGAAGAAGAATGAGATGCCGACGTATTTTCCGACGGAGA TTTCTCAACTCGACTGAGTACATCAGTGACACGATGCGTACTTCATTTTATCACCAGCAAGATG AAGAGCTAGCAATGAGTAATGCTCCCATGTATACTCGAAGAAGATA
C03	LOC100361060	100361060	large subunti ribosomal protein L36e	TCACCAAGCACACCAAGTTCGTGCGAGATATGATCCGGGAGGTGTGCGGCTTCGCGCCCTACG AGCGGCGTGCCATGGAGCTGCTCAAGGTGTCCAAGGACAAGCGAGCACTCAAGTTTATCAAGA AGAGGGTGGGCACGCACATCCGGGCCAAGAGAAAGAGGGAGGAGCTGAGCAACGTGCTGGCA GCCATGCGGAAG
C04	Crb1	304825	CRUMBs homolg 1 (NOTCH)	ACTGCCCCTTTGATGATACTTCTAGGACATTTTATGGAGGAGAAGACTGCTCTGAAATTCTCCT GGGTTGCACTCATCACCAGTGTCTGAACAATGGAAAATGTATCCCTCACTTCCAAAACGGCCA GCACGAATTCACCTGCCAGTGTCCTTCTGGCTACGCCGGTCCACTGTGTGAAACTGTCACCACA CTTTCTTTT
C05	Mvb12b	362118	ESCRT-1 Complex subunit MVB12, multivesicular body subunit 12B	CTCCCTCCCCGGGAACGTTGTTCATAATTGTGACTAATGTGTGTGCTGTTAGTGACCAGAGGCT CCTGTGTGATGACCACTTACCCCACCAAGAAAGAAAACTCCTCCCTTACCTGGAGTCACCCATG AGGGCCTGGGCACATACTCCATCCACCCAGTGACACTCACTGGCTACCCTCCAACTGACCATCA CTGACCAC
C06	Ramp3	56820	RAMP3	CCCGAGCAGAAAGAGAGATGAGCACATTCTCTGTTGGACATGAAGGGTAGTCGGGGGGATTG GGGAATGGAGTTGTTAGGAGTCATGTGTGACCTACGGACCTGCCTGTCTTCTAGGCGATCTGCC ATGATTCTGTGTCCAGTGTGGGCTGGAGCTGTGATTTGTTTAACCCTTCAGACCCCTACCCTGA AGATAGAGAG
C07	Il9r	24500	interleukin 9 receptor	CAGCCATCTGCCTACCTGCCCCAGGAGGACTGGGCCCCACTGGGCTCTGCCAGGCCGCCCCCTC TAGACTCAGACAGTGGCAGCAGTGACTACTGCATGCTGGACTGCCGTGAGGAGTATGACCTCT CAGTCTTCCCAGAACACACCCTGAGTCCCGAGTTCACACTGGCTCAGCCTGTGGCCCTTGCTGT GTCTAGCAGG
C08	Tmprss11f	498345	Protein Tmprss11f	GATGTGGGATAAGAATGTCATCTTCCAACATCCCATTACCAGCATCCTCTACTACTGAACGAAT TGTCCAAGGGAGGGAAACAGCTATGGAAGGGGAGTGGCCATGGCAGGCTAGCCTACAGCTCA TAGGGGCTGGCCATCAGTGTGGAGCCACGCTCATCAGCAACACATGGCTGCTCACAGCAGCTC ATTGCTTCTGGAA
C09	Abcg3l3	305142	ATP-binding cassette subfamily G member 2 and 3	CTGACGAACATGAAGACCTTTATGAGAGACTACATCAAGTCACAGAAAAATTGGCCAATATGT ATGCCCAGTCACCCTTACACAGTGACACAAGAGCCAAACTGGATCAACTCTTGGGGGAACAGA AGCAGGACAGGAGATCAGCTATGGAGACCACATTTGTCACCCCTTTCTGGCATCAGTTCGGGT GGATTACCCTT

C10	Rpl7a	296596	lRP-L7Ae, RPL7A, large subunit ribosomal protein L7Ae	GGCAGGACATCCAGCCCAAAAGAGATCTCACGCGCTTCGTCAAATGGCCCCGCTACATCAGGC TGCAGCGGCAAAGAGCCATCCTCTATAAGCGGCTCAAAGTACCTCCTGCCATCAACCAGTTCA CCCAGGCCCTGGACAGGCAAACAG
C11	Cox6c	54322	cytochrome c oxidase subunit 6c, subunit 3	GACATTGGCTACCATGAGTTCCGGTGCTCTGTTGCCGAAACCACAGATGCGTGGTCTTCTGGCC AAGCGTCTGCGGGTTCATATTGTTGGCGCATTCGTTGTGGCCCTAGGAGTTGCTGCTGCCTATA AG
C12	Timp1	116510	TIMP metallopeptidase inhibitor 1	GTGTTTCCCTGTTCAGCCATCCCTTGCAAACTGGAGAGTGACAGTCATTGCTTGTGGACAGATC AGATCCTCATGGGCTCTGAGAAGGGCTACCAGAGCGATCACTTTGCCTGCCTGCCACGGAATC CAGATTTGTGCACCTGGCAATACCTTGGGGTCTCGATGACCCGAAGCCTTCCCCTGGCAAAAGC TGAAGCCTG
D01	Ankrd35	365881	ankyrin repeat domain 35	TGGAGCCAGAGGAGAGCCCTTAGGGGCCCCTGGAGGGGAACAGGCCTTAGGAGGAGGCCTGG CAAAGGGACAGCTGGAGAAAGAGGTGTCAGCTCTGAGACTGAGCAATAGCAATTTGCTGGAG GAATTGGAAGAGTTGGGGCGTGAGAGACAACGGTTGCAGGGAGAGCTGCAGTCCTTGACCCA GAAGCTACAACGGG
D02	Arhgap4	246249	ankyrin repeat domain 35	TGATGCGCGGGCAGTTGAGTGAGCAGCTTCATTGCCTGGAGCTTCAGGGAGAGCTGCGGCGGG ATTTGCTGCTGGAGCTAGCTGAGTTCATGCGGCGTCGAGCAGAGGTGGAGCTGGAGTATTCTC GGGGCCTGGACAAGTTGGCTGAACGCTTTACTAGCCGCAGTGGACGCCTTGGAGGCAGCAGCC GGGAGCAGCAAAGTTTCCG
D03	Prickle3	317380	prickle homolog 3	CACTCCATGCCTGAACTGGGGCTTCGCAGTGCTCCTGAGCCACCTACAGAATCCCCTGGCCATC CTGCCCTGCACCCAGATGATAACACCACCTTTGGTCGCCAGAGTACGCCTCGTGTCAGCTTCCG AGACCCTCTGGTATCTGAAGGAGGTCCACGAAGGACCCTTAGTGCACCTCCAGCCCAGCGCCG TAGACCGCG
D04	Hnrnpa1	29578	heterogeneous nuclear ribonucleoprotein A1	GATTCTCAGAGACCAGGTGCCCACTTAACTGTGAAGAAGATCTTTGTTGGCGGTATTAAAGAA GACACTGAAGAACATCACCTACGAGATTATTTTGAGCAGTATGGGAAAATTGAAGTGATTGAA ATTATGACTGACAGAGGCAGTGGAAAAAAGAGGGGATTTGCGTTTGTCACCTTTGATGACCAT GACTCTGTGGATAAGATTGTTA
D05	Hmgn5b	681284	high mobility group nucleosome binding domain 5B	AGACACTGAAGGAGATGGAGGAGAAAAGAAAGAAGCAGTGGTAACAAAAGGCAAAAATGAT GAGCTAGAAGCAAACATTCAAGATGTGGAGAAAGATGAAGATGAAAAAGAGCACGAAGATAC AGGTGAGGAGGGAGAAGATGGGGAAAGGGAAGGAGGCCTAAAAGAGAAACCAGATGTAGCT GAAATCGAAGACGCAA

D06	Pigx	288041	phosphatidylinositol glycan, class x	GCAGTGATGGTATCAGAGAGTTTTAATCTAGAAGCCCCCAGCTATTTATCCACAGAGTCTGCGGTCCTCATTTATGCCCGGCAGGACGCACAGTGCATCGACTGCTTCCAGGCCTTCCTACCTGTGCACTATCGATATCACCGTCCACATAAGAAGGATGGAGACACCCTCATTGTGGTCAACAACCCTGACTTACTGATGCACTGTGACCAAG
D07	Palb2	293452	partner and localiser of BRCA2	AACCTATAAATAAAGGCTTTCCTTGTGACGCTTCGTTACAAAGCGACCATCTTGATGAGGAGACTGGAGAAAACATCTCTCAGATACTTGATGGTGATCCTCAGTCCTTTAACTGTGAAAGTGGCCAAGAAGTCTTACATACACCAAGAGCAGGTGACATCCAAGGACAATTTTTACATAGCACCAGCAGCCCTGATGGT
D08	Phkg1	29353	phosphorylase kinase, gamma 1	GTCATCTGTCTAACTGTGCTGGCCTCGGTAAGGATCTACTACCAGTACCGTCGGGTGAAGCCGGTAACCAGGGAGATCGTCATCCGAGACCCCTACGCCCTACGGCCATTGCGCAGACTCATCGACGCCTATGCTTTCCGCATCTACGGCCACTGGGTGAAGAAAGGGCAACAGCAGAACAGAGCTGCCCTCTTCGAGAA
D09	Calm1	24242	calmodulin 1	TACAGTATAAATACTCGTACTACCTTATAAGGAAGCACTTAGTGGACTCCTTCAAGTTCCATTTGCTAATGATTAACACACTGTCTGGGCTGGCCAGTTTCTCATGCATGCAGCTTGGTGATTGAGCACAGTCAGGCCTTTGTATTAAAACTGAAAAATGGAAAAAACAAATTCAAACTCTCAGATGGCTTCTAGTTCAA
D10	Cetn2	84593	centrin-2	ATGTTGATTGGTCTAGCTCGCCTCTGGCGTAGCCAATTGACGCTCACAGCACGATTTTGCCCAATGAGGCCAATCTTTGGCTGCCTACGCATCGCCCTTTGGCCCTTGGGCGTGCTTTGCCAGGTCAGCCCCACCTCCTCGTTCCCAAACCAATGGGAAGCGGGCTGTGCGCGCAGGGAGCAGTGGGAAAGCCGCCAAGG
D11	Galnt1	79214	UDP-N-acetyl-alpha-D-galactosamine:polypeptide N-acetylgalactosaminyltransferase 1 (GalNAc-T1)	ACTTTTTGAAAAGACCTCTAGAGAGTTATGTGAAAAAGCTTAAAGTGCCAGTTCATGTAATTCGAATGGAACAACGTTCTGGGTTGATCAGAGCTAGATTAAAAGGAGCTGCTGTGTCCAAAGGCCAAGTGATCACCTTCTTAGATGCTCACTGCGAGTGCACAGTAGGGTGGCTGGAGCCTCTGTTAGCCCGGATCAAACATGACAG
D12	LOC100910152	100910152	histone H2A	TACCTGGCGGCGGTGCTGGAGTACCTGACGGCCGAGATCCTGGAACTGGCGGGCAACGCGGCGAGGGACAACAAGAAGACGCGCATCATCCCTCGCCACCTGCAGCTGGCTATCCGCAACGACGAAGAGCTCAACAAGCTTCTGGGCCGTGTGACCATCGCGCAGGGCGGTGTCCTGCCCAACATCCAGGCCGTGCTGCT
E01	Gatm	81660	glycine amidinotransferase	CTTGGAGGATCCTTAACAGGATGGGTGCAGCGAACTTTCCAGAGCACCCAGGCAGCTACAGCTTCCTCCCAAAATTCCTGTGCAGCTGAAGACAAGGCCACCCACCCCCTGCCCAAGGACTGCCCTGTCTCCTCTTACAACGAATGGGACCCTTTAGAGGAAGTGATAGTGGGCAGAGCTGAAAATGCCTGTGTCCCACCATTCACAGTGGAGGTGAAG

E02	Gpr165	296866	G protein-coupled receptor 165	GTCCAAGATGGATAAGTTAGCAGACCACATGTCAAACACGGGGGACCTGGCTGACACATCAGG TCCCCTAGATTTGGAAATTGTATCCCAGGATGAGCAGGTGCAATTCTGGTTAGTGGTAGGGTAC ACCATAGTGGTCTTTGCTGCCATCATAGGCAACTGGGTCTTAAACCACATCATTATGAAGTATA AGAGGGTAC
E03	Spag8	362508	sperm-associated antigen 8	ATCTTTTGATATACAGCCCAGCTCTGAAGGACTAGAGTCCACTTCAGAACCCATTCCTTCTTCG GGTAGCAGTCCTAAGCCTACCGTACAGACCGGAGCTGCCCCATCATCTGCAGTATGTCGAGGA GTTCCTTCGCCGTATTGTGTGTTTACAGATCCCTCCTCTGACAGTCTTTATGAAGCAACCTGCCC CGCACCCC
E04	Hnrnpa3	362152	heterogeneous nuclear ribonucleoprotein A3	AAGTTTACTATTGCATGGACCAGCAGGGACAGTCAGTTTAGTTATGTGTTTTTAGTCTTCCCCA AAACCCATCACACCAACAGTCTGGTCTCACTGTTGTCCTAGCTTGGAACTCAGTCCACCAGCCT TCTGTCACCCAAGTGCTGGGATTAAAGGGTGGTGCCTATATGACAACTCATTCCTTTAAAAAAA AAAATCCA
E05	Spatc1	315091	spermatogenesis and centriole associated 1	GCCTCCCTAAACCCCAGTAGCCACAAGTTGGATGAGGACCTATGCCAGACACTCACACAGCGT TATGTGAGCATCATGAACAGGCTGCAGAGCCTAGGCTACAATGGACGGGTGCATCCAGCACTG ACAGAGCAGCTGGTGAACGCATATGGCATCTTGCGTGAGAGGCCTGAGCTGGCAGCATCTGAA GGTGGTACCTA
E06	Slc26a1	64076	sulphate anion transporter 1	CAAGGTCTGTTTCCTGTCATACGCTGGCTGCCCCAGTACCGCCTTAAGGAATACCTGGCAGGTG ATGTCATGTCGGGATTGGTCATTGGCATTATCCTGGTGCCACAGGCCATAGCCTACTCACTGCT GGCTGGGTTGCAGCCCATCTACAGTCTCTACACTTCCTTCTTCGCCAACCTTATCTACTTCCTCA TGGGTAC
E07	LOC1003 65845	10036584 5	RIKEN cDNA gene, 1110034G24Rik, rCG26214-like	CACTGCCAGGCTCTGGGGATCCGCTCTCTGCACCTGTGTGTCAGTGCCTGTCTCAGACCATCTC TGAGCTCGAGGGCCAGGAGAGCCAAAAGTATGCTCTCCGCAGTTTCCAGATGGCCCGGGTCAT CTTCAGCCGGGATGGCTGCTCTACCTTACAGCGGCATTCCAGGGAAACCCGCTTCTACCCACTA GAGCAAGAA
E08	S1pr2	29415	sphingosine-1-phosphate receptor 2	AATTGTCTGGACCATCTGGAGGCTTGCTCCACTGTGCTGCCCCTCTATGCTAAGCACTATGTGC TCTGCGTGGTCACCATCTTCTCTGTCATCTTACTGGCTATCGTGGCCTTGTACGTCCGAATCTAC TTCGTAGTCCGCTCAAGCCATGCGGACGTTGCTGGTCCTCAGACGCTGGCCCTGCTCAAGACAG TCACCAT
E09	Prok2	192206	Prokineticin-2	GGACTTACCGATGGAAAGGAAGAGAGAACTGCTTTGACCTTGACCTGCTTGGAAAGGATGCTT GGAAGGAGAAATGCTGATTGGGTCTTGGTTTGCATGAGAAAAGGCAAGCACCAGGAGGAGGG CCCAGCAGCTCAGAGAGGTGGGTGTAGCCTGCTGTTCCTGCAAAGGGCCTTTCCTTTCTGGTTC CTCCTTGTATCCTTCAGTACCTAG

E10	Zfp862	681217	Zinc finger protein 863	CATGCCCTGGCCGCCAAGGACCCCGTCTGGGCAGCCCACCTTCAGAATCTCAGGGAGAGTCCT GCAGATCTCCTGGCCAGCCCTGAACACCTCCTCACTGCAGACAATCCCACATTCTACCTGCCAG GGCCTCTGGGAAACTTTGATGGCATAGATGAGCTTCTGTCCAGCCCAAGAGCTGAACCAGAGG ACACCTCAGG
E11	Rpl8	26962	ribosomal protein L8	CCCAGCTGAATATTGGCAATGTTTTGCCCGTGGGCACCATGCCTGAGGGTACTATCGTGTGTTG TCTGGAGGAGAAGCCTGGGGACAGGGGCAAGCTGGCACGAGCCTCCGGGAACTATGCTACAG TCATCTCCCACAACCCAGAGACCAAGAAGACCCGAGTGAAGCTGCCTTCAGGGTCCAAGAAGG TCATTTCCTCTGCTAACCGAGCTGTTGTTG
E12	Hmgb1	25459	high mobility group protein B1	AAGACCTGAGAATGTATCCCCAAAAGCGTGAGCTTAAAATACAAGATTGCTGTACTATTTGTT GACCTTAGTCCCAGCGAAGGCTATCATGAGAAGCTGGCTGTAATGCCTTTGCCCTTCTATCTAA ATACGGATTGCTCAGGAAACTTGACTGTTTAAAGGTATATTTAATTAGTTGAGCCAGCTTTTAA AATTATGCC
F01	Utp14a	317579	UTP14, U3 small nucleolar ribonucleoprotein, homolog A (yeast)	CATCCAGAATCCCATAGGGTCCACATGGATCACCCAGCGAGCATTCCAAAAGCTGACTGCTCC CAAGGTTGTGACCAAGCCAGGCCATATTATCAAGCCCATAACAGCAGACGATGTGGGTCGCCA ATCTTCCCCAAGGTCTGACCTGTCTGTCATGCAGACCAATCCAAAACGACACTGCAAACATCA AAAGCAACTGA
F02	P4hb	25506	prolyl 4-hydroxylase, beta polypeptide	ATCCTGTTCATCTTCATCGATAGTGACCACACTGACAACCAGCGCATACTTGAGTTCTTTGGCC TGAAGAAGGAGGAATGTCCAGCTGTGCGGCTTATTACCCTGGAGGAAGAGATGACCAAGTACA AACCGGAGTCAGACGAGCTGACAGCTGAGAAGATCACACAATTTTGCCACCACTTCCTGGAGG GCAAGATCAAG
F03	Kcna7	365241	ribosomal protein L7a	AGTGGTCACCATGACCACGGTCGGCTACGGGGACATGGCACCTGTCACCGTGGGTGGCAAGAT CGTGGGCTCTCTGTGTGCCATTGCAGGCGTGCTCACCATCTCTCTGCCGGTGCCTGTCATCGTCT CCAACTTCAGCTACTTTTACCACCGGGAGACAGAGGGCGAAGAGGCAGGGATGTACAGCCATG TGGACACAC
F04	Mettl20	316976	Methyltransferase-like protein 20	ACAGTGGGGAGCTGTTTGGATCTTAAGATGAAAGCCTACCTGGAGGAAAACACTGAAGTCACC AGCAGTGGCAGCCTTACCCCTGAAATCCAGTTACGGCTTTTAACCCCCAGGTGCAAGTTTTGGT GGGAAAGGGCTGACCTGTGGCCCTACAGTGATCCCTACTGGGCTATCTACTGGCCAGGAGGCC AGGCTCTGTC
F05	Mtnr1a	114211	melatonin receptor type 1A	TACCCATTTCCCTTGGCGCTGACGTCTATACTTAACAATGGATGGAACCTGGGATATCTGCATT GTCAAGTTAGTGCCTTCCTAATGGGCCTGAGTGTCATTGGCTCGGTATTCAACATCACCGGGAT CGCTATGAACCGCTACTGCTACATTTGCCACAGTCTCAAGTATGATAGGATATACAGTAACAA GAATTCCCT

F06	Opcml	116597	opioid binding protein/cell adhesion molecule-like	GTGTACCATAGATGACCGGGTCACCAGAGTAGCCTGGCTAAACCGCAGCACAATCCTCTACGC TGGGAATGACAAGTGGTCCATAGACCCTCGAGTGATCATCTTGGTCAACACGCCTACCCAGTA CAGTATCATGATCCAGAATGTGGATGTTTATGACGAAGGTCCGTACACCTGCTCTGTGCAGACA GACAATCACCCCAAAACCTCCCGGGTCCACCTCATAGTGCAAG
F07	Kifc2	300053	kinesin-like protein KIFC2 precursor	CGCCCAGCGAGTGGGTCAAGTGGAACTGGGGCCTGCCCGGCGCCGTAGAACCCCACGCTCTGG GACCCCTTCTTCTCTCAGTACTGACACCCCTCTCACTGGAACTTCCTGCACCCCTACACCATCTC CTGGCAGCCCTCCCAGTCCCAGCCCCAACAGCTGTTCTGGCTTGACTCTTGAACCTCCAGGGGA CCTGCCTC
F08	Astn2	100361323	astrotactin 2	GGTCCTCAGGCCAGGGAGAGCTTCCGCTCCACCAGACTACAGGCACACAACTCAGTCATCGGT GTGCCTATCCGGGAAACCCCCATCCTAGATGACTATGACTATGAAGAGGAAGAGGACCCACCC AGGCGGGCCAACCATGTCTCCCGTGAGGATGAGTTTGATAGCCAGATGACCCATGCCCTGGAC AGCTTGGGAAG
F09	LOC100359664	100359664	mitochondrial transcription termination factor-like	TGAAATTGTAAATAGTTTGGAGTGTTCTCCTGAATCCTTCTTTCTGTCTAATAACAACCTAAACT TAGAGAATAACATAAAGTTCCTCTGCTCTGTTGGCTTGACTCATAAATGCCTCTGCCGACTGTT GACCAGTGCTCCCAGGACCTTCTCCAACAGTCTGAATTTGAATAAACAAATGGTTGAATATTTG CAGGAAA
F10	Itga2	170921	integrin, alpha 2 (CD49B, alpha 2 subunit of VLA-2 receptor)	GGCGTCCTGAACCAGCACCAGTTTCTTGAAGGACCTGAAGGCACTGGAAATGCTCGGTTTGGT TCAGCAATTGCAGCCCTTTCAGACATCAACATGGATGGCTTTAATGATGTGATTGTTGGTTCGC CTGTAGAGAATGAGAACTCTGGAGCTGTGTACATCTACAATGGCCACCAGGGTACCATTCGCA CCAAGTACTC
F11	Ppp1r3e	691447	protein phosphatase 1, regulatory (inhibitor) subunit 3E	AGAGATCTGGAAGCAAGCAGGACGGATATTCTGACACCGGGGACTGGCCGCTAAAGGAAGGG AAAAATGGTCAAGGAAACCAAGCAGGCCGGGTACGTGGGGTGACGGCAAGGAGAGTCCACAG CCAGCAGCTGCCGAGCAGCCCTGCACCTTATGATCGGACATAGAGCCGGCGGGAGAGCGAGG ACGCGCCGGGCACT
F12	Tmem176b	171411	transmembrane protein 176B	GGCCACATATCACGGCTGCTCCTCCTGGCTTGCTCTGCTACAGCTGCAGCTGCTACCGTTATGG GTGTGAAAAGCCTCATCTGGCAAACCAGTGCTTCCTACTACTTCGAGATCAGTTCCACATGTGA CTCCTTACAACCAAGCATTGTCGATAGGTTTCGGTCAGTGCGATTCACTGACGACTCAGACTGG AGGACAGA
G01	Egr4	25129	early growth response 4	ACAGACTCCTGCTTCCTGGAGGGCCCTGCACCCACGCCCCCTTCGGGCCTCAGCTACAGCGGCA GCTTCTTCATCCAGGCGGTTCCCGAACACCCGCACGACCCGGAGGCCCTCTTCAACCTCATGTC TGGCATCTTGGGCTTGGCACCCTTCCCTAGCCCCGAGGCGGCAGCGTCTCGGTCCCCCCTGGAT GTCCCTTT

G02	Cyp1a1	24296	cytochrome P450, family 1, subfamily A, polypeptide 1	ATAGCCTCAGACCCAACACTGGCATCCTCTTGCTACTTGGAAGAGCACGTGAGCAAAGAGGCTGAATACTTAATCAGCAAGTTCCAGAAGCTGATGGCAGAGGTTGGCCACTTCGACCCTTTCAAGTATTTGGTGGTGTCAGTGGCCAATGTCATCTGTGCCATATGCTTTGGCAGACGTTATGACCACGATGACCAAGA
G03	Izumo1	499152	izumo sperm-egg fusion 1	ATGGGGCTACATTTTACACTCTTGCTGGCAGCTCTTGCCAACTGCCTGTGTCCAGCAAGGCTCTGCATCATATGTGACCCGTTTGTGGTGGCTGCAATAAAGACTTTGGAGCAGAATTACCTGCCTACCCACCTGGCGCCCGAGCATCACGAAGATGTAATGAAGAGGGTAGAGCAGGAAGTGAGGAACTTCGCTGATCTGCCCTTGAATCAGAATACCTTTCTGGGGGTTGTAG
G04	Lama2	309368	laminin, alpha 2	ATGGCCTCAATCAGTTTGGCCTGACCACCAACGTTAGGTTCCGAGGCTGCATCCGATCTCTGAAGCTCACCAAAGGGACAGGCAAGCCGCTGGAGGTTAATTTTGCCAAGGCTCTGGAACTGAGGGGTGTTCAACCTGTATCATGCCCAACTACCTAATAAAGATAAGTTCAATCCGGAGAAGAATTCACCAAGACAAGT
G05	Nxf2	308653	nuclear RNA export factor 2	AATTTGCATCATGAACGATGAGTTGATTGTGAGGAATGCCAGTCCCAAAGAGATACAAAAGGCCTTCACATCGTCGCCTGCACCCGACACTTCTCTCAAGCCTTTACTCTCTGCAGAGCAGCAGGAAATGGTGAAGTCTTTCTCTGTGCAATCTGGAATGAAACTTGATTGGTCTCAGAA
G06	Ryr3	170546	ryanodine receptor 3	GCCGGATACCCAGAGCTGTGGCCTCCATCAACCAGCATCTGCTGAAGTCAGATGATGTGGTGAGCTGCTGCCTTGACCTTGGAGTACCCAGCATTTCTTTCCGAATCAATGGACAACCTGTGCAGGGAATGTTTGAGAATTTCAACACAGATGGACTCTTTTTCCCCGTGATGAGTTTTTCGGCTGGTGTCAA
G07	Steap1	297738	six transmembrane epithelial antigen of the prostate 1	TTACCCATTAGTCGCTTCCCGCGAACAGTATTTTTATAAGATCCCGATCCTGGTCGTTAACAAAGTCTTGCCAATGGTCTCCATTACCCTCTTGGCATTGGTTTATCTGCCAGGAGAGATAGCGGCAGTTGTGCAGCTTCGCAATGGGACCAAGTACAAGAAGTTCCCACCCTGGTTAGACAGATGGATGCTGGCGAGGA
G08	Stk32b	305431	serine/thr eonine kinase 2B	GTACTCCTTCCAGGATGAGGAAGACATGTTCATGGTGGTGGACCTGCTGCTGGGCGGGGACCTGCGCTACCACCTACAGCAGAACGTGCACTTCACAGAGGGAGCCGTGAAGCTCTACGTCTGTGAGCTGGCCCTGGCACTGGAGTACCTGCAGAGGTACCACATCATCCACAG
G09	Vom2r52	297590	vomeronasal 2 receptor, 52	ATTGGGATATCACCACATTATCCTTTCGACAAAATCTAAGTTATACATATTTTGGTGGAGAATTATCATTTTCTGTTCACACAGATGAAATTCTGGGATTCAAAGATTTTCTCAGAAGTGTCCAACCTAGGAAATACCCTCAAGATATCTTTATCCAGGATGTGTGGTCGATCTTATTTGAATGTCCATATACTTATCTA

G10	Ar	24208	androgen receptor	CCGAATGCAAAGGTCTTTCCCTGGACGAAGGCCCGGGCAAAGGCACTGAAGAGACTGCTGAGT ATTCCTCTTTCAAGGGAGGTTACGCCAAAGGGTTGGAAGGTGAGAGTCTGGGCTGCTCTGGCA GCAGTGAAGCAGGTAGCTCTGGGACACTTGAGATCCCGTCCTCACTGTCTCTGTATAAGTCTGG AGCAGTAGAC
G11	Capn6	83685	calpain 6	GTGGAGATGAACCGAAGATTCCGCCTTCATCACCTGTATATTCAGGAGCGAGCTGGAACTTCC ACCTATATCGACACCCGTACCGTGTTTCTGAGCAAGTATCTGAAGAAGGGCAACTATGTTCTTG TTCCAACTATGTTCCAGCATGGCCGTACCAGCGAATTTCTACTGAGGATCTTCTCGGAAGTGCC TGTCCAGCTCAG
G12	Ccr7	287673	chemokine (C-C motif) receptor 7	ACATCCTCTTCCTCATGATCCTTCCCTTCTGGGCCTACAGCGAAGCCAAGTCCTGGATCTTTGGT GCCTACCTGTGTAAGAGCATCTTTGGCATCTACAAGTTAAGCTTCTTCAGCGGGATGTTGCTGC TCCTGTGTATCAGCATTGACCGCTATGTGGCCATCGTCCAGGCCGTGTCAGCCCACCGGCACCG CGCCCGC
H01	Cyp17a1	25146	cytochrome P450, family 17, subfamily A, polypeptide 1	GGTCAAGTCAAAGACGCCCGGTGCCAAGCTCCCCAGGAGCCTTCCATCCCTGCCCCTGGTGGG CAGTCTGCCGTTTCTCCCCAGACGTGGTCATATGCATGTCAACTTCTTCAAGCTACAGGAAAAG TATGGTCCCATCTATTCTCTTCGCCTGGGTACCACAACTACAGTGATCATCGGCCACTATCAGC TGGCCAGGG
H02	Epha5	79208	EPH receptor A5	GACCTTTAACATGTATTATTTTGAGTCGGATGATGAGAATGGGAGAAATATCAAAGAGAACCA GTACATCAAGATCGATACCATTGCTGCTGATGAGAGCTTCACCGAACTTGACCTTGGAGACCG GGTCATGAAGCTGAATACGGAGGTCAGAGATGTAGGACCTCTGAGCAAAAAGGGATTTTATCT TGCTTTCCAAG
H03	Ftl1l1	501644	ferritin, light polypeptide	TGGGCTTCTTTTTTGATCGGGATGACGTGGCTTTGGAGGGCGTAGGCCACTTCTTCGGAGAATT GGCCGAGGAGAAGCGCGAGGGCGCCGAGCATCTCCTCAAGTTGCAGAACGAACGCGGGGGCC GTGCACTCTTCCAGGATGTGCAGAAGCCATCTCAAGATGAGTGGGGTAAAACCCTGGAGGCCA TGGAAGCTGCC
H04	Hfm1	690161	HFM1, ATP-dependent DNA helicase homolog (S. cerevisiae)	CATACATGAACAGGATTACCTAAATTTAGGAGGATTAAATAACAATGACATGTCACATACAGC TGGCAAGCTAGTGTACGGTTCTTCTCAAAAATATAAAAACCACATGGGGGATGAGAGTCCACC GACAAAGAGTGGTCCTGGTGATGCAAAGCTGCATACTGCTGCTGAGGACAGAGAGGGCACATC AGCACTCAAAA
H05	Itga10	310683	integrin, alpha 10	CAAAATTTGCTGATGCTCCAGGGAACCCTTCAGCCAGACCGCTCCCAGGATTCTCGGTTTGGCT TTGCTATGGCTGCTCTTCCTGATCTGAACCACGACGGTTTCAGTGATGTAGCAGTGGGGGCACC TCTGGAGGATGGCCACCAGGGAGCACTGTACCTGTATCACGGAACCCAAACTGGAATCAGGCC ACATCCTACCCAG

H06	Kcne2	171138	potassium voltage-gated channel, Isk-related family, member 2	CTGTACCTCATGGTGATGATCGGCATGTTCGCCTTCATCGTGGTGGCCATCCTGGTGAGCACGG TGAAGTCGAAGCGGCGGGAGCACTCCCAGGACCCGTACCACCAGTACATCGTGGAGGATTGGC AGCAGAAGTATAGGAGTCAGATCTTGCATCTGGAAGACTCCAAGGCCACCATCCATGAGAACC TGGGGGCGAC
H07	Muc6	282586	mucin 6, oligomeric mucus/gel-forming	GTGGGAGTGCCTGGAACCTTGAAGAGTCTAAGGGTTCTCCAGCCGGGGTGGGGAACTCCTTAT GCATTCCTACAGGAACCAACGGTATCACCCCACAGGTCCTGGTAGAGAAGAAGTACATGGGCA AGCTATGTGGACTGTGTGGGAACTTTGATGGAAAGATAGACAATGAATTTCTCAGTGAGGATG GTAAGCTGGGT
H08	Nexn	246172	nexilin (F actin binding protein)	ATTCTGCTTTCTTCATCTAAACCTGTCCCCAAATCCTATGTGCCAAAACTCGGCAAGGGAGATG TAAAGGATAAATTTGAAGCCATGCAGAGGGCCAGGGAAGAAAGAAATCAAAGGCGATCTAGA GACGAAAAGCAAAGAAGAAAAGAACAATATATTAGAGAAAGAGAATGGAACAGGAGAAAGC AGGAG
H09	Odf4	303236	outer dense fiber of sperm tails 4	TCCGAGTTCAGCCTGCTGGCCTTCCTCCTGCTCCTGCTCATGGTCTTCTCCAAGAAATGGTTGTA TCCTTCTAAGAGTCGTTTCCATCAGCGCTACCCCCAAAACATCACCAAGAGAGTCTACACCTCC ATCCACAGTATGTCCACAGGACTCCTGTACATCTGCATATCTAAAAGCTGCCTCAGCTCAGACA ATGAGGA
H10	Plekho2	315764	pleckstrin homology domain containing, family O member 2	TTGGGGACCTACTCAGAGAAAGCCCTCAGCATCCACGACTGCCCAAGGAAAAGTTGTACCGGG CCCAGCTGGAAGTGAAGGTGGCTTCGAAACAGACAGAGAAATTGTTGAATCAGGTGCTGGGCA GTGAGCCGCCACCTGTGTGTGCCGAGTCATTGCTCAGCCAGGCTGTGGAGCAACTGAGGCAGG CCACCCAGGTC
H11	Clca5	308016	chloride channel calcium activated 5	TCTGAAAGTGACTGTGGCCTCCCGTGCCTCCAGTCTGGCCGTGTCCCCAGCCACCGTGGACGCC TTTGTGGAAAGGGACAGCACCTATTTTCCTCAGCCGGTGATAATTTATGCAAACGTGAGGAAG GGTCTGTACCCCATACTCAATGCCACTGTGATGGCAACGGTTGAGCCTGAGGCTGGAGACCCT GTTGTGCTGC
H12	Il7	25647	interleukin 7	AACAAAGCCTCGGCCTTCGGGAAGCTACTCAAGCCTTGGCTGCAAAGTCACAAAGCCCATTTG GATCTGCTTTCAAAGATTAACCACTCAGGGACATTGAACAATGATCATGCTGGTATGTGGGTTA TGGATTCTTTTTGA
I01	Thsd7b	289007	thrombospondin, type I, domain containing 7B	CCTCAGCCTCCCACAGAGCAAGCCTGCCTCATCCCTTGCCCCAGGGACTGTGTTGTATCTGAGT TCTCCCCGTGGTCCACCTGCCCTGAAGGGTGTGGGAAGAAGCTGCAGCATAGAACTCGTGTGG CCATCGCACCCCCTCTGTATGGAGGTCTGCAGTGCCCAAATCTCACTGAGTCCAGAGCCTGTGA GGCTCCAAT

I02	Tlr5	289337	toll-like receptor 5	GCTTTACCGCCAACTTCATAGAGTTATCTGAAAATGGGCTAGAAAATCTGTCTGACCTCTACTT CCTCCTGCGAATCCCCGGTCTCCAGTTTCTCATCCTAAATCAGAACCGCCTTTCGTCCTGCAGC AATGTGGACTACGCCCCTTCCCAGAACCTGAGCTTAGAACAGCTTTTCCTTGCAGAGAACATGC TACAGCTC
I03	Barhl2	65050	BarH-like homeobox 2	CTTCCACCTCTTCCTTTTTAATTAAGGACATCTTGGGAGACAGCAAACCCCTGGCGGCTTGTGC ACCCTACAGCACCAGCGTTTCTTCTCCTCATCACACCCCGAAGCAGGAGTGCAACGCGGCGCA CGAGAGCTTCAGGCCAAAGCTGGAGCAGGAGGACAGCAAAACCAAGCTGGACAAGAGGGAA GACTCTCAGAGC
I04	Cbln2	291388	cerebellin 2 precursor	GCTCAGAACGACACGGAGCCCATCGTGCTAGAGGGCAAGTGCCTGGTAGTGTGCGATTCCAGT CCATCGGGGGATGGCGCTGTCACTTCTTCCCTGGGCATATCTGTGCGCTCAGGCAGTGCCAAGG TGGCCTTCTCCGCTACTCGGAGCACCAACCACGAGCCTTCAGAGATGAGCAACCGTACCATGA CCATCTACTT
I05	Olfml2a	296708	olfactomedin-like 2A	CTACACGGTGGACACTTACAACCAGCATGAAGGCCAAGTGGCCTATGCGTTCGATACCCACAC CGGCACTGATGCTTACCCACAGTTGCCCTTCCTCAATGAATATTCCTATACCACCCAGGTTGAC TACAACCCCAAGGAGCGGGTGCTCTATGCCTGGGACAATGGCCACCAGCTCACCTACACTCTC CACTTTGTCG
I06	Aldh2	29539	aldehyde dehydrogenase 2 family (mitochondrial)	TGGACTGGGCTGTGGAACAGGCCCACTTTGCCCTGTTCTTCAACCAGGGCCAGTGCTGTTGTGC GGGCTCCCGGACCTTCGTGCAGGAGGATGTGTATGATGAATTCGTGGAACGCAGTGTGGCCCG GGCCAAGTCTCGGGTGGTCGGGAACCCTTTCGACAGCCGGACGGAGCAGGGGCCGCAG
I07	Tirap	680127	toll interleukin 1 receptor domain protein	ACTGGTTCAGGCAGGCTCTGTTGAAGAAGCCCAAGAAGATGCCAATCTCCCAGGAAAGCCACC TCAGTGATGGTTCACAGACAGCCACACAGGATGGTCTCTCACCCTCCAGCGGCAGTTCACCTCG GAGTCATAGTTCATCCCAGAGCCAAAGCTCAACCCCGAGCTGCAGTTCAGGAATGTCTCCTAC CTCACCACCA
I08	Grid2	79220	Glutamate receptor, ionotropic, delta 2	CATGTGAACTTATGAACCAGGGCATCTTGGCCTTGGTCAGCTCCATTGGTTGCACATCTGCTGG GTCCCTCCAGTCTTTGGCAGACGCCATGCATATCCCTCACCTCTTCATTCAGCGTTCAACAGCT GGGACCCCAAGAAGTGGCTGCGGCCTCACCAGGAGCAACAGAAACGATGACTATACCCTTTCA GTTCGTCCACCTGTCTACTTGAATGAAGTCATCCTAAGAGTAGTCACAGAGTATGCATGGCAGA AATTTATTATCTTCTATGATAGTGAATATG
I09	Llph	299818	LLP homolog, long-term synaptic facilitation (Aplysia)	ATGGCTAAAAGCTTGCGGAGTAAGTGGAAAAGGAAGATGCGCGCTGAGAAGAGAAAGAAGAA TGCGCCAAGGGAACTTAACAGACTCAAAAGTATCCTCAAAGTTGACGGCGATGCTTTAATGAA AGATGTTGAAGAAATAGCCACTGTGGTGGTACCCAAACATTACCAGGAGAAAATGCAGTGTGA TGTCGCTGTGGATGATGAAAAGG

I10	RT1-CE7	368153	RT1 class I, locus CE7	GCTCGCACTCGCTGCGGTATTTCACCACGGCGCTGTCCCGGCCCGGCCTCGGGGAGCCCCGGTTCATCTCTGTCGGCTACGTGGACGACACGGAGTTCGTGCGCTTCGACAGCGACGCGGAGAATCCGAGATACGAGCCGCGGGCGCCGTGGATGGAGCGGGAGGGGCTGGAGTATTGGGAGCAGCAGACACGGAGAGCC
I11	Actc1	29275	actin, alpha cardiac muscle	GGTGTCATGGTAGGTATGGGGCAGAAAGACTCCTATGTAGGTGACGAGGCTCAGAGCAAGCGAGGCATCCTGACTCTGAAGTACCCCATAGAGCACGGCATTATCACCAACTGGGACGACATGGAGAAGATCTGGCACCACACCTTCTACAATGAGCTCCGTGTGGCCCCTGAGGAGCACCCGACCCTGCTCACTGAGGC
I12	Itgb1bp2	317258	integrin beta 1 binding protein (melusin) 2	AGATGAAGACGAGGAAGAAGCTATGGGGGAATAGGAACAGCAGACAGTTGAGTTTCTAGGCAGGCCCTCAGTGACTGCCTTAGAATCTCAGAGACCAGGATAGGGTTGACTATGTGGTGTCATTGAGCAGCAGGAGGCTGAAGGAAGAGATAACAAAATGTCCAAACTGCTGCTGCCCCCTAATAAACCTTACATTCTGC
J01	Lag3	297596	lymphocyte-activation gene 3	TGACTCCTAAATCCTTCGGGTTACCTGGCTCCCCGCAGAAGCTGTTATGTGAGGTAGTCCCGGCATCTGGAGAAGGAAGATTTGTGTGGCGCCCCCTCAGCGATCTGTCCAGGAGTTCCCTGGGCCCTGTGCTGGAGTTGCAGGAGGCCAAGCTTCTGGCTGAGCAATGGCAGTGTCAGCTGTATGAGGGCCAGAAACTT
J02	Olfml1	361621	Olfactomedin-like-1	CCAGGAATTCTCAAAAAACCTATCCACCATGCTGGGGAGGTGTCAGACCCACACGAATGAGTACAGGAGTGCAGTGGATAACCTTGCCCTGAGAGTGGAGCGTGCCCAGCGGGAGATCGACTACCTGCAATACCTCAGGGAATCTGACTTCTGCGTTGAATCGGAGGAGAAGACATCAGCTGAAAAGGTGCTTCAAGAAG
J03	S100a4	24615	S100 calcium binding protein A4	AGAAGGACAGACGAAGCTGCATTCCAGAAGCTGATGAACAACTTGGACAGCAACAGGGACAATGAAGTTGACTTCCAGGAGTACTGTGTCTTCCTGTCCTGCATTGCCATGATGTGCAATGAATTCTTTGAGGGCTGCCCAGATAAGGAGCCCCGGAAGAAGTGA
J04	Tmem182	501129	transmembrane protein 182	GTGTCCTGTTTTCCCTGGTGGTGATACTGTATGTCATCTGGGTCCAGGCAGTGTCTGACATGGAAAGCTACAGAGCCTCGAAAATGAAAGACTGCTGGGAGTTCACGCCTTCTGTTCTGTACGGCTGGTCGTTTTTTCTGGCCCCGGCTGGAGTATTTTTCTCTCTGCTCGCTGGGCTACTCTTTCTTGTTGTTGGGTGGCATATCCAGACGCATCACTAA
J05	Tulp2	361576	tubby-like protein 2	ACAGTGCTTGGAACATGACCTGCCCCATGCCTCGCACTCCAGGTCCTCGGCTCGGGGAGGACATGGAAGCTTACGTGTTGCTCCCTGCACCCCGAGAACACATGGTGCAGTGCCGCATCGTCCGAAACAAGCATGGAGTGGACAAGGGCATGTTCCCTTCCTACTACCTCTACCTGGAGGCAGAGGATGGTGTAGCAGTA

J06	Ucn3	498791	urocortin-3	TCTCAGACGCTGTGGGTGGGAATGGAGGTAGAAGCATCCGGTACAGATACCAATCCCAAGCAC AGCCCAAAGGAAAGCTGTACCCGGACAAGGTCAAAAACGACCGGGGCACCAAGTTCACTCTG TCCCTCGACGTTCCCACTAACATCATGAACATCCTCTTCAACATTGACAAGGCCAAGAATTTGC GAGCCAAGGCA
J07	Zeb2	311071	zinc finger E-box-binding homeobox 2	TGGTGAACTATGACAACGTAGTGGACGCAGGTTCCGAAACAGACGAGGAGGACAAGCTGCAC ATTGCTGAGGATGACGGCATTGCAAACCCTCTGGACCAGGAGACGAGTCCAGCTAGCATGCCC AACCACGAGTCCTCCCCACACATGAGCCAAGGCCTGCTACCAAGAGAGGAAGAAGAAGACGA GATAAGGGAGAGC
J08	Apoe	25728	apolipoprotein E	GAGCAGACCCAGCAGATACGCCTGCAGGCCGAGATCTTCCAGGCCCGCATCAAGGGCTGGTTC GAGCCGCTAGTGGAAGACATGCAGCGCCAGTGGGCAAACCTAATGGAGAAGATACAGGCCTC TGTGGCTACCAACTCCATTGCCTCCACCACAGTGCCCCTGGAGAATCAATGATCATCCCTCACC TACGCCCTGCC
J09	Atp6v1g2	368044	ATPase, H+ transporting, lysosomal 13kDa, V1 subunit G2	GCCATGGGCTCTCAGGGGAACCTGTCTGCTGAGGTGGAGCAGGCCACGAGACGTCAGGTTCAG GGCATGCAGAGCTCCCAGCAGAGAAATCGGGAGCGAGTCCTGACTCAGCTTCTTGGCATGGTC TGTGACGTCAGACCCCAGGTCCACCCCAACTATCGGATTACTGTCTAG
J10	Erbb3	29496	v-erb-b2 avian erythroblastic leukemia viral oncogene homolog 3	GATTCTGCGGTTTTGGGGGGTCGTGAACAGTTCTCCCGTCCCATCTCTCTGCACCCAATTCCAC GGGGGCGTCCAGCATCAGAGTCATCAGAGGGCCACGTGACAGGCTCTGAGGCTGAACTCCAAG AGAAAGTGTCAGTGTGTAGGAGCCGAAGCCGGAGTCGGAGCCCGCGGCCTCGTGGGGACAGT GCCTACCATTC
J11	Adm	25026	adrenomedullin	CTCCGGGCAGGGGTCTGAGCCACTGCCTTGCCCGCTCATAAACTGGTTTTCTCACGGGGCATAC GCCTCATTACTACTTGAACTTTCCAAAACCTAGCGAGGAAAAGTGCAATGCTTGTTATACAGCC AAAGGTAACTATCATATTTAAGTTTGTTGATGTCAAGAGGTTTTTTTTTTTGTAACTTCAAATAT ATAGAAA
J12	Lhx3	170671	LIM homeobox protein 3	GCGCTTCGGGACCAAGTGCGCCGCATGCCAGCTGGGCATCCCGCCCACGCAGGTGGTGCGGCG CGCCCAGGACTTCGTGTACCACCTGCATTGCTTCGCCTGCGTGGTTTGCAAGCGGCAGCTGGCC ACGGGGGACGAGTTCTACCTCATGGAAGACAGCCGGCTGGTGTGCAAGGCGGACTACGAAAC AGCCAAGCAGCGAG
K01	Alb	24186	Albumin	CACACTCTCTTCGGAGACAAGTTATGCGCCATTCCAAAGCTTCGCGACAACTACGGTGAACTG GCTGACTGCTGTGCAAAACAAGAGCCCGAAAGAAACGAGTGTTTCCTGCAGCACAAGGATGAC AACCCCAACCTGCCACCCTTCCAGAGGCCGGAGGCTGAGGCCATGTGCACCTCCTTCCAGGAG AACCCTACCAGCTTTCTGGGACA

K02	Sstr1	25033	Somatostatin receptor 1	CAGCCTGAGAATCTGGAATCTGGAGGCGTTTTCCGTAATGGCACCTGCGCTTCCAGGATCAGC ACGCTTTGAGGCCGGACGCTAACCGGAGGGGGAGAGTGGTCAGAAAGGTGGAGAGGGGAAGC AGGTGGGAGGGAATGATAGCCGCACACCAGGTGCTATGGGAGTAGTGCGTGACAGCGATGCA GCGCCCCTGTTTA
K03	Igfbp1	25685	Insulin-like growth factor binding protein 1	CGCCGAGACACAAACCCAGCGAGCATTGAACACTGCACACGGCCATCTGCCCAGAGAGCTGTG ACCACCACTTCCGCTACTATCTACTCAGAAAGTCGTGACTACTGAGCCACTGCTGCCTGCCCAG ATTCTCATCCACCGCCTGCTGCGTCTGGTTGCGATGCCGGAGTTCCTAACTGTTGTTTCTTGGCC GTTCCTGA
K04	Ppargc1b	291567	Peroxisome proliferative activated receptor, gamma, coactivator 1 beta	AAAGAGGATGAGGAGGTGGGAGAGGATTGCCCAAGCCCCTGGCCAGCTCCAGCGTCTCCCCA AGACTCACTAGGACAGGACACGGCCAACCCCAACAGTGCCCAAGTTCCCAAGGACGACGTGA GGGCCATGGTACAGCTCATTCGCTACATGCATACCTACTGCCTGCCTCAGAGGAAGCTGCCCCA ACGGGCCTCAGA
K05	Cdh3	116777	Cadherin 3, type 1, P-cadherin (placental)	GAGTGGGGAAGTCGATTCAAGAAACTGGCTGACATGTATGGTGGCGGTGAGGATGACTAGACT GGCCGGCCATGCTGTCCAGGCAAGAACTACAGACAGGTCACAGCAGCATCTCAGGGGAGCTCT CACTCCTGCTCCTGAGGACTCTGAAGCTCGCCAGGAAGTCGCCCGCAAAGCAGGCTGCATCTG ACATGAAGGCT
K06	Vdac1	83529	voltage-dependent anion channel 1	GAAAAAAAATGCTAAAATCAAGACAGGGTACAAGAGGGAGCATATCAACCTGGGCTGTGATG TGGACTTTGACATCGCTGGGCCCTCAATCCGGGGCGCTCTGGTGCTTGGCTATGAGGGTTGGCT GGCTGGCTACCAGATGAATTTTGAGACCTCGAAGTCCCGAGTGACCCAGAGCAACTTTGCAGT TGGCTACAAGACGGACGAATTCCAGCTTCATACTAATGT
K07	Eif4e	117045	translation initiation factor 4E	AGGTTTGTTGTTTAAGAAGACACCTTCTGAGTATCCTCACAGGAGACTGCGTCACGCAATCGAG ATTGGGAGCTGAACCAAAGCCTCATCAAAGCAGAGTGGACTGCACTGAAGCTGACTCCATCCA AGTGTTGCTAAGATATAAGAGAAGTCTCATTCGCCTTTGTCTTGTACTTCTGTGTTCATTCTCCT CCCCCACC
K08	Mthfr	362657	5,10-methylenetetrahydrofolate reductase (NADPH) (predicted)	CAGGAATCCAGCCATGTCGAACGAGGCCAGAAGAAGTGGCAGCCCCAGCCCCCGATCTGAGG GCAGCAGCAGTGGCAGCGAGAGTTCCAAGGACAGTTCCAGATGTTCCACCCCCAGCCTGGACC CGGACCGGCACGAGAGACTGCGGGAGAAGATGAGACGCAGAATGGACTCTGGTGACAAGTGG TTCTCCCTGGAGTTCTTCCCTCCTCGGACAGCTGAGGGAGCTGTTAACCTCATCTCGAG
K09	Itgb4	25724	integrin beta 4	CGAGTCTGCCTTCCACTATGAGGCTGATGGTGCCAACGTGCTGGCCGGCATCATGAACCGCAA TGATGAGAAGTGCCACCTGGATGCCACAGGCGCCTACACCCAGTATAAGACCCAGGACTACCC ATCTGTGCCCACACTGGTTCGCCTGCTTGCCAAACACAACATTATCCCCATCTTTGCCGTCACC AACTACTCTT

K10	Zhx2	314988	Zinc fingers and homeoboxes 2	CCGGGGAGACCAACTTCAAGCTGAAGTTAATCAAGCGTAATAATCAGACGGTCCTAGAGCAGT CCATCGAGGCCACCAACCACGTTGTGTCCATCACTGCCAGTGCTCCTGGAAGTAGTGATAATG ACCCCGGGGTCTCAGTAGGTAAGACTGCCACGGTGAAGACAGGAAAGCAGAAGGCAGATGCC AAGAAAGTGCCC
K11	Nr4a1	79240	Nuclear receptor subfamily 4, group A, member 1	CCACATCTTCTTCCTCGTCCTCGGCCACCTCTCCCGCGTCGGCTTCCTTTAAGTTTGAGGACTTT CAGGTGTATGGCTGCTACCCTGGCACCCTGAGCGGCCCATTAGACGAGACCCTGTCCTCCAGTG GCTCTGATTACTATGGAAGCCCCTGCTCAGCCCCGTCACCACCTACACCCAACTTCCAGCCATC CCAGCTC
K12	Tp53	24842	Tumor protein p53	TGATCAAGAAAGTGGGGCCTGACTCAGACTGACAGCCTCTGCATCCTGTCCCCATCACCAGCCT CCCCGTCCCCTCCTTTCTTGCCATTTTATGACTTTAGGGCTTGTTATGAGAGCTGACAAGACAAT GCTAGTCCCTTCACTGCCTTTTTTTACCTTGTAGATAGTACTCGGCCCCCTCTATGCAAACTGGT TCCTGG
L01	Pkn3	296619	Protein kinase N3	CCTGTACTGTGAGAAGCGGATCCTGGAGACTGTGGGTCGTACAGGGCACCCGTTCTTGCTCTCT CTCCTTGCCTGCATCCAGACCTCCAGTCACGCCTGCTTTGTTACTGAGTTTCTGCCCGGAGGAG ACCTCATGATGCAGATCCACGAGGATGTCTTTCCTGAGCCCCAGGCCTG
L02	Ltb	361795	Lymphotoxin B	CCGATCCCCGTCTGCATCCTCAGAGATCCTATTCTTCCAGGAATCTAGATCCCACATCCCAGCG CCCTGTTGCACAGCCCTCTCGGGAGGCATCTGCATGGGTGACCACCCTGTCCCCAGCTGTGGAT TCTATACTAGATCCAGGGGTTCAACAGCTGCCATTGGGGGAACCAGAAACTGACTTCAGCCCC GAGCTTCCT
L03	Krt10	450225	Keratin 10	CAGCTTCGGTGGAGGAAGCTTCGGTGGAGGAAGCTTCGGCGGTGGGCTTGGAGGAGATGGTGG TGGCCTTCTCTCTGGAAATGAAAAGGTGACCATGCAGAACCTGAATGACCGCCTGGCCTCCTA CATGAACAAGGTCCGGGATCTGGAAGAGTCAAACTATGAGCTGGAGGGTAAAATCAAGGAGT GGTACGAGAAGC
L04	Arhgef26	310460	Rho guanine nucleotide exchange factor 26	GAGCACCCCTGGGCCCCGAAGGGGAGGAAAGCGAAGCCGACAACGACATAGACAGCCCGGGC TCCCTTCGGCGAGGCTTGCGGTCCACATCTTACCGAAGGGCAGTGGTCAGCGGTTTTGATTTTG ACAGTCCCACCAGCTCAAAGAAGAAGAACAGAATGTCCCAGCCTGTCCTGAAGGCGGTAATGG AAGACAAGGAG
L05	Angptl6	298698	Angiopoietin-like 6 (predicted)	GTGGGCTTTGGACGACCGGATGGAGAATACTGGCTGGGCTTGGAACCCGTGCATCAGGTGACT AGCCGCGGGGACCACGAGCTGCTGATACTCTTAGAGGACTGGGGGGGCCGTGGGGCACGCGC CCACTATGACAGCTTCTCCTTGGAACCCGAGAGTGACCACTACCGGCTGCGGCTTGGCCAGTAC CATGGTGATGC

L06	Itgb3bp	362548	Integrin beta 3 binding protein (beta3-endonexin)	ATGGGTTCTGGCCTTAGACTTCCTGCACCCTCATTTTCTTGCACACGTTCGGGCTCTTTCTCGCG TGGAGACTGTTTCGGAGGAGCCGCATTCGGTGTGACACCTCATTCAGTGCTTACTACGCGGGCT TTTTACACTTCCGCGTTTGTGGTTTCTCAATTGGTTCTGTCCAGCAACGGAGTCCCGAAATGCC
L07	Itga2b	685269	(integrin alpha 2B)	GAGGCATGACCTACTGGTGGGGGCTCCATTATACATGGAGAGCAGGGTGGACCGAAAGCTGGC CGAGGTGGGCCGTGTATACTTGTTTCTGCAGCCTAAGGGTCTCCAGGCTCTGAGCTCACCCACT CTCGTGCTGACCGGCACTCAGGTGTATGGGAGATTTGGATCTGCCATTGCACCCCTGGGTGACC TCAACCGAGACGGCTATAATG
L08	Lmx1b	114501	LIM homeobox trancription factor	GCTCTTCGCGGCAAAGTGCAGCGGCTGCATGGAGAAGATCGCACCCACTGAGTTCGTCATGCG GGCGCTCGAGTGTGTGTACCACCTGGGCTGTTTCTGCTGCTGTGTGTGCGAGAGGCAGCTGCGG AAGGGTGATGAGTTCGTGCTCAAGGAGGGCCAGCTGCTGTGCAAGGGTGACTACGAGAAGGA GAAAGACCTCCTCAGCTCCGTGAGCCCGGATGAGTCTGACTCTG
L09	Sfrp4	89803	secreted frizzled related protein 4	GGGAGTGCGCGGAGCGCCCTGCGAGGCTGTGCGCATCCCCATGTGTAGGCACATGCCCTGGAA CATCACCCGGATGCCCAACCACCTGCACCACAGCACTCAGGAGAACGCCATCCTGGCCATCGA GCAGTACGAGGAGCTGGTAGACGTGAACTGCAGCTCTGTACTGCGCTTCTTTCTCTGTGCCATG TACGCACCCA
L10	Vim	81818	vimentin	AATGAGTCCCTGGAGCGCCAGATGCGTGAAATGGAAGAGAATTTTGCCCTTGAAGCTGCTAAC TACCAGGACACTATTGGCCGCCTGCAGGATGAGATCCAGAACATGAAGGAAGAGATGGCTCGC CACCTTCGTGAATACCAGGACCTGCTCAATGTAAAGATGGCTCTTGACATTGAGATCGCCACCT ACAGGAAGCT
L11	Casp4	114555	caspase 4, apoptosis related cysteine peptidase	GGCATGGAATCAGAAATGAAAGACTTTGCTGCACTCTCAGAGCACCAAACATCAGACAGCACA TTCCTGGTGTTAATGTCTCATGGCACATTGCAGGGCCTTTGTGGAACAATGCACAGTGAAGCAA CTCCAGATGTGCTATTATATGATACTATCTATCAGATATTTAACAATTGTCACTGTCCAGGTCTA CGAGACAAACCCAAAGTCATCATTGTGCAGGCCTGCAGAGGTG
L12	Cpne4	367160	Copine IV	CAATATTTCATCCTGCTGATCCTGACAGACGGTGTCATCACAGACATGGCTGACACCCGGGAG GCCATCGTCCATGCCTCCCACCTTCCCATGTCCGTCATCATCGTGGGAGTGGGGAACGCCGACT TCAGTGACATGCAGATGCTGGACGGTGACGACGGAATTCTAAGGTCACCCAAGGGAGAGCCTG TCCTTCGAGACATCGTCCAGTTTGTGCCCTTCCGGAACTTCAAACAT
M01	RGD1306556	288744	similar to hypothetical protein A530094D01	ATGGCAACTCGGGTCGAAGTTGGCTCTATCGCATCCCTGAGGGCGGGGCCCGCCGGCCTTGGT GACATCGGCAGGGAGGAAACCCTGAAGAGGACCTACTTTTGCCAGACTGGGGACCTCCCTGGG GCGTCCTCCACCAGGATCCGAAGTGCAAAGAACCCCCTCCAGGCCCACCTGTTCCCACTACCC ATTGCGCCCAA

M02	Kcnq1	84020	Potassium voltage-gated channel, subfamily Q, member 1	GTGACACAACTGGACCAGAGACTGGTGATCATCACAGACATGCTCCACCAACTGCTGTCCCTG CAACAAGGTGGTCCAACCTGCAACAACAGGTCACAAGTCGTAGCCAGTGATGAAGGTGGCTCC ATCAACCCTGAGCTCTTCCTGCCCAGCAACAGCCTGCCCACCTATGAACAGCTGACTGTGCCCC AGACAGGCCCTGATGAAGGCTCCTGA
M03	Notch2	29492	Notch gene homolog 2 (Drosophila)	CCTGGAGCTCTGGGACAGAAAGTACAGACTCCTCAGAAGCTGAGGACAGTTCATCTTCTTCAT CTTGGGTGAGGTCATCAAAGTCCTCCTCCTCTTCTTCCTCAGCCCCGTCCTTCTCCGCTCCAGTG TCTGTTCCTGCTGGGGTTCCCACAGACTGACCATCAGCGTTGGCTGAGTCCTCAGGCTTCCCTG GAGGACTG
M04	Phactr3	362284	Phosphatase and actin regulator 3	ATGGATGTGCGTCTGTCCAGGACATCGAGCATGGAGCGGGGCAAGGAGAGGGATGAGGCGTG GAGCTTTGACGGGGCCTCAGAGAACAAGTGGACTGCTGCCAAAGACTCTGAGGAGAACAAGG AGAATCTGATTCTGAGCTCCGAGCTCAAGGATGACTTGCTTCTGTATCAGGATGAAGAGGCGC TCAACGACTCCAT
M05	Abcb1b	24646	ATP-binding cassette, sub-family B (MDR/TAP), member 1B	TTTCTAGATGGCAAAGAAATAAAACAACTCAACGTCCAGTGGCTCCGCGCCCACCTGGGCATT GTGTCCCAGGAGCCCATCCTGTTTGACTGCAGCATCACCGAGAACATCGCCTACGGAGACAAC AGCCGTGTCGTGTCTCATGAGGAGATCGTGAGGGCCGCCAGGGAGGCCAACATCCACCAGTTC ATCGACTCACTGCCTGAG
M06	Kitlg	60427	KIT ligand	CCGGGACTGAGAGTGCCGCGGGAAAGCAACGGCCAAGGACGGGGCGCTGCGCTCGAGCTACC CAATGCTGGGACTATCTGCAGCCGCTGCTCGTGCAATATGCTGGAGCTCCAGAACAGCTAAAC GGAGTCGCCACACCGCTGCCTGGGCTGGATCGCAGCGCTGCCTTTCCTTATGAAGAAGACACA A
M07	Sik1	59329	salt-inducible kinase 1	GGCTGAAGGCCTTCCGGCAGCAGCTAAGGAAAAACGCGAGGACCAAGGGGTTCCTGGGACTG AACAAGATCAAAGGATTGGCCCGTCAGGTGTGCCAGTCCTCCATCCGAGGTTCCCGGGGAGGG ATGAGTACCTTCCACACCCCGGCCCCAAGCTCAGGTCTGCAAGGCTGCACGGCCAGCAGTCGC GAGGGCAGGAGCCTGCTCGAAGAGGTGCTGCACCAGCAGAG
M08	Cd247	25300	CD247 molecule	GGTCTCAGCACTGCCACCAAGGACACCTATGACGCCCTGCATATGCAGACCCTGCCCCCTCGCT AACAGCCAGGGGATTTCTCACTCAAAGGCTTCACCTGCTGACGTCACTTGTGAAGGACGAGGA CAAAGCATTTACAACTCAGTTTATTAACTTCACAGACACCGTTTCCTGAAGAGGATGCTTCTCC CACTTGTCA
M09	Cd59	25407	CD59 molecule, complement regulatory protein	GAAAGCAAGTCTATCAACAGTGTTGGAGATTTTCGGATTGTAATGCCAAGTTCATTTTGAGCCG ACTAGAAATCGCAAACGTACAATACAGATGCTGCCAGGCGGACTTGTGTAACAAAAGCTTCGA AGACAAGCCAAACAATGGGGCAATCTCCCTATTGGGGAAGACAGCGTTGCTGGTGACCTCGGT TCTGGCGGCCATTTTGAAGCCTTGTTTCTAA

M10	Meis1	686117	Meis homeobox 1	TACGACGATCTACCCCATTATGGGGGCATGGATGGAGTAGGCATCCCCTCCACGATGTATGGG GACCCGCATGCAGCCAGGTCTATGCAGCCGGTCCACCACCTGAACCACGGGCCTCCTCTGCAC TCTCATCAGTACCCGCACACAGCTCATACCAACGCCATGGCCCCCAGCATGGGCTCCTCAGTCA ATGACGCTTTAAAGAGAGATAAAGATGCCATTTATGG
M11	Mt1a	24567	metallothionein 1a	GCTGCTGCTCCTGCTGCCCCGTGGGCTGCTCCAAATGTGCCCAGGGCTGTGTCTGCAAAGGTGC CTCGGACAAGTGCACGTGCTGTGCCTGAAGTGACGAACAGTGCTGCTGCCCTCAGGTGTAAAT AATTTCCGGACCAACTCAGAGTCTTGCCGTACACCTCCACCCAGTTTACTAAACCCCGTTTTCT ACCGAGCATGTGAATAATAAAAGCCTGTTTATTCT
M12	Tnfrsf25	500592	tumor necrosis factor receptor superfamily, member 25	ATGGAGGAGGTGCCTAGGAGGGAGAGGTCGCCTTCTGGGGCAGCCACAGCTGGGTCAGCTGC ACGTGTTCTCCAGCCTCTGTTCCTACCATCGCTGCTGCTGCTGCTGCTACTGCTGCTTGGTGGCC ATGGCCAGGGTGGTACGCCCGGCAGGTGTGACTGTGCCAGTGAGCCACAGAAGAGGTATGGCC AGCTTTGTTGCAGGGGCTGCCCAAAGG
N01	Il15	25670	interleukin 15	CCTCCGCCTGCTGCCCAGAGGCAGCACAGCTCCATGCATTCGTGATCTGCTGGGAAACCAAGC TGCCTAACAGGAAACGGTTGAGCCATTTGGATCCCATGAACCCTCGGGAATGAAGAGAGGGAA AGGGCTTTTCTCGGACTTATTTTTGCTTGCTTATTTTTAATTTATTACTTCAGTTGTGCATATTTG TAATATAA
N02	Rpl37	81770	ribosomal protein L37	ACATGGATTCCGTGAAGGAACAACACCTAAACCCAAGAGGGCAGCTGTTGCAGCATCCAGTTC ATCTTGAGGATTTCAATCGGTCATAAAATAAATGTTCTGGTTTCA
N03	Tgm1	60335	transglutaminase 1	GAAACAATCCTGAGGTGGGCAAGGGCACCCACGTGATCATCCCAGTGGGTAAGGGAGGCAGC GGTGGCTGGAAGGCCCAAGTGACTAAGACCAATGGACACAACCTAACCCTGCGCGTCCACACC TCCCCTAATGCCATCATTGGCAAGTTTCAATTCACTGTCCGTACACGCTCAGAGGCTGGCGAGT TCCAGCTGCCC
N04	Col18a1	85251	collagen, type XVIII, alpha 1	GACAACGAGGTAGCTGCCTTGCAACCTCCATTGGTACAGCTTCATGAGGGCAGTTCATATACCC GGAGGGAGCACTCCTATCCCACGGCACGACCCTGGCGAGCAGATGACATCTTGGCCAACCCAC CACGTCTGCCGGACCGCCAGCCTTACCCGGGAGTTCCACACCACCACCACCACCACCACC ACCACAGTTC
N05	Fbxl2	363156	F-box and leucine-rich repeat protein 2	AGCTTGTCCCACTGTGAGCTCATCACCGATGAAGGGATCCTACACTTGAGCAGCAGCACCTGT GGGCACGAGAGACTCCGGGTACTGGAGCTGGACAACTGCCTTCTTGTCACTGACGCCTCACTG GAGCACCTGGAGAACTGCCGGGGCTTGGAGAGACTGGAGCTGTACGACTGCCAGCAGGTCACC CGTGCAGGCATCAAGCGTATGCGG

N06	Tdrd5	289129	tudor domain containing 5	CCATTCCAGATGAATCCACCAAAGGAATAGCAAGTTTGGTTGCAAAGCAGAGAAGGAGCCATAAGGTCCGAAACTCCATGCAAAAGGGAAGAAGCAGCGTTTGCTCCGGCCGCGTGCCTTACCGCGGAAGGGTGCCCCCTATTCTCCCGGCAGTAGTGAAGAGTGAGTTGAAAGACCTTTTGGCATTGTCTCCTGTTCTC
N07	Antxr1	362393	anthrax toxin receptor 1	GAAAGAAAGAAAGGAGGGGAAGAAGGGGAGGGAGCAAAGACACCGCACTGCCCCAACCAAGAACAATTTGAAAACCCACCCCATCATACTTAAAAATCTAGGACAAAGAGCCGTCGGGACGGAACTGCTTCGACTGCAAAGCTTCGAGCGCAGCTTGGGAGCCGCCTGGTGGCCCGAGCCCGAGAGCTCCACAGAGCAGA
N08	Slamf1	498286	signaling lymphocytic activation molecule family member 1	AAGCATCCGCATCCTTGTCACGATGGCAAGGTCTCCAGGAAGCAAAACCAACAAGAAAATAGTGTCTTTTGATCTCTCGAAAGGGGGCTACCCAGATCACCTGGAGGATGGCTACCAGTTTCAATCCAAAAACCTAAGCCTGAAGATCCTAGGGAACAGGAGGGAGAGTGAAGGCTTGTACTTTGTGACCGTGGAAGAGA
N09	Htr1d	25323	5-hydroxytryptamine (serotonin) receptor 1D, G protein-coupled	TACCCCAGCCAACTATCTCATTGGCTCCTTGGCCACCACCGACCTCCTGGTTTCTATCTTGGTCATGCCCATCAGCATAGCCTATACCACCACCCGTACCTGGAACTTTGGCCAGATCCTGTGTGACATCTGGGTGTCTTCTGACATCACATGCTGTACGGCCTCCATCCTGCATCTCTGTGTCATCGCTCTGGACAGAT
N10	Nid2	302248	nidogen 2 (osteonidogen)	AGAATCGATGTGTCTTTCAATTCAGAGGTTAATCCCACGTCTCCAGATTCTGATCACGCTTCTCCTTTGCCACACCCAGCACCTGGTAACTGGCCATCCTACCGGGAAACAGAATCGGCTTCTTTGGACCCTCAAACCAAACAGGGGCCACCTGTGGGAGAGGTAGAGGTCCTGGATTTCAAGGACCCAGCAGAACTTTT
N11	Degs2	314438	delta(4)-desaturase, sphingolipid 2	CCAAGTACCCATCCATCAAGGCCCTGATGCGGCCAGACCCCAACATCAAGTGGACCGTGCTGGGAATGGTACTGGTGCAGGTGCTGGCCTGCTGGCTGGTACGGGGGCTCTCTTGGCGATGGTTGCTGTTTTGGGCCTATGCCTTTGGCGGCTGCATCAACCACTCACTGACACTGGCCATCCATGACATCTCGCACAAC
N12	Taar4	294122	trace amine-associated receptor 4	GACCAACTTCCTTATTCTCTCCATGGCTACCACAGACTTCCTGTTGAGCTGCGTGGTCATGCCCTTCAGTATGGTCCGGTCTATCGAGTCGTGCTGGTACTTCGGAGACCTCTTTTGCAAAGTCCACAGCTGCTGTGACATCATGCTCTGTACCACCTCCATTTTCCACCTCTGTTTCATCTCAGTGGACCGCCACTATG
O01	Gnmt	25134	glycine N-methyltransferase	TAAGTTTCGGCTCTCTTACTACCCACACTGTTTGGCGTCTTTCACGGAGTTGGTCCAAGAAGCCTTTGGGGGCAGGTGCCAGCACAGCGTCCTGGGTGACTTCAAGCCTTACAGGCCCGGCCAGGCCTACGTTCCCTGCTACTTCATCCACGTGCTCAAGAAGACAGGCTGAGCCTGGCTCCGGCTCCCACCCTAAGACC

O02	Zfp704	310233	zinc finger protein 704	AGGGTCTCAGCGGGTCCTGGAAGGAAGGCGCACCATCCAGCAGCAGCAGCAGTGGCTACTGG AGCTGGAGCGCTCCGAGTGACCAGTCCAACCCCTCCACACCCTCTCCGCCACTGTCGGCTGACA GCTTCAAGCCCTTCCGTAGCCCTGTTCCACTTGACGATGGCATCGATGAGGCAGAGGCCAGCA ACCTGCTCTTCGACGAGCCCATTCCCAGGAAGAGAAAG
O03	Kif26a	314473	kinesin family member 26A	TGCCCATTATCCCAGCCCTGAGTCGACGCAGGCCCTCCGAGGGACCCCGGGACGCTGACCACT TCCGCTGTAGTACTTTTGCAGAGCTGCAGGAGCGCCTGGAGTGTATAGATGGCAGTGAGGGAT TCCCTGGTCCCCAGGGCGGCTCTGACGGAGCCCAAGCCAGCCCCTCTCGGGGCAGCAGGAAAC CCTCCTTACCT
O04	Slc12a1	25065	solute carrier family 12 (sodium/potassium/chloride transporter), member 1	ATGTCAGTCAACATCCCTTCCAACTCAGTGCCCAGTGGTGCCAGTCGTTTCCAAGTCCATGTTA TAAATGAGGGCCATGGCAGTGGTGCAGCCATGAGTGACAGCACGGACCCCCCACATTATGAAG AGACCTCTTTCGGGGATGAAGCCCAAAACAGACTGAAAATCAGCTTTAGGCCTGGGAATCAGG AGTGCTATGA
O05	Mpa2l	305139	similar to guanylate binding protein family, member 6	CTATGTTACAGAACTCACTAAGCTGATCAGAGCAAGGTCTTCCCCAAATCCTGATGGAATCAA GAATTCCACAGAGTTTGTGAGTTTCTTTCCAGACTTTGTCTGGACTGTTCGAGATTTCATGCTGG AGCTGACGTTAAATGGGAAAAACATCACAAGTGATGAGTACCTAGAGAATGCCCTGAAATTGA TCCCAG
O06	Fam109b	688685	family with sequence similarity 109, member B	AGGGCTGTTGCCAGTCGCAGTAAATCTCAGGCTCCTGACCACCGGGCTCCAGGTCCTGAGAAT GGCCACTTTCTCCCTAGGGACGGCAATTCCATGGGTACTGTGGAAGAAAGGGGAATCCGGCCA ATAGGACGGGATTTGACTGAGTGGGAGTTACAGGGCCCTGCTAGCCTCCTCCTCAGCATGGGG CAGAGCCCCGT
O07	Sidt1	288109	SID1 transmembrane family, member 1	ACGAGTCGAGTTCCAGTCCTGGAAGGCAGATGTCTTCTTCCGATGGTGGGCAGCCATGCCACTC AGACACGGACAGCTCTGTGGAGGAGAGTGACTTCGACACTATGCCAGACATCGAAAGTGACA AAAACGTCATCCGGACCAAG
O08	Chrna2	170945	Cholinergic receptor, nicotinic, alpha polypeptide 2 (neuronal)	TGCAGATGGGGAGTTTGCGGTGACCCACATGACCAAGGCTCACCTCTTCTTCACGGGCACTGTG CACTGGGTGCCCCCAGCCATCTACAAGAGCTCCTGCAGCATCGATGTGACCTTCTTCCCCTTCG ACCAGCAGAACTGCAAGATGAAGTTTGGCTCCTGGACATATGACAAGGCCAAGATCGATCTGG AGCAGATGG
O09	Mast4	100912235	microtubule associated serine/threonine kinase family member 4	GCTACGGCGCAGATGGAAGACCGTCTGAAGGAAATCGTCACCAGCTACTCTCCAGACAACGTC CTCCCCTTGGCCGACGGGGTGCTTAGCTTCACTCACCATCAGATCATTGAGCTGGCTCGTGACT GTCTGGATAAATCCCACCAGGGTCTCATCACGTCAAGATATTTCCTTGAGTTGCAGCACAAGCT GGATAAGTTGCTGCAGGAG

O10	Gpr27	65275	G protein-coupled receptor 27	GGGCCCACGCCACCTGCGCTCGTGGGCATCAGGCCTGCAGGCCCGGGCCGCGGAGCCCGGCGC CTCCTGGTGCTGGAGGAATTCAAGACGGAGAAGAGGCTGTGCAAGATGTTCTACGCCATCACG CTGCTCTTCCTGCTCCTCTGGGGGCCCTATGTGGTTGCCAGTTACCTGCGCGTCCTGGTGCGGCC CGGAGCTGT
O11	Anxa8	306283	annexin A8	ACTTTTGAACCATAGGGAGCTTCCTCTACACTAGAGAATACTCTGGGGGAACACAGCCACTGA AGGAGCCCAGCAATACCAACAGCTCCGAGTGCGGAAGGGAATAGACTCATACCAGTAGAGCA CCGAGCGCAAACGCGTGCTGGGCACCTTCCTCGTCTCAAGCTGGGGTGCTTCCAGAGTGAAAG CTGAGGTTCTGG
O12	Ano9	499287	anoctamin 9	TGATCCAGTATGGCTTCACCACCATCTTTGTGGCCGCGTTCCCGCTCGCGCCCCTGTTGGCGCTC TTCAGCAACCTTGTGGAGATCCGCCTGGATGCCATCAAGATGGTCAGACTACAGCGGCGCCTG GTTCCTCGCAAGGCTAAGGACATAG
P01	Sgk2	171497	serum/glucocorticoid regulated kinase 2	GAGGGACCCGCTGACTTGAAAACTTTGACCCAGAGTTCACCCAGGAGGCTGTGTCCAAGTCCA TTGGCTGCACCCCTGACACCATGTCCAGCAGTTCTGGGGCCTCAAGTGCATTCCTCGGATTCTC CTATGCACAGGATGATGATGACATCTTGGACTCTTGA
P02	Kcnj12	117052	potassium inwardly-rectifying channel, subfamily J, member 12	CTGGGATCTGGCAGCCTCCCCCCGGCGTCTGAGTACCCCAACCTTGGCCACCTTCCCCTGGAAG TCTCAGGAACCCGGGGCTGAGATGTCTTCCCAGAATAGTCCCCGGGTTCCCCAGCCCCGCCAA CCCTCTGCCTCCTGGCCTAGACAGAAACAGCATCCACCATTACAGCCCCGAGCCTCAGCTACA AAGGCCCATG
P03	Plekhg1	679812	pleckstrin homology domain containing, family G (with RhoGef domain) member 1	ATGGAGCTTTCCGACAGTGACCGACCCATCAGCTTCGGCTCCACCTCATCCTCGGCCTCCTCCA GGGACAGCCATGGTTCCTTTGGCAGCAGAATGACTTTGGTTTCAAATAGCCACTTGGGCTTATT TCACCAGGATAAAGAAGCTGGGGCCATAAAGCTGGAGCTGGTACCAGCGCAACCATTTTCCAG CAGCGAGCT
P04	Cd6	25752	CD6 molecule	GAATCGGGCTGCTACAGAGGCTGCATGCAACGCACTGGGCTGTGGCGATTTGGGAAACTTTAC CCACCTGGCGCCACCCACCTCTGAGCGTCCACCAGGAGCCACTTCCCGGAACACTAGCAGCTC CAGGAATACGACATGGGCGGGGGCACCAACTGTGAGATGCCACGGAGCCAATTGGCAACTCT GCAAGGTGGAGG
P05	Emp3	81505	epithelial membrane protein 3	GTGCGGCTGTGTTCTCCGGGGCACTGATCTATGCCATCCATGCTAAGGAGATCCTGGCAAAGC ACCCGAGTGGAGGCAGCTTCGGCTACTGCTTCGCCCTGGCCTGGGTGGCCTTTCCACTCGCCCT GGTCAGTGGCATCATCTACATCCACCTGCGGAAACGAGAATGA

P06	Tas1r1	29407	taste receptor, type 1, member 1	TGCTGCGTCAGCCCCTCTTTTCTCTCGGGTTTGCCATCTTCCTCTCCTGCCTGACAATCCGCTCC TTCCAACTGGTCATCATCTTCAAGTTTTCTACCAAGGTGCCCACATTCTACCGTACCTGGGCCC AAAACCATGGTGCAGGTCTATTCGTCATTGTCAGCTCCACGGTCCATTTGCTCATCTGTCTCAC ATGGCTT
P07	Cckar	24889	cholecystokinin A receptor	TGTTACTTGCAGAAGTCCCGGCCCCCGAGGAAGCTGGAGCTTCAGCAGCTGTCTAGCGGCAGC GGTGGCAGCAGACTCAACCGGATCAGGAGCAGCAGTTCAGCTGCCAACCTGATAGCCAAGAA GCGCGTGATCCGCATGCTCATTGTCATCGTGGTCCTCTTCTTCCTGTGCTGGATGCCCATCTTCA GCGCCAACGC
P08	Lsamp	29561	limbic system-associated membrane protein	GTGTGTGGTAGAAGACAAGAACTCGAAAGTGGCCTGGTTGAACCGCTCTGGCATCATCTTCGC TGGACACGACAAGTGGTCTCTGGACCCTCGGGTTGAGCTGGAGAAACGCCATGCTCTGGAATA CAGCCTCCGAATCCAGAAGGTGGATGTCTATGATGAAGGATCCTACACATGCTCAGTTCAGAC ACAGCATGAGCCCAAGACCTCTCAAGTTTACTTGATTGTACAAG
P09	Rph3a	171039	rabphilin 3A homolog (mouse)	GTCTGGAAGCGCTCGGGAGCATGGTTCTTCAAGGGTTTCCCAAAACAGGTCCTTCCACAGCCC ATGCCTATAAAGAAGACCAAGCCCCAGCAGCCTGCTGGTGAGCCGGCCACCCAGGAGCAGCCT ACACCCGAGTCCAGGCATCCAGCCAGAGCTCCAGCTCGAG
P10	Npffr2	78964	neuropeptide FF receptor 2	GGCCAAACCAGGAAATGAGGAGGATCTACACCACCGTGCTCTTTGCCACTATCTACCTGGCTC CACTCTCCCTCATTGTTATCATGTATGCAAGGATTGGGGCTTCCCTCTTCAAGACCTCAGCACA CAGCACAGGTAAGCAGCGCCTGGAGCAGTGGCATGTATCCAAGAAGAAACAGAAGGTCATCA AGATGCTGCTG
P11	P2rx2	114115	purinergic receptor P2X, ligand-gated ion channel, 2	CAAGTAGATGGCCTGTGACCCTTGCCCTTGTCTTGGGCCAGATCCCTCCCCCACCTAGTCACTA CTCCCAGGATCAGCCACCCAGCCCTCCATCAGGTGAAGGACCAACTTTGGGAGAAGGGGCAGA GCTACCACTGGCTGTCCAGTCTCCTCGGCCTTGCTCCATCTCTGCTCTGACTGAGCAGGTGGTG GACACACTT
P12	Glp1r	25051	Glucagon-like peptide 1 receptor	GTCCAGATGGAGTTTCGGAAGAGCTGGGAGCGCTGGAGGCTGGAGCGCTTGAACATCCAGAG GGACAGCAGCATGAAACCCCTCAAGTGTCCCACCAGCAGTGTCAGCAGTGGGGCCACGGTGGG CAGCAGCGTGTATGCAGCCACCTGCCAAAATTCCTGCAGCTGA

APPENDIX 5: PUBLISHED ARTICLES

Recent advances in understanding GLP-1R (glucagon-like peptide-1 receptor) function

Cassandra Koole*, Kavita Pabreja*, Emilia E. Savage*, Denise Wootten*, Sebastian G.B. Furness*, Laurence J. Miller†, Arthur Christopoulos* and Patrick M. Sexton*[1]

*Monash Institute of Pharmaceutical Sciences and Department of Pharmacology, Monash University, 381 Royal Parade, Parkville 3052, Victoria, Australia, and †Department of Molecular Pharmacology and Experimental Therapeutics, 13400 E. Shea Blvd., Scottsdale, AZ 85259, U.S.A.

Abstract

Type 2 diabetes is a major global health problem and there is ongoing research for new treatments to manage the disease. The GLP-1R (glucagon-like peptide-1 receptor) controls the physiological response to the incretin peptide, GLP-1, and is currently a major target for the development of therapeutics owing to the broad range of potential beneficial effects in Type 2 diabetes. These include promotion of glucose-dependent insulin secretion, increased insulin biosynthesis, preservation of β-cell mass, improved peripheral insulin sensitivity and promotion of weight loss. Despite this, our understanding of GLP-1R function is still limited, with the desired spectrum of GLP-1R-mediated signalling yet to be determined. We review the current understanding of GLP-1R function, in particular, highlighting recent contributions in the field on allosteric modulation, probe-dependence and ligand-directed signal bias and how these behaviours may influence future drug development.

Introduction

Type 2 DM (diabetes mellitus) is a global epidemic, with worldwide prevalence increasing exponentially and future projections estimating that almost 10% of the adult population will suffer from the condition by the year 2030 [1]. A complex disease, arising from multiple aetiological factors including genetic predisposition and modern lifestyle, Type 2 DM is typically diagnosed by chronic hyperglycaemia; however, the two distinct features allowing disease progression are impaired β-cell function and a target organ reduction in sensitivity to insulin. In the later stages of the condition, the continual demand for elevated insulin to compensate for insulin insensitivity results in β-cell exhaustion and glucose toxicity [2]. Aside from these characteristic traits of Type 2 DM, there are also many other associated pathophysiologies including vascular dysfunction, the consequences of which include retinopathy, nephropathy, neuropathy and atherosclerosis, the latter increasing the risk of heart attack and stroke in addition to significantly increasing the risk of cardiovascular mortality [2]. The evolution of understanding into both the physiology of glucose homoeostasis as well as the pathophysiology of Type 2 DM has highlighted the importance of endogenously produced incretin hormones in facilitating nutrient-induced insulin biosynthesis and secretion, as well as preserving β-cell function, decreasing β-cell apoptosis, slowing gastric emptying, and enhancing insulin sensitivity at peripheral tissues (reviewed in [3]). This article provides a brief overview of the GLP-1R (glucagon-like peptide-1 receptor), the major target of incretin mimetic therapies, and highlights some of the previous work on this receptor.

Key words: allosteric modulation, biased signalling, G-protein-coupled receptor, glucagon-like peptide-1 receptor, glucagon-like peptide-1, probe-dependence.

Abbreviations used: BETP, 4-(3-(benzyloxy)phenyl)-2-(ethylsulfinyl)-6-(trifluoromethyl) pyrimidine; DM, diabetes mellitus; DPPIV, dipeptidyl peptidase IV; EGFR, epidermal growth factor receptor; ERK1/2, extracellular-signal-regulated kinase 1 and 2; GLP-1R, glucagon-like peptide-1 receptor; GPCR, G-protein-coupled receptor; GRK, G-protein-coupled receptor kinase; PAM, positive allosteric modulator; PI3K, phosphoinositide 3-kinase; PK, protein kinase.

[1]To whom correspondence should be addressed (email patrick.sexton@monash.edu).

Physiology of the incretin system

Accounting for as much as 70% of insulin secreted from pancreatic β-cells following nutrient consumption, incretin hormones are key mediators in communicating nutrient content of the gastrointestinal tract to insulin producing pancreatic β-cells [3]. The principal incretin hormones include GLP-1, primarily expressed in L cells of the ileum and colon, and gastric inhibitory polypeptide/glucose-dependent insulinotropic polypeptide, primarily expressed in K cells of the duodenum and jejunum. Although secreted levels of both incretin hormones are reduced in Type 2 DM subjects, only GLP-1 has been observed to retain its potent insulinotropic activity, and has therefore attracted significant interest in the development of Type 2 DM therapeutics [4].

The principal stimuli for GLP-1 secretion is nutrient content of the gastrointestinal tract [5]; however, the mechanisms behind GLP-1 secretion are complex and largely unclear, with multiple factors thought to impact on its release, including neural and endocrine factors (reviewed in [6]). GLP-1 is rapidly secreted postprandially, peaking at 10–15 min followed by a sustained peak at 30–60 min [5]. The insulinotropic effects induced by secreted GLP-1 are mediated through interaction with its transmembrane expressed GPCR (G-protein-coupled receptor), the GLP-1R, promoting intracellular signalling mechanisms to aid in increasing the expression, biosynthesis and secretion of insulin from pancreatic β-cells in a glucose-dependent manner [7]. Highlighting the importance of GLP-1-mediated

signalling in the endocrine pancreas, all studies of *GLP-1R*$^{-/-}$ mice observe at least a modest reduction in glucose tolerance and impaired glucose-stimulated insulin secretion [8]. In addition to glucoregulation, GLP-1 has a fundamental role in increasing neogenesis, proliferation and decreasing apoptosis of pancreatic β-cells in animal models, leading to an increase in β-cell mass and subsequently aiding the glucose-dependent augmentation of insulin secretion [9].

Aside from the pancreatic effects, there is significant evidence illustrating biological actions of GLP-1 via its receptor in other tissues (extensively reviewed in [3]). Briefly, GLP-1 activity suppresses appetite and inhibits gastric emptying, in turn influencing ingestive behaviour. Other roles include inhibition of glucagon release and augmenting glycogen synthase activity in muscle, adipose and hepatic cells, favouring incorporation of glucose into glycogen. Furthermore, GLP-1 and GLP-1-related peptides enhance peripheral insulin sensitivity and reduce steatosis. In the nervous system, GLP-1 augments neogenesis, proliferation and anti-apoptotic behaviour of neuronal cells, enhancing memory, and spatial and associative learning. Other documented roles include contribution to normal cardiovascular, respiratory and renal function. The diverse and beneficial actions of GLP-1 have consequently attracted significant attention in the development of therapeutics that mimic the endogenous GLP-1 system, particularly for the management of Type 2 DM.

GLP-1 receptor

The GLP-1R is a 463-amino-acid transmembrane-spanning protein belonging to the family B/secretin GPCRs, mediating the effects of both endogenous GLP-1 peptides [four forms: GLP-1(1–36)NH_2, GLP-1(7–36)NH_2, GLP-1(1–37) and GLP-1(7–37)], as well as the endogenous peptide oxyntomodulin and exogenous peptide exendin-4 (Figure 1A). Characteristic of family B GPCRs, the GLP-1R possesses a long extracellular N-terminus with an α-helical region, five β-strands forming two antiparallel β-sheets and six conserved cysteine residues that form disulfide interactions [10–12]. Together, these features allow the receptor to adopt the classic 'Sushi domain' or 'short consensus repeat', which aids N-terminal stability and confers a high level of structural homology within the N-terminal regions of family B GPCRs. The large extracellular N-terminus has a significant role in peptide binding, supported by GLP-1 binding the isolated N-terminus of the GLP-1R [13] and crystal structures of the isolated GLP-1R N-terminus in complex with GLP-1 and exendin peptides [11,12]. Specifically, the C-terminus of the peptide interacts with the N-terminus of the receptor, which is proposed to be responsible for ligand recognition and specificity, while the N-terminus of the peptide is proposed to associate with the core of the receptor, and is suggested to have a major influence in signalling specificity and transmission [14,15]. This widely accepted two-domain model of ligand binding is also experimentally supported by chimaeric receptors [16,17], photolabile peptide cross-linking [18–20], and to some extent, mutagenesis analysis [21–25]. However, despite the seemingly abundant data, there is still a wide knowledge gap with respect to the complete structure of any receptor in this family, as well as whether a definitive binding crevice exists that is common across all receptors of the family. Furthermore, the orientation of the receptor N-terminus in relation to the transmembrane bundle is uncertain, and has been inherently difficult to establish either experimentally or using molecular modelling [15,20].

GLP-1R signalling and regulation

The physiological changes observed with increases in GLP-1, including increases in insulin secretion and β-cell mass, rely on signalling via GLP-1R-mediated intracellular pathways (Figure 2). The GLP-1R is a pleiotropically coupled receptor, with evidence for signalling via multiple G-protein-coupled pathways including $G_{\alpha s}$, $G_{\alpha i}$, $G_{\alpha o}$ and $G_{\alpha q/11}$ [26,27]. However, the GLP-1R is most well documented for its role in $G_{\alpha s}$ coupling, favouring production of cAMP through increasing enzymatic activity of adenylate cyclase [7]. This subsequently promotes increases in both PKA (protein kinase A) and Epac2 (exchange protein activated by cAMP-2), which is directly involved in enhancing proinsulin gene transcription [28]. Furthermore, GLP-1R activation induces membrane depolarization of β-cells through inhibition of K^+ channels, allowing VDCCs (voltage-dependent Ca^{2+} channels) to open and acceleration of Ca^{2+} influx to occur, resulting in the exocytosis of insulin from β-cells. Therefore the production of cAMP and influx of Ca^{2+} are vital components in the biosynthesis and secretion of insulin. GLP-1R activity also promotes EGFR (epidermal growth factor receptor) transactivation, PI3K (phosphoinositide 3-kinase) activity, IRS-2 (insulin receptor substrate-2) signalling, and subsequently, ERK1/2 (extracellular-signal-regulated kinase 1 and 2) activity, as well as nuclear translocation of PKCζ to mediate β-cell proliferation and differentiation as well as promote insulin gene transcription (reviewed in [3]). Aside from G-protein-coupled pathways, there are recently emerging studies suggesting that GRK (GPCR kinase) and β-arrestin recruitment are involved in optimal GLP-1R function [29–32]. Clear evidence for this is seen in β-cell knockdown of β-arrestin-1, that results in attenuated cAMP and consequently diminished insulin secretion [29]. There is also evidence supporting β-arrestin-1-mediated ERK1/2 activation as a mechanism for β-cell preservation [32]. Although GRKs and β-arrestins are well documented for their role in regulating cell-surface receptor function and expression through receptor desensitization and internalization, it is unclear how these scaffolding proteins regulate this process at the GLP-1R.

GLP-1 mimetics in the treatment of Type II DM

With the ability to address almost all manifestations of Type 2 DM, the GLP-1R system has become one of the

Figure 1 | Peptide and small molecule ligands of the GLP-1R

(**A**) Peptide ligands of the GLP-1R, including four endogenous forms of GLP-1, two of which have glycine residues extended at the C-terminus [GLP-1(1–37) and GLP-1(7–37)] and two of which have undergone C-terminal amidation (GLP-1(1–36)NH_2 and GLP-1(7–36)NH_2). DPPIV degradation yields N-terminally truncated metabolites GLP-1(9–37) and GLP-1(9–36)NH_2. The endogenous agonist oxyntomodulin and the exogenous agonist exendin-4 share high homology in the N-terminal region of the peptide. The clinically used GLP-1 analogue, liraglutide (NN2211), shares the same amino acid sequence as GLP-1(7–37), but with modifications as indicated. (**B**) Compound 2 (6,7-dichloro2-methylsulfonyl-3-t-butylaminoquinoxaline), synthetic allosteric agonist and positive modulator of cAMP formation. (**C**), Boc5, synthetic allosteric agonist in cAMP formation. (**D**) S4P, synthetic allosteric agonist in cAMP formation. (**E**) Quercetin (3,3′,4,5,7-pentahydroxyflavone), naturally occurring PAM (positive allosteric modulator) of intracellular Ca^{2+} mobilization. (**F**) Compound B/BETP, 4-(3-(benzyloxy)phenyl)-2-(ethylsulfinyl)-6-(trifluoromethyl)pyrimidine, synthetic allosteric agonist in cAMP formation.

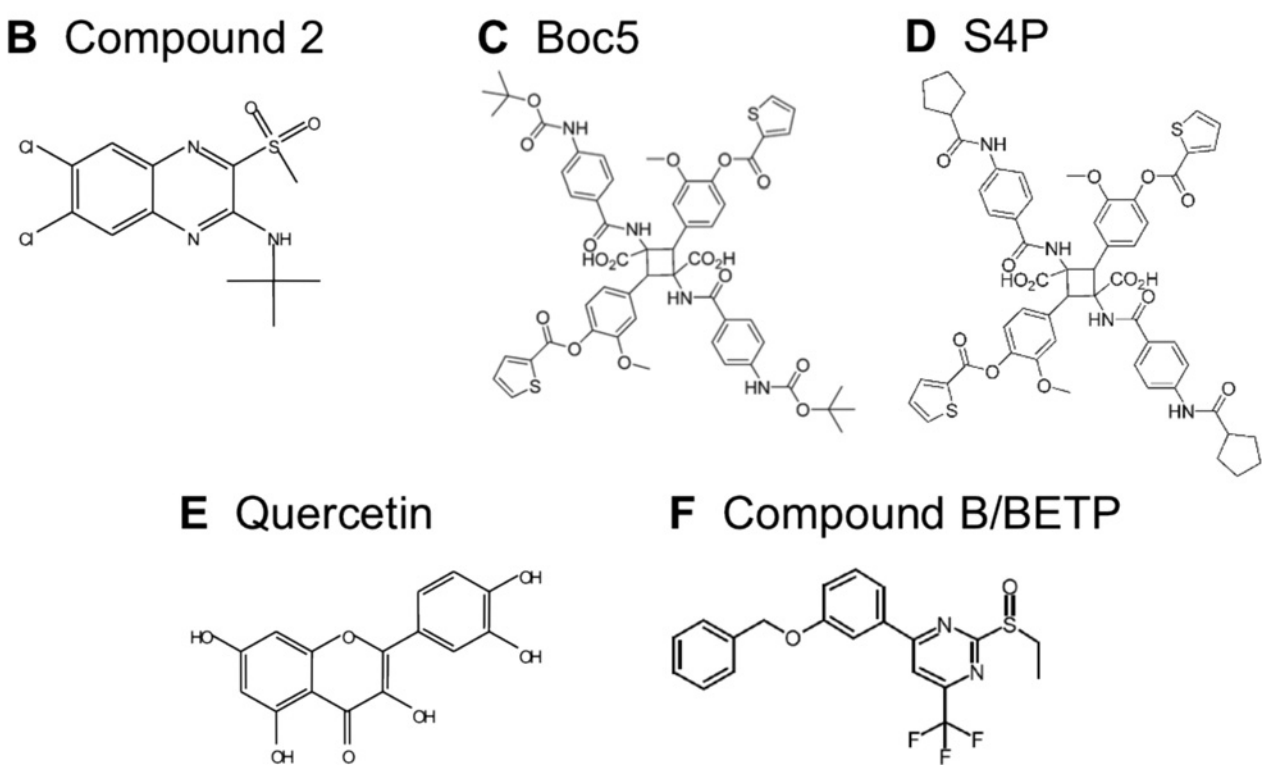

most appealing targets in the development of therapies for management of the condition. However, the leading problem in enhancing this system with GLP-1 administration directly is the rapid breakdown of the peptides by the enzyme DPPIV (dipeptidyl peptidase IV) into low activity metabolites. As such, the most prominent avenue of drug development aims to imitate endogenous peptide activity but limit peptide breakdown (GLP-1 mimetics). The most well-known GLP-1 mimetic prescribed for the management of Type 2 DM is exenatide (Byetta®), a synthetically produced equivalent

Figure 2 | GLP-1R-mediated signalling in pancreatic β-cells

Signalling in pancreatic β-cells via the classical GLP-1R-coupled $G_{\alpha s}$ pathway mediates increases in cAMP to up-regulate PKA and Epac2 (exchange protein activated by cAMP 2), enhancing $_{i}Ca^{2+}$ (intracellular Ca^{2+}) mobilization and calcineurin/NFAT (nuclear factor of activated T cells). In association with increases in $_{i}Ca^{2+}$ through inhibition of K^{+} channels and acceleration of Ca^{2+} influx through VDCCs (voltage-dependent Ca^{2+} channels), these pathways lead to increases in insulin biosynthesis and secretion (green). Activation of proto-oncogene tyrosine kinase src (c-src), increases in β-cellulin and subsequent transactivation of EGFR aid in increasing PI3K, IRS-2 and PKB (Akt) to enhance β-cell neogenesis and proliferation (blue). This is also facilitated in part by PKA-mediated increases in MAPKs (mitogen-activated protein kinases) and cyclin-D1. Inhibition of caspases, FoxO1 (forkhead box protein O1) and NF-κB (nuclear factor κB), in addition to regulation of CREB (cAMP-response-element-binding protein) and protein survival factors Bcl-2 and Bcl-XL, aid in the inhibition of apoptosis (orange), a process also mediated by β-arrestin-1 and the pERK1/2 (phosphorylation of ERK1/2). ER (endoplasmic reticulum) stress reduction (pink) involves the up-regulation of multiple transcription factors, including ATF-4 (activating transcription factor-4), CHOP [C/EBP (CCAAT/enhancer-binding protein)-homologous protein], and Gadd34 (growth arrest and DNA damage-inducible protein), which inhibits the dephosphorylation of eIF2α (eukaryote initiation factor 2 α). Cross-talk exists between most pathways, including the regulation of the important promotor of insulin gene transcription, synthesis and secretion, Pdx-1 (pancreas duodenum homeobox-1) via both cAMP-dependent and IRS-dependent mechanisms.

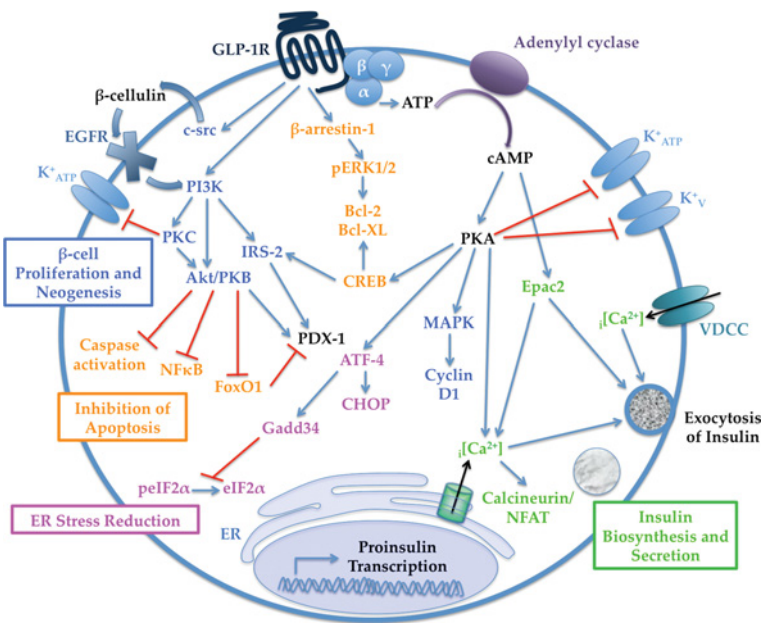

of the venom-derived peptide exendin-4 (Figure 1A). Similar to GLP-1, exendin-4 decreases plasma glucose levels immediately following nutrient ingestion in both healthy and diabetic subjects, promotes β-cell proliferation, and augments the synthesis and secretion of insulin [33]. However, unlike GLP-1, exendin-4 is resistant to the proteolytic activity of DPPIV, prolonging its activity *in vivo*.

Unlike exendin-4, all other GLP-1 mimetics are synthetically developed, modified GLP-1 peptides that are designed to take advantage of the peptide's specificity for the receptor, but have alterations to enhance stability and/or function *in vivo*. These modifications typically involve the substitution of Ala^{8} of the GLP-1 peptide, such that the peptide becomes resistant to enzymatic degradation by DPPIV. Examples of this include (Val^{8})GLP-1, (Thr^{8})GLP-1, (Ser^{8})GLP-1 and (Gly^{8})GLP-1, each of which display insulinotropic activity and enhanced metabolic stability [34].

Peptide modifications through fatty acid derivatization have also been pursued in order to extend biological half-life in plasma. A well-recognized example of this is liraglutide (NN2211, Victoza®), which covalently couples a hexadecanoic fatty acid at the Lys^{26} residue of the GLP-1 peptide, as well as containing an arginine substitution at residue 34 [35] (Figure 1A). Similar to GLP-1 and exendin-4, liraglutide significantly improves glycaemic control, enhances β-cell function and promotes weight loss, and, similar to exendin-4, has a significantly improved plasma half-life due to DPPIV resistance [33].

There are many other synthetically engineered peptide analogues for the GLP-1R that have been shown to have insulinotropic activity and enhanced metabolic stability, including the GLP-1 analogues LY315902 and CJC-1131 and the albumin-conjugated dimeric GLP-1 analogue, albiglutide [34,36], and exendin-4 analogues AC3174 and CJC-1134-PC

[36,37]. In another previous study, modification through biotin and polyethylene glycol labelling of GLP-1 and exendin-4 peptides have been explored as a means to aid oral delivery of antidiabetic treatments through enhancing intestinal absorption [38].

Collectively, synthetically produced GLP-1 and exendin-4 analogues illustrate that biological activity can be mimicked and in some cases favourably enhanced. However, generation and application of peptides remains a difficult and complex task, with peptide stability and administration route a major challenge, as well as controversy over the long-term consequences of use, including reports of pancreatitis and C-cell hyperplasia, a precursor for thyroid cancer [39,40]. In addition, all analogous peptides are coupled to some extent with adverse side effects, the most prominent being nausea. For this reason, there is significant interest in novel treatments that have similar physiological effects to GLP-1, but which can be administered orally and eliminate, or at least minimize, side effects.

Biased signalling

GPCRs are widely accepted to be promiscuous, signalling via multiple G-protein-dependent and -independent mechanisms on receptor activation. It has become increasingly evident that in such pleiotropically coupled receptor systems, receptor activation can engender differential effects via multiple pathways depending on the ligand present in the system. This phenomenon is termed 'biased signalling', but may also be referred to as ligand-directed signalling, ligand-directed stimulus bias, functional selectivity or stimulus trafficking, and is a result of different ligands stabilizing distinct receptor conformations, which subsequently influence the nature and strength of pathway coupling that may include alterations to G-protein coupling profiles, but also to non-G-protein signalling pathways such as those mediated by β-arrestins [41]. Biased signalling has been observed at many receptors including the pituitary adenylate cyclase-activating polypeptide receptor, 5-hydroxytryptamine 2c receptor, μ-opioid receptor, dopamine receptors, V_2 vasopressin receptor, β_2-adrenergic receptor and recently at the GLP-1R [41,42].

Recent analytical advances in the field have demonstrated that bias in a system can be quantified through estimating τ/K_A ratios, where τ equates to the efficacy in the system [24,25]. This is a novel method to determine signalling bias in a system where profound reversal of potencies is not observed. At the GLP-1R, all peptide agonists preferentially activate cAMP over ERK1/2 and Ca^{2+} *in vitro*. However, the relative degree of bias is variable between ligands, with truncated GLP-1 peptides and exendin-4 having greater bias towards cAMP than full-length GLP-1 peptides and oxyntomodulin (Figure 3) [24,25,42]. This is particularly important to consider in pharmacological characterization of any receptor, and may have the potential to be exploited in the rational design of therapeutics that target pathways associated with beneficial effects over pathways that are associated with detrimental effects.

Figure 3 | Biased signalling at the GLP-1R

Degree of bias of GLP-1R peptide agonists for (**A**) cAMP/pERK1/2, (**B**) pERK1/2/$_i$Ca^{2+} and (**C**), cAMP/$_i$Ca^{2+} relative to the values for GLP-1(7–36)NH_2 (control agonist), where τ is coupling efficacy, corrected for cell-surface expression (c), and K_A is the affinity of the agonist. Statistical significance of changes in coupling efficacy in comparison with GLP-1 (7–36)NH_2 is indicated with an asterisk ($^*P<0.05$). Data taken from [42].

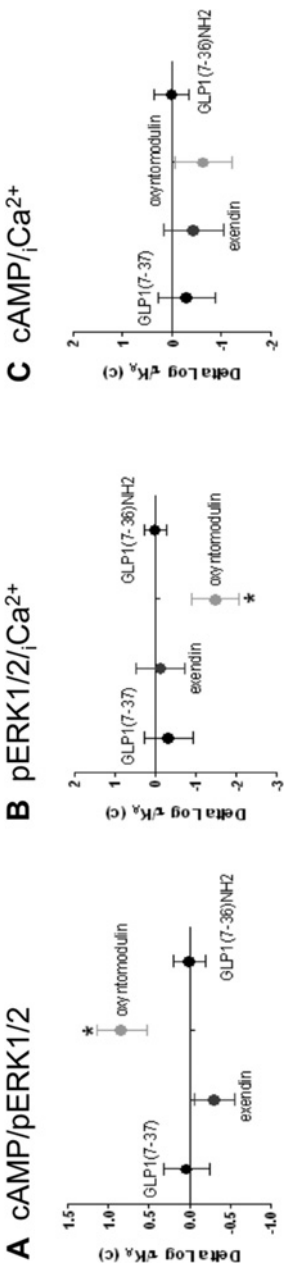

Allosteric modulation

Aside from both the endogenous and exogenous peptide agonists, there have been several synthetic and naturally occurring ligands of the GLP-1R that have been proposed to act allosterically, that is, at sites distinct to the endogenous ligand (Figures 1B–1F). From a therapeutic perspective, ligands acting allosterically have several major advantages,

including enhanced receptor subtype selectivity, the ability to simultaneously bind to the receptor with the endogenous ligand (restoring physiologically relevant temporal control), inducing a new repertoire of receptor conformations and therefore influencing receptor activity, and in particular for peptide-activated receptors, the potential for oral administration. With respect to the GLP-1R, allosteric ligands that enhance the insulinotropic effects of the system are desired [PAMs (positive allosteric modulators)].

At present, very few allosterically acting ligands have been identified for the GLP-1R. The Novo Nordisk compounds 2-(2′-methyl)thiadiazolylsulfanyl-3-trifluoromethyl-6,7-dichloroquinoxaline (compound 1) and 6,7-dichloro-2-methylsulfonyl-3-t-butylaminoquinoxaline (compound 2) [43] were the first non-peptide agonists identified for the GLP-1R, the latter of which demonstrates glucose-dependent insulin release via the GLP-1R [44,45]. Similarly, the cyclobutanes Boc5 and S4P stimulate GLP-1R activity, whereas the inability to fully inhibit ^{125}I-GLP-1(7–36)NH_2 binding suggests an allosteric mechanism of action [43,46]. Although S4P is only a partial agonist in GLP-1R-expressing immortal cell lines, Boc5 is a fully efficacious agonist with maximal responses for decreasing plasma glucose and reducing nutrient intake in obese mice, comparable with the native GLP-1 peptide [47]. Unlike the compounds detailed above, quercetin (3,3′,4,5,7-pentahydroxyflavone) is a naturally occurring compound belonging to the flavonoid family, and has been observed to allosterically enhance GLP-1 efficacy and potency in intracellular Ca^{2+} mobilization *in vitro* [42,48]. The most recently identified allosterically acting synthetic ligand of the GLP-1R, 4-(3-(benzyloxy)phenyl)-2-(ethylsulfinyl)-6-(trifluoromethyl)pyrimidine (BETP or compound B), increases glucose-dependent insulin release from normal and diabetic human islet cells [49]. Support for an allosteric mode of action is seen in the removal of the GLP-1R N-terminus, which does not influence the activity of the compound [49].

Although several additional synthetic small molecule ligands have been reported to increase GLP-1R-mediated cAMP production, increase plasma GLP-1 levels or decrease acute nutrient intake (reviewed in [50]), they have not been fully characterized pharmacologically, and thus it remains to be determined whether they are true GLP-1R ligands. Although allosteric modulation is fast gaining traction as a desired therapeutic approach to many disorders and conditions, there are many challenges in the identification and application of allosteric modulators. One most prominent complexity is that of probe-dependence, which describes the extent and direction of allosteric modulation on an orthosteric ligand (the probe), and is correlated with the co-operativity between the allosteric and orthosteric ligand in the system (reviewed in [51]). Indeed, this has already been observed at the GLP-1R *in vitro* and *in vivo*, with differential effects observed between orthosterically acting peptide ligands and the allosteric ligands BETP or compound 2, with preferential enhancement of signalling via oxyntomodulin relative to GLP-1 or exendin-4 [42,52]. Intriguingly, these allosteric compounds also markedly enhance the activity of the inactive metabolite of GLP-1 (GLP-1(9–36)NH_2), suggesting that therapies directed to altering metabolite activity may be possible [53]. Although the physiological importance of probe-dependence is yet to be determined, it illustrates an important consideration when pharmacologically characterizing allosteric ligands at receptors possessing multiple orthosteric ligands.

Conclusions

The rapidly increasing incidence of Type 2 DM and significant impact on quality-of-life demands the development of superior therapeutics for the management of the condition. Despite the GLP-1R having a pivotal role in glucose homoeostasis and currently being a highly valued therapeutic target, there are still significant knowledge gaps that limit understanding of this complex receptor system, particularly with respect to receptor structure and the nature of allosterism. In addition, the physiological importance of biased signalling and probe-dependence remains largely unexplored. Further research into these aspects of receptor function will have an impact on the future design and development of therapeutics for the management of Type 2 DM.

Funding

This work was supported by the National Health and Medical Research Council of Australia (NHMRC) [grant numbers 519461 and 1002180], with Senior Research Fellowship awarded to A.C. and Principal Research Fellowship awarded to P.M.S.

References

1 Shaw, J.E., Sicree, R.A. and Zimmet, P.Z. (2010) Global estimates of the prevalence of diabetes for 2010 and 2030. Diabetes Res. Clin. Pract. **87**, 4–14
2 Ross, S.A., Gulve, E.A. and Wang, M. (2004) Chemistry and biochemistry of Type 2 diabetes. Chem. Rev. **104**, 1255–1282
3 Baggio, L.L. and Drucker, D.J. (2007) Biology of incretins: GLP-1 and GIP. Gastroenterology **132**, 2131–2157
4 Nauck, M.A., Heimesaat, M.M., Orskov, C., Holst, J.J., Ebert, R. and Creutzfeldt, W. (1993) Preserved incretin activity of glucagon-like peptide 1 [7–36 amide] but not of synthetic human gastric inhibitory polypeptide in patients with Type-2 diabetes mellitus. J. Clin. Invest. **91**, 301–307
5 Herrmann, C., Goke, R., Richter, G., Fehmann, H.C., Arnold, R. and Goke, B. (1995) Glucagon-like peptide-1 and glucose-dependent insulin-releasing polypeptide plasma levels in response to nutrients. Digestion **56**, 117–126
6 Reimann, F. (2010) Molecular mechanisms underlying nutrient detection by incretin-secreting cells. Int. Dairy J. **20**, 236–242
7 Drucker, D.J., Philippe, J., Mojsov, S., Chick, W.L. and Habener, J.F. (1987) Glucagon-like peptide I stimulates insulin gene expression and increases cyclic AMP levels in a rat islet cell line. Proc. Natl. Acad. Sci. U.S.A. **84**, 3434–3438
8 Scrocchi, L.A., Brown, T.J., MaClusky, N., Brubaker, P.L., Auerbach, A.B., Joyner, A.L. and Drucker, D.J. (1996) Glucose intolerance but normal satiety in mice with a null mutation in the glucagon-like peptide 1 receptor gene. Nat. Med. **2**, 1254–1258
9 Farilla, L., Bulotta, A., Hirshberg, B., Li Calzi, S., Khoury, N., Noushmehr, H., Bertolotto, C., Di Mario, U., Harlan, D.M. and Perfetti, R. (2003) Glucagon-like peptide 1 inhibits cell apoptosis and improves glucose responsiveness of freshly isolated human islets. Endocrinology **144**, 5149–5158

10 Bazarsuren, A., Grauschopf, U., Wozny, M., Reusch, D., Hoffmann, E., Schaefer, W., Panzner, S. and Rudolph, R. (2002) *In vitro* folding, functional characterization, and disulfide pattern of the extracellular domain of human GLP-1 receptor. Biophys. Chem. **96**, 305–318
11 Runge, S., Thogersen, H., Madsen, K., Lau, J. and Rudolph, R. (2008) Crystal structure of the ligand-bound glucagon-like peptide-1 receptor extracellular domain. J. Biol. Chem. **283**, 11340–11347
12 Underwood, C.R., Garibay, P., Knudsen, L.B., Hastrup, S., Peters, G.H., Rudolph, R. and Reedtz-Runge, S. (2010) Crystal structure of glucagon-like peptide-1 in complex with the extracellular domain of the glucagon-like peptide-1 receptor. J. Biol. Chem. **285**, 723–730
13 Wilmen, A., Goke, B. and Goke, R. (1996) The isolated N-terminal extracellular domain of the glucagon-like peptide-1 (GLP)-1 receptor has intrinsic binding activity. FEBS Lett. **398**, 43–47
14 Al-Sabah, S. and Donnelly, D. (2003) A model for receptor-peptide binding at the glucagon-like peptide-1 (GLP-1) receptor through the analysis of truncated ligands and receptors. Br. J. Pharmacol. **140**, 339–346
15 Coopman, K., Wallis, R., Robb, G., Brown, A., Wilkinson, G.F., Timms, D. and Willars, G.B. (2011) Residues within the transmembrane domain of the glucagon-like peptide-1 receptor involved in ligand binding and receptor activation. Mol. Endocrinol. **25**, 1804–1818
16 Runge, S., Wulff, B.S., Madsen, K., Brauner-Osborne, H. and Knudsen, L.B. (2003) Different domains of the glucagon and glucagon-like peptide-1 receptors provide the critical determinants of ligand selectivity. Br. J. Pharmacol. **138**, 787–794
17 Graziano, M.P., Hey, P.J. and Strader, C.D. (1996) The amino terminal domain of the glucagon-like peptide-1 receptor is a critical determinant of subtype specificity. Recept. Channels **4**, 9–17
18 Chen, Q., Pinon, D.I., Miller, L.J. and Dong, M. (2009) Molecular basis of glucagon-like peptide 1 docking to its intact receptor studied with carboxyl-terminal photolabile probes. J. Biol. Chem. **284**, 34135–34144
19 Chen, Q., Pinon, D.I., Miller, L.J. and Dong, M. (2010) Spatial approximations between residues 6 and 12 in the amino-terminal region of glucagon-like peptide 1 and its receptor: a region critical for biological activity. J. Biol. Chem. **285**, 24508–24518
20 Miller, L.J., Chen, Q., Lam, P.C., Pinon, D.I., Sexton, P.M., Abagyan, R. and Dong, M. (2011) Refinement of glucagon-like peptide 1 docking to its intact receptor using mid-region photolabile probes and molecular modeling. J. Biol. Chem. **286**, 15895–15907
21 Lopez de Maturana, R., Treece-Birch, J., Abidi, F., Findlay, J.B. and Donnelly, D. (2004) Met-204 and Tyr-205 are together important for binding GLP-1 receptor agonists but not their N-terminally truncated analogues. Protein Pept. Lett. **11**, 15–22
22 Lopez de Maturana, R. and Donnelly, D. (2002) The glucagon-like peptide-1 receptor binding site for the N-terminus of GLP-1 requires polarity at Asp198 rather than negative charge. FEBS Lett. **530**, 244–248
23 Xiao, Q., Jeng, W. and Wheeler, M.B. (2000) Characterization of glucagon-like peptide-1 receptor-binding determinants. J. Mol. Endocrinol. **25**, 321–335
24 Koole, C., Wootten, D., Simms, J., Miller, L.J., Christopoulos, A. and Sexton, P.M. (2012) Second extracellular loop of human glucagon-like peptide-1 receptor (GLP-1R) has a critical role in GLP-1 peptide binding and receptor activation. J. Biol. Chem. **287**, 3642–3658
25 Koole, C., Wootten, D., Simms, J., Savage, E.E., Miller, L.J., Christopoulos, A. and Sexton, P.M. (2012) Second extracellular loop of human glucagon-like peptide-1 receptor (GLP-1R) differentially regulates orthosteric but not allosteric agonist binding and function. J. Biol. Chem. **287**, 3659–3673
26 Hallbrink, M., Holmqvist, T., Olsson, M., Ostenson, C.G., Efendic, S. and Langel, U. (2001) Different domains in the third intracellular loop of the GLP-1 receptor are responsible for $G_{\alpha s}$ and $G_{\alpha i}/G_{\alpha o}$ activation. Biochim. Biophys. Acta **1546**, 79–86
27 Montrose-Rafizadeh, C., Avdonin, P., Garant, M.J., Rodgers, B.D., Kole, S., Yang, H., Levine, M.A., Schwindinger, W. and Bernier, M. (1999) Pancreatic glucagon-like peptide-1 receptor couples to multiple G proteins and activates mitogen-activated protein kinase pathways in Chinese hamster ovary cells. Endocrinology **140**, 1132–1140
28 Holz, G.G. (2004) Epac: a new cAMP-binding protein in support of glucagon-like peptide-1 receptor-mediated signal transduction in the pancreatic β-cell. Diabetes **53**, 5–13
29 Sonoda, N., Imamura, T., Yoshizaki, T., Babendure, J.L., Lu, J.C. and Olefsky, J.M. (2008) β-arrestin-1 mediates glucagon-like peptide-1 signaling to insulin secretion in cultured pancreatic beta cells. Proc. Natl. Acad. Sci. U.S.A. **105**, 6614–6619
30 Jorgensen, R., Kubale, V., Vrecl, M., Schwartz, T.W. and Elling, C.E. (2007) Oxyntomodulin differentially affects glucagon-like peptide-1 receptor β-arrestin recruitment and signaling through $G_{\alpha s}$. J. Pharmacol. Exp. Ther. **322**, 148–154
31 Jorgensen, R., Martini, L., Schwartz, T.W. and Elling, C.E. (2005) Characterization of glucagon-like peptide-1 receptor β-arrestin 2 interaction: a high-affinity receptor phenotype. Mol. Endocrinol. **19**, 812–823
32 Quoyer, J., Longuet, C., Broca, C., Linck, N., Costes, S., Varin, E., Bockaert, J., Bertrand, G. and Dalle, S. (2010) GLP-1 mediates anti-apoptotic effect by phosphorylating Bad through a β-arrestin 1-mediated ERK1/2 activation in pancreatic β -cells. J. Biol. Chem. **285**, 1989–2002
33 Barnett, A.H. (2009) New treatments in Type 2 diabetes: a focus on the incretin-based therapies. Clin. Endocrinol. (Oxford, U.K.) **70**, 343–353
34 Green, B.D. and Flatt, P.R. (2007) Incretin hormone mimetics and analogues in diabetes therapeutics. Best Pract. Res. Clin. Endocrinol. Metab. **21**, 497–516
35 Knudsen, L.B., Nielsen, P.F., Huusfeldt, P.O., Johansen, N.L., Madsen, K., Pedersen, F.Z., Thogersen, H., Wilken, M. and Agerso, H. (2000) Potent derivatives of glucagon-like peptide-1 with pharmacokinetic properties suitable for once daily administration. J. Med. Chem. **43**, 1664–1669
36 Christensen, M. and Knop, F.K. (2010) Once-weekly GLP-1 agonists: how do they differ from exenatide and liraglutide? Curr. Diab. Rep. **10**, 124–132
37 Hargrove, D.M., Kendall, E.S., Reynolds, J.M., Lwin, A.N., Herich, J.P., Smith, P.A., Gedulin, B.R., Flanagan, S.D., Jodka, C.M., Hoyt, J.A. et al. (2007) Biological activity of AC3174, a peptide analog of exendin-4. Regul. Pept. **141**, 113–119
38 Chae, S.Y., Jin, C.H., Shin, H.J., Youn, Y.S., Lee, S. and Lee, K.C. (2008) Preparation, characterization, and application of biotinylated and biotin-PEGylated glucagon-like peptide-1 analogues for enhanced oral delivery. Bioconjugate Chem. **19**, 334–341
39 Parks, M. and Rosebraugh, C. (2010) Weighing risks and benefits of liraglutide: the FDA's review of a new antidiabetic therapy. N. Engl. J. Med. **362**, 774–777
40 Olansky, L. (2010) Do incretin drugs for Type 2 diabetes increase the risk of acute pancreatitis? Cleveland Clin. J. Med. **77**, 503–505
41 Kenakin, T. (1995) Agonist-receptor efficacy. II. Agonist trafficking of receptor signals. Trends Pharmacol. Sci. **16**, 232–238
42 Koole, C., Wootten, D., Simms, J., Valant, C., Sridhar, R., Woodman, O.L., Miller, L.J., Summers, R.J., Christopoulos, A. and Sexton, P.M. (2010) Allosteric ligands of the glucagon-like peptide 1 receptor (GLP-1R) differentially modulate endogenous and exogenous peptide responses in a pathway-selective manner: implications for drug screening. Mol. Pharmacol. **78**, 456–465
43 Teng, M., Johnson, M.D., Thomas, C., Kiel, D., Lakis, J.N., Kercher, T., Aytes, S., Kostrowicki, J., Bhumralkar, D., Truesdale, L. et al. (2007) Small molecule ago-allosteric modulators of the human glucagon-like peptide-1 (hGLP-1) receptor. Bioorg. Med. Chem. Lett. **17**, 5472–5478
44 Knudsen, L.B., Kiel, D., Teng, M., Behrens, C., Bhumralkar, D., Kodra, J.T., Holst, J.J., Jeppesen, C.B., Johnson, M.D., de Jong, J.C. et al. (2007) Small-molecule agonists for the glucagon-like peptide 1 receptor. Proc. Natl. Acad. Sci. U.S.A. **104**, 937–942
45 Irwin, N., Flatt, P.R., Patterson, S. and Green, B.D. (2010) Insulin-releasing and metabolic effects of small molecule GLP-1 receptor agonist 6,7-dichloro-2-methylsulfonyl-3-N-tert-butylaminoquinoxaline. Eur. J. Pharmacol. **628**, 268–273
46 Chen, D., Liao, J., Li, N., Zhou, C., Liu, Q., Wang, G., Zhang, R., Zhang, S., Lin, L., Chen, K. et al. (2007) A nonpeptidic agonist of glucagon-like peptide 1 receptors with efficacy in diabetic db/db mice. Proc. Natl. Acad. Sci. U.S.A. **104**, 943–948
47 Su, H., He, M., Li, H., Liu, Q., Wang, J., Wang, Y., Gao, W., Zhou, L., Liao, J., Young, A.A. and Wang, M.W. (2008) Boc5, a non-peptidic glucagon-like peptide-1 receptor agonist, invokes sustained glycemic control and weight loss in diabetic mice. PLoS ONE **3**, e2892
48 Wootten, D., Simms, J., Koole, C., Woodman, O.L., Summers, R.J., Christopoulos, A. and Sexton, P.M. (2011) Modulation of the glucagon-like peptide-1 receptor signaling by naturally occurring and synthetic flavonoids. J. Pharmacol. Exp. Ther. **336**, 540–550
49 Sloop, K.W., Willard, F.S., Brenner, M.B., Ficorilli, J., Valasek, K., Showalter, A.D., Farb, T.B., Cao, J.X., Cox, A.L., Michael, M.D. et al. (2010) Novel small molecule glucagon-like peptide-1 receptor agonist stimulates insulin secretion in rodents and from human islets. Diabetes **59**, 3099–3107
50 Wang, M.W., Liu, Q. and Zhou, C.H. (2010) Non-peptidic glucose-like peptide-1 receptor agonists: aftermath of a serendipitous discovery. Acta Pharmacol. Sin. **31**, 1026–1030

51 Keov, P., Sexton, P.M. and Christopoulos, A. (2011) Allosteric modulation of G protein-coupled receptors: a pharmacological perspective. Neuropharmacology **60**, 24–35
52 Willard, F.S., Wootten, D., Showalter, A.D., Savage, E.E., Ficorilli, J., Farb, T.B., Bokvist, K., Alsina-Fernandez, J., Furness, S.G., Christopoulos, A. et al. (2012) Small molecule allosteric modulation of the glucagon-like peptide-1 receptor enhances the insulinotropic effect of oxyntomodulin. Mol. Pharmacol. **82**, 1066–1073
53 Wootten, D., Savage, E.E., Valant, C., May, L.T., Sloop, K.W., Ficorilli, J., Showalter, A.D., Willard, F.S., Christopoulos, A. and Sexton, P. (2012) Allosteric modulation of endogenous metabolites as an avenue for drug discovery. Mol. Pharmacol. **82**, 281–290

Received 24 September 2012
doi:10.1042/BST20120236

BJP British Journal of Pharmacology

DOI:10.1111/bph.12313
www.brjpharmacol.org

Themed Section: Molecular Pharmacology of GPCRs

REVIEW

Molecular mechanisms underlying physiological and receptor pleiotropic effects mediated by GLP-1R activation

K Pabreja, M A Mohd, C Koole, D Wootten and S G B Furness

Drug Discovery Biology, Monash Institute of Pharmaceutical Sciences, Monash University, Parkville, Vic., Australia

Correspondence
Sebastian George Barton Furness, Drug Discovery Biology Laboratory Monash Institute of Pharmaceutical Sciences Monash University, 399 Royal Parade, Parkville, Vic. 3052, Australia. E-mail: sebastian.furness@monash.edu

Keywords
type 2 diabetes; glucagon-like peptide-1 receptor; GLP-1; GLP-1R; GPCR; G protein-coupled receptor

Received
6 May 2013
Revised
10 July 2013
Accepted
19 July 2013

The incidence of type 2 diabetes in developed countries is increasing yearly with a significant negative impact on patient quality of life and an enormous burden on the healthcare system. Current biguanide and thiazolidinedione treatments for type 2 diabetes have a number of clinical limitations, the most serious long-term limitation being the eventual need for insulin replacement therapy (Table 1). Since 2007, drugs targeting the glucagon-like peptide-1 (GLP-1) receptor have been marketed for the treatment of type 2 diabetes. These drugs have enjoyed a great deal of success even though our underlying understanding of the mechanisms for their pleiotropic effects remain poorly characterized even while major pharmaceutical companies actively pursue small molecule alternatives. Coupling of the GLP-1 receptor to more than one signalling pathway (pleiotropic signalling) can result in ligand-dependent signalling bias and for a peptide receptor such as the GLP-1 receptor this can be exaggerated with the use of small molecule agonists. Better consideration of receptor signalling pleiotropy will be necessary for future drug development. This is particularly important given the recent failure of taspoglutide, the report of increased risk of pancreatitis associated with GLP-1 mimetics and the observed clinical differences between liraglutide, exenatide and the newly developed long-acting exenatide long acting release, albiglutide and dulaglutide.

LINKED ARTICLES
This article is part of a themed section on Molecular Pharmacology of GPCRs. To view the other articles in this section visit http://dx.doi.org/10.1111/bph.2014.171.issue-5

Abbreviations
ADP, adenosine diphosphate; ANS, autonomic nervous system; ATP, adenosine triphosphate; Bad, Bcl-2-associated death promoter; cAMP, cyclic adenosine monophosphate; CREB, cAMP response element binding protein; DPPIV, dipeptidyl peptidase IV; EGF-R1, epidermal growth factor receptor; Epac2, exchange protein directly activated by cAMP 2; GCGR, glucagon receptor; GIP, gastric inhibitory polypeptide; GLP-1, glucagon-like peptide-1; GLP-1R, glucagon-like peptide-1 receptor; GLP-2, glucagon-like peptide-2; GPCR, G protein-coupled receptor; GRK, G protein-coupled receptor kinase; GSIS, glucose stimulated insulin secretion; ICV, introcerebroventricular; K_{ATP}, ATP sensitive potassium channel (potassium inwardly-rectifying channel, subfamily J); MAPK, mitogen activated protein kinase; NFAT, nuclear factor of activated T-cells; PACAP, pituitary adenylate cyclase activating polypeptide; PDX-1, pancreatic-duodenum homeobox-1; PI3K, phosphoinositide 3-kinase; PKA, protein kinase A; Rab3A, Ras-associated protein 3A; Rap1, Ras-proximate-1; Rim2, regulating synaptic membrane exocytosis 2; SNAP25, synaptosomal-associated protein 25; T2DM, type 2 diabetes mellitus; VDCC, voltage-dependant calcium channel; VIP, vasoactive intestinal peptide

The incretin effect

The observation that oral glucose administration results in significantly higher pancreatic insulin secretion compared with intravenous dosing to the same plasma concentration gave rise to the idea of an entero-insular axis that was responsible for this enhancement (Elrick *et al.*, 1964; Mcintyre *et al.*, 1964). The implication being that there was glucose sensing

Table 1

Comparison of therapies for type 2 diabetes in terms of therapeutic outcome and adverse events (TZDs = thiazolidinedione; HbA1c = glycated haemaglobin)

					GLP-1 mimetics	
	Sulfonyl-ureas	**Metformin**	**TZDs**	**DPPIV inhibitors**	**Short acting**	**Long acting**
Insulin secretion	Increased	No effect	No effect	Glucose-dependent increase	Glucose-dependent increase	Glucose-dependent increase
Beta cell glucose sensitivity	No effect	Increased	No effect	Increased	Increased	Increased
Target tissue insulin sensitivity	No effect	Increased	Increased	Unclear	Unclear	Unclear
Beta cell mass	No protection from loss	No protection from loss	No protection from loss	Unclear	Probably increased	Probably increased
HbA1c	Reduced	Reduced	Reduced	Reduced	Reduced	Reduced
Satiety	No effect	No effect	No effect	Increased	Increased	Increased
Gastric emptying	No effect	No effect	No effect	Reduced	Reduced	Small reduction
Weight	Increase	Neutral	Increase	Neutral	Sustained loss	Sustained loss
Long-term insulin dependency	Yes	Yes	Yes	Unlikely	Unlikely	Unlikely
Pancreatitis	Not reported	Not reported	Not reported	Increased risk	Increased risk	Increased risk
Adverse GIT effects	Broad spectrum GIT AEs	Mostly absent	Mostly absent	Some nausea	Some nausea	Some nausea
Hypoglycemia	At risk	Low risk	None	None	None	None

within the gastrointestinal tract or hepatic system that resulted in potentiated insulin secretion, called the incretin effect, a concept dating back to the late 19th century (reviewed in Creutzfeldt, 1979). It was shown that two gut-derived hormones gastric inhibitory polypeptide [GIP (Dupre *et al.*, 1973)] and glucagon-like peptide-1 [GLP-1 (Kreymann *et al.*, 1987)], known as incretins, were secreted in response to meal ingestion and could stimulate insulin secretion, thereby making a significant contribution to overall postprandial insulin release. Both GIP and GLP-1 have no effect on insulin secretion in the absence of elevated plasma glucose obviating the risk of hypoglycaemia (Nauck *et al.*, 1993a). However, the insulinotropic effects of GIP are lost in type 2 diabetics (T2DM) (Nauck *et al.*, 1993b), while these effects from GLP-1 are maintained, leaving GLP-1 as the primary candidate incretin for clinical use.

The insulinotropic action of GLP-1 appears to be entirely mediated by the GLP-1 receptor (GLP-1R) (Scrocchi *et al.*, 1996) [we note that the official NC-IUPHAR nomenclature (Alexander *et al.*, 2013) for this receptor is GLP-1 and have used GLP-1R to aid distinction between ligand and receptor]. Activation of the GLP-1R on pancreatic β-islets results in potentiation of glucose-dependent insulin secretion as well as improvements in beta cell function and mass in animal models (Xu *et al.*, 1999; Perfetti *et al.*, 2000; Stoffers *et al.*, 2000; Tourrel *et al.*, 2001; Farilla *et al.*, 2002; Rolin *et al.*, 2002; Wang and Brubaker, 2002; Bock *et al.*, 2003; Sturis *et al.*, 2003; Gedulin *et al.*, 2005), although some of this effect may be mediated centrally and will be discussed later. Its activation forms the basis of two classes of glucose lowering agents, incretin mimetics (i.e. GLP-1 receptor agonists) and inhibitors of dipeptidyl peptidase IV (DPPIV or CD26) (incretin enhancers), an enzyme responsible for cleavage of GLP-1 to inert metabolites.

Biology of GLP-1 synthesis, secretion and metabolism

Tissue-specific post-translational cleavage of proglucagon generates glucagon in pancreatic α-cells (Patzelt *et al.*, 1979) and GLP-1, GLP-2, oxyntomodulin and glicentin in intestinal L-cells (Orskov *et al.*, 1987; Eissele *et al.*, 1992) and the brain (Drucker and Asa, 1988; Larsen *et al.*, 1997). GLP-1(1-37) is processed in intestinal L-cells into two equipotent circulating molecular forms GLP-1(7-36) amide and GLP-1(7-37) (Holst *et al.*, 1987; Kreymann *et al.*, 1987; Mojsov *et al.*, 1987). In humans, GLP-1(7-36) amide represents the majority of circulating active GLP-1 secreted in response to nutrient ingestion (Orskov *et al.*, 1994) and will henceforth referred to simply as GLP-1. GLP-1 is secreted in a biphasic pattern with early phase beginning within 5–15 min and prolonged second phase observed from 30 to 60 min of meal ingestion (Herrmann *et al.*, 1995). GLP-1 is rapidly cleaved between positions 8 and 9 by the widely expressed serine protease DPPIV into GLP-1(9-36)amide (and GLP-1(9-37)) giving a circulation half life of 2–3 min (Mentlein *et al.*, 1993b; Deacon *et al.*, 1995; Kieffer *et al.*, 1995; Hansen *et al.*, 1999). These DPPIV-processed GLP-1 peptides have low *in vitro* affinity and activity at the classically defined human GLP-1R (Knudsen and Pridal, 1996; Montrose-Rafizadeh *et al.*, 1997a) but have

been shown to have cardioprotective and glucoregulatory actions when pharmacologically dosed (Nikolaidis *et al.*, 2005; Meier *et al.*, 2006; Elahi *et al.*, 2008) and, in model animals, may exert effects independent of GLP-1R (Ban *et al.*, 2008; 2010). The relevance of the pharmacological effects of these metabolites is unclear, particularly given they are subject to rapid renal clearance with a half-life of less than 5 min (Ruiz-Grande *et al.*, 1993; Meier *et al.*, 2004). GLP-1 is also a substrate for the metalloendopeptidase enzyme neprylisin, also known as neutral endopeptidase 24.11 (Hupe-Sodmann *et al.*, 1995). A single study in the pig demonstrated that neprylisin is responsible for degrading almost half the circulating GLP-1 (Plamboeck *et al.*, 2005), consistent with findings that the GLP-1 analogue liraglutide is also degraded by neprylsin in humans (Malm-Erjefält *et al.*, 2010). Neprylisin cleaves GLP-1 at a number of positions (Hupe-Sodmann *et al.*, 1995) and although it is theorized that these products could have mitochondrial effects (Tomas and Habener, 2010), their physiological concentrations make this unlikely.

As mentioned above, oxyntomodulin (OXM) is also a product of tissue specific cleavage of proglucagon. OXM consists of amino acids 33–69 of proglucagon and is a cleavage product of glicentin containing the full 29 amino acids of glucagon with an 8 amino-acid carboxy terminal extension (for a comprehensive review, see Holst, 2007). In both intestinal L-cells and cells of the nucleus of the solitary tract in the brain processing of proglucagon generates GLP-1, GLP-2 and glicentin which is only partly processed into OXM (Mojsov *et al.*, 1986; Orskov *et al.*, 1987; Larsen *et al.*, 1997). In the intestinal L-cells all these peptides are co-secreted in response to food intake (reviewed in Pocai, 2012). OXM is a low potency full agonist for cyclic adenosine monophosphate (cAMP) accumulation from the GLP-1R (Schepp *et al.*, 1996; Jorgensen *et al.*, 2007) and the glucagon receptor (GCGR) (Jorgensen *et al.*, 2007). It is also a full agonist for recruitment of G protein-coupled receptor kinase (GRK) 2, β-arrestin 1 and β-arrestin 2 to the GCGR; however, at the GLP-1R, OXM is only a partial agonist for these interactions (Jorgensen *et al.*, 2007). Despite this, OXM has a higher affinity for the GLP-1R than GCGR and thus, GLP-1R is proposed as the primary receptor for this peptide.

The GLP-1 receptor: structure and expression

In humans, GLP-1R is a 463 amino acid G protein-coupled receptor (GPCR) belonging to the secretin-like family (also referred to as Family B). This is a small family of only 15 GPCRs including receptors for secretin, GIP and vasoactive intestinal peptide (VIP). Structural characteristics of this receptor family include: a relatively long, extracellular N-terminal domain responsible for high affinity binding of endogenous peptide ligands; six highly conserved cysteine residues in the extracellular domain that form three conserved disulphide bridges; an amino terminal signal peptide, several N-linked glycosylation sites and of course the characteristic seven transmembrane bundle shared by all GPCRs (reviewed in Furness *et al.*, 2012).

The sites of GLP-1R expression in both model organisms and humans have been investigated using a variety of techniques of varying sensitivity and resolution. Potential roles for the receptor in physiological processes that are regulated by its ligands may be predicted by its location. In many cases there are significant shortcomings in the molecular identification of sites of expression of the GLP-1R and in these cases better molecular and functional data would be invaluable.

Expression of the GLP-1R has been demonstrated in pancreatic islets of rodents and humans (Orskov and Poulsen, 1991; Campos *et al.*, 1994; Körner *et al.*, 2007), which is consistent with the large amount of data demonstrating GLP-1 potentiation of glucose stimulated insulin secretion (GSIS). Insulin-secreting beta cells comprise 65–80% of the cells of the pancreatic islet with glucagon-secreting α-cells comprising 15–20% and somatostatin secreting δ-cells 3–10% (reviewed in In't Veld and Marichal, 2010). Based on the central location of mRNA (Bullock *et al.*, 1996; Moens *et al.*, 1996; Hörsch *et al.*, 1997) and autoradiographic GLP-1 signal (Orskov and Poulsen, 1991) and further confirmed with immunoflourescence (Tornehave *et al.*, 2008), GLP-1R is expressed on beta cells, and this expression is consistent with expression on insulinomas from rodents and humans (Göke *et al.*, 1989; Gefel *et al.*, 1990; Fehmann and Habener, 1991; Lankat-Buttgereit *et al.*, 1994). There have been reports that the GLP-1R is also expressed on both α (glucagon) and δ-(somatostatin) cells in rodents (Heller and Aponte, 1995; Heller *et al.*, 1997); however, this is not supported in immunoflourescent experiments on human islets (Tornehave *et al.*, 2008) and remains controversial. In addition to expression on islet beta cells, GLP-1R is present on the ductal exocrine cells [acinar (Xu *et al.*, 2006; Gier *et al.*, 2012)], an observation that may be important in relation to pancreatitis associated with the use of GLP-1 mimetics (see later).

GLP-1 has a number of physiological effects related to energy homeostasis and cardiovascular function that are mediated to some extent by the autonomic nervous system (ANS) and visceral afferent neurons. In both animals and humans, GLP-1 enhances satiety (Tang-Christensen *et al.*, 1996; Turton *et al.*, 1996; Flint *et al.*, 1998; Näslund *et al.*, 1998; Williams *et al.*, 2009; Kanoski *et al.*, 2011; Renner *et al.*, 2012) and inhibition of gastric emptying (Imeryüz *et al.*, 1997; Näslund *et al.*, 1998; Delgado-Aros *et al.*, 2002; Schirra *et al.*, 2002; 2006; Nagell *et al.*, 2006; Hayes *et al.*, 2008; Hellström *et al.*, 2008). Inhibition of gastric emptying is regulated primarily by the ANS and satiety is modulated by both vagal afferents and direct effects on the hypothalamus with suppression of GLP-1-dependent satiety upon vagotomy (Abbott *et al.*, 2005). There is some evidence for a GLP-1-dependent decrease in gastric acid secretion mediated by the ANS (Wettergren *et al.*, 1994; 1997; 1998). In addition to these ANS-mediated gastrointestinal effects, there are also energy homeostatic effects that appear to have some ANS contribution. In humans, depending on experimental setting, there is a GLP-1-dependent (and insulin/glucagon independent) decrease in hepatic glucose production (Prigeon *et al.*, 2003; Seghieri *et al.*, 2013), an effect that can be replicated using intracerebroventricular (ICV) administration of GLP-1 in rodents (Sandoval *et al.*, 2008; Burmeister *et al.*, 2012). In mice, ICV administration of GLP-1 stimulates thermogenesis in brown adipose (Lockie *et al.*, 2012) and

lipid deposition in white adipose is decreased (Nogueiras *et al.*, 2009). In addition, there is also evidence for GLP-1R-dependent ANS regulation of the cardiovascular system in rodents (Barragán *et al.*, 1999; Yamamoto *et al.*, 2002; Cabou *et al.*, 2008; Griffioen *et al.*, 2011), but this does not appear to be the case in humans (Bharucha *et al.*, 2008). Within the central nervous system mRNA for the GLP-1R can be detected in the thalamus, hypothalamus and brainstem in both rodents (Shughrue *et al.*, 1996; Merchenthaler *et al.*, 1999; Yamamoto *et al.*, 2003) and humans (Alvarez *et al.*, 2005) and is consistent with rodent *in situ* radioligand binding data (Göke *et al.*, 1995). These central GLP-1Rs may be stimulated by circulating GLP-1, for example in privileged areas such as the subfornical organ and the area postrema which have been shown to bind peripherally administered GLP-1 (Orskov *et al.*, 1996a), or, alternatively, may be stimulated by GLP-1 release from neurons projecting from the nucleus of the solitary tract (Jin *et al.*, 1988). There is indirect evidence in model animals for GLP-1R expression on vagal afferent nerve terminals of the hepatic portal vein (Nakabayashi *et al.*, 1996; Nishizawa *et al.*, 1996; Balkan and Li, 2000; Baumgartner *et al.*, 2010) with cell bodies in the nodose ganglion (Nakagawa *et al.*, 2004; Vahl *et al.*, 2007). Vahl *et al.* (Vahl *et al.*, 2007) use immunocytochemistry to demonstrate GLP-1R expression in hepatic portal vein nerve terminals; however, it must be noted that the antibody used is no longer available from AbCam, and the replacement does not recognize the GLP-1R (Panjwani *et al.*, 2013). Similar indirect evidence suggests GLP-1R expression on enteric neurons that communicate with the vagus nerve (Washington *et al.*, 2010).

There are conflicting reports on GLP-1/GLP-1 mimetic-dependent effects on insulin sensitivity in man with some showing no effect (Orskov *et al.*, 1996b; Vella *et al.*, 2000; 2002) and some showing enhanced sensitivity (Egan *et al.*, 2002; Zander *et al.*, 2002; Meneilly *et al.*, 2003). From the preceding discussion on the ANS, changes in liver and adipose insulin sensitivity may be influenced by the ANS (either directly or indirectly, for example via the adrenal gland, e.g. Yamamoto *et al.*, 2002; 2003); however, there may also be direct GLP-1R-mediated effects on these tissues. Whether the GLP-1R is expressed in these insulin target tissues remains contentious due to the nature of the functional experiments performed. All three tissue types are marked by unusual pharmacology in which the truncated form of exendin (exendin 9-39), which is normally considered an antagonist, as well as the pro-GLP-1 peptide GLP-1(1-36NH_2), which is generally considered low affinity (e.g. Koole *et al.*, 2010) both act as potent agonists in regulation of glucose uptake and metabolism in these cell types (Villanueva-Peñacarrillo *et al.*, 1995; Montrose-Rafizadeh *et al.*, 1997b; Wang *et al.*, 1997; Luque *et al.*, 2002; González *et al.*, 2005). This has led a number of researchers to propose that a second GLP-1 receptor exists. The characterization of exendin 9-39 and pro-GLP-1 pharmacologies as low affinity and antagonistic ligands is based on observations in transfected cell lines. The downstream pathways linking GLP-1R to glucose uptake and metabolism are not established in these cell types. It is therefore possible that these peptides have alternative, GLP-1R-dependent pharmacologies depending on cell background, particularly given the widespread heterodimerization of family B GPCRs (Harikumar *et al.*, 2008).

Beyond the above tissues, which are obvious physiological targets for GLP-1, GLP-1R expression has been reported on kidney (Korner *et al.*, 2007; Schlatter *et al.*, 2007) and lung (Kanse *et al.*, 1988; Richter *et al.*, 1990; 1993; Korner *et al.*, 2007), although expression in the human lung is restricted to small vessels (Korner *et al.*, 2007).

Molecular mechanisms underlying GLP-1R physiology

GLP-1 has multiple physiological effects that include potentiation of glucose-dependent insulin secretion, up-regulation of insulin biosynthesis, increasing beta cell mass, suppression of glucagon secretion, delaying gastric emptying, reducing appetite, improved glucose disposal and insulin sensitivity in adipose, muscle and liver as well as improving cardiovascular function and cardiovascular protective effects. In addition, GLP-1 has been reported to have anabolic effects on bone and effects on learning and memory that are beyond the scope of this review (During *et al.*, 2003; Yamada *et al.*, 2008).

The best studied molecular pathways underlying this physiology are those in the pancreas, in particular, the beta cells (Figure 1). GLP-1, acting via the GLP-1R, causes acute potentiation of GSIS, regulated primarily by signalling through the stimulatory G_α ($G_{\alpha s}$) subunit to activate adenylate cyclase and increase intracellular cAMP (Drucker *et al.*, 1987; Holst *et al.*, 1987; Mojsov *et al.*, 1987). Acute GSIS in pancreatic beta cells occurs primarily via changes in the energy balance within the cell [adenosine triphosphate (ATP)/adenosine diphosphate (ADP)], dependent on glucose catabolism. Glucose transporters are not rate limiting for glucose catabolism in beta cells, rather glucokinase provides the rate limiting step and is therefore considered the glucose sensor having high cooperativity for glucose binding and an enzymatic inflection point of ~4 mM. Increases in plasma glucose above this inflection point results in increased rates of glucose catabolism via the glycolytic and oxidative phosphorylation pathways in cytoplasm and mitochondria, respectively. The increase in ATP/ADP ratio acts on ATP sensitive potassium channels (K_{ATP}). Binding of ATP to the pore forming subunits ($K_{ir6.2}$) (Gribble *et al.*, 1998) and release of ADP from the regulatory subunits (SUR1) (Gribble *et al.*, 1997) result in channel closure leading to membrane depolarization stimulating the opening of voltage-dependent calcium channels (VDCCs) and insulin exocytosis (for reviews on GSIS see Matschinsky *et al.*, 1993; 1998; Schuit *et al.*, 2001). *In vitro* evidence from both rodent and human pancreatic islets demonstrates that GLP-1R-mediated increases in intracellular second messenger cAMP potentiates GSIS (reviewed in Gromada *et al.*, 1998). Increases in intracellular cAMP act on the K_{ATP} channel to increase its sensitivity to ATP (i.e. left shift the ATP curve). This occurs via two intermediates, protein kinase A (PKA) and the guanine nucleotide exchange factor Epac2 (Ozaki *et al.*, 2000; Kang *et al.*, 2001; Eliasson *et al.*, 2003). Both SUR1 and $K_{ir6.2}$ subunits contain consensus PKA phophorylation sites, and GLP-1R-dependent activation of PKA leads to phosphorylation of SUR1 subunits lowering their affinity for ADP (Light, 2002); however, PKA activation also changes the dynamics of exo-

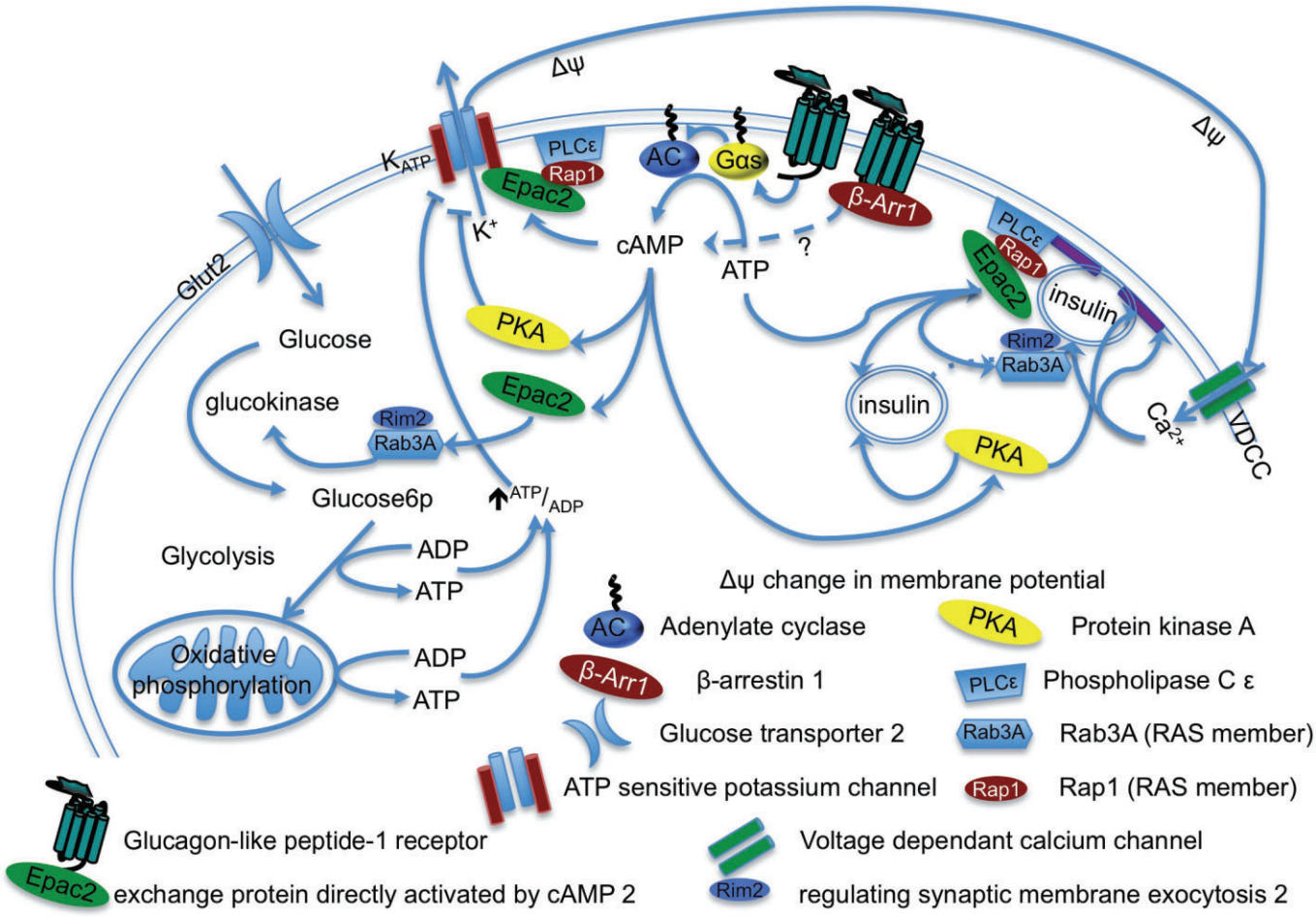

Figure 1

Cartoon depicting the major pathway by which a pancreatic beta cell secretes insulin in response to increases in plasma glucose. The various pathways that originate from GLP-1R activation and converge to potentiate glucose stimulated insulin secretion are depicted. See text for a full description.

cytosis (Eliasson *et al.*, 2003; Hatakeyama *et al.*, 2006; 2007) by phosphoylating snapin that acts to regulate vesicle assembly along with synaptosomal-associated protein 25 and Epac2 (Song *et al.*, 2011). Similarly, cAMP-dependent activation of Epac2 in beta cells increases the sensitivity of the K_{ATP} channel to ATP (Kang *et al.*, 2008) and also the dynamics of vesicle priming and fusion (Hatakeyama *et al.*, 2007; Shibasaki *et al.*, 2007; Kang *et al.*, 2008; Dzhura *et al.*, 2011) thus potentiating GSIS. Epac2 activation probably converges with PKA-dependent activation of snapin (above), but additionally the activation of the small GTPase, Rap1 (Shibasaki *et al.*, 2007) and its target phospholipase C-ε (Dzhura *et al.*, 2011) may independently potentiate vesicle priming. These GLP-1R-dependent effects to directly potentiate GSIS are $G_{\alpha s}$/cAMP dependent; however, data from the INS-1 insulinoma using supraphysiological GLP-1 stimulation in combination with β-arrestin 1 knockdown demonstrate a proportion of the cAMP/GSIS response to be β-arrestin 1 dependent (Sonoda *et al.*, 2008). Based on the observed clinical differences in effects of GLP-1 mimetics (see later), a better understanding of the requirement for this β-arrestin 1-dependent cAMP/GSIS response may be required for the development of small molecule drugs. In addition to post-glucokinase effects, GLP-1R-mediated activation of Epac2 acting in a Rim2/Rab3A-dependent manner (in rodent cell lines and islets) acutely decreases the K_m (but not Vmax) of glucokinase (Park *et al.*, 2012), thus providing an additional sensitization to GSIS, albeit at supraphysiological GLP-1 concentrations.

In addition to acute potentiation of GSIS, GLP-1R activation improves medium- and long-term insulin secretion via a number of mechanisms. In insulinoma cell lines, GLP-1R activation leads to increases in insulin expression. This effect is due to both stabilization of insulin mRNA and increases in insulin transcription (Fehmann and Habener, 1992; Wang *et al.*, 1995). GLP-1R activation in insulinoma cell lines activates cAMP response element binding protein (CREB) and NFAT in both PKA dependent and independent manners to activate insulin transcription (Skoglund *et al.*, 2000; Kemp and Habener, 2001; Chepurny, 2002; Lawrence *et al.*, 2002). The molecular pathways that connect GLP-1R to insulin transcription are however unclear, as it has been shown that GLP-1R activation can induce insulin expression indepen-

dent of cAMP, PKA and Epac2. Insulin secretion is also dependent on beta cell mass, and GLP-1R activation is associated with trophic and protective effects including proliferation, anti-apoptosis and stimulation of islet neogenesis. In insulinoma cell lines activation of GLP-1R generates cell autonomous signalling via β-arrestin 1 to inhibit the activity of pro-apoptotic protein Bad (Quoyer *et al.*, 2010) and paracrine pro-proliferative effects via post-transcriptional up-regulation of epidermal growth factor receptor (EGF-R1) (Buteau *et al.*, 2003; Cornu *et al.*, 2010). Isolated human islets are also protected from apoptosis by GLP-1 (Farilla *et al.*, 2003); however, this may be compensatory due to loss of tonic stimulation of cAMP (compare Xie *et al.*, 2007 and Preitner *et al.*, 2004). In glucose intolerant rats, GLP-1 increases beta cell mass correlating with induction of expression of the beta cell transcriptional regulator pancreatic-duodenum homeobox-1 (PDX-1) (Perfetti *et al.*, 2000). GLP-1R-dependent activation of PDX-1 is also seen in model insulinomas and is dependent on a cAMP/PKA pathway (Wang *et al.*, 2001), and induction of PDX-1 expression is likely to contribute directly to islet neogenesis (Hui *et al.*, 2001; Bulotta *et al.*, 2002). In addition to these direct effects, vagal innervation of the pancreas is well documented to regulate beta cell mass (e.g. Lausier *et al.*, 2010; Llewellyn-Smith and Verberne, 2013), and GLP-1R activation stimulates pancreas projecting vagal neurons (Wan *et al.*, 2007a,b). Beyond GLP-1R-mediated effects on the endocrine pancreas, rodent models show significant adverse effects in exocrine pancreas. In a 10 weeks trial in rats, exendin treatment resulted in significant acinar cell death and inflammation (Nachnani *et al.*, 2010) and in a mouse model of pancreatic intraepithelia neoplasia, exendin treatment significantly accelerated metaplasia and lesion formation (Gier *et al.*, 2012). While there is no mechanistic data to explain these exocrine pancreatic effects, recent meta analysis on the incidence of pancreatitis in T2DM patients shows a doubling in relative risk for those using GLP-1 therapies (Singh *et al.*, 2013). The pleiotropic effects on beta cell function and mass are clinically very important as preservation of pancreatic function is one of the key advantages to GLP-1-based therapies. It is also imperative that the nature of GLP-1 pathways that form the molecular basis for pancreatitis be established. These pathways may be via changes in pancreatic morphology due to accelerated beta cell neogenesis or via direct effects on acinar cells that express GLP-1R.

The ability of GLP-1 to suppress glucagon secretion from pancreatic α-cells is regarded as important for its glucoregulatory effects. Under conditions of hyperinsulinaemic-euglycaemic clamp, GLP-1 does not inhibit glucagon secretion in humans (Meneilly *et al.*, 2003). This suggests that GLP-1-dependent regulation of glucagon secretion is not mediated by direct effects on pancreatic α-cells but rather is mediated by a combination of pancreatic paracrine (Franklin *et al.*, 2005) and ANS signalling (Llewellyn-Smith and Verberne, 2013).

The ANS effects of GLP-1 are critical for the success of GLP-1 mimetics as treatments for T2DM. The effect of GLP-1 mimetics on postprandial glucose excursion is largely via slowing in gastric emptying (Meier *et al.*, 2005; Linnebjerg *et al.*, 2008); however, this effect is subject to tachyphylaxis (Nauck *et al.*, 2011) and as a result, long-acting GLP-1 analogues are less efficacious in controlling postprandial glucose excursion (Degn *et al.*, 2004; Buse *et al.*, 2009). GLP-1-dependent decreases in gastric emptying appear to be mediated by the ANS (Nagell *et al.*, 2006; Holmes *et al.*, 2009) suggesting that the sites of GLP-1R expression responsible for gastric emptying are sites in which GLP-1R is subject to agonist mediated desensitization. In contrast, similar weight loss is observed in T2DM patients receiving both long- and short-acting GLP-1 mimetics (Drucker *et al.*, 2008; Buse *et al.*, 2009), consistent with the gastric motility independent decrease in food intake seen in ICV-treated rats (Turton *et al.*, 1996) that is apparently not subject to GLP-1R desensitization. It is therefore likely that there are some sites in these pathways where GLP-1R is desensitized and some are not and this is likely to be an important consideration for the design of small molecule GLP-1R agonists. There is one site in which GLP-1R stimulation has been shown to result in neuronal depolarization (e.g. Wan *et al.*, 2007a,b; Holmes *et al.*, 2009); however, there is no data that address the pathways immediately downstream of the GLP-1R that cause depolarization, and there is no data that allow this site to be extrapolated to sites important for gastric emptying and satiety. An understanding of the subsets of neurons activated and the downstream pathways required for the therapeutic effects is important as there are clear differences in the anorectic effects of different GLP-1R agonists. In rodents, GLP-1 and exendin drive similar reductions in food intake when administered peripherally, but exendin is far more potent when administered ICV (Barrera *et al.*, 2009); in clinical trials, high molecular weight GLP-1 mimetics (e.g. Albiglutide and Dulaglutide) fail to provide weight loss benefits seen with peptide mimetics (Rosenstock *et al.*, 2009; Grunberger *et al.*, 2012) suggesting differential access by these ligands to central GLP-1R.

As part of its overall glucoregulatory role, GLP-1 can act to inhibit endogenous glucose production in the liver both acutely (Meneilly *et al.*, 2003; Prigeon *et al.*, 2003) and over the long term (Egan *et al.*, 2002; Zander *et al.*, 2002). Although GLP-1 binding has been demonstrated on rat hepatocyte membranes (Villanueva-Peñacarrillo *et al.*, 1995), there is no convincing evidence that GLP-1 agonists exert a direct effect on liver metabolism, rather GLP-1 effects on hepatic function, where they occur, are likely to be centrally mediated (although this may be indirect). In human adipocytes, there is one report showing GLP-1 potentiation of glucose uptake via phosphoinositide 3-kinase (PI3K) and mitogen-activated protein kinase pathways (Sancho *et al.*, 2007). In this report, exendin 9-39 also stimulates PI3K activity that contrasts to the traditional view of this ligand as an antagonist. In addition, the data from the mouse suggest that, rather than stimulating glucose uptake and therefore lipogenesis, GLP-1 acts to increase lipolysis. Given one of the useful clinical outcomes of GLP-1 mimetics is sustained weight loss, a better understanding of the effects on adipose physiology is required.

Our understanding of the underlying molecular basis of GLP-1's pleiotropic effects would benefit greatly from high quality antibodies directed against GLP-1R and a GLP-1R reporter mouse so the precise location of receptors in different tissues could be fully characterized. Better characterization of pathways leading to translational and post-translational control of gene expression by GLP-1R activation

is required. Additionally, comprehensive studies that provide pharmacological or biochemical characterization of GLP-1R on tissues such as liver and adipose would greatly enhance our understanding of the underlying physiology.

Challenges for incretin therapies for T2DM

Currently there are no therapeutically approved small molecule GLP-1R agonists. As discussed above, the therapeutic usefulness of GLP-1 (peptide) is limited by its metabolic instability. Thus, therapeutic strategies for increasing active GLP-1 concentrations include DPP4 resistant GLP-1 mimetics such as exenatide and liraglutide or DPP4 inhibitors such as vildagliptin and sitagliptin that are approved as monotherapies and/or adjuvant drugs with oral antidiabetic compounds, depending on the country of approval.

Approved DPPIV inhibitors (known as gliptins) show very good selectivity for DPPIV over the structurally related enzymes DPPVIII and DPPIX (Brandt *et al.*, 2005; Kim *et al.*, 2005; Feng *et al.*, 2007; Wang *et al.*, 2012). DPPIV inhibitors produce modest changes in circulating levels of active GLP-1 (GLP-1(7-36)NH_2) levels ranging from twofold to fourfold depending on the study (Ahrén *et al.*, 2004; Herman *et al.*, 2005; Dai *et al.*, 2008; Henry *et al.*, 2011). For healthy individuals, this corresponds to an increase in fasted GLP-1 to ~3 pM and postprandial peak of ~18 pM, compared with T2DM patients where reduced GLP-1 secretion is observed and the plasma concentrations are roughly half. Although the available data indicate that DPPIV inhibition is a promising treatment for type 2 diabetes, gliptins are clinically less effective than GLP-1 mimetics (reviewed in Brown and Evans, 2012; Reid, 2012; Scheen, 2012). There are also concerns that prolonged inhibition of DPPIV activity could lead to adverse side effects. Substrate cleavage by DPPIV occurs at penultimate L-proline or L-alanine residues (Kenny *et al.*, 1976). Some known and putative *in vivo* substrates of DPPIV include substance P (Heymann and Mentlein, 1978; Kato *et al.*, 1978), neuropeptide Y and peptide YY (Mentlein *et al.*, 1993a), endomorphin-1 (Bird *et al.*, 2001), pituitary adenylate cyclase activating peptide 38 (PACAP 38) (Lambeir *et al.*, 2001); GLP-1 and GIP (Mentlein *et al.*, 1993b), GLP-2 (Drucker *et al.*, 1997) and various chemokines such as CCL5 (regulated on activation, normal T-cell expressed and secreted, RANTES) and CCL11 (eotaxin) (Oravecz *et al.*, 1997), CCL22 (macrophage derived chemokine, MDC) (Proost *et al.*, 1999), CCL3L1 (LD78β) (Proost *et al.*, 2000) and CXCL12 (stromal-cell-derived factor 1, SDF-1) (Proost *et al.*, 1998). Thus, inhibition of DPPIV could potentially extend the circulating half-lives of these biologically active peptides which might conceivably affect/modulate vasoreactivity, nociception, energy homeostasis (food intake, lipid metabolism, thermogenesis and glucose control), proliferation, angiogenesis, immune response, behavioural stress response, gastrointestinal motility and growth.

Currently there are a number of GLP-1 analogues that have been approved or are in clinical trials for treatment of T2DM (Figure 2). The main drawback of all GLP-1 analogues is the need for parenteral administration. There has therefore been substantial effort to extend the half-life of these mimetics. Two synthetic analogues of exendin-4, exenatide and lixisenatide, were isolated from the saliva of the Gila monster (*Heloderma suspectum*). These two analogues are naturally resistant to DPPIV; exenatide and lixisenatide, which has a 6 amino acid polylysine extension at the C-terminus, have circulating half lives of around 4 h but have been formulated

Figure 2

A schematic of the various GLP-1 mimetics discussed in the text. Differences in sequence with respect to native GLP-1 are shown in red. Albiglutide is a genetic fusion of a GLP-1 concatamer to human albumin (blue), and Dulaglutide is a genetic fusion of GLP-1 via a linker (red) to the Fc domain of human IgG4 (blue).

for once a day injection. Liraglutide is based on the mammalian GLP-1 sequence with a glutamate and 16 carbon fatty acid conjugated to the ε-amino group of lysine26 and a substitution of lysine34 with arginine. This modification increases albumin binding to 99%, thus protecting liraglutide from DPPIV degradation and giving it an 11–13 h half life. Taspoglutide is also based on mammalian GLP-1 with substitution of Ala8 and Ala35 with methylated derivatives, thus protecting the peptide from DPPIV and giving a half-life of 10 h. Albiglutide uses two molecules of gly8 substituted GLP-1 sequences covalently coupled to human albumin and has a half life of 6–8 days. Dulaglutide uses two molecules of a position 8 valine substituted GLP-1 sequence fused via a linker to human IgG4-Fc domain and has a half life of 4 days. Lastly exenatide-LAR is a microsphere formulated extended release formulation of exendin that is suitable for once a week injection. These GLP-1 analogues are very selective for GLP-1R acitivation and do not suffer from the potential off target affects of DPPIV inhibitors. Clinically, all GLP-1 mimetics are better at lowering fasting and postprandial plasma glucose, glycosylated haemaglobin levels and weight compared with DPPIV inhibitors (Table 1; Arnolds *et al.*, 2010; Pratley *et al.*, 2010; 2011; Berg *et al.*, 2011). In spite of these positive attributes, there are differences in the clinical outcomes from trials using these different analogues that point to differential GLP-1R activation or signal bias by these ligands as well as safety concerns. In spite of the relatively minor changes in sequence for taspoglutide compared with mammalian GLP-1, this drug has now been withdrawn from clinical trials due to unacceptably high incidence of nausea and vomiting as well as systemic and injection site allergic reactions (Rosenstock *et al.*, 2013). It is unclear why this mimetic displays such a different emetic effect compared with liraglutide that has similar pharmacokinetics, however we would speculate that this may be due to differences in the mechanism of GLP-1R activation or access. Additionally, GLP-1 desensitization may play an important role in the tolerability of GLP-1 mimetics. All GLP-1 mimetics have nausea and vomiting as side effects; however, these side effects generally subside over time. It is therefore possible that the clinical difference seen with taspoglutide is due to failure of reeptor desensitization. Although exenatide-LAR, albiglutide and dulaglutide offer the benefit of once weekly injection, these long-acting analogues do not offer the same level of weight reduction seen with the short-acting analogues and this appears to be due to their reduced ability to promote satiety. The large conjugates, albiglutide and dulaglutide, also appear to be poor potentiators of GLP-1R anorectic effects, and this is probably due to the inability of these large molecules to access areas of the central nervous system (CNS) important for this effect. Alternatively, all long-acting mimetics may be less effective at promoting satiety due to them causing receptor desensitization in parts of the ANS responsible for satiety. If this is the case, a thorough understanding of the different neuronal types and the mechanisms for GLP-1R desensitization in these neurons will be necessary. Lastly, although evidence has not been published for albiglutide and dulaglutide, both DPPIV inhibitors and GLP-1 mimetics double the risk of pancreatitis, a condition associated with serious morbidity. This effect is almost certainly due to GLP-1R activation on acinar cells of the exocrine pancreas leading to their apoptosis and metaplasia and causing associated inflammation. In pancreatic beta cells, GLP-1R activation has anti-apoptotic and pro-proliferative effects, whereas in acinar ductal cells, it appears to be pro-apoptotic and drive metaplastic differentiation. In a subset of neurons responsible for GLP-1-mediated gastric emptying, sustained activation does not appear to be susceptible to tachyphylaxis whereas the neurons responsible for appetite suppression are. It may well be possible to generate small molecule ligands for the GLP-1R that display a suitable bias profile so as to bypass the pancreatic intraepithelial neoplasty while improving the weight loss profile through lack of receptor desensitization in the CNS. For these challenges to be met, a better understanding or key aspects of GLP-1R physiology and underlying molecular signalling is required.

Acknowledgements

This work was funded by Program Grant 519461 and Project Grant 436780 from the National Health and Medical Research Council (NHMRC) of Australia. We would like to thank Dane D. Jensen for helpful discussions and John B. Furness for critical evaluation of the manuscript.

Conflict of interest

None declared.

References

Abbott CR, Monteiro M, Small CJ, Sajedi A, Smith KL, Parkinson JR *et al.* (2005). The inhibitory effects of peripheral administration of peptide YY 3–36 and glucagon-like peptide-1 on food intake are attenuated by ablation of the vagal–brainstem–hypothalamic pathway. Brain Res 1044: 127–131.

Ahrén B, Landin-Olsson M, Jansson P-A, Svensson M, Holmes D, Schweizer A (2004). Inhibition of dipeptidyl peptidase-4 reduces glycemia, sustains insulin levels, and reduces glucagon levels in type 2 diabetes. J Clin Endocrinol Metab 89: 2078–2084.

Alexander SPH, Benson HE, Faccenda E, Pawson AJ, Sharman JL, Catterall WA, Spedding M, Peters JA, Harmar AJ and CGTP Collaborators (2013). The Concise Guide to PHARMACOLOGY 2013/14: G Protein-Coupled Receptors. Br J Pharmacol 170: 1459–1581.

Alvarez E, Martinez MD, Roncero I, Chowen JA, Garcia-Cuartero B, Gispert JD *et al.* (2005). The expression of GLP-1 receptor mRNA and protein allows the effect of GLP-1 on glucose metabolism in the human hypothalamus and brainstem. J Neurochem 92: 798–806.

Arnolds S, Dellweg S, Clair J, Dain M-P, Nauck MA, Rave K *et al.* (2010). Further improvement in postprandial glucose control with addition of exenatide or sitagliptin to combination therapy with insulin glargine and metformin: a proof-of-concept study. Diabetes Care 33: 1509–1515.

Balkan B, Li X (2000). Portal GLP-1 administration in rats augments the insulin response to glucose via neuronal mechanisms. Am J Physiol Regul Integr Comp Physiol 279: R1449–R1454.

Ban K, Noyan-Ashraf MH, Hoefer J, Bolz S-S, Drucker DJ, Husain M (2008). Cardioprotective and vasodilatory actions of glucagon-like peptide 1 receptor are mediated through both glucagon-like peptide 1 receptor-dependent and -independent pathways. Circulation 117: 2340–2350.

Ban K, Kim KH, Cho CK, Sauve M, Diamandis EP, Backx PH *et al.* (2010). Glucagon-like peptide (GLP)-1(9-36)amide-mediated cytoprotection is blocked by exendin(9-39) yet does not require the known GLP-1 receptor. Endocrinology 151: 1520–1531.

Barragán JM, Eng J, Rodríguez R, Blázquez E (1999). Neural contribution to the effect of glucagon-like peptide-1-(7-36) amide on arterial blood pressure in rats. Am J Physiol 277: E784–E791.

Barrera JG, D'Alessio DA, Drucker DJ, Woods SC, Seeley RJ (2009). Differences in the central anorectic effects of glucagon-like peptide-1 and exendin-4 in rats. Diabetes 58: 2820–2827.

Baumgartner I, Pacheco-López G, Rüttimann EB, Arnold M, Asarian L, Langhans W *et al.* (2010). Hepatic-portal vein infusions of glucagon-like peptide-1 reduce meal size and increase c-Fos expression in the nucleus tractus solitarii, area postrema and central nucleus of the amygdala in rats. J Neuroendocrinol 22: 557–563.

Berg JK, Shenouda SK, Heilmann CR, Gray AL, Holcombe JH (2011). Effects of exenatide twice daily versus sitagliptin on 24-h glucose, glucoregulatory and hormonal measures: a randomized, double-blind, crossover study. Diabetes Obes Metab 13: 982–989.

Bharucha AE, Charkoudian N, Andrews CN, Camilleri M, Sletten D, Zinsmeister AR *et al.* (2008). Effects of glucagon-like peptide-1, yohimbine, and nitrergic modulation on sympathetic and parasympathetic activity in humans. Am J Physiol Regul Integr Comp Physiol 295: R874–R880.

Bird AP, Faltinek JR, Shojaei AH (2001). Transbuccal peptide delivery: stability and in vitro permeation studies on endomorphin-1. J Control Release 73: 31–36.

Bock T, Pakkenberg B, Buschard K (2003). The endocrine pancreas in non-diabetic rats after short-term and long-term treatment with the long-acting GLP-1 derivative NN2211. Apmis 111: 1117–1124.

Brandt I, Joossens J, Chen X, Maes M-B, Scharpé S, De Meester I *et al.* (2005). Inhibition of dipeptidyl-peptidase IV catalyzed peptide truncation by Vildagliptin ((2S)-{[(3-hydroxyadamantan-1-yl)amino] acetyl}-pyrrolidine-2-carbonitrile). Biochem Pharmacol 70: 134–143.

Brown DX, Evans M (2012). Choosing between GLP-1 receptor agonists and DPP-4 inhibitors: a pharmacological perspective. J Nutr Metab 2012: 1–10.

Bullock BP, Heller RS, Habener JF (1996). Tissue distribution of messenger ribonucleic acid encoding the rat glucagon-like peptide-1 receptor. Endocrinology 137: 2968–2978.

Bulotta A, Hui H, Anastasi E, Bertolotto C, Boros LG, Di Mario U *et al.* (2002). Cultured pancreatic ductal cells undergo cell cycle re-distribution and beta-cell-like differentiation in response to glucagon-like peptide-1. J Mol Endocrinol 29: 347–360.

Burmeister MA, Ferre T, Ayala JE, King EM, Holt RM, Ayala JE (2012). Acute activation of central GLP-1 receptors enhances hepatic insulin action and insulin secretion in high-fat-fed, insulin resistant mice. Am J Physiol Endocrinol Metab 302: E334–E343.

Buse JB, Rosenstock J, Sesti G, Schmidt WE, Montanya E, Brett JH *et al.* (2009). Liraglutide once a day versus exenatide twice a day for type 2 diabetes: a 26-week randomised, parallel-group, multinational, open-label trial (LEAD-6). Lancet 374: 39–47.

Buteau J, Foisy S, Joly E, Prentki M (2003). Glucagon-like peptide 1 induces pancreatic β-cell proliferation via transactivation of the epidermal growth factor receptor. Diabetes 52: 124–132.

Cabou C, Campistron G, Marsollier N, Leloup C, Cruciani-Guglielmacci C, Pénicaud L *et al.* (2008). Brain glucagon-like peptide-1 regulates arterial blood flow, heart rate, and insulin sensitivity. Diabetes 57: 2577–2587.

Campos RV, Lee YC, Drucker DJ (1994). Divergent tissue-specific and developmental expression of receptors for glucagon and glucagon-like peptide-1 in the mouse. Endocrinology 134: 2156–2164.

Chepurny OG (2002). Exendin-4 as a stimulator of rat insulin I gene promoter activity via bZIP/CRE interactions sensitive to serine/threonine protein kinase inhibitor Ro 31-8220. Endocrinology 143: 2303–2313.

Cornu M, Modi H, Kawamori D, Kulkarni RN, Joffraud M, Thorens B (2010). Glucagon-like peptide-1 increases beta-cell glucose competence and proliferation by translational induction of insulin-like growth factor-1 receptor expression. J Biol Chem 285: 10538–10545.

Creutzfeldt W (1979). The incretin concept today. Diabetologia 16: 75–85.

Dai H, Gustavson SM, Preston GM, Eskra JD, Calle R, Hirshberg B (2008). Non-linear increase in GLP-1 levels in response to DPP-IV inhibition in healthy adult subjects. Diabetes Obes Metab 10: 506–513.

Deacon CF, Johnsen AH, Holst JJ (1995). Degradation of glucagon-like peptide-1 by human plasma in vitro yields an N-terminally truncated peptide that is a major endogenous metabolite in vivo. J Clin Endocrinol Metab 80: 952–957.

Degn KB, Juhl CB, Sturis J, Jakobsen G, Brock B, Chandramouli V *et al.* (2004). One week's treatment with the long-acting glucagon-like peptide 1 derivative liraglutide (NN2211) markedly improves 24-h glycemia and alpha- and beta-cell function and reduces endogenous glucose release in patients with type 2 diabetes. Diabetes 53: 1187–1194.

Delgado-Aros S, Kim D-Y, Burton DD, Thomforde GM, Stephens D, Brinkmann BH *et al.* (2002). Effect of GLP-1 on gastric volume, emptying, maximum volume ingested, and postprandial symptoms in humans. Am J Physiol Gastrointest Liver Physiol 282: G424–G431.

Drucker DJ, Asa S (1988). Glucagon gene expression in vertebrate brain. J Biol Chem 263: 13475–13478.

Drucker DJ, Philippe J, Mojsov S, Chick WL, Habener JF (1987). Glucagon-like peptide I stimulates insulin gene expression and increases cyclic AMP levels in a rat islet cell line. Proc Natl Acad Sci U S A 84: 3434–3438.

Drucker DJ, Shi Q, Crivici A, Sumner-Smith M, Tavares W, Hill M *et al.* (1997). Regulation of the biological activity of glucagon-like peptide 2 in vivo by dipeptidyl peptidase IV. Nat Biotechnol 15: 673–677.

Drucker DJ, Buse JB, Taylor K, Kendall DM, Trautmann M, Zhuang D *et al.* (2008). Exenatide once weekly versus twice daily for the treatment of type 2 diabetes: a randomised, open-label, non-inferiority study. Lancet 372: 1240–1250.

Dupre J, Ross SA, Watson D, Brown JC (1973). Stimulation of insulin secretion by gastric inhibitory polypeptide in man. J Clin Endocrinol Metab 37: 826–828.

During MJ, Cao L, Zuzga DS, Francis JS, Fitzsimons HL, Jiao X *et al.* (2003). Glucagon-like peptide-1 receptor is involved in learning and neuroprotection. Nat Med 9: 1173–1179.

Dzhura I, Chepurny OG, Leech CA, Roe MW, Dzhura E, Xu X *et al.* (2011). Phospholipase C-ε links Epac2 activation to the

potentiation of glucose-stimulated insulin secretion from mouse islets of Langerhans. Islets 3: 121–128.

Egan JM, Meneilly GS, Habener JF, Elahi D (2002). Glucagon-like peptide-1 augments insulin-mediated glucose uptake in the obese state. J Clin Endocrinol Metab 87: 3768–3773.

Eissele R, Göke R, Willemer S, Harthus HP, Vermeer H, Arnold R *et al*. (1992). Glucagon-like peptide-1 cells in the gastrointestinal tract and pancreas of rat, pig and man. Eur J Clin Invest 22: 283–291.

Elahi D, Egan JM, Shannon RP, Meneilly GS, Khatri A, Habener JF *et al*. (2008). GLP-1 (9-36) amide, cleavage product of GLP-1 (7-36) amide, is a glucoregulatory peptide. Obesity (Silver Spring) 16: 1501–1509.

Eliasson L, Ma X, Renström E, Barg S, Berggren P-O, Galvanovskis J *et al*. (2003). SUR1 regulates PKA-independent cAMP-induced granule priming in mouse pancreatic B-cells. J Gen Physiol 121: 181–197.

Elrick H, Stimmler L, Hlad CJ, Arai Y (1964). Plasma insulin response to oral and intravenous glucose administration. J Clin Endocrinol Metab 24: 1076–1082.

Farilla L, Hui H, Bertolotto C, Kang E, Bulotta A, Di Mario U *et al*. (2002). Glucagon-like peptide-1 promotes islet cell growth and inhibits apoptosis in Zucker diabetic rats. Endocrinology 143: 4397.

Farilla L, Bulotta A, Hirshberg B, Li Calzi S, Khoury N, Noushmehr H *et al*. (2003). Glucagon-like peptide 1 inhibits cell apoptosis and improves glucose responsiveness of freshly isolated human islets. Endocrinology 144: 5149–5158.

Fehmann HC, Habener JF (1991). Homologous desensitization of the insulinotropic glucagon-like peptide-I (7-37) receptor on insulinoma (HIT-T15) cells. Endocrinology 128: 2880–2888.

Fehmann HC, Habener JF (1992). Insulinotropic hormone glucagon-like peptide-I(7-37) stimulation of proinsulin gene expression and proinsulin biosynthesis in insulinoma beta TC-1 cells. Endocrinology 130: 159–166.

Feng J, Zhang Z, Wallace MB, Stafford JA, Kaldor SW, Kassel DB *et al*. (2007). Discovery of alogliptin: a potent, selective, bioavailable, and efficacious inhibitor of dipeptidyl peptidase IV. J Med Chem 50: 2297–2300.

Flint A, Raben A, Astrup A, Holst JJ (1998). Glucagon-like peptide 1 promotes satiety and suppresses energy intake in humans. J Clin Invest 101: 515–520.

Franklin I, Gromada J, Gjinovci A, Theander S, Wollheim CB (2005). β-cell secretory products activate α-cell ATP-dependent potassium channels to inhibit glucagon release. Diabetes 54: 1808–1815.

Furness SG, Wootten D, Christopoulos A, Sexton PM (2012). Consequences of splice variation on secretin family G protein-coupled receptor function. Br J Pharmacol 166: 98–109.

Gedulin BR, Nikoulina SE, Smith PA, Gedulin G, Nielsen LL, Baron AD *et al*. (2005). Exenatide (exendin-4) improves insulin sensitivity and {beta}-cell mass in insulin-resistant obese fa/fa Zucker rats independent of glycemia and body weight. Endocrinology 146: 2069–2076.

Gefel D, Hendrick GK, Mojsov S, Habener J, Weir GC (1990). Glucagon-like peptide-I analogs: effects on insulin secretion and adenosine 3′,5′-monophosphate formation. Endocrinology 126: 2164–2168.

Gier B, Matveyenko AV, Kirakossian D, Dawson D, Dry SM, Butler PC (2012). Chronic GLP-1 receptor activation by exendin-4 induces expansion of pancreatic duct glands in rats and accelerates formation of dysplastic lesions and chronic pancreatitis in the Kras(G12D) mouse model. Diabetes 61: 1250–1262.

Göke R, Trautmann ME, Haus E, Richter G, Fehmann HC, Arnold R *et al*. (1989). Signal transmission after GLP-1(7-36)amide binding in RINm5F cells. Am J Physiol 257: G397–G401.

Göke R, Larsen PJ, Mikkelsen JD, Sheikh SP (1995). Distribution of GLP-1 binding sites in the rat brain: evidence that exendin-4 is a ligand of brain GLP-1 binding sites. Eur J Neurosci 7: 2294–2300.

González N, Acitores A, Sancho V, Valverde I, Villanueva-Peñacarrillo ML (2005). Effect of GLP-1 on glucose transport and its cell signalling in human myocytes. Regul Pept 126: 203–211.

Gribble FM, Tucker SJ, Ashcroft FM (1997). The essential role of the Walker A motifs of SUR1 in K-ATP channel activation by Mg-ADP and diazoxide. EMBO J 16: 1145–1152.

Gribble FM, Tucker SJ, Haug T, Ashcroft FM (1998). MgATP activates the beta cell KATP channel by interaction with its SUR1 subunit. Proc Natl Acad Sci U S A 95: 7185–7190.

Griffioen KJ, Wan R, Okun E, Wang X, Lovett-Barr MR, Li Y *et al*. (2011). GLP-1 receptor stimulation depresses heart rate variability and inhibits neurotransmission to cardiac vagal neurons. Cardiovasc Res 89: 72–78.

Gromada J, Holst JJ, Rorsman P (1998). Cellular regulation of islet hormone secretion by the incretin hormone glucagon-like peptide 1. Pflugers Arch 435: 583–594.

Grunberger G, Chang A, Garcia Soria G, Botros FT, Bsharat R, Milicevic Z (2012). Monotherapy with the once-weekly GLP-1 analogue dulaglutide for 12 weeks in patients with type 2 diabetes: dose-dependent effects on glycaemic control in a randomized, double-blind, placebo-controlled study. Diabet Med 29: 1260–1267.

Hansen L, Deacon CF, Orskov C, Holst JJ (1999). Glucagon-like peptide-1-(7-36)amide is transformed to glucagon-like peptide-1-(9-36)amide by dipeptidyl peptidase IV in the capillaries supplying the L cells of the porcine intestine. Endocrinology 140: 5356–5363.

Harikumar KG, Morfis MM, Sexton PM, Miller LJ (2008). Pattern of intra-family hetero-oligomerization involving the G-protein-coupled secretin receptor. J Mol Neurosci 36: 279–285.

Hatakeyama H, Kishimoto T, Nemoto T, Kasai H, Takahashi N (2006). Rapid glucose sensing by protein kinase A for insulin exocytosis in mouse pancreatic islets. J Physiol (Lond) 570: 271–282.

Hatakeyama H, Takahashi N, Kishimoto T, Nemoto T, Kasai H (2007). Two cAMP-dependent pathways differentially regulate exocytosis of large dense-core and small vesicles in mouse beta-cells. J Physiol (Lond) 582: 1087–1098.

Hayes MR, Skibicka KP, Grill HJ (2008). Caudal brainstem processing is sufficient for behavioral, sympathetic, and parasympathetic responses driven by peripheral and hindbrain glucagon-like-peptide-1 receptor stimulation. Endocrinology 149: 4059–4068.

Heller RS, Aponte GW (1995). Intra-islet regulation of hormone secretion by glucagon-like peptide-1-(7–36) amide. Am J Physiol 269: G852–G860.

Heller RS, Kieffer TJ, Habener JF (1997). Insulinotropic glucagon-like peptide I receptor expression in glucagon-producing alpha-cells of the rat endocrine pancreas. Diabetes 46: 785–791.

Hellström PM, Näslund E, Edholm T, Schmidt PT, Kristensen J, Theodorsson E *et al*. (2008). GLP-1 suppresses gastrointestinal

motility and inhibits the migrating motor complex in healthy subjects and patients with irritable bowel syndrome. Neurogastroenterol Motil 20: 649–659.

Henry RR, Smith SR, Schwartz SL, Mudaliar SR, Deacon CF, Holst JJ *et al*. (2011). Effects of saxagliptin on β-cell stimulation and insulin secretion in patients with type 2 diabetes. Diabetes Obes Metab 13: 850–858.

Herman GA, Stevens C, Van Dyck K, Bergman A, Yi B, De Smet M *et al*. (2005). Pharmacokinetics and pharmacodynamics of sitagliptin, an inhibitor of dipeptidyl peptidase IV, in healthy subjects: results from two randomized, double-blind, placebo-controlled studies with single oral doses. Clin Pharmacol Ther 78: 675–688.

Herrmann C, Göke R, Richter G, Fehmann HC, Arnold R, Göke B (1995). Glucagon-like peptide-1 and glucose-dependent insulin-releasing polypeptide plasma levels in response to nutrients. Digestion 56: 117–126.

Heymann E, Mentlein R (1978). Liver dipeptidyl aminopeptidase IV hydrolyzes substance P. FEBS Lett 91: 360–364.

Holmes GM, Browning KN, Tong M, Qualls-Creekmore E, Travagli RA (2009). Vagally mediated effects of glucagon-like peptide 1: in vitro and in vivo gastric actions. J Physiol (Lond) 587: 4749–4759.

Holst JJ (2007). The physiology of glucagon-like peptide 1. Physiol Rev 87: 1409–1439.

Holst JJ, Orskov C, Vagn Nielsen O, Schwartz TW (1987). Truncated glucagon-like peptide I, an insulin-releasing hormone from the distal gut. FEBS Lett 211: 169–174.

Hörsch D, Göke R, Eissele R, Michel B, Göke B (1997). Reciprocal cellular distribution of glucagon-like peptide-1 (GLP-1) immunoreactivity and GLP-1 receptor mRNA in pancreatic islets of rat. Pancreas 14: 290–294.

Hui H, Wright C, Perfetti R (2001). Glucagon-like peptide 1 induces differentiation of islet duodenal homeobox-1-positive pancreatic ductal cells into insulin-secreting cells. Diabetes 50: 785–796.

Hupe-Sodmann K, McGregor GP, Bridenbaugh R, Göke R, Göke B, Thole H *et al*. (1995). Characterisation of the processing by human neutral endopeptidase 24.11 of GLP-1(7-36) amide and comparison of the substrate specificity of the enzyme for other glucagon-like peptides. Regul Pept 58: 149–156.

Imeryüz N, Yeğen BÇ, Bozkurt A, Coşkun T, Villanueva-Peñacarrillo ML, Ulusoy NB (1997). Glucagon-like peptide-1 inhibits gastric emptying via vagal afferent-mediated central mechanisms. Am J Physiol 273: G920–G927.

In't Veld P, Marichal M (2010). Microscopic anatomy of the human islet of Langerhans. Adv Exp Med Biol 654: 1–19.

Jin SL, Han VK, Simmons JG, Towle AC, Lauder JM, Lund PK (1988). Distribution of glucagonlike peptide I (GLP-I), glucagon, and glicentin in the rat brain: an immunocytochemical study. J Comp Neurol 271: 519–532.

Jorgensen R, Kubale V, Vrecl M, Schwartz TW, Elling CE (2007). Oxyntomodulin differentially affects glucagon-like peptide-1 receptor beta-arrestin recruitment and signaling through Galpha(s). J Pharmacol Exp Ther 322: 148–154.

Kang G, Chepurny OG, Holz GG (2001). cAMP-regulated guanine nucleotide exchange factor II (Epac2) mediates Ca2+-induced Ca2+ release in INS-1 pancreatic β-cells. J Physiol (Lond) 536: 375–385.

Kang G, Leech CA, Chepurny OG, Coetzee WA, Holz GG (2008). Role of the cAMP sensor Epac as a determinant of KATP channel ATP sensitivity in human pancreatic β-cells and rat INS-1 cells. J Physiol (Lond) 586: 1307–1319.

Kanoski SE, Fortin SM, Arnold M, Grill HJ, Hayes MR (2011). Peripheral and central GLP-1 receptor populations mediate the anorectic effects of peripherally administered GLP-1 receptor agonists, liraglutide and exendin-4. Endocrinology 152: 3103–3112.

Kanse SM, Kreymann B, Ghatei MA, Bloom SR (1988). ScienceDirect.com – FEBS Letters – Identification and characterization of glucagon-like peptide-1 7–36 amide-binding sites in the rat brain and lung. FEBS Lett 241: 209–212.

Kato T, Nagatsu T, Fukasawa K, Harada M, Nagatsu I, Sakakibara S (1978). Successive cleavage of N-terminal Arg1–Pro2 and Lys3-Pro4 from substance P but no release of Arg1-Pro2 from bradykinin, by X-Pro dipeptidyl-aminopeptidase. Biochim Biophys Acta 525: 417–422.

Kemp DM, Habener JF (2001). Insulinotropic hormone glucagon-like peptide 1 (GLP-1) activation of insulin gene promoter inhibited by p38 mitogen-activated protein kinase. Endocrinology 142: 1179–1187.

Kenny AJ, Booth AG, George SG, Ingram J, Kershaw D, Wood EJ *et al*. (1976). Dipeptidyl peptidase IV, a kidney brush-border serine peptidase. Biochem J 157: 169–182.

Kieffer TJ, McIntosh CH, Pederson RA (1995). Degradation of glucose-dependent insulinotropic polypeptide and truncated glucagon-like peptide 1 in vitro and in vivo by dipeptidyl peptidase IV. Endocrinology 136: 3585–3596.

Kim D, Wang L, Beconi M, Eiermann GJ, Fisher MH, He H *et al*. (2005). (2R)-4-oxo-4-[3-(trifluoromethyl)-5,6-dihydro[1,2,4]triazolo [4,3-a]pyrazin-7(8H)-yl]-1-(2,4,5-trifluorophenyl)butan-2-amine: a potent, orally active dipeptidyl peptidase IV inhibitor for the treatment of type 2 diabetes. J Med Chem 48: 141–151.

Knudsen LB, Pridal L (1996). Glucagon-like peptide-1-(9-36) amide is a major metabolite of glucagon-like peptide-1-(7-36) amide after in vivo administration to dogs, and it acts as an antagonist on the pancreatic receptor. Eur J Pharmacol 318: 429–435.

Koole C, Wootten D, Simms J, Valant C, Sridhar R, Woodman OL *et al*. (2010). Allosteric ligands of the glucagon-like peptide 1 receptor (GLP-1R) differentially modulate endogenous and exogenous peptide responses in a pathway-selective manner: implications for drug screening. Mol Pharmacol 78: 456–465.

Korner J, Bessler M, Inabnet W, Taveras C, Holst JJ (2007). Exaggerated glucagon-like peptide-1 and blunted glucose-dependent insulinotropic peptide secretion are associated with Roux-en-Y gastric bypass but not adjustable gastric banding. Surg Obes Relat Dis 3: 597–601.

Körner M, Stöckli M, Waser B, Reubi JC (2007). GLP-1 receptor expression in human tumors and human normal tissues: potential for in vivo targeting. J Nucl Med 48: 736–743.

Kreymann B, Williams G, Ghatei MA, Bloom SR (1987). Glucagon-like peptide-1 7-36: a physiological incretin in man. Lancet 2: 1300–1304.

Lambeir AM, Durinx C, Proost P, Van Damme J, Scharpé S, De Meester I (2001). Kinetic study of the processing by dipeptidyl-peptidase IV/CD26 of neuropeptides involved in pancreatic insulin secretion. FEBS Lett 507: 327–330.

Lankat-Buttgereit B, Göke R, Stöckmann F, Jiang J, Fehmann HC, Göke B (1994). Detection of the human glucagon-like peptide 1(7-36) amide receptor on insulinoma-derived cell membranes. Digestion 55: 29–33.

Larsen PJ, Tang-Christensen M, Holst JJ, Orskov C (1997). Distribution of glucagon-like peptide-1 and other

preproglucagon-derived peptides in the rat hypothalamus and brainstem. Neuroscience 77: 257–270.

Lausier J, Diaz WC, Roskens V, LaRock K, Herzer K, Fong CG *et al.* (2010). Vagal control of pancreatic β-cell proliferation. Am J Physiol Endocrinol Metab 299: E786–E793.

Lawrence MC, Bhatt HS, Easom RA (2002). NFAT regulates insulin gene promoter activity in response to synergistic pathways induced by glucose and glucagon-like peptide-1. Diabetes 51: 691–698.

Light PE (2002). Glucagon-like peptide-1 inhibits pancreatic ATP-sensitive potassium channels via a protein kinase A- and ADP-dependent mechanism. Mol Endocrinol 16: 2135–2144.

Linnebjerg H, Park S, Kothare PA, Trautmann ME, Mace K, Fineman M *et al.* (2008). Effect of exenatide on gastric emptying and relationship to postprandial glycemia in type 2 diabetes. Regul Pept 151: 123–129.

Llewellyn-Smith IJ, Verberne AJM (2013). Central Regulation of Autonomic Functions. Oxford University Press: Oxford.

Lockie SH, Heppner KM, Chaudhary N, Chabenne JR, Morgan DA, Veyrat-Durebex C *et al.* (2012). Direct control of brown adipose tissue thermogenesis by central nervous system glucagon-like peptide-1 receptor signaling. Diabetes 61: 2753–2762.

Luque MA, González N, Márquez L, Acitores A, Redondo A, Morales M *et al.* (2002). Glucagon-like peptide-1 (GLP-1) and glucose metabolism in human myocytes. J Endocrinol 173: 465–473.

McIntyre N, Holdsworth CD, Turner DS (1964). New interpretation of oral glucose tolerance. Lancet 2: 20–21.

Malm-Erjefält M, Bjørnsdottir I, Vanggaard J, Helleberg H, Larsen U, Oosterhuis B *et al.* (2010). Metabolism and excretion of the once-daily human glucagon-like peptide-1 analog liraglutide in healthy male subjects and its in vitro degradation by dipeptidyl peptidase IV and neutral endopeptidase. Drug Metab Dispos 38: 1944–1953.

Matschinsky F, Liang Y, Kesavan P, Wang L, Froguel P, Velho G *et al.* (1993). Glucokinase as pancreatic beta cell glucose sensor and diabetes gene. J Clin Invest 92: 2092.

Matschinsky FM, Glaser B, Magnuson MA (1998). Pancreatic beta-cell glucokinase: closing the gap between theoretical concepts and experimental realities. Diabetes 47: 307–315.

Meier JJ, Nauck MA, Kranz D, Holst JJ, Deacon CF, Gaeckler D *et al.* (2004). Secretion, degradation, and elimination of glucagon-like peptide 1 and gastric inhibitory polypeptide in patients with chronic renal insufficiency and healthy control subjects. Diabetes 53: 654–662.

Meier JJ, Kemmeries G, Holst JJ, Nauck MA (2005). Erythromycin antagonizes the deceleration of gastric emptying by glucagon-like peptide 1 and unmasks its insulinotropic effect in healthy subjects. Diabetes 54: 2212–2218.

Meier JJ, Gethmann A, Nauck MA, Götze O, Schmitz F, Deacon CF *et al.* (2006). The glucagon-like peptide-1 metabolite GLP-1-(9-36) amide reduces postprandial glycemia independently of gastric emptying and insulin secretion in humans. Am J Physiol Endocrinol Metab 290: E1118–E1123.

Meneilly GS, McIntosh CHS, Pederson RA, Habener JF, Ehlers MRW, Egan JM *et al.* (2003). Effect of glucagon-like peptide 1 (7-36 amide) on insulin-mediated glucose uptake in patients with type 1 diabetes. Diabetes Care 26: 837–842.

Mentlein R, Dahms P, Grandt D, Krüger R (1993a). Proteolytic processing of neuropeptide Y and peptide YY by dipeptidyl peptidase IV. Regul Pept 49: 133–144.

Mentlein R, Gallwitz B, Schmidt WE (1993b). Dipeptidyl-peptidase IV hydrolyses gastric inhibitory polypeptide, glucagon-like peptide-1(7-36)amide, peptide histidine methionine and is responsible for their degradation in human serum. Eur J Biochem 214: 829–835.

Merchenthaler I, Lane M, Shughrue P (1999). Distribution of pre-pro-glucagon and glucagon-like peptide-1 receptor messenger RNAs in the rat central nervous system. J Comp Neurol 403: 261–280.

Moens K, Heimberg H, Flamez D, Huypens P, Quartier E, Ling Z *et al.* (1996). Expression and functional activity of glucagon, glucagon-like peptide I, and glucose-dependent insulinotropic peptide receptors in rat pancreatic islet cells. Diabetes 45: 257–261.

Mojsov S, Heinrich G, Wilson IB, Ravazzola M, Orci L, Habener JF (1986). Preproglucagon gene expression in pancreas and intestine diversifies at the level of post-translational processing. J Biol Chem 261: 11880–11889.

Mojsov S, Weir GC, Habener JF (1987). Insulinotropin: glucagon-like peptide I (7-37) co-encoded in the glucagon gene is a potent stimulator of insulin release in the perfused rat pancreas. J Clin Invest 79: 616–619.

Montrose-Rafizadeh C, Yang H, Rodgers BD, Beday A, Pritchette LA, Eng J (1997a). High potency antagonists of the pancreatic glucagon-like peptide-1 receptor. J Biol Chem 272: 21201–21206.

Montrose-Rafizadeh C, Yang H, Wang Y, Roth J, Montrose MH, Adams LG (1997b). Novel signal transduction and peptide specificity of glucagon-like peptide receptor in 3T3-L1 adipocytes. J Cell Physiol 172: 275–283.

Nachnani JS, Bulchandani DG, Nookala A, Herndon B, Molteni A, Pandya P *et al.* (2010). Biochemical and histological effects of exendin-4 (exenatide) on the rat pancreas. Diabetologia 53: 153–159.

Nagell CF, Wettergren A, Ørskov C, Holst JJ (2006). Inhibitory effect of GLP-1 on gastric motility persists after vagal deafferentation in pigs. Scand J Gastroenterol 41: 667–672.

Nakabayashi H, Nishizawa M, Nakagawa A, Takeda R, Niijima A (1996). Vagal hepatopancreatic reflex effect evoked by intraportal appearance of tGLP-1. Am J Physiol 271: E808–E813.

Nakagawa A, Satake H, Nakabayashi H, Nishizawa M, Furuya K, Nakano S *et al.* (2004). Receptor gene expression of glucagon-like peptide-1, but not glucose-dependent insulinotropic polypeptide, in rat nodose ganglion cells. Auton Neurosci 110: 36–43.

Näslund E, Gutniak M, Skogar S, Rössner S, Hellström PM (1998). Glucagon-like peptide 1 increases the period of postprandial satiety and slows gastric emptying in obese men. Am J Clin Nutr 68: 525–530.

Nauck MA, Bartels E, Orskov C, Ebert R, Creutzfeldt W (1993a). Additive insulinotropic effects of exogenous synthetic human gastric inhibitory polypeptide and glucagon-like peptide-1-(7-36) amide infused at near-physiological insulinotropic hormone and glucose concentrations. J Clin Endocrinol Metab 76: 912–917.

Nauck MA, Heimesaat MM, Orskov C, Holst JJ, Ebert R, Creutzfeldt W (1993b). Preserved incretin activity of glucagon-like peptide 1 [7-36 amide] but not of synthetic human gastric inhibitory polypeptide in patients with type-2 diabetes mellitus. J Clin Invest 91: 301–307.

Nauck MA, Kemmeries G, Holst JJ, Meier JJ (2011). Rapid tachyphylaxis of the glucagon-like peptide 1-induced deceleration of gastric emptying in humans. Diabetes 60: 1561–1565.

Nikolaidis LA, Elahi D, Shen Y-T, Shannon RP (2005). Active metabolite of GLP-1 mediates myocardial glucose uptake and improves left ventricular performance in conscious dogs with dilated cardiomyopathy. Am J Physiol Heart Circ Physiol 289: H2401–H2408.

Nishizawa M, Nakabayashi H, Uchida K, Nakagaw A, Niijima A (1996). The hepatic vagal nerve is receptive to incretin hormone glucagon-like peptide-l, but not to glucose-dependent insulinotropic polypeptide, in the portal vein. J Auton Nerv Syst 61: 149–154.

Nogueiras R, Perez-Tilve D, Veyrat-Durebex C, Morgan DA, Varela L, Haynes WG *et al.* (2009). Direct control of peripheral lipid deposition by CNS GLP-1 receptor signaling is mediated by the sympathetic nervous system and blunted in diet-induced obesity. J Neurosci 29: 5916–5925.

Oravecz T, Pall M, Roderiquez G, Gorrell MD, Ditto M, Nguyen NY *et al.* (1997). Regulation of the receptor specificity and function of the chemokine RANTES (regulated on activation, normal T cell expressed and secreted) by dipeptidyl peptidase IV (CD26)-mediated cleavage. J Exp Med 186: 1865–1872.

Orskov C, Poulsen SS (1991). Glucagonlike peptide-I-(7-36)-amide receptors only in islets of Langerhans. Autoradiographic survey of extracerebral tissues in rats. Diabetes 40: 1292–1296.

Orskov C, Holst JJ, Poulsen SS, Kirkegaard P (1987). Pancreatic and intestinal processing of proglucagon in man. Diabetologia 30: 874–881.

Orskov C, Rabenhøj L, Wettergren A, Kofod H, Holst JJ (1994). Tissue and plasma concentrations of amidated and glycine-extended glucagon-like peptide I in humans. Diabetes 43: 535–539.

Orskov C, Poulsen SS, Møller M, Holst JJ (1996a). Glucagon-like peptide I receptors in the subfornical organ and the area postrema are accessible to circulating glucagon-like peptide I. Diabetes 45: 832–835.

Orskov L, Holst JJ, Møller J, Orskov C, Møller N, Alberti KG *et al.* (1996b). GLP-1 does not acutely affect insulin sensitivity in healthy man. Diabetologia 39: 1227–1232.

Ozaki N, Shibasaki T, Kashima Y, Miki T, Takahashi K, Ueno H *et al.* (2000). cAMP-GEFII is a direct target of cAMP in regulated exocytosis. Nat Cell Biol 2: 805–811.

Panjwani N, Mulvihill EE, Longuet C, Yusta B, Campbell JE, Brown TJ *et al.* (2013). GLP-1 receptor activation indirectly reduces hepatic lipid accumulation but does not attenuate development of atherosclerosis in diabetic male ApoE-/- mice. Endocrinology 154: 127–139.

Park JH, Kim SJ, Park SH, Son DG, Bae JH, Kim HK *et al.* (2012). Glucagon-like peptide-1 enhances glucokinase activity in pancreatic β-cells through the association of Epac2 with Rim2 and Rab3A. Endocrinology 153: 574–582.

Patzelt C, Tager HS, Carroll RJ, Steiner DF (1979). Identification and processing of proglucagon in pancreatic islets. Nature 282: 260–266.

Perfetti R, Zhou J, Doyle ME, Egan JM (2000). Glucagon-like peptide-1 induces cell proliferation and pancreatic-duodenum homeobox-1 expression and increases endocrine cell mass in the pancreas of old, glucose-intolerant rats. Endocrinology 141: 4600–4605.

Plamboeck A, Holst JJ, Carr RD, Deacon CF (2005). Neutral endopeptidase 24.11 and dipeptidyl peptidase IV are both mediators of the degradation of glucagon-like peptide 1 in the anaesthetised pig. Diabetologia 48: 1882–1890.

Pocai A (2012). Unraveling oxyntomodulin, GLP1's enigmatic brother. J Endocrinol 215: 335–346.

Pratley R, Nauck M, Bailey T, Montanya E, Cuddihy R, Filetti S *et al.* (2011). One year of liraglutide treatment offers sustained and more effective glycaemic control and weight reduction compared with sitagliptin, both in combination with metformin, in patients with type 2 diabetes: a randomised, parallel-group, open-label trial. Int J Clin Pract 65: 397–407.

Pratley RE, Nauck M, Bailey T, Montanya E, Cuddihy R, Filetti S *et al.* (2010). Liraglutide versus sitagliptin for patients with type 2 diabetes who did not have adequate glycaemic control with metformin: a 26-week, randomised, parallel-group, open-label trial. Lancet 375: 1447–1456.

Preitner F, Ibberson M, Franklin I, Binnert C, Pende M, Gjinovci A *et al.* (2004). Gluco-incretins control insulin secretion at multiple levels as revealed in mice lacking GLP-1 and GIP receptors. J Clin Invest 113: 635–645.

Prigeon RL, Quddusi S, Paty B, D'Alessio DA (2003). Suppression of glucose production by GLP-1 independent of islet hormones: a novel extrapancreatic effect. Am J Physiol Endocrinol Metab 285: E701–E707.

Proost P, Struyf S, Schols D, Durinx C, Wuyts A, Lenaerts JP *et al.* (1998). Processing by CD26/dipeptidyl-peptidase IV reduces the chemotactic and anti-HIV-1 activity of stromal-cell-derived factor-1alpha. FEBS Lett 432: 73–76.

Proost P, Struyf S, Schols D, Opdenakker G, Sozzani S, Allavena P *et al.* (1999). Truncation of macrophage-derived chemokine by CD26/ dipeptidyl-peptidase IV beyond its predicted cleavage site affects chemotactic activity and CC chemokine receptor 4 interaction. J Biol Chem 274: 3988–3993.

Proost P, Menten P, Struyf S, Schutyser E, De Meester I, Van Damme J (2000). Cleavage by CD26/dipeptidyl peptidase IV converts the chemokine LD78beta into a most efficient monocyte attractant and CCR1 agonist. Blood 96: 1674–1680.

Quoyer J, Longuet C, Broca C, Linck N, Costes S, Varin E *et al.* (2010). GLP-1 mediates antiapoptotic effect by phosphorylating Bad through a beta-arrestin 1-mediated ERK1/2 activation in pancreatic beta-cells. J Biol Chem 285: 1989–2002.

Reid T (2012). Choosing GLP-1 receptor agonists or DPP-4 inhibitors: weighing the clinical trial evidence. Clin Diabetes 30: 3–12.

Renner E, Puskás N, Dobolyi A, Palkovits M (2012). Glucagon-like peptide-1 of brainstem origin activates dorsomedial hypothalamic neurons in satiated rats. Peptides 35: 14–22.

Richter G, Göke R, Göke B, Arnold R (1990). Characterization of receptors for glucagon-like peptide-1(7-36)amide on rat lung membranes. FEBS Lett 267: 78–80.

Richter G, Feddersen O, Wagner U, Barth P, Göke R, Göke B (1993). GLP-1 stimulates secretion of macromolecules from airways and relaxes pulmonary artery. Am J Physiol 265: L374–L381.

Rolin B, Larsen MO, Gotfredsen CF, Deacon CF, Carr RD, Wilken M *et al.* (2002). The long-acting GLP-1 derivative NN2211 ameliorates glycemia and increases beta-cell mass in diabetic mice. Am J Physiol Endocrinol Metab 283: E745–E752.

Rosenstock J, Reusch J, Bush M, Yang F, Stewart M, Albiglutide Study Group (2009). Potential of albiglutide, a long-acting GLP-1 receptor agonist, in type 2 diabetes: a randomized controlled trial exploring weekly, biweekly, and monthly dosing. Diabetes Care 32: 1880–1886.

Rosenstock J, Balas B, Charbonnel B, Bolli GB, Boldrin M, Ratner R *et al.* (2013). The fate of taspoglutide, a weekly GLP-1 receptor agonist, versus twice-daily exenatide for type 2 diabetes: the T-emerge 2 trial. Diabetes Care 36: 498–504.

Ruiz-Grande C, Alarcón C, Alcántara A, Castilla C, López Novoa JM, Villanueva-Peñacarrillo ML *et al.* (1993). Renal catabolism of truncated glucagon-like peptide 1. Horm Metab Res 25: 612–616.

Sancho V, Nuche B, Arnés L, Cancelas J, González N, Díaz-Miguel M *et al.* (2007). The action of GLP-1 and exendins upon glucose transport in normal human adipocytes, and on kinase activity as compared to morbidly obese patients. Int J Mol Med 19: 961–966.

Sandoval DA, Bagnol D, Woods SC, D'Alessio DA, Seeley RJ (2008). Arcuate glucagon-like peptide 1 receptors regulate glucose homeostasis but not food intake. Diabetes 57: 2046–2054.

Scheen AJ (2012). DPP-4 inhibitors in the management of type 2 diabetes: a critical review of head-to-head trials. Diabetes Metab 38: 89–101.

Schepp W, Dehne K, Riedel T, Schmidtler J, Schaffer K, Classen M (1996). Oxyntomodulin: a cAMP-dependent stimulus of rat parietal cell function via the receptor for glucagon-like peptide-1 (7-36)NH2. Digestion 57: 398–405.

Schirra J, Wank U, Arnold R, Göke B, Katschinski M (2002). Effects of glucagon-like peptide-1(7-36)amide on motility and sensation of the proximal stomach in humans. Gut 50: 341–348.

Schirra J, Nicolaus M, Roggel R, Katschinski M, Storr M, Woerle HJ *et al.* (2006). Endogenous glucagon-like peptide 1 controls endocrine pancreatic secretion and antro-pyloro-duodenal motility in humans. Gut 55: 243–251.

Schlatter P, Beglinger C, Drewe J, Gutmann H (2007). Glucagon-like peptide 1 receptor expression in primary porcine proximal tubular cells. Regul Pept 141: 120–128.

Schuit FC, Huypens P, Heimberg H, Pipeleers DG (2001). Glucose sensing in pancreatic β-cells a model for the study of other glucose-regulated cells in gut, pancreas, and hypothalamus. Diabetes 50: 1–11.

Scrocchi LA, Brown TJ, MaClusky N, Brubaker PL, Auerbach AB, Joyner AL *et al.* (1996). Glucose intolerance but normal satiety in mice with a null mutation in the glucagon-like peptide 1 receptor gene. Nat Med 2: 1254–1258.

Seghieri M, Rebelos E, Gastaldelli A, Astiarraga BD, Casolaro A, Barsotti E *et al.* (2013). Direct effect of GLP-1 infusion on endogenous glucose production in humans. Diabetologia 56: 156–161.

Shibasaki T, Takahashi H, Miki T, Sunaga Y, Matsumura K, Yamanaka M *et al.* (2007). Essential role of Epac2/Rap1 signaling in regulation of insulin granule dynamics by cAMP. Proc Natl Acad Sci U S A 104: 19333–19338.

Shughrue PJ, Lane MV, Merchenthaler I (1996). Glucagon-like peptide-1 receptor (GLP1-R) mRNA in the rat hypothalamus. Endocrinology 137: 5159–5162.

Singh S, Chang H-Y, Richards TM, Weiner JP, Clark JM, Segal JB (2013). Glucagonlike peptide 1-based therapies and risk of hospitalization for acute pancreatitis in type 2 diabetes mellitus: a population-based matched case-control study. JAMA Intern Med 173: 534–539.

Skoglund G, Hussain MA, Holz GG (2000). Glucagon-like peptide 1 stimulates insulin gene promoter activity by protein kinase A-independent activation of the rat insulin I gene cAMP response element. Diabetes 49: 1156–1164.

Song W-J, Seshadri M, Ashraf U, Mdluli T, Mondal P, Keil M *et al.* (2011). Snapin mediates incretin action and augments glucose-dependent insulin secretion. Cell Metab 13: 308–319.

Sonoda N, Imamura T, Yoshizaki T, Babendure JL, Lu J-C, Olefsky JM (2008). Beta-Arrestin-1 mediates glucagon-like peptide-1 signaling to insulin secretion in cultured pancreatic beta cells. Proc Natl Acad Sci U S A 105: 6614–6619.

Stoffers DA, Kieffer TJ, Hussain MA, Drucker DJ, Bonner-Weir S, Habener JF *et al.* (2000). Insulinotropic glucagon-like peptide 1 agonists stimulate expression of homeodomain protein IDX-1 and increase islet size in mouse pancreas. Diabetes 49: 741–748.

Sturis J, Gotfredsen CF, Rømer J, Rolin B, Ribel U, Brand CL *et al.* (2003). GLP-1 derivative liraglutide in rats with beta-cell deficiencies: influence of metabolic state on beta-cell mass dynamics. Br J Pharmacol 140: 123–132.

Tang-Christensen M, Larsen PJ, Göke R, Fink-Jensen A, Jessop DS, Møller M *et al.* (1996). Central administration of GLP-1-(7-36) amide inhibits food and water intake in rats. Am J Physiol 271: R848–R856.

Tomas E, Habener JF (2010). Insulin-like actions of glucagon-like peptide-1: a dual receptor hypothesis. Trends Endocrinol Metab 21: 59–67.

Tornehave D, Kristensen P, Rømer J, Knudsen LB, Heller RS (2008). Expression of the GLP-1 receptor in mouse, rat, and human pancreas. J Histochem Cytochem 56: 841–851.

Tourrel C, Bailbé D, Meile MJ, Kergoat M, Portha B (2001). Glucagon-like peptide-1 and exendin-4 stimulate beta-cell neogenesis in streptozotocin-treated newborn rats resulting in persistently improved glucose homeostasis at adult age. Diabetes 50: 1562–1570.

Turton MD, O'Shea D, Gunn I, Beak SA, Edwards CM, Meeran K *et al.* (1996). A role for glucagon-like peptide-1 in the central regulation of feeding. Nature 379: 69–72.

Vahl TP, Tauchi M, Durler TS, Elfers EE, Fernandes TM, Bitner RD *et al.* (2007). Glucagon-like peptide-1 (GLP-1) receptors expressed on nerve terminals in the portal vein mediate the effects of endogenous GLP-1 on glucose tolerance in rats. Endocrinology 148: 4965–4973.

Vella A, Shah P, Basu R, Basu A, Holst JJ, Rizza RA (2000). Effect of glucagon-like peptide 1(7-36) amide on glucose effectiveness and insulin action in people with type 2 diabetes. Diabetes 49: 611–617.

Vella A, Shah P, Reed A, Adkins A, Basu R, Rizza R (2002). Lack of effect of exendin-4 and glucagon-like peptide-1-(7, 36)-amide on insulin action in non-diabetic humans. Diabetologia 45: 1410–1415.

Villanueva-Peñacarrillo ML, Delgado E, Trapote MA, Alcántara A, Clemente F, Luque MA *et al.* (1995). Glucagon-like peptide-1 binding to rat hepatic membranes. J Endocrinol 146: 183–189.

Wan S, Browning KN, Travagli RA (2007a). Glucagon-like peptide-1 modulates synaptic transmission to identified pancreas-projecting vagal motoneurons. Peptides 28: 2184–2191.

Wan S, Coleman FH, Travagli RA (2007b). Glucagon-like peptide-1 excites pancreas-projecting preganglionic vagal motoneurons. Am J Physiol Gastrointest Liver Physiol 292: G1474–G1482.

Wang A, Dorso C, Kopcho L, Locke G, Langish R, Harstad E *et al.* (2012). Potency, selectivity and prolonged binding of saxagliptin to DPP4: maintenance of DPP4 inhibition by saxagliptin in vitro and ex vivo when compared to a rapidly-dissociating DPP4 inhibitor. BMC Pharmacol 12: 2.

Wang Q, Brubaker PL (2002). Glucagon-like peptide-1 treatment delays the onset of diabetes in 8 week-old db/db mice. Diabetologia 45: 1263–1273.

Wang X, Zhou J, Doyle ME, Egan JM (2001). Glucagon-like peptide-1 causes pancreatic duodenal homeobox-1 protein translocation from the cytoplasm to the nucleus of pancreatic β-cells by a cyclic adenosine monophosphate/protein kinase A-dependent mechanism. Endocrinology 142: 1820–1827.

Wang Y, Egan JM, Raygada M, Nadiv O, Roth J, Montrose-Rafizadeh C (1995). Glucagon-like peptide-1 affects gene transcription and messenger ribonucleic acid stability of components of the insulin secretory system in RIN 1046-38 cells. Endocrinology 136: 4910–4917.

Wang Y, Kole HK, Montrose-Rafizadeh C, Perfetti R, Bernier M, Egan JM (1997). Regulation of glucose transporters and hexose uptake in 3T3-L1 adipocytes: glucagon-like peptide-1 and insulin interactions. J Mol Endocrinol 19: 241–248.

Washington MC, Raboin SJ, Thompson W, Larsen CJ, Sayegh AI (2010). Exenatide reduces food intake and activates the enteric nervous system of the gastrointestinal tract and the dorsal vagal complex of the hindbrain in the rat by a GLP-1 receptor. Brain Res 1344: 124–133.

Wettergren A, Petersen H, Orskov C, Christiansen J, Sheikh SP, Holst JJ (1994). Glucagon-like peptide-1 7-36 amide and peptide YY from the L-cell of the ileal mucosa are potent inhibitors of vagally induced gastric acid secretion in man. Scand J Gastroenterol 29: 501–505.

Wettergren A, Wøjdemann M, Meisner S, Stadil F, Holst JJ (1997). The inhibitory effect of glucagon-like peptide-1 (GLP-1) 7-36 amide on gastric acid secretion in humans depends on an intact vagal innervation. Gut 40: 597–601.

Wettergren A, Wøjdemann M, Holst JJ (1998). Glucagon-like peptide-1 inhibits gastropancreatic function by inhibiting central parasympathetic outflow. Am J Physiol 275: G984–G992.

Williams DL, Baskin DG, Schwartz MW (2009). Evidence that intestinal glucagon-like peptide-1 plays a physiological role in satiety. Endocrinology 150: 1680–1687.

Xie T, Chen M, Zhang Q-H, Ma Z, Weinstein LS (2007). Beta cell-specific deficiency of the stimulatory G protein alpha-subunit Gsalpha leads to reduced beta cell mass and insulin-deficient diabetes. Proc Natl Acad Sci U S A 104: 19601–19606.

Xu G, Stoffers DA, Habener JF, Bonner-Weir S (1999). Exendin-4 stimulates both beta-cell replication and neogenesis, resulting in increased beta-cell mass and improved glucose tolerance in diabetic rats. Diabetes 48: 2270–2276.

Xu G, Kaneto H, Lopez-Avalos MD, Weir GC, Bonner-Weir S (2006). GLP-1/exendin-4 facilitates beta-cell neogenesis in rat and human pancreatic ducts. Diabetes Res Clin Pract 73: 107–110.

Yamada C, Yamada Y, Tsukiyama K, Yamada K, Udagawa N, Takahashi N *et al.* (2008). The murine glucagon-like peptide-1 receptor is essential for control of bone resorption. Endocrinology 149: 574–579.

Yamamoto H, Lee CE, Marcus JN, Williams TD, Overton JM, Lopez ME *et al.* (2002). Glucagon-like peptide-1 receptor stimulation increases blood pressure and heart rate and activates autonomic regulatory neurons. J Clin Invest 110: 43–52.

Yamamoto H, Kishi T, Lee CE, Choi BJ, Fang H, Hollenberg AN *et al.* (2003). Glucagon-like peptide-1-responsive catecholamine neurons in the area postrema link peripheral glucagon-like peptide-1 with central autonomic control sites. J Neurosci 23: 2939–2946.

Zander M, Madsbad S, Madsen JL, Holst JJ (2002). Effect of 6-week course of glucagon-like peptide 1 on glycaemic control, insulin sensitivity, and β-cell function in type 2 diabetes: a parallel-group study. Lancet 359: 824–830.

Journal of Biomolecular Screening
2015, Vol. 20(5) 646–654

DOI: 10.1177/1087057114563025
jbx.sagepub.com
SAGE

Detection and Quantification of Allosteric Modulation of Endogenous M_4 Muscarinic Acetylcholine Receptor Using Impedance-Based Label-Free Technology in a Neuronal Cell Line

Amy N. Y. Chen[1], Daniel T. Malone[1], Kavita Pabreja[1], Patrick M. Sexton[1], Arthur Christopoulos[1], and Meritxell Canals[1]

Abstract

Allosteric modulators of G protein–coupled receptors have the potential to achieve greater receptor subtype selectivity compared with ligands targeting the orthosteric site of this receptor family. However, the high attrition rate in GPCR drug discovery programs has highlighted the need to better characterize lead compounds in terms of their allosteric action, as well as the signals they elicit. Recently, the use of label-free technologies has been proposed as an approach to overcome some limitations of endpoint-based assays and detect global changes in the ligand-stimulated cell. In this study, we assessed the ability of an impedance-based label-free technology, xCELLigence, to detect allosteric modulation in a neuronal cell line natively expressing rodent M_4 muscarinic acetylcholine receptors. We were able to demonstrate that positive allosteric modulation of the endogenous M_4 muscarinic acetylcholine receptor can be detected using this technology. Importantly, the allosteric parameters estimated from the label-free approach are comparable to those estimated from endpoint-based assays.

Keywords

label-free technology, cell impedance, G protein–coupled receptor, positive allosteric modulator, muscarinic acetylcholine receptor

Introduction

G protein–coupled receptors (GPCRs) are the largest family of mammalian cell-surface receptors. These receptors are important in the function of all organ systems, with over 30% of marketed drugs interacting with GPCRs to exert their therapeutic effect.[1] However, GPCR drug discovery efforts still suffer from a very high attrition rate, suggesting that much remains to be learned about the complexity of GPCR signaling.

Traditionally, drug discovery at GPCRs has been based on screening compounds using endpoint-based assays, where compounds are defined by their ability to alter a distinct signaling event in a cell. However, the realization that GPCRs adopt different active conformations that recruit or disrupt different signaling components has highlighted the caveats of such approaches as only one signaling event can be measured per assay and often at only one time point.[2,3] In addition, many endpoint-based assays require cell lines to express reporter proteins or to overexpress the receptor of interest, and therefore, such manipulations can alter the physiological relevance of a cellular environment.

Recently, the use of label-free technologies has been proposed as an approach to overcome these limitations and to detect real-time global changes in the ligand-stimulated cell.[4,5] Label-free technologies have been used in the study of GPCRs, particularly receptor de-orphanization programs, as an unbiased approach that does not discriminate between specific signaling events in a cell.[4,5] Moreover, although these approaches require prior knowledge of receptor expression, they can be of use when the G protein coupling preferences of the receptor are unknown. Currently, the two main label-free technologies used for receptor-mediated

[1]Drug Discovery Biology, Monash Institute of Pharmaceutical Sciences, Monash University, Parkville, Victoria, Australia

Received Aug 27, 2014, and in revised form Oct 16, 2014. Accepted for publication Nov 16, 2014.

Corresponding Author:
Meritxell Canals, Drug Discovery Biology, Monash University, 381 Royal Parade, Parkville VIC 3052, Australia.
Email: meri.canals@monash.edu

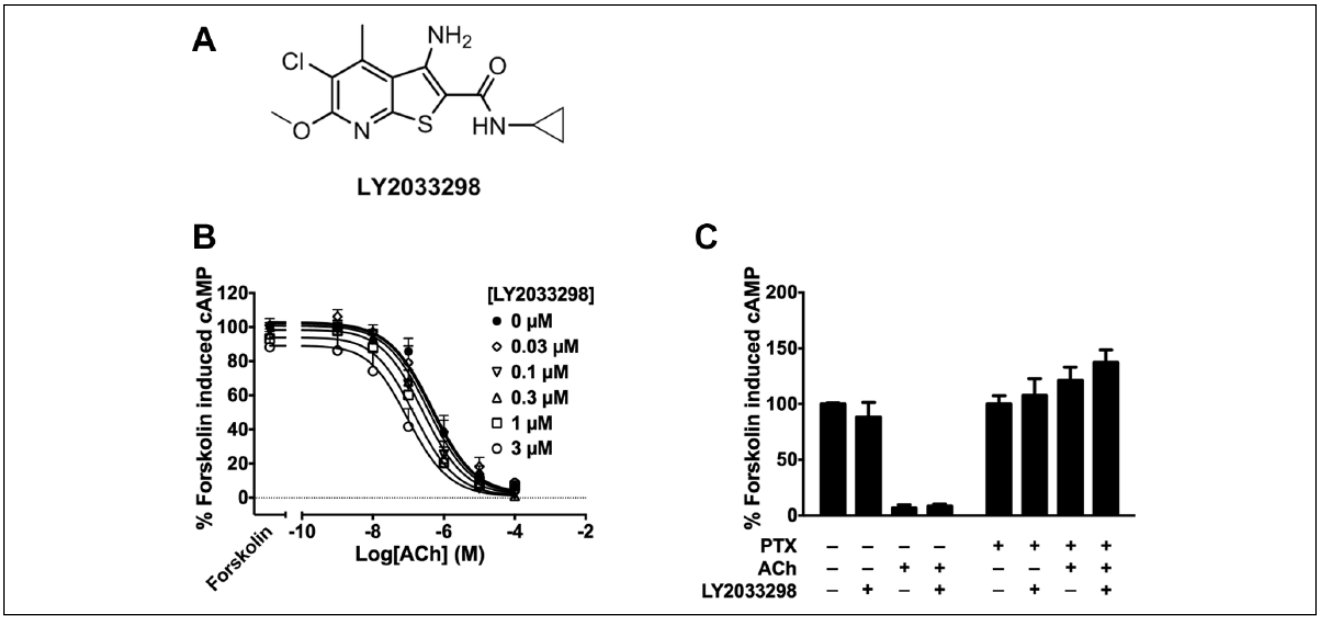

Figure 1. LY2033298 potentiates inhibition of forskolin-induced cAMP by acetylcholine (ACh). (**A**) Chemical structure of the M_4 muscarinic acetylcholine receptor (mAChR) PAM, LY2033298. (**B**) Concentration-response curves of ACh inhibition of forskolin-induced cAMP production with increasing concentrations of LY2033298 measured using a bioluminescence resonance energy transfer (BRET)–based cAMP sensor. Curves shown represent the best fit of the operational model of allosterism, equation (1); $n = 4$. (**C**) In cells treated with pertussis toxin (PTX; 25 ng/mL for 24 h), ACh (100 μM) in the absence and presence of LY2033298 (3 μM) lost the ability to inhibit forskolin-induced cAMP production; $n = 2$–4. Data presented as mean ± SEM.

signaling assays are impedance based and optical based. Impedance-based technologies, such as xCELLigence (Roche Diagnostics GmbH, Mannheim, Germany, and ACEA Biosciences, San Diego, CA)[6] and CellKey (MDS Analytical Technologies, Sunnyvale, CA),[7] use a microelectrode array to measure the changes in impedance of the electrical current applied to a cell layer. On the other hand, optical-based technologies, such as EPIC (Corning, Inc, Corning, NY).[8] and BIND (SRU Biosystems, Woburn, MA),[9] measure the change in refraction index as a function of mass redistribution of the cell layer. Both technologies are sensitive to changes in cell morphology, adhesion, and cytoskeleton reorganization.[4,5]

Most current GPCR-based therapeutics target the orthosteric binding site of these receptors—namely, the site where the endogenous ligands bind.[10] Therefore, a major limitation of these drugs is the occurrence of side effects that can be caused by the drug acting on other subtypes of the target GPCR due to sequence conservation at the orthosteric site. This has led to a focus on the development of allosteric modulators as potentially more selective therapeutic ligands.[11–13] Allosteric modulators bind to GPCRs at a site that is topographically distinct from the orthosteric binding site and is frequently less conserved.[14] Allosteric modulators can alter the affinity and/or efficacy of the orthosteric ligand and can sometimes have efficacy in the absence of the orthosteric ligand. Due to these properties, there is potential for allosteric modulators to be not only more subtype selective than current orthosteric drugs but also to maintain the spatiotemporal control of receptor activity. This type of treatment can be beneficial in a number of disease states, particularly ones where current treatments based on orthosteric targeting of GPCRs are suboptimal, such as schizophrenia.[15]

Antipsychotics currently on the market for the treatment of schizophrenia are associated with a range of side effects, including movement, cardiovascular, and metabolic adverse effects.[16] Consequently, there have been intensive efforts toward developing novel therapeutics for schizophrenia that have high receptor subtype selectivity and lower occurrence of side effects. The muscarinic acetylcholine receptor (mAChR) subtypes 1, 4, and 5 have all been implicated in schizophrenia,[15] and selective M_4 mAChR agonism, in particular, has antipsychotic effects.[17] Xanomeline, an M_1/M_4 mAChR-preferring orthosteric agonist, significantly improved both positive and negative symptoms in people with schizophrenia compared with a placebo-treated group in a pilot study.[18] However, the presence of gastrointestinal-related adverse effects mediated by xanomeline acting on peripheral mAChRs prevented it from undergoing further clinical development. This paved way for the development of M_4 mAChR-positive allosteric modulators (PAMs), with LY2033298 (**Fig. 1A**) being the first to show efficacy in vivo.[19,20] In cellular assays, LY2033298 has functional selectivity for the M_4 mAChR over other mAChR subtypes in the

presence of the endogenous orthosteric agonist, acetylcholine (ACh).[19]

As label-free technologies detect global cellular changes upon receptor activation, they are ideal systems to evaluate and/or screen for allosteric modulation of GPCRs in native systems endogenously expressing the receptor of interest. Indeed, in the past few years, potentiation of orthosteric ligands by allosteric modulators has been measured using both impedance-based[21] and optical-based[22] technologies. However, these experiments were performed in recombinant cells where the receptors of interest have been heterologously expressed. To date, no study has investigated whether these approaches are sensitive enough to detect and quantify allosteric modulation of endogenously expressed GPCRs.

In the present study, we assessed the ability of an impedance-based technology, xCELLigence, to detect allosteric modulation in a neuronal cell line that natively expresses rodent M_4 mAChRs. We demonstrate that the positive allosteric modulation of agonist-induced impedance at the endogenous M_4 mAChR could be detected and quantified with this technology. Importantly, the allosteric parameters estimated from the xCELLigence data are comparable to those estimated from endpoint-based assays.

Materials and Methods

Materials

LY2033298 was prepared as a 10-mM stock in DMSO distributed in 100-µL aliquots and stored at −20 °C. Prior to its use, LY2033298 was diluted in the corresponding buffer for each assay.

Cell Culture

NG108-15 cells (American Type Culture Collection, Manassas, VA) were grown and maintained in high glucose Dulbecco's modified Eagle's medium without sodium pyruvate supplemented with 10% fetal bovine serum and sodium hypoxanthine, aminopterin, and thymidine (HAT) supplement (Life Technologies, Mulgrave, VIC, Australia). Cells were maintained at 37 °C in a humidified incubator containing 5% CO_2.

NG108-15 Membrane Preparation

When cells were approximately 90% confluent, they were detached using 2 mM EDTA in phosphate-buffered saline (150 mM NaCl, 16 mM Na_2HPO_4, 4 mM NaH_2PO_4) and centrifuged (300 × *g*, 4 °C, 10 min). The resulting pellets were resuspended in 30 mL of ice-cold buffer containing 20 mM HEPES and 10 mM EDTA at pH 7.4. The cell suspension was homogenized using a Polytron homogenizer (PT 1200 CL; Kinematica, Basel, Switzerland), with three 10-s bursts and 30-s periods of cooling on ice between each burst. The cell homogenate was centrifuged (300 × *g*, 4 °C, 10 min), and the supernatant was transferred to new tubes and recentrifuged (30,000 × *g*, 4 °C, 1 h) in a Sorval centrifuge. The pellet was resuspended in 5 mL of buffer (20 mM HEPES and 0.1 mM EDTA, pH 7.4) and briefly homogenized to ensure uniform consistency. The cell homogenate was then separated into 250-µL aliquots and stored at −80 °C. The protein concentration was determined by the method of Bradford.

[^{3}H]N-Methylscopolamine Binding Assay

Saturation binding assay was performed by incubating 5 µg of NG108-15 membrane with increasing concentrations of [^{3}H]N-methylscopolamine (NMS) (85.5 Ci/mmol; PerkinElmer, Waltham, MA) in HEPES binding buffer (20 mM HEPES, 100 mM NaCl, and 10 mM $MgCl_2$, pH 7.4) for 1 h at 37 °C. Binding was terminated by fast-flow filtration onto GF/B-grade filter paper (Whatman, Maidstone, UK) using a Brandel harvester, followed by three washes with ice-cold 0.9% NaCl. Nonspecific binding was defined in the presence of 10 µM atropine, and bound radioactivity was measured in a Tri-Carb 2900TR liquid scintillation counter (PerkinElmer).

cAMP Biosensor Assay

cAMP levels were measured using the bioluminescence resonance energy transfer (BRET) sensor, cAMP sensor using YFP-Epac-RLuc (CAMYEL; American Type Culture Collection). NG108-15 cells were seeded at 2,000,000 per 10-cm culture dish in culture medium and grown overnight. The cells were transfected with 2 µg CAMYEL using polyethylenimine. Cells were seeded into poly-D-lysine (Sigma-Aldrich, Castle Hill, NSW, Australia)–coated 96-well Cultureplates (PerkinElmer) 24 h posttransfection and assayed at 48 h posttransfection. For pertussis toxin (PTX) experiments, cells were treated with PTX 25 ng/mL for 24 h before assaying. Prior to the start of the assay, cells were allowed to equilibrate in Hanks' balanced salt solution (HBSS) at 37 °C. Under low light conditions, coelenterazine h was added at a final concentration of 5 µM 15 min prior to BRET detection. ACh and LY2033298 were added simultaneously 5 min after coelenterazine h. Forskolin was then added at a final concentration of 0.1 µM after a further 5 min. BRET readings were captured with a LUMIstar Omega instrument (BMG LabTech, Offenburg, Germany) that allows for sequential integration of the signals detected at 475 ± 30 and 535 ± 30 nm, using filters with the appropriate band pass.

ERK1/2 Phosphorylation Assay

ERK1/2 phosphorylation was measured using the AlphaScreen SureFire phospho-ERK kit (TGR Biosciences, Adelaide, SA, Australia). NG108-15 cells were seeded at

30,000 cells per well into a transparent 96-well plate coated with poly-D-lysine and grown overnight in culture medium with 2.5% fetal bovine serum (FBS). The next day, culture medium was aspirated, and the cells were rinsed with phosphate-buffered saline and incubated for 4 h in culture medium with 0.5% FBS before assaying. For PTX experiments, cells were treated with PTX 25 ng/mL for 20 h before assaying. ERK1/2 phosphorylation time course experiments were initially performed at least twice to determine the time at which the ligands were able to elicit the maximum ERK1/2 phosphorylation response (7.5 min for both ACh and LY2033298). Functional interaction experiments were performed at 37 °C with simultaneous addition of increasing concentrations of ACh in the absence or presence of increasing concentrations of LY2033298. ACh 10 μM was used as a positive control. Ligand stimulation was terminated by removal of medium, and cells were lysed by addition of cold 100 μL SureFire lysis buffer (PerkinElmer) to each well. Lysates were shaken in plates for 5 min at room temperature (RT) prior to transferring 5 μL lysate to a white 384-well Proxiplate (PerkinElmer). Under low light conditions, 8 μL of a 240:1440:7:7 mixture of SureFire activation buffer/SureFire reaction buffer/AlphaScreen acceptor beads/AlphaScreen donor beads was added to each sample well. Plates were incubated in the dark at 37 °C for 1 h and read with a Fusion-α plate reader (PerkinElmer) using standard AlphaScreen settings.

Cellular Impedance Assay

The label-free technology, xCELLigence Real-Time Cell Analyzer (RTCA) single-plate (SP) instrument (Roche Diagnostics GmbH and ACEA Biosciences), was used to measure changes in cellular impedance over time, which was defined as the cell index variable. Prior to the start of the assay, background cell index readings of each well of the 96-well E-plate (Roche Applied Science and ACEA Biosciences) were taken with culture medium in the absence of cells. This background reading was subtracted from all subsequent cell index values measured after addition of cells. NG108-15 cells were then seeded at 30,000 cells per well in culture medium with 2.5% FBS and grown for 16 h at 37 °C. Medium was then manually aspirated and replaced with culture medium with 0.5% FBS. The E-plate was inserted into the RTCA SP device station for both the cells and the system to equilibrate for 4 h at 37 °C. Immediately after simultaneous additions of increasing concentrations of ACh in the absence or presence of LY2033298, cell index values were obtained at 15-s intervals for 90 min. Data were baseline corrected with cell index values from the time point immediately prior to ligand addition and normalized to vehicle-treated wells. Importantly, DMSO concentration was maintained at a constant 0.05% across the plate. Data from the first 20 to 30 min following ligand addition were used to calculate the area under the curve (AUC) of the peak. For PTX experiments, AUC was calculated from the first 30 min immediately after ligand addition.

Data Analysis

Data from the xCELLigence system were analyzed and extracted with RTCA software 1.2.1.1002 (ACEA Biosciences). Data were analyzed with GraphPad Prism 6.00 (GraphPad Software, La Jolla, CA). Allosterism can be quantified by applying the operational model of allosterism to the ACh and LY2033298 interaction data to obtain the best-fit curve data, equation (1),[23] where E_m is the maximal effect of the pathway; $[A]$ and $[B]$ are concentrations of the orthosteric agonist and the allosteric modulator, respectively; K_A and K_B are the equilibrium dissociation constant of the orthosteric agonist and allosteric modulator, respectively; τ_A and τ_B are operational measures of the respective signaling efficacies of orthosteric agonist and allosteric modulator that incorporate receptor expression levels and efficiency of stimulus-response coupling; α is the cooperativity factor of the allosteric effect of the modulator on orthosteric agonist binding affinity, whereas β is that of the signaling efficacy; and n is the transducer slope factor linking occupancy to response.

$$E = \frac{E_m}{1+\left[\frac{\left([A]K_B + K_A K_B + K_A[B] + \alpha[A][B]\right)}{\left(\tau_A[A]\left(K_B + \alpha\beta[B]\right) + \tau_B[B]K_A\right)}\right]^n} \quad (1)$$

All affinity, potency, and cooperativity values were estimated as logarithms[24] and statistical comparisons between values were by one-way analysis of variance using a Tukey's multiple-comparison posttest to determine significant differences.

Results and Discussion

We have previously characterized LY2033298 (**Fig. 1A**) as a potent M_4 mAChR PAM of ACh affinity and function in cells overexpressing human M_4 mAChR.[20] In the same study, we found both LY2033298 agonism and potentiation of the ACh response (cooperativity) were markedly reduced when tested in NG108-15 cells that natively express rodent M_4 mAChR. Although these results could be due to the species variability described for LY2033298,[25] they could also be a consequence of different M_4 mAChR expression levels in the different cell lines. Thus, we initially assessed M_4 mAChR expression levels in NG108-15 cells by [^{3}H]NMS in membrane saturation radioligand binding experiments (data not shown). The B_{max} obtained in these experiments was 0.17 ± 0.04 pmol/mg of membrane protein (n = 4),

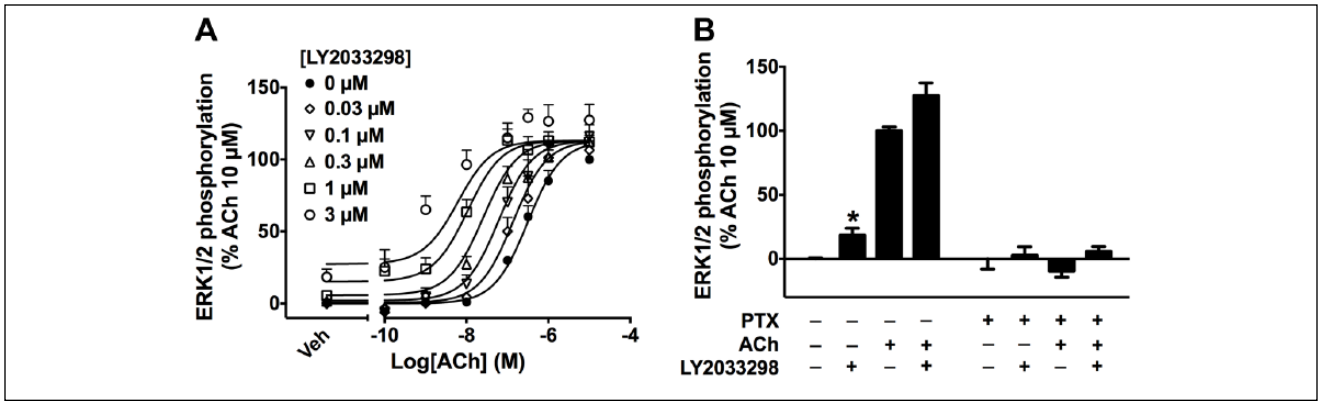

Figure 2. LY2033298 potentiates acetylcholine (ACh)–induced ERK1/2 phosphorylation. (**A**) Concentration-response curves of ACh-induced ERK1/2 phosphorylation with increasing concentrations of LY2033298. Curves shown represent the best fit of the operational model of allosterism, equation (1); $n = 3$. (**B**) In cells treated with pertussis toxin (PTX; 25 ng/mL for 20 h), ACh (10 μM) in the absence and presence of LY2033298 (3 μM) lost the ability to phosphorylate ERK1/2. Asterisk indicates significant difference in LY2033298 (3 μM)–induced ERK1/2 phosphorylation compared with vehicle (one-way analysis of variance with Dunnett's multiple-comparisons test; $*p < 0.05$); $n = 2–3$. Data presented as mean ± SEM.

which is markedly lower than that of human M_4 mAChR heterologously expressed in FlpIn Chinese hamster ovary (CHO) cells (1.1 ± 0.2 pmol/mg[26]).

To compare the allosteric properties of LY2033298 in NG108-15 cells using the xCELLigence system, we first characterized the effects of the PAM using two classical endpoint-based assays. M_4 mAChR predominantly couples to $G\alpha_i$ proteins, the activation of which inhibits production of cAMP by adenylyl cyclase, as well as promoting ERK1/2 phosphorylation further downstream in the signal transduction pathway. We explored the ability of LY2033298 to modulate ACh-mediated inhibition of cAMP accumulation using a BRET sensor, cAMP sensor using YFP-Epac-RLuc (CAMYEL).[27,28] Briefly, the CAMYEL sensor has yellow fluorescent protein (YFP; acceptor) and *Renilla* luciferase (*R*luc; donor) on either termini of the Epac1 protein. Binding of cAMP to Epac1 induces a change in conformation, increasing the distance between YFP and *R*luc, resulting in a decrease of the BRET signals. Increasing concentrations of ACh alone resulted in a concentration-dependent inhibition of forskolin-induced cAMP accumulation (**Fig. 1B**). Coaddition of LY2033298 caused a potentiation of ACh-mediated inhibition of forskolin-induced cAMP accumulation (**Fig. 1B**).

ERK1/2 phosphorylation was analyzed using the AlphaScreen SureFire Phospho-ERK1/2 assay, based on the transfer of oxygen radicals from the donor to the acceptor beads, which detect total or phosphorylated ERK1/2, respectively. ACh induced ERK1/2 phosphorylation in a concentration-dependent manner (**Fig. 2A**). As seen with the cAMP BRET assay, costimulation of LY2033298 potentiated ACh response, although the potentiation was greater in the ERK1/2 phosphorylation assay. In terms of allosteric agonism, while LY2033298 alone only weakly inhibited cAMP accumulation, it showed significant agonism in ERK1/2 phosphorylation ($p < 0.05$; one-way analysis of variance [ANOVA] with Dunnett's multiple-comparisons test; **Figs. 1C**, **2B**).

The allosteric effect of LY2033298 was quantified by fitting concentration-response curves to the operational model of allosterism, equation (1),[23] to yield the allosteric parameters shown in **Table 1**. The ability of LY2033298 to potentiate the ACh-mediated response (denoted as functional cooperativity, αβ) in the ERK1/2 phosphorylation assay was significantly higher than that estimated from the cAMP BRET assay (αβ, 127 vs. 12, respectively; $p < 0.01$; one-way ANOVA with Tukey's multiple-comparisons test). ACh and LY2033298 efficacy (τ_A and τ_B, respectively), although not significant, were estimated to be marginally higher in ERK1/2 phosphorylation than the cAMP BRET assay (τ_A, 231 vs. 147, respectively; τ_B, 0.66 vs. 0.14, respectively).

We then confirmed the contribution of $G\alpha_i$ proteins to M_4 mAChR-mediated signals in NG108-15 cells. In cells treated with PTX, which prevents the coupling of $G\alpha_i$ proteins to GPCRs, the inhibition of forskolin-induced cAMP accumulation mediated by either ACh (100 μM) or ACh + LY2033298 (3 μM) was completely abolished, confirming the involvement of $G\alpha_i$ proteins in these responses (**Fig. 1C**). This was also observed in the ERK1/2 phosphorylation assay, where the signals mediated by either ligand were abolished in PTX-treated cells (**Fig. 2B**).

Next, we investigated the ACh response in NG108-15 cells using the xCELLigence label-free system. This system measures the change in cellular impedance using microelectrodes lined on the bottom of the wells of a 96-well

Table 1. Operational Model Parameters for Functional Interaction between ACh and LY2033298 at the M_4 Muscarinic Acetylcholine Receptor (mAChR).

Parameter	cAMP	pERK	xCELLigence
pEC_{50} [a]	6.28 ± 0.12	6.64 ± 0.08	6.59 ± 0.04
pK_B [b]	5.54	5.54	5.54
Log$\alpha\beta$ [c]	1.08 ± 0.15 ($\alpha\beta$ = 12; 95% CI = 6–23)	2.10 ± 0.10** ($\alpha\beta$ = 127; 95% CI = 81–199)	1.87 ± 0.06* ($\alpha\beta$ = 74; 95% CI = 56–98)
Logτ_A [d]	2.17 ± 0.09 (τ_A = 147; 95% CI = 96–223)	2.23 ± 0.07 (τ_A = 231; 95% CI = 170–316)	2.28 ± 0.05 (τ_A = 191; 95% CI = 151–240)
Logτ_B [e]	−0.86 ± 0.25 (τ_B = 0.14; 95% CI = 0.05–0.43)	−0.18 ± 0.12 (τ_B = 0.66; 95% CI = 0.39–1.12)	−0.78 ± 0.10 (τ_B = 0.17; 95% CI = 0.10–0.26)

Parameter values were estimated from the operational model of allosterism, equation (1), presented as mean ± SEM; n = 3–4. CI, confidence interval.
[a]Negative logarithm of the concentration of acetylcholine (ACh) that produces half the maximal agonist response.
[b]Negative logarithm of the equilibrium dissociation constant of LY2033298; value was fixed to that determined from radioligand binding assays at the mouse M_4 mAChR expressed in Chinese hamster ovary cells.[20]
[c]Logarithm of the product of the binding (α) and efficacy (β) cooperativity factors between ACh and LY2033298. Antilogarithm shown in parentheses. Asterisks indicate significant difference compared with cAMP bioluminescence resonance energy transfer assay value (one-way analysis of variance, Tukey's multiple comparisons test; *p < 0.05, **p < 0.01).
[d]Logarithm of the operational efficacy parameter of ACh as an orthosteric agonist. Antilogarithm shown in parentheses.
[e]Logarithm of the operational efficacy parameter of LY2033298 as an allosteric agonist. Antilogarithm shown in parentheses.

plate (E-plate). As the cells adhere to the microelectrodes, the local ionic environment changes, which leads to an increase in impedance.[6] Therefore, the change in cell adhesion and/or morphology is reflected in a change in impedance.[4–6] Of note, the DMSO content was kept constant across the plate, as DMSO itself changes cellular impedance.[4]

Immediately after addition of ACh, there was a sharp increase in impedance, which reached a maximum within 10 min (**Fig. 3A–E**, black lines). There was a concentration-dependent increase in the maximum impedance reached by ACh (**Fig. 3F**, filled circles). The return to baseline produced a more gradual slope that decayed slowly back to the baseline (**Fig. 3A–E**).

As shown in the impedance traces (**Fig. 3A–E**), coaddition of LY2033298 potentiated an ACh-mediated response, and this potentiation reached a limit at the highest concentrations of modulator. Of note, increasing concentrations of the PAM increased the peak height, although not the width, of ACh-mediated impedance.

Concentration-response curves were obtained by calculating the AUC of the impedance peaks, and allosteric parameters were estimated through analysis of the data with equation (1) (**Fig. 3F** and **Table 1**). The potency of ACh in all three assays (cAMP inhibition, ERK phosphorylation, and cellular impedance) was similar (**Table 1**). This is in contrast to a previous study with the C5a receptor where the potency of the agonists tested was consistently lower in label-free assays compared with endpoint-based assays.[29] The potentiation of ACh-mediated impedance by LY2033298 using the label-free approach was similar to the cooperativity estimated for ERK1/2 phosphorylation and significantly higher than that for the inhibition of cAMP accumulation ($\alpha\beta$, 74 vs. 12, respectively; $p < 0.05$; one-way ANOVA with Dunnett's multiple-comparisons test). However, LY2033298 agonism (τ_B) as estimated by xCELLigence was similar to that by the cAMP BRET assay (τ_B, 0.17 vs. 0.14, respectively).

Interestingly, in cells treated with PTX, the impedance change induced by ACh (100 μM) was significantly impaired (**Fig. 4**). These results suggest that the overall changes in morphology of NG108-15 cells induced by ACh are predominately $G\alpha_i$ protein dependent. Interestingly, upon PTX treatment, the LY2033298 (3 μM)–induced impedance, both in the absence and in the presence of ACh, fell into the negative range, which was a phenomenon not seen in cells with intact $G\alpha_i$ protein activity (**Fig. 4**). These results suggest LY2033298 may be able to activate signaling pathways that are PTX insensitive. Although these data need further exploration, our cAMP data (**Fig. 1C**) show that in the presence of PTX, LY2033298 does not elicit changes in cAMP, suggesting that the unmasking of a $G\alpha_s$-mediated response is highly unlikely.

Label-free technologies on their own do not allow the determination of the precise intracellular pathways activated by a particular receptor or whether the different signaling pathways are modulated by an allosteric ligand. The deconvolution of label-free traces into specific signaling cascades can be achieved using pharmacological inhibitors. However, it is worth noting that activation of intracellular signaling cascades is cell type dependent, and as such, the interpretation of impedance traces is highly restricted to a particular cell system. Previous publications that have deconvoluted label-free traces into signaling pathways have also highlighted its cell type dependency. Stallaert et al.[30] used xCELLigence profiles in combination with pharmacological inhibitors to cluster and classify different β2-adrenergic receptor (β2AR) ligands in HEK293S cells overexpressing this receptor or in rat aortic smooth muscle cells endogenously expressing β2AR. While

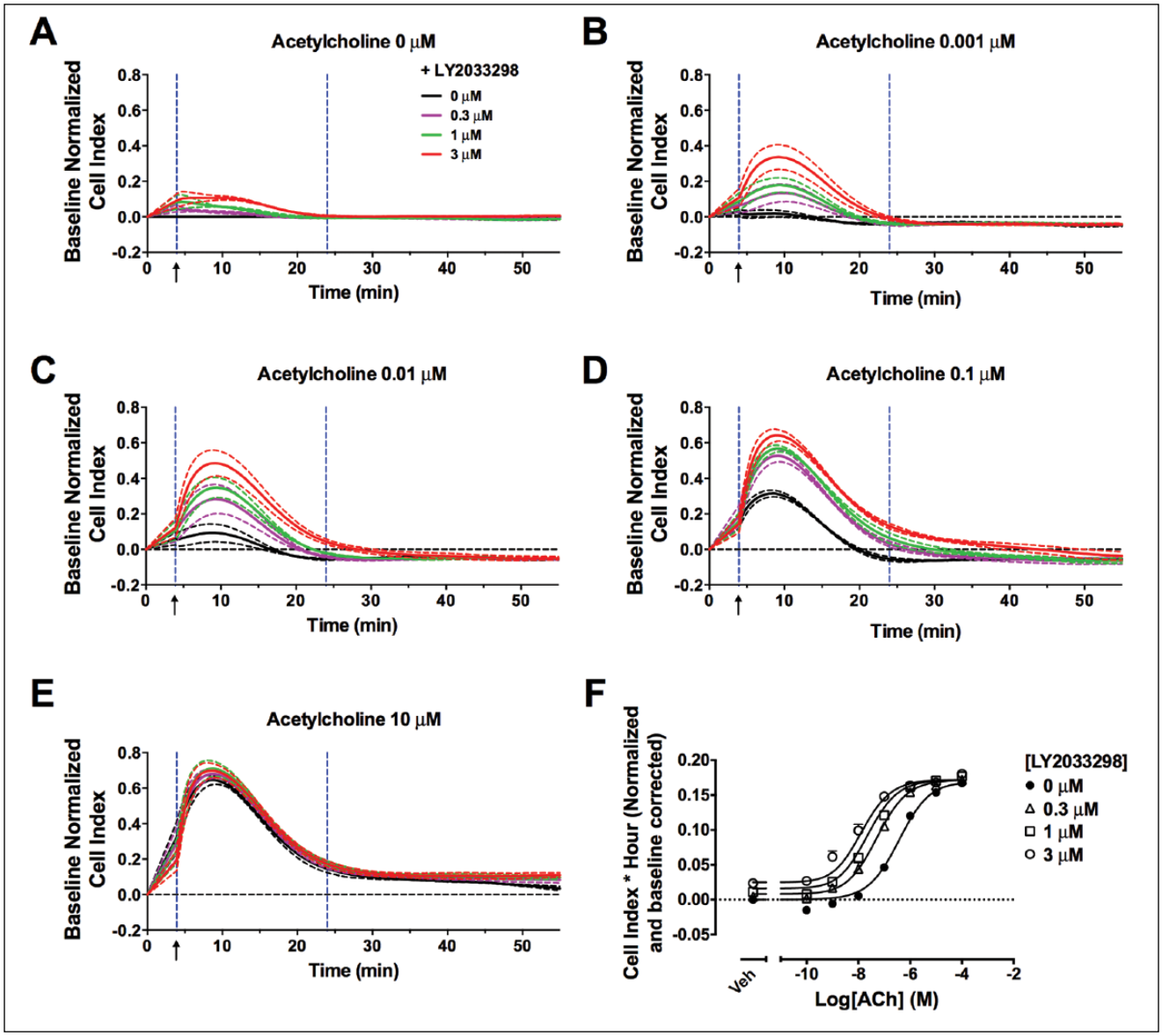

Figure 3. Positive allosteric modulation of acetylcholine (ACh) by LY2033298 can be detected with xCELLigence. Change in impedance induced by ACh (**A**) 0, (**B**) 0.001, (**C**) 0.01, (**D**) 0.1, and (**E**) 10 μM with increasing concentrations of LY2033298, which showed a sharp increase in ACh responses immediately after ligand stimulation, and the responses were potentiated by LY2033298. Traces of impedance profiles (mean ± SEM) shown were measured from three independent xCELLigence experiments. DMSO was constant across the plate at 0.05%. Black arrows indicate the time at which ligands were added. Vertical blue dotted lines indicate the data section used to calculate the area under the curve. (**F**) Concentration-response curves of ACh-induced change in cell index with increasing concentrations of LY2033298. Curves shown represent the best fit of the operational model of allosterism, equation (1); *n* = 3. Data presented as mean ± SEM.

the clustering of ligands remained unaltered, the impedance profiles of the ligands were markedly different. Schröder et al.[31] dissected the signaling patterns of several GPCRs with differential G protein coupling preferences using dynamic mass redistribution (DMR). This study also revealed a cell type dependency of the DMR response. Taking these studies into consideration, we would anticipate that in a different cell line, the impedance traces would change but the allosteric modulation would remain. Indeed, in preliminary studies using CHO FlpIn cells overexpressing the M_4 mAChR, the impedance traces were different from those observed in NG108-15 cells; however, LY2033298 allosteric modulation could be readily observed and quantified (data not shown).

Our results show that the potentiation of an orthosteric ligand by an allosteric modulator can be detected and quantified by xCELLigence in a neuronal cell line that

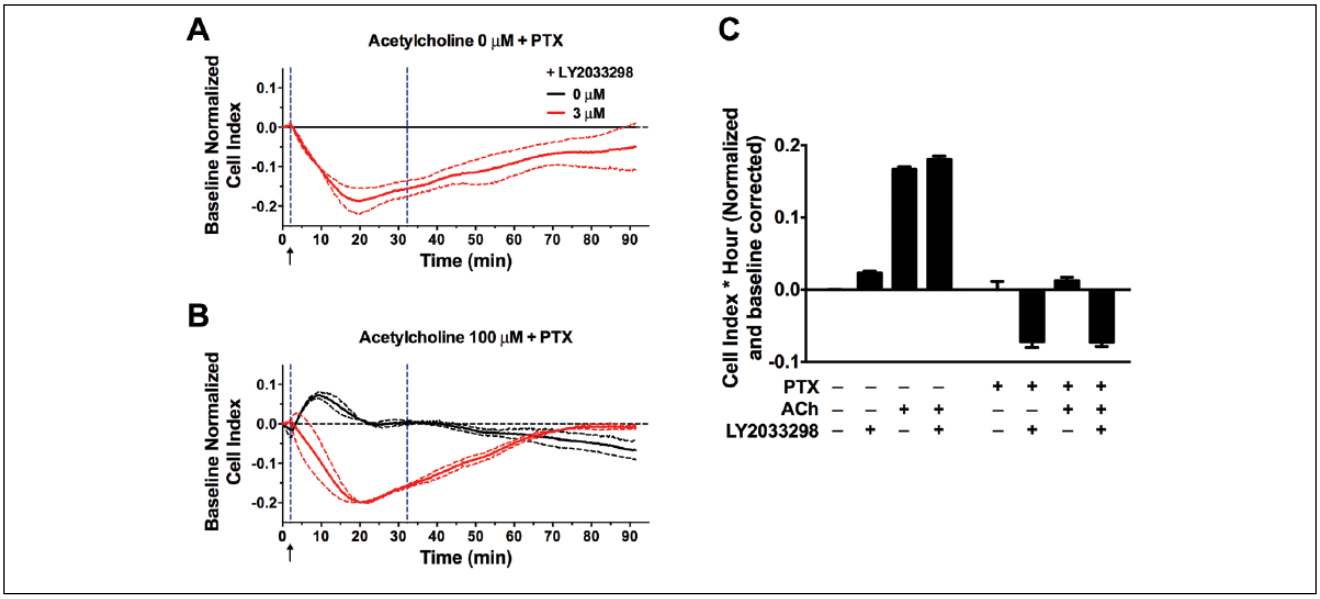

Figure 4. Overall change in impedance induced by acetylcholine (ACh) is predominately $G\alpha_i$ protein dependent. (**A**, **B**) Inhibition of $G\alpha_i$ protein activation by overnight treatment with pertussis toxin (PTX; 25 ng/mL for 20 h) diminished ACh (100 μM) alone response. However, costimulation with LY2033298 (3 μM) or LY2033298 alone led to a transient decrease in impedance. DMSO was constant across the plate at 0.05%. Black arrows indicate the time at which ligands were added. Vertical blue dotted lines indicate the data section used to calculate the area under the curve. (**C**) In cells treated with PTX, the ACh (100 μM)–induced response was greatly diminished. Cells stimulated with LY2033298 (3 μM), both in the presence and in the absence of ACh, showed a decrease in cell index that was not seen in PTX-untreated cells; n = 2–3. Data presented as mean ± SEM.

endogenously expresses the receptor of interest. To show this, we have used a prototypical GPCR with known G protein coupling preferences. However, our data also show that this approach is also amenable to screen for allosteric modulators in the absence of information about G protein coupling preferences.

In addition to allosterism, label-free approaches have previously been used to investigate another GPCR signaling paradigm, termed *biased agonism* or *functional selectivity*, where ligands that bind to the same GPCR preferentially activate one signaling pathway over another, leading to diverse physiological outcomes.[30] Both types of GPCR behaviors provide additional scope for the development of novel potential treatments with improved target selectivity and reduced occurrence of side effects.[3] The ability of impedance-based technology to detect and quantify allosteric and ligand-biased signaling in native environments can substantially aid the characterization of novel GPCR ligands.

Acknowledgments

LY2033298 was a generous gift from Christian C. Felder (Eli Lilly & Co., USA).

Declaration of Conflicting Interests

The authors declared no potential conflicts of interest with respect to the research, authorship, and/or publication of this article.

Funding

The authors disclosed receipt of the following financial support for the research, authorship, and/or publication of this article: This work was funded by the National Health and Medical Research Council of Australia (NHMRC) (program grant APP1055134) to A.C. and P.M.S.; M.C. is a Monash fellow; A.C. and P.M.S. are principal research fellows of the NHMRC.

References

1. Muller, C. E.; Schiedel, A. C.; Baqi, Y. Allosteric Modulators of Rhodopsin-Like G Protein–Coupled Receptors: Opportunities in Drug Development. *Pharmacol. Ther*. **2012**, *135*, 292–315.
2. Galandrin, S.; Oligny-Longpre, G.; Bouvier, M. The Evasive Nature of Drug Efficacy: Implications for Drug Discovery. *Trends Pharmacol. Sci*. **2007**, *28*, 423–430.
3. Kenakin, T.; Miller, L. J. Seven Transmembrane Receptors as Shapeshifting Proteins: The Impact of Allosteric Modulation and Functional Selectivity on New Drug Discovery. *Pharmacol. Rev*. **2010**, *62*, 265–304.
4. Halai, R.; Cooper, M. A. Using Label-Free Screening Technology to Improve Efficiency in Drug Discovery. *Expert Opin. Drug Discov*. **2012**, *7*, 123–131.
5. Scott, C. W.; Peters, M. F. Label-Free Whole-Cell Assays: Expanding the Scope of GPCR Screening. *Drug Discov. Today* **2010**, *15*, 704–716.
6. Yu, N.; Atienza, J. M.; Bernard, J.; et al. Real-Time Monitoring of Morphological Changes in Living Cells by Electronic Cell

Sensor Arrays: An Approach to Study G Protein–Coupled Receptors. *Anal. Chem*. **2006**, *78*, 35–43.
7. Verdonk, E.; Johnson, K.; McGuinness, R.; et al. Cellular Dielectric Spectroscopy: A Label-Free Comprehensive Platform for Functional Evaluation of Endogenous Receptors. *Assay Drug Dev. Technol*. **2006**, *4*, 609–619.
8. Fang, Y. Label-Free Cell-Based Assays with Optical Biosensors in Drug Discovery. *Assay Drug Dev. Technol*. **2006**, *4*, 583–595.
9. Cunningham, B. T.; Li, P.; Schulz, S.; et al. Label-Free Assays on the BIND System. *J. Biomol. Screen*. **2004**, *9*, 481–490.
10. Nickols, H. H.; Conn, P. J. Development of Allosteric Modulators of GPCRs for Treatment of CNS Disorders. *Neurobiol. Dis*. **2014**, *61*, 55–71.
11. Wang, L.; Martin, B.; Brenneman, R.; et al. Allosteric Modulators of G Protein–Coupled Receptors: Future Therapeutics for Complex Physiological Disorders. *J. Pharmacol. Exp. Ther*. **2009**, *331*, 340–348.
12. Conn, P. J.; Christopoulos, A.; Lindsley, C. W. Allosteric Modulators of GPCRs: A Novel Approach for the Treatment of CNS Disorders. *Nat. Rev. Drug Discov*. **2009**, *8*, 41–54.
13. Melancon, B. J.; Hopkins, C. R.; Wood, M. R.; et al. Allosteric Modulation of Seven Transmembrane Spanning Receptors: Theory, Practice, and Opportunities for Central Nervous System Drug Discovery. *J. Med. Chem*. **2012**, *55*, 1445–1464.
14. Gregory, K. J.; Valant, C.; Simms, J.; et al. The Emergence of Allosteric Modulators for G Protein–Coupled Receptors. In *GPCR Molecular Pharmacology and Drug Targeting*. Ed: Annette Gilchrist. John Wiley: New York, **2010**; pp. 61–87.
15. Foster, D. J.; Choi, D. L.; Conn, P. J.; et al. Activation of M_1 and M_4 Muscarinic Receptors as Potential Treatments for Alzheimer's Disease and Schizophrenia. *Neuropsychiatr. Dis. Treat*. **2014**, *10*, 183–191.
16. Muench, J.; Hamer, A. M. Adverse Effects of Antipsychotic Medications. *Am. Fam. Physician* **2010**, *81*, 617–622.
17. Dencker, D.; Wortwein, G.; Weikop, P.; et al. Involvement of a Subpopulation of Neuronal M_4 Muscarinic Acetylcholine Receptors in the Antipsychotic-Like Effects of the M_1/M_4 Preferring Muscarinic Receptor Agonist Xanomeline. *J. Neurosci*. **2011**, *31*, 5905–5908.
18. Shekhar, A.; Potter, W. Z.; Lightfoot, J.; et al. Selective Muscarinic Receptor Agonist Xanomeline as a Novel Treatment Approach for Schizophrenia. *Am. J. Psychiatry* **2008**, *165*, 1033–1039.
19. Chan, W. Y.; McKinzie, D. L.; Bose, S.; et al. Allosteric Modulation of the Muscarinic M_4 Receptor as an Approach to Treating Schizophrenia. *Proc. Natl. Acad. Sci. U. S. A*. **2008**, *105*, 10978–10983.
20. Leach, K.; Loiacono, R. E.; Felder, C. C.; et al. Molecular Mechanisms of Action and In Vivo Validation of an M_4 Muscarinic Acetylcholine Receptor Allosteric Modulator with Potential Antipsychotic Properties. *Neuropsychopharmacology* **2010**, *35*, 855–869.
21. Peters, M. F.; Knappenberger, K. S.; Wilkins, D.; et al. Evaluation of Cellular Dielectric Spectroscopy, a Whole-Cell, Label-Free Technology for Drug Discovery on G(i)-Coupled GPCRs. *J. Biomol. Screen*. **2007**, *12*, 312–319.
22. Klein, M. T.; Vinson, P. N.; Niswender, C. M. Approaches for Probing Allosteric Interactions at 7 Transmembrane Spanning Receptors. *Prog. Mol. Biol. Transl. Sci*. **2013**, *115*, 1–59.
23. Leach, K.; Sexton, P. M.; Christopoulos, A. Allosteric GPCR Modulators: Taking Advantage of Permissive Receptor Pharmacology. *Trends Pharmacol. Sci*. **2007**, *28*, 382–389.
24. Christopoulos, A. Assessing the Distribution of Parameters in Models of Ligand-Receptor Interaction: To Log or Not to Log. *Trends Pharmacol. Sci*. **1998**, *19*, 351–357.
25. Suratman, S.; Leach, K.; Sexton, P.; et al. Impact of Species Variability and 'Probe-Dependence' on the Detection and In Vivo Validation of Allosteric Modulation at the M4 Muscarinic Acetylcholine Receptor. *Br. J. Pharmacol*. **2011**, *162*, 1659–1670.
26. Nawaratne, V.; Leach, K.; Suratman, N.; et al. New Insights into the Function of M_4 Muscarinic Acetylcholine Receptors Gained Using a Novel Allosteric Modulator and a DREADD (Designer Receptor Exclusively Activated by a Designer Drug). *Mol. Pharmacol*. **2008**, *74*, 1119–1131.
27. Xu, Y.; Kanauchi, A.; von Arnim, A. G.; et al. Bioluminescence Resonance Energy Transfer: Monitoring Protein-Protein Interactions in Living Cells. *Methods Enzymol*. **2003**, *360*, 289–301.
28. Jiang, L. I.; Collins, J.; Davis, R.; et al. Use of a cAMP BRET Sensor to Characterize a Novel Regulation of cAMP by the Sphingosine 1-Phosphate/G13 Pathway. *J. Biol. Chem*. **2007**, *282*, 10576–10584.
29. Halai, R.; Croker, D. E.; Suen, J. Y.; et al. A Comparative Study of Impedance versus Optical Label-Free Systems Relative to Labelled Assays in a Predominantly Gi Coupled GPCR (C5aR) Signalling. *Biosensors* **2012**, *2*, 273–290.
30. Stallaert, W.; Dorn, J. F.; van der Westhuizen, E.; et al. Impedance Responses Reveal Beta(2)-Adrenergic Receptor Signaling Pluridimensionality and Allow Classification of Ligands with Distinct Signaling Profiles. *PLoS One* **2012**, *7*, e29420.
31. Schröder, R.; Janssen, N.; Schmidt, J.; et al. Deconvolution of Complex G Protein–Coupled Receptor Signaling in Live Cells Using Dynamic Mass Redistribution Measurements. *Nat. Biotechnol*. **2010**, *28*, 943–949.